Visual and sedimentological characterisation of cold-water coral mounds

From a single coral up to a large mound

Lies De Mol

2012

Thesis submitted for the degree of Doctor of Science: Geology

Promoters: Prof. Dr. Jean-Pierre Henriet and Prof. Dr. Marc De Batist

Visual and sedimentological characterisation of cold-water coral mounds

From a single coral up to a large mound

Visuele en sedimentologische karakterisatie van koudwaterkoraalheuvels

Van een enkel koraal tot een grote koraalheuvel

This research was financially supported by the Agency for Innovation by Science and Technology (IWT).

Members of the reading committee:

Prof. Dr. J.-P. Henriet	Ghent University - Belgium
Prof. Dr. F. Boulvain	Université de Liège - Belgium
Prof. Dr. D. Blamart	CEA/CNRS - Université de Versailles - France

Members of the examination committee:

Prof. Dr. J. Verniers	Ghent University - Belgium
Prof. Dr. J.-P. Henriet	Ghent University - Belgium
Prof. Dr. M. De Batist	Ghent University - Belgium
Prof. Dr. D. Van Rooij	Ghent University - Belgium
Prof. Dr. S. Louwye	Ghent University - Belgium
Prof. Dr. A. Vanreusel	Marine Biology - Ghent University - Belgium
Prof. Dr. F. Boulvain	Université de Liège - Belgium
Prof. Dr. D. Blamart	CEA/CNRS - Université de Versailles - France

To refer to this thesis:
De Mol, L., 2012. Visual and sedimentological characterisation of cold-water coral mounds – From a single coral up to a large mound. PhD thesis, Ghent University, Belgium.

In Dutch: Visuele en sedimentologische karakterisatie van koudwaterkoraalheuvels – Van een enkel koraal tot een grote koraalheuvel. Doctoraatsthesis, Universiteit Gent, België.

Table of contents

Appendices on DVD

ROV pictures R/V Belgica cruises (2008, 2009 and 2010)

ROV video R/V Belgica 08/13a cruise Bay of Biscay

ROV video R/V Belgica 09/14b cruise Gulf of Cadiz

ROV video oysters (supplementary data Deep-Sea Research)

Acknowledgements - Dankwoord

First of all, I would like to thank my two promoters Prof. Dr. Jean-Pierre Henriet and Prof. Dr. Marc De Batist. Jean-Pierre, you gave me the opportunity to apply a second time for funding for four years of PhD research and I am glad that I took that opportunity. Although I was not familiar with cold-water coral mound research, you gave me the time to find my way in the subject. Even with a really busy schedule you always made the time to answer questions, discuss problems and read my manuscripts. Although I do not always agree with your opinion, I appreciated your valuable comments and tips, especially during the last months! During my PhD, you gave me the chance to go at sea, to go to conferences, to follow courses… I learnt a lot during the past five years! As your last PhD student, I must say: enjoy your retirement!!! Tist, thanks for being my official promoter during the last year! I will never forget the five years I have spent at the RCMG!

A special thanks goes to David and Hans for all their help during my PhD! Thanks a lot for helping me in the lab, giving me advice, careful reading of all the manuscripts and answering lots of questions!!! Jasper, thanks for sharing an office with me for four years. Although we had some disagreements (especially about the room temperature), I really enjoyed my time there! Wim, thanks for the nice chats and always willing to help me! I will definitely never forget our trip to Baku in Azerbaijan! Marcske, Lieven, Katrien, Maarten, Matthias, Tine, Andres, Mieke, Dries, Jeroen, Koen, Jens, Rindert, Sonia, Anneleen, Davy, Vera, Els, Isabelle, Peter, Jeffrey, Thomas, Willem, Sebastien, Mario, Arne, Tom, Anita, Javiera and Athanas, thanks a lot for the nice time at the RCMG, the trips to the Delhaize and the scientific and social discussions during lunch time! Part of this thesis could not have been made without the help of students. Therefore I would like to thank Zoë, Wencke, Alexander, Cindy and Elke†. I also would like to thank the other geology people from the S8: Danielle, Kurt, Cilia, Ingrid, Stijn, Johan, Ann, Thomas, Koen, Kenneth, Jan, Carolien, Veerle, Jan, Tim and Marijn!

The team from the UGCT, especially Veerle Cnudde, Jan Dewanckele and Matthieu Boone, and Henry Houbrechts from the Ghent Unviversity Hospital, are thanked for helping me with the CT scanning! Henk de Haas, Furu Mienis, Henko de Stigter, Cees van der Land, Rineke Gieles and Alina Stadnitskaia, thanks a lot for all your help during my stay at the NIOZ! Erwan Le Guilloux and Olivier Soubigou (Ifremer), thanks for giving me an introduction in Adelie and in ROV interpretation! Norbert Frank (LSCE), many thanks for the (last-minute) U-series dating of my coral samples, although it was not easy to find some well-preserved and unaltered specimens! Dominique Blamart (LSCE), thanks for providing the stable carbon and oxygen isotope results! Stéphanie Larmagnat (Université Laval), thanks for your help with the histological thin sections and SEM observations of the Belgica 09/14 boxcore samples! I really enjoyed your stay in Belgium! Veerle Huvenne, thanks for reading some of my

manuscripts and giving me advice during my PhD! Mieke Thierens, thanks a lot for your last-minute help and advice!

I also would like to thank the coral community as well as the people from the HERMES, HERMIONE and MiCROSYSTEMS projects for the nice chats and discussions on conferences. The shipboard scientific parties and the crew of the R/V Belgica 07/13, 08/13, 09/14 and 10/17 cruises and the R/V Marion Dufresne 169 cruise are thanked for the nice time and good cooperation on board! After 82 days at sea I will probably never get used to sea sickness!

Verder wil ik ook mijn collega's, Marc, Koen, Helga, Hilde en Patrik, bij de Dienst Continentaal Plat (FOD Economie) bedanken voor hun steun tijdens de laatste maanden van mijn doctoraat. Het was niet altijd eenvoudig om mijn nieuwe job te combineren met het schrijven van een doctoraat maar uiteindelijk heb ik toch de eindstreep behaald! Na het Issyk-Kul meer, de Golf van Cadiz en de Golf van Biscaje, kan ik mij nu volledig toeleggen op het Belgisch deel van de Noordzee!

Karen, bedankt voor de dagelijkse koffiepauzes op de S8 en voor je luisterend oor! Ondertussen woon je aan de andere kant van het Kanaal maar Skype is toch een goede uitvinding! Kristien, Koen DB, Katrijn, Roeland, Thijs, Vic, Ineke, Koen D, Svea, Natalie, Jurgen en Ferike, bedankt voor de gezellige en ontspannende etentjes en weekendjes! Jullie zijn gewoon fantastisch! Els, bedankt voor de leuke babbels en om er gewoon altijd te zijn voor mij! Gentse BC en in het bijzonder mijn ploegleden van 5G wil ik bedanken voor het bezorgen van sportieve ontspanning, leuke badmintonmatchen en vooral gezellige nabesprekingen in de cafetaria! Jacques, Marleen, Heidi, Patrick, Lisa en Lars, bedankt voor de leuke familiebijeenkomsten en weekendjes!

Mama en papa, bedankt om altijd voor mij klaar te staan, om mij te steunen in mijn (studie)keuzes (ook als ik kwam vertellen dat ik geologie ging studeren), om naar mij te luisteren als het even wat minder ging, om blijven interesse te tonen in wat ik deed voor mijn doctoraat, om mijn artikels te lezen… Kortom, bedankt voor alles!!! Zonder jullie had ik dit nooit bereikt…

Jeroen… Mijn doctoraat heeft een belangrijke rol gespeeld de laatste vier jaar maar ondanks de ups en downs ben je mij altijd blijven steunen en blijven moed geven om verder te doen. Bedankt dat je er altijd voor mij bent!

Summary

Cold-water corals are widely distributed along the northeast Atlantic margin. They are able to form habitats which vary in size from small patches (few metres in size) to large reef structures (covering several kilometres). Additionally, they can even build up large mound structures up to 300 m high. The discovery of large cold-water coral mound provinces along the European continental margin belongs to one of the most spectacular discoveries of the past decade. Since then, these coral mounds became a hot topic within deep-water research resulting in many multidisciplinary studies (e.g. sedimentological, (micro)biological, palaeontological, geophysical, biochemical). At present, more than one thousand mounds have already been identified within different mound provinces along the European and Moroccan continental margins. The best studied examples along the NE Atlantic margin can be found in the Porcupine Seabight and on the margins of the Rockall Trough.

Within the Gulf of Cadiz submarine ridges and steep fault escarpments occur, which could favour the settlement of scleractinians and facilitate the build-up of cold-water coral mounds, if the appropriate environmental conditions are met. One of these sites is the Pen Duick Escarpment, situated in the El Arraiche mud volcano field on the Moroccan continental margin. Up to now, 15 cold-water coral mounds have been identified on top of this escarpment with an average elevation of 15 m. This research will focus on three of these mounds: Alpha, Beta and Gamma Mound. First, the surface and the uppermost decimetres of these mounds will be discussed, followed by a detailed study of three gravity cores in order to unveil the architectural framework of the cold-water coral build-ups. Compared to the mounds in the Porcupine Seabight and on the margins of the Rockall Trough, the Pen Duick mounds are much smaller in size, suggesting a younger age, and making them ideal to study the initial build-up and evolution of the mounds. However, little is known about these mounds.

The second part of this thesis focuses on the presence of cold-water corals and associated oysters along the continental margin in the Bay of Biscay, where no coral mounds are observed. In contrast to these well studied areas in the Porcupine Seabight and the Rockall Trough, coral occurrences within the Bay of Biscay, and more specifically the Armorican margin, are less investigated.

Gulf of Cadiz

Three cold-water coral mounds on top of the Pen Duick Escarpment were investigated, using video observations and boxcore samples. A detailed study of the present distribution of fossil cold-water corals on the Pen Duick Escarpment, the role of cold-water coral rubble

fields, the presence of authigenic carbonate slabs and the growth and distribution of these corals in the past is presented. Up to 40 m high cold-water coral mounds covered with fossil corals were observed, which is in contrast with the cold-water coral mounds on the Irish margin that are covered with a living coral cover. The mounds surfaces revealed a patchwork of facies: soft sediment with/without cold-water coral rubble, dense coral rubble fields and carbonate slabs. This patchwork can be explained by a complex process of deposition, non-deposition and erosion, triggered by changes in bottom current strength and direction, and changes in the morphology of the escarpment. Bottom samples showed that *Lophelia pertusa*, *Madrepora oculata* and *Dendrophyllia* sp. were the most common cold-water coral species. U/Th dating of the corals revealed that *Lophelia pertusa* and *Madrepora oculata* thrived in the Gulf of Cadiz during glacial periods, while *Dendrophyllia* sp. was able to survive after the Younger Dryas event (interglacial periods). *Dendrophyllia* sp. will thus appear after the extinction of *Lophelia pertusa* and *Madrepora oculata*. In a next step, gravity cores from these three coral mounds were investigated using CT scanning, magnetic susceptibility, X-ray fluorescence, grain-size analysis, end-member modelling, stable carbon and oxygen isotope analysis, and U-series dating in order to reconstruct different phases of mound and coral growth, assess the impact of early diagenesis on the sedimentary record and to link these processes with specific palaeoenvironmental conditions. This study shows that diagenetic processes, like dissolution of carbonates, the formation of pyrite and carbonate precipitation, play an important role in mound build-up. However, we looked further and tried to unravel paleoenvironmental signals from the input of terrigenous sediment in a cold-water coral mound which is not significantly altered by diagenetic processes. The growth and evolution of the Pen Duick mounds is linked to climatic changes on the NW African continent. *Lophelia pertusa* and *Madrepora oculata* are the dominant species within the mounds, indicating intense coral growth during glacial periods. Additionally, mound growth is also related to glacial times (mainly to Marine Isotopic Stages 2-4 and 8) due to the high input of aeolian dust during these periods. During interglacials coral growth is very limited and will result in slowing down or interrupting the mound building process due to the input of the more fine-grained fluvial sediments.

Bay of Biscay

In 1948, Le Danois reported for the first time the occurrence of living cold-water coral reefs, the so-called “massifs coralliens”, along the European Atlantic continental margin. In 2008, a cruise with R/V Belgica was set out to re-investigate these cold-water corals in the Penmarc’h and Guilvinec Canyons along the Gascogne margin of the Bay of Biscay. During this cruise, an area of 560 km^2 was studied using multibeam swath bathymetry, CTD casts, ROV observations and USBL-guided boxcoring. Based on the multibeam data and the ROV video imagery, two different cold-water coral reef settings were distinguished. In water depths ranging from 260 to 350 m, mini mounds up to 5 m high, covered by dead cold-water coral rubble, were observed. In between these mounds, soft sediment with a patchy

distribution of gravel was recognised. The second setting (350-950 m) features hard substrates with cracks, spurs, cliffs and overhangs. In water depths of 700 to 950 m, both living and dead cold-water corals occur. Occasionally, they form dense coral patches with a diameter of about 10-60 m, characterised by mostly stacked dead coral rubble and a few living specimens. U/Th datings indicate a shift in cold-water coral growth after the Late Glacial Maximum (about 11.5 ka BP) from shallow to deep-water settings. The living cold-water corals from the deeper area occur in a water density (sigma-theta) of 27.35 – 27.55 $kg.m^{-3}$, suggested to be a prerequisite for the growth and distribution of cold-water coral reefs along the northern Atlantic margin. In contrast, the dead cold-water coral fragments in the shallow area occur in a density range of 27.15-27.20 $kg.m^{-3}$ which is slightly outside the density range where living cold-water corals normally occur. The presented data suggest that this prerequisite is also valid for coral growth in the deeper canyons (>350 m) in the Bay of Biscay. Next to the presence of cold-water corals, we also report the northernmost and deepest known occurrence of deep-water pycnodontine oysters, based on two surveys along the French Atlantic continental margin to the La Chapelle continental slope (2006) and the Guilvinec Canyon (2008). The combined use of multibeam bathymetry, seismic profiling, CTD casts and a remotely operated vehicle (ROV) made it possible to describe the physical habitat and to assess the oceanographic control for the recently described species *Neopycnodonte zibrowii*. These oysters have been observed in vivo in depths from 540 to 846 m, colonising overhanging banks or escarpments protruding from steep canyon flanks. Especially in the Bay of Biscay, such physical habitats may only be observed within canyons, where they are created by both long-term turbiditic and contouritic processes. Frequent observations of sand ripples on the seabed indicate the presence of a steady, but enhanced bottom current of about 40 cm s^{-1}. The occurrence of oysters also coincides with the interface between the Eastern North Atlantic Water and the Mediterranean Outflow Water. A combination of this water mass mixing, internal tide generation and a strong primary surface productivity may generate an enhanced nutrient flux, which is funnelled through the canyon. When the ideal environmental conditions are met, up to 100 individuals per m^2 may be observed. These deep-water oysters require a vertical habitat, which is often incompatible with the requirements of other sessile organisms, and are only sparsely distributed along the continental margins. The discovery of these giant oyster banks illustrates the rich biodiversity of deep-sea canyons and their underestimation as true ecosystem hotspots.

Samenvatting

Koudwaterkoralen zijn wijdverspreid langsheen de noordoostelijke Atlantische rand. Ze zijn in staat om habitats te vormen die variëren in grootte van kleine groepjes (enkele meters) tot grote riffen (enkele kilometers). Daarnaast zijn ze ook in staat om grote heuvelstructuren te vormen die tot 350 m hoog kunnen worden. De ontdekking van grote koraalheuvelprovincies langsheen de Europese continentale rand behoort tot één van de meest spectaculaire ontdekkingen van het laatste decennium. Sindsdien zijn deze koraalheuvels een hot topic binnen het diepzeeonderzoek wat leidt tot vele multidisciplinaire studies (sedimentologisch, (micro)biologisch, paleontologisch, geofysisch, biochemisch). Momenteel werden reeds een duizendtal koraalheuvels geïdentificeerd binnen verschillende provincies langsheen de Europese en Marokkaanse continentale randen. De best bestudeerde exemplaren langs de noordoostelijke Atlantische rand zijn te vinden in de Porcupine Seabight en langsheen de randen van de Rockall Trough.

In de Golf van Cadiz komen onderwaterruggen en steile breukwanden voor die een ideaal substraat kunnen vormen voor koralen en die de aanzet kunnen geven tot het opbouwen van koraalheuvels indien de ideale omgevingscondities aanwezig zijn. Eén van deze locaties is de Pen Duick Escarpment, gelegen in het El Arraiche moddervulkaanveld op de Marokkaanse continentale rand. Tot nu werden reeds 15 koraalheuvels, met een gemiddelde hoogte van 15 m, ontdekt op de top van deze klif. Dit onderzoek zal zich toeleggen op drie van deze koraalheuvels: Alpha, Beta en Gamma Mound. In eerste instantie zal het oppervlak en de bovenste decimeters van de koraalheuvels worden besproken, waarna een gedetailleerde studie volgt van drie sedimentkernen met als doel om de opbouw van deze koraalheuvels te achterhalen. In vergelijking met de koraalheuvels in de Porcupine Seabight en op de randen van de Rockall Trough zijn de Pen Duick koraalheuvels veel kleiner in grootte, wat wijst op een jongere ouderdom. Dit maakt dat ze ideaal zijn voor de studie van de initiële groei en evolutie van koraalheuvels. Weinig is echter gekend over deze koraalheuvels in de zuidelijke Golf van Cadiz.

Het tweede deel van deze thesis richt zich op de aanwezigheid van koudwaterkoralen en oesters langsheen de continentale rand in de Golf van Biscaje, waar geen koraalheuvels werden geobserveerd. In vergelijking met de goed bestudeerde gebieden in de Porcupine Seabight en de Rockall Trough, is het voorkomen van koralen in de Golf van Biscaje, en meer specifiek langsheen de Armoricaanse rand, tot op heden weinig onderzocht.

Golf van Cadiz

Drie koudwaterkoraalheuvels op de top van de Pen Duick Escarpment werden bestudeerd aan de hand van video-observaties en bodemstalen. Een gedetailleerde studie van de huidige verdeling van fossiele koudwaterkoralen op de Pen Duick Escarpment, de rol van koraalgruisvelden, het voorkomen van carbonaatkorsten en de groei en verdeling van deze koralen in het verleden wordt voorgesteld. Tot 40 m hoge koraalheuvels bedekt met fossiele koralen werden geobserveerd, dit in groot contrast met de koraalheuvels langsheen de Ierse rand die bedekt zijn met een levend koraalrif. Het oppervlak van de heuvels vertoont een patchwork van facies: zacht sediment met/zonder koraalgruis, dikke koraalgruisvelden en carbonaatkorsten. Dit patchwork kan verklaard worden door een complex proces van afzetting, niet-afzetting en erosie, aangestuurd door veranderingen in de sterkte en de richting van bodemstromingen, en veranderingen in de morfologie van de klif. Bodemstalen tonen aan dat *Lophelia pertusa*, *Madrepora oculata* en *Dendrophyllia* sp. de meest voorkomende koraalsoorten zijn. U/Th dateringen van deze koralen wijzen erop dat *Lophelia pertusa* en *Madrepora oculata* voornamelijk voorkwamen in de Golf van Cadiz tijdens glaciale perioden, terwijl *Dendrophyllia* sp. in staat is om te overleven na het Younger Dryas (interglaciale perioden). *Dendrophyllia* sp. zal dus pas verschijnen na het uitsterven van *Lophelia pertusa* en *Madrepora oculata*. In een volgende stap werden sedimentkernen van deze drie koraalheuvels onderzocht aan de hand van CT scans, magnetische susceptibiliteit, X-stralen fluorescentie, korrelgrootte-analyse, eindtermmodellering, stabiele koolstof- en zuurstofisotopenanalyse, en U/Th datering. Dit zal ons in staat stellen om verschillende fases in de groei van koralen en koraalheuvels te reconstrueren, de impact van vroege diagenese op het sedimentair archief na te gaan, en deze verschillende processen te linken aan specifieke omgevingscondities tijdens het verleden. Deze studie toont aan dat diagenetische processen, zoals oplossing van carbonaten, de vorming van pyriet en carbonaatprecipitatie, een belangrijke rol spelen in de opbouw van de koraalheuvels. We trachten echter verder te kijken en de signalen van terrigene input te achterhalen in een koraalheuvel die niet significant is aangetast door diagenetische processen. De groei en evolutie van de Pen Duick koraalheuvels is gelinkt aan klimaatsveranderingen op het NW Afrikaanse continent. *Lophelia pertusa* en *Madrepora oculata* zijn de dominante species in de koraalheuvels, die wijzen op intense koraalgroei tijdens glaciale perioden. Daarbovenop kan de groei van koraalheuvels eveneens gelinkt worden aan deze glaciale tijden (voornamelijk tijdens de Marien Isotopische Periodes 2-4 en 8) door de hoge input van eolisch stof tijdens deze periodes. Tijdens interglacialen is koraalgroei zeer beperkt wat leidt tot het vertragen van de opbouw van koraalheuvels of zelfs het helemaal stopzetten van dit proces door de input van fijner, fluviatiel materiaal.

Golf van Biscaje

In 1948 rapporteerde Le Danois voor het eerst het voorkomen van levende koudwater-koraalriffen, de zogenoemde “massifs coralliens”, langsheen de Europese Atlantische continentale rand. In 2008 werd een campagne georganiseerd met het onderzoeksschip Belgica om deze koralen opnieuw te gaan bekijken in de Penmarc’h en Guilvinec Canyons langsheen de Gascogne rand in de Golf van Biscaje. Tijdens deze campagne werd een gebied van 560 km² bestudeerd aan de hand van multibeam bathymetrie, CTD, ROV observaties en USBL geleide staalname. Op basis van de multibeam data en de ROV videobeelden werden twee verschillende koraalrifgebieden onderscheiden. In waterdieptes van 260 tot 350 m werden mini-heuvels tot 5 m hoog bedekt met dood koraalgruis waargenomen. Tussen deze mini-heuvels vonden we zacht sediment met hier en daar grind. Het tweede gebied (350-950 m) is gekenmerkt door hard substraat met breuken en kliffen. In waterdieptes van 700 tot 950 m werden zowel levende als dode koralen waargenomen. Occasioneel vormden deze koralen dichte koraalvelden met een diameter van ongeveer 10-60 m, gekenmerkt door voornamelijk dood koraalgruis met bovenop een paar levende koralen. U/Th dateringen wijzen op een verandering in koraalgroei na het laatste glaciaal maximum (ongeveer 11.500 jaar geleden) van het ondiepe naar het diepe gebied. De levende koudwaterkoralen uit het diepe gebied komen voor in een waterdichtheid (sigma-theta) van 27.35 – 27.55 $kg.m^{-3}$, wat overeenstemt met één van de eerder voorgestelde voorwaarden voor de groei en verdeling van koudwater-koraalriffen langsheen de noordelijke Atlantische rand. In tegenstelling tot het diepe gedeelte komen de koraalfragmenten uit het ondiepe deel voor in een dichtheid van 27.15-27.20 $kg.m^{-3}$, wat net buiten het interval voor levende koralen valt. Deze data toont aan dat deze voorwaarde ook geldig is voor koraalgroei in diepe canyons (>350 m) in de Golf van Biscaje. Naast het voorkomen van koudwaterkoralen melden we ook het meest noordelijke en diepste voorkomen van diepwater pycnodontine oesters, gebaseerd op twee campagnes langsheen de Frans Atlantische continentale rand nabij de La Chapelle continentale helling (2006) en de Guilvinec Canyon (2008). Het gecombineerd gebruik van multibeam bathymetrie, seismische profielen, CTD en ROV data maakte het mogelijk om de fysische habitat te beschrijven alsook de oceanografische context van de recent beschreven *Neopycnodonte zibrowii* soort te onderzoeken. Deze oesters werden levend geobserveerd in dieptes van 540 tot 846 m, waarbij ze overhangende banken of kliffen op steile wanden in canyons koloniseren. In de Golf van Biscaje kunnen zulke fysische habitats enkel voorkomen in canyons, waar ze worden gecreëerd door langdurige turbiditische activiteit en contouritische processen. Frequente observaties van zandribbels op de zeebodem wijzen op een gematigde, maar toenemende bodemstroming van ongeveer 40 cm s^{-1}. De aanwezigheid van oesters komt ook overeen met de overgang tussen de oostelijke Noord-Atlantische watermassa (ENAW) en de uitstromende watermassa uit de Middellandse Zee (MOW). Een combinatie van menging van deze watermassa’s, interne getijdeontwikkeling en een sterke primaire oppervlakteproductiviteit kan zorgen voor een toegenomen nutriëntenstroom, die gekanaliseerd wordt doorheen de canyon. Wanneer de ideale omgevingscondities worden

bereikt, kunnen tot 100 individuen per m² worden waargenomen. Deze diepwateroesters hebben nood aan een verticaal habitat, wat vaak niet samengaat met de vereisten van andere sessiele organismen, en komen slechts sporadisch voor langsheen continentale randen. De ontdekking van deze grote oesterbanken illustreert de rijke biodiversiteit van diepzee canyons en hun onderschatting als echte ecosysteem hotspots.

List of acronyms

AAIW	Antarctic Intermediate Water
AOM	Anaerobic oxidation of methane
AI	Atlantic Inflow Water
CAT	Computed axial tomography
CPD	Critical-point drying
CT	Computed tomography
CTD	Conductivity, temperature and depth
DIC	Dissolved inorganic carbon
DTM	Digital terrain model
EM	End-member
EMMA	End-member modelling algorithm
ENACW	Eastern North Atlantic Central Water
ENAW	Eastern North Atlantic Water
FDOM	Fluorescent dissolved organic matter
GAPS	Global acoustic positioning system
GIS	Geographic information system
GPS	Global positioning system
ICP-QMS	Inductively coupled plasma-quadrupole mass spectrometry
ICPMS	Inductively coupled plasma mass spectrometry
INS	Inertial Navigation System
IODP	Integrated Ocean Drilling Program
ISOM	Induced and supported organomineralisation
ISOW	Iceland-Scotland Overflow Water
LDW	Lower Deep Water
LSW	Labrador Sea Water
MC-ICPMS	Multi-collector inductively coupled plasma mass spectrometry
MIS	Marine isotope stage
ML	Mediterranean Lower Core
MOW	Mediterranean Outflow Water
MU	Mediterranean Upper Core
NACW	North Atlantic Central Water
NADW	North Atlantic Deep Water
NASW	North Atlantic Superficial Water
NSAL	Northern branch of the Saharan air layer
OFOP	Ocean Floor Observation Protocol
PDB	Pee Dee Belemnite
PDE	Pen Duick Escarpment

ROV	Remotely Operated Vehicle
RV	Research vessel
SAIW	Sub Antarctic Intermediate Water
SEM	Scanning electron microscopy
SI	International System of Units
SMTZ	Sulphate-methane transition zone
TIMS	Thermal ionisation mass spectrometry
TMS	Tethered Management System
TWT	Two-way travel time
USBL	Ultra Short Base Line
XRD	X-ray diffraction
XRF	X-ray fluorescence

Part 1

Introduction & methodology

Chapter 1

Introduction

1.1 Cold-water corals

1.1.1 General

In contrast to their tropical counterparts in warm, shallow seas, cold-water corals prefer cold, dark waters of the deep ocean, where no light penetrates. They belong to the phylum of the Cnidaria which is subdivided in five classes, namely the Anthozoa (true corals, sea anemones and sea pens), the Cubozoa (box jellies), the Hydrozoa (siphonophores, hydroids, fire corals and medusae), the Scyphozoa (jellyfish) and the Staurozoa (stalked jellyfish). Cold-water coral ecosystems are mainly formed by members of the class Anthozoa, namely the Scleractinia (stony corals), the Antipatharia (black corals) and the Octocorallia (true soft corals), and by members of the class Hydrozoa, namely the Stylasteridae (lace corals) (Freiwald et al., 2004; Roberts et al., 2009).

The most spectacular cold-water coral reefs are constructed by Scleractinia or stony corals. These corals lack the symbiotic light-dependant zooxanthellate algae, making it possible to survive at greater depths than the warm-water corals. They live fixed in place and are known as stony corals due to their hard calcareous skeleton ($CaCO_3$). Scleractinia are suspension feeders, using their adhesive tentacles for catching food, mainly plankton and dissolved organic matter. At present, about 1488 scleractinian coral species have been described (Roberts et al., 2009), of which 672 species belong to the non-symbiotic group (Cairns, 2001). Solitary as well as colonial corals exist but only a few of the latter ones can create extensive reef frameworks. These reefs can vary in size from small reef patches, about 1 m high and a few metres wide, up to large reefs, e.g. the Sula ridge which is 14 km long and 35 m high (Freiwald et al., 2002).

Fig. 1.1 *Pictures showing the two most important framework-building cold-water coral species observed in reefs along the NE Atlantic margin:* Lophelia pertusa *(left) and* Madrepora oculata *(right) (image courtesy: RCMG – Ghent University).*

The main framework-building species along the NE Atlantic continental margin are *Lophelia pertusa* (Linnaeus, 1758) and to a lesser extent *Madrepora oculata* (Linnaeus, 1758) (Fig. 1.1) (Freiwald et al., 2004; Le Danois, 1948; Rogers, 1999; Zibrowius, 1980). *L. pertusa* forms bush-like colonies which can create structures of several metres, which are built up by thousands of polyps (Freiwald et al., 2004). It is known as the white coral, although several colour variations with yellow, orange and red are observed. *M. oculata* is also a colonial coral with a zig-zag type of branching pattern; however, it is much more fragile than *L. pertusa*, which limits its framework-building capacity. For this reason, *M. oculata* is mostly found in association with *L. pertusa* (Freiwald et al., 2004). In general, the polyps of *M. oculata* are also smaller than the polyps of *L. pertusa*. The solitary coral *Desmophyllum dianthus* (Esper, 1794) and the yellow coral *Dendrophyllia cornigera* (Lamarck, 1816) are also often observed in cold-water coral reefs (Fig. 1.2) (Le Danois, 1948; Zibrowius, 1980). Linear growth rates of cold-water corals are estimated between 2 and 25 mm yr^{-1} (Freiwald, 2002; Sabatier et al., 2012).

Fig. 1.2 *Pictures showing the solitary coral* Desmophyllum dianthus *(left) and the yellow colonial coral* Dendrophyllia cornigera *(right) (sources: Woods Hole Oceanographic Institution and Yves Gladu).*

At present, human activity is a major threat for cold-water coral ecosystems, e.g. commercial bottom trawling, hydrocarbon exploration and production, cable and pipeline placement, and waste disposal. Bottom trawling can cause severe physical damage to the reefs, which will take several hundreds or thousands of years to recover. Additionally, it reduces the structural complexity, and thus the species diversity (Freiwald et al., 2004). Another very important threat is ocean acidification due to increasing CO_2 levels in the atmosphere. This will shallow the aragonite dissolution depth, especially at higher latitudes and in the deep sea.

1.1.2 Distribution

Cold-water corals are found all over the world: in fjords, along continental margins, and around submarine banks and seamounts (Freiwald et al., 2004). While warm-water corals are restricted to more tropical regions (between 30°N and 30°S), cold-water corals are observed throughout many of the world's oceans (Fig. 1.3). They are usually found below the photic zone in water depths between 200 and 1000 m, although the shallowest specimen of *L. pertusa* was found at 38 m water depth in the Trondheimsfjord (Norway) while the deepest one has been observed at 3383 m in the New England seamount chain (North Atlantic) (Freiwald et al., 2004).

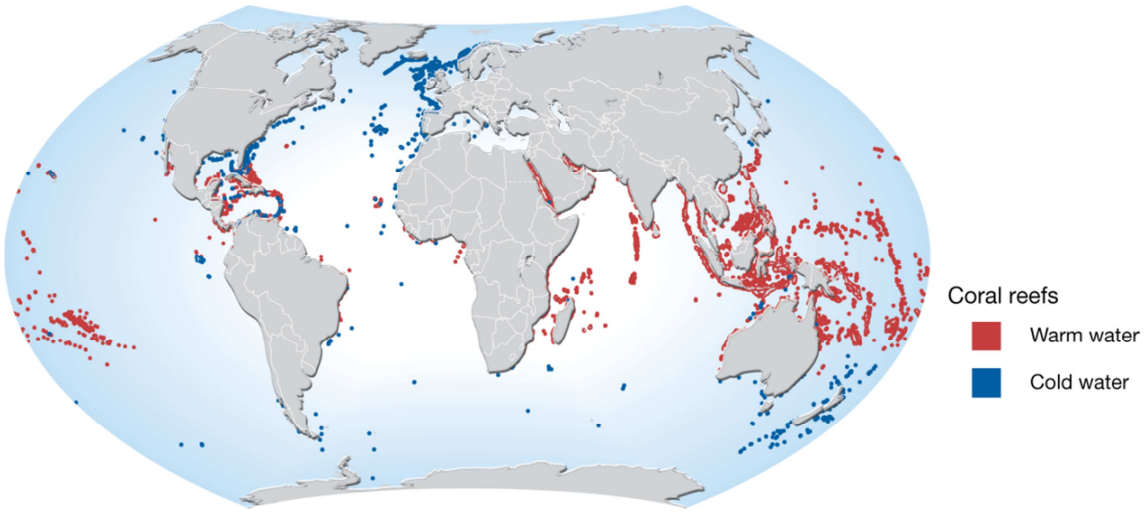

Fig. 1.3 *Distribution of cold-water and tropical coral reefs (source: UNEP/GRID-Arendal Maps and Graphics Library, February 2008, http://maps.grida.no/go/graphic/distribution-of-coldwater-and-tropical-coral-reefs).*

Both *L. pertusa* (Fig. 1.4) and *M. oculata* (Fig. 1.5) have a cosmopolitan distribution, although they have been found most frequently in the northeast Atlantic, e.g. off Norway (Fosså et al., 2005; Fosså et al., 2002; Freiwald et al., 1997; Freiwald et al., 1999; Hovland et al., 2005; Lindberg et al., 2007; Mortensen et al., 2001), in the Rockall Trough and on the Rockall Bank (Akhmetzhanov et al., 2003; de Haas et al., 2009; Kenyon et al., 2003; Masson et al., 2003; van Weering et al., 2003; Wienberg et al., 2008), in the Porcupine Seabight and on the Porcupine Bank (De Mol et al., 2007; De Mol et al., 2002; Dorschel et al., 2009; Eisele et al., 2008; Foubert et al., 2005; Huvenne et al., 2005; Huvenne et al., 2007; Rüggeberg et al., 2005), on the Hatton Bank (Roberts et al., 2008), in the Bay of Biscay (De Mol et al., 2011b; Reveillaud et al., 2008), on the Galicia Bank (Duineveld et al., 2004), in the Gulf of Cadiz (Foubert et al., 2008; Wienberg et al., 2009) and off Mauritania (Colman et al., 2005). *L. pertusa* is also observed in parts of the Mediterranean Sea (Freiwald et al., 2009; Taviani et al., 2005a; Taviani et al., 2009; Zibrowius, 1980), off Angola (Le Guilloux et al., 2009), in the Gulf of Mexico (Becker et al., 2009; Cordes et al., 2008; Schroeder, 2002), in the Caribbean Sea (Cairns, 1979; Grasmueck et al., 2006; Paull et al., 2000), off Brazil (Sumida et al., 2004) and in a few locations in the Indian and Pacific Oceans (Cairns, 1984; Etnoyer and Morgan,

2005; Matsumoto, 2005; Zibrowius, 1973). The northernmost occurrence of *L. pertusa* is reported from the south-western Barents Sea near Hjelmsøybank (Fosså et al., 2000) while the southernmost location is on the sub-Antarctic Macquarie Ridge off New Zealand (Cairns, 1982). *M. oculata* is, besides the NE Atlantic, most abundant in the Mediterranean Sea and in the western Atlantic. The northernmost location is found in the Andfjord in northern Norway (Zibrowius, 1980) and the southernmost in the sub-Antarctic Drake Passage (Cairns, 1982). *M. oculata* occur in water depths between 55 m and 2000 m (Zibrowius, 1980).

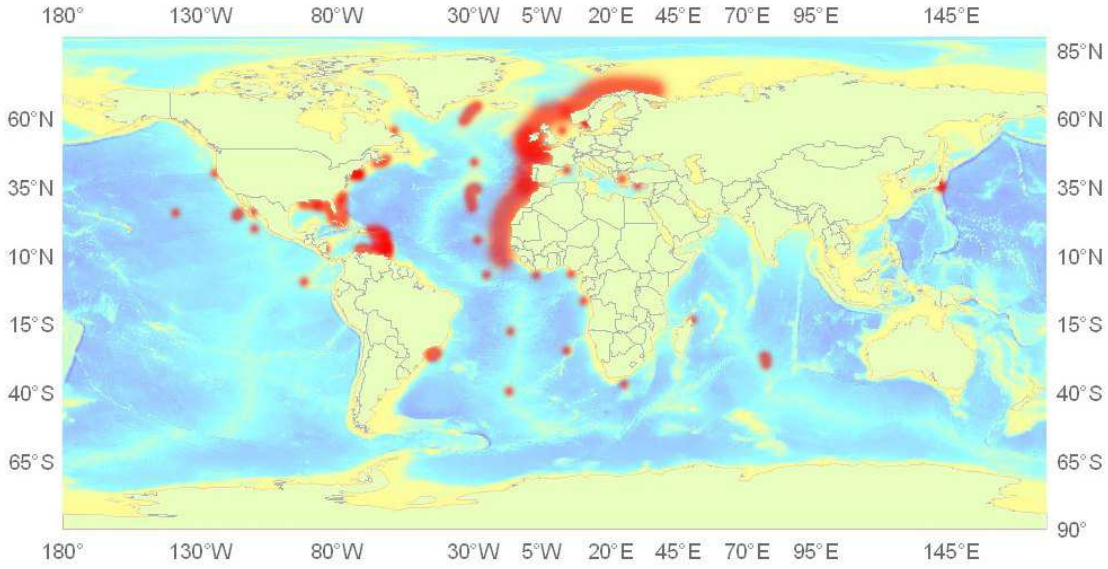

Fig. 1.4 *Distribution of* Lophelia pertusa *(after Freiwald et al., 2004; source: http://www.lophelia.org).*

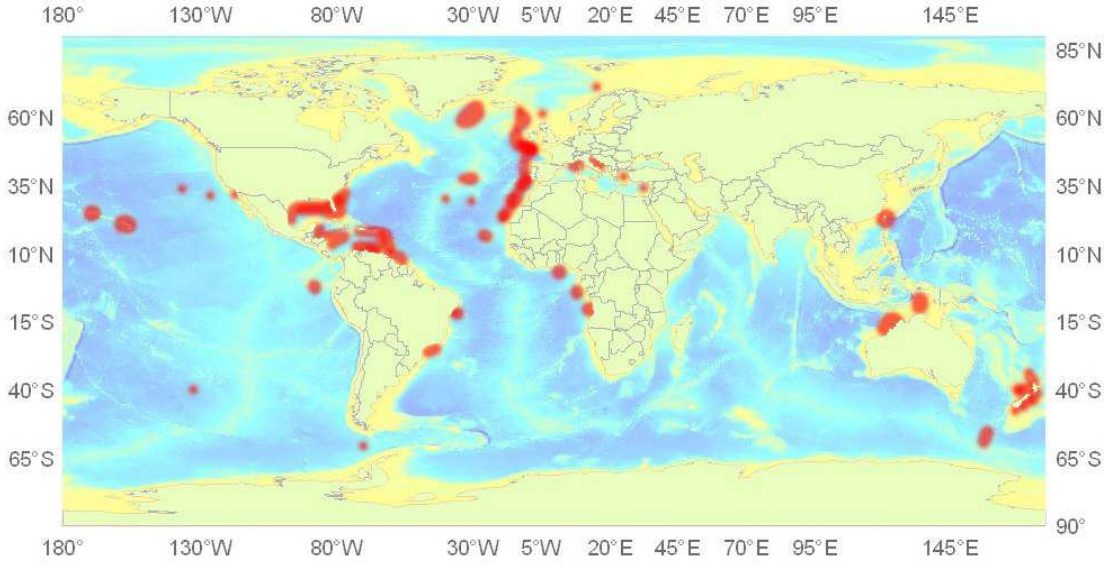

Fig. 1.5 *Distribution of* Madrepora oculata *(after Freiwald et al., 2004; source: http://www.lophelia.org).*

1.1.3 Environmental conditions

Cold-water corals need a hard substrate to settle on, like boulders, moraine ridges, oceanic banks, seamounts, sedimentary mounds and occasionally artificial substrates (e.g. wrecks and oil rigs) (Freiwald et al., 2004; Rogers, 1999). They prefer temperatures of 4-13 °C (Freiwald, 2002), a salinity varying between 32 and 38.8 ‰ (Strømgren, 1971; Taviani et al., 2005b) and dissolved oxygen values of 4.3-7.2 ml l^{-1} (Davies et al., 2008), although some examples have been found outside these limits. Recently, Dullo et al. (2008) showed the importance of a density envelope for living *Lophelia* reefs of sigma-theta σ_θ = 27.35 to 27.65 kg m^{-3}, which is determined by the salinity and temperature at a pressure of one atmosphere. Cold-water corals feed on zooplankton and suspended particulate organic matter provided by strong topographically guided bottom currents, which additionally prevent the deposition of sediments (Frederiksen et al., 1992; Freiwald, 2002; Kiriakoulakis et al., 2004; White et al., 2005).

1.1.4 Biodiversity

Cold-water corals are complex habitats providing hard bottom substrate, refuge and nursery areas for a highly diverse assemblage of deep-sea species. Although the cold-water coral associated fauna is still poorly studied it is thought to be much more diverse than the one found in bare seafloor sediments (Henry and Roberts, 2007). Existing information on biodiversity of cold-water coral reefs results from visual surveys of the megafauna based on video images and the identification of macrofauna species present in samples of the coral framework, debris and surrounding sediments.

Living corals are protected on the outside by a mucus layer. Mucus free parts of the coral skeleton and coral debris on the other hand are especially vulnerable to the attachment of a variety of invertebrates like other anthozoans, hydrozoans, crinoids, sponges, bryozoans, molluscs and brachiopods (Beuck and Freiwald, 2005). The physical structure of the corals is also the habitat of more mobile species, mostly crustaceans, polychaetes, gastropods and echinoderms. Studies of species diversity in samples from reef habitats show high diversity associated with the coral framework (e.g. Jensen and Frederiksen, 1992) and some evidence of characteristic reef species (e.g. Freiwald and Schonfeld, 1996; Henry and Roberts, 2007) but the endemicity is usually low. Already 1300 species have been recorded with *Lophelia pertusa* reefs in the northeast Atlantic (Roberts et al., 2006). Also on a smaller scale, cold-water coral habitats have an important influence on meiofaunal biodiversity (Raes and Vanreusel, 2006).

1.2 Cold-water coral mounds

1.2.1 General

A cold-water coral mound is a topographic structure that has accumulated through successive periods of reef development, sedimentation and (bio)erosion and that owes its origin to the framework-building capacity of cold-water corals (Freiwald, 2002; Roberts et al., 2006). Coral mounds vary in shape and size, reflecting different stages of development and morphological responses to environmental controls on growth processes (Roberts et al., 2009). They can range from small features of a few metres high and tens of metres across (e.g. Moira Mounds in the Porcupine Seabight) up to giant mounds of hundreds of metres high and a few kilometres across (e.g. Logachev Mounds on the southeastern slope of the Rockall Bank). Mounds tend to cluster in mound provinces where specific environmental conditions favour coral growth (Roberts et al., 2006). Cold-water coral mounds can be covered with a thriving cold-water coral community (e.g. Thérèse Mound and Galway Mound in the Porcupine Seabight), although most mound tops and flanks are covered by dead coral rubble (De Mol et al., 2002). Some mound provinces may even be entirely buried by sediment, e.g. the Magellan mounds in the Porcupine Basin (Huvenne et al., 2003).

1.2.2 Distribution

The knowledge about the distribution of cold-water coral mounds is limited and biased by mainly Atlantic mound research (Roberts et al., 2009). In the Atlantic Ocean, coral mounds are observed along the upper and mid-slopes of the continental margins, e.g. in the Porcupine Seabight (De Mol et al., 2002; Hovland et al., 1994; Huvenne et al., 2007; Huvenne et al., 2003; Van Rooij et al., 2003), in the Rockall Trough (Akhmetzhanov et al., 2003; Huvenne et al., 2009; Kenyon et al., 2003; Masson et al., 2003; Mienis et al., 2006; O'Reilly et al., 2003; van Weering et al., 2003; Wheeler et al., 2008), in the Mediterranean Sea (Comas and Pinheiro, 2007), in the Gulf of Cadiz (Foubert et al., 2008; Van Rensbergen et al., 2005; Wienberg et al., 2009), along the Mauritanian margin (Colman et al., 2005; Eisele et al., 2011), in the Florida-Hatteras Strait (Grasmueck et al., 2006; Paull et al., 2000); and on the flanks of larger oceanic banks, e.g. on the Chatham Rise, on West African seamounts, on the Hatton (Roberts et al., 2008), Rockall (Wienberg et al., 2008) and Porcupine Banks (De Mol et al., 2002). The combination of water masses with the appropriate temperature range and sites with strong currents and high food supply make continental margins ideal locations for repeated cold-water coral reef growth (Freiwald, 2002; Kenyon et al., 2003). Additionally, internal tides and waves along these continental margins may supply food particles to the corals (Roberts et al., 2009). The best studied mounds are located in the Porcupine Seabight (e.g. Magellan, Hovland and Belgica mound provinces) and the Rockall Trough region (e.g. Pelagia, Logachev and Darwin mound provinces).

1.2.3 Mound formation

Two hypotheses have been proposed the past years to explain the presence of large mound clusters along continental margins. The first hypothesis relates the presence of coral reefs to light hydrocarbon seepage (Henriet et al., 1998; Hovland, 1990; Hovland et al., 1994). In this case, deep-seated faults act as conduits for the seepage of hydrocarbons. Once at the seafloor, these hydrocarbons attract microbial communities and nutrients which are beneficial for coral growth or form a lithified layer which creates a suitable substrate for coral settlement. Although cold-water corals have been observed in the vicinity of cold seeps and near fault zones (Henriet et al., 1998; Hovland et al., 1998; Hovland and Risk, 2003; Masson et al., 2003; Sumida et al., 2004), no direct relationship with hydrocarbons have been found yet (Masson et al., 2003; Mienis et al., 2007; Williams et al., 2006). The second hypothesis links the presence of cold-water corals and the formation of coral mounds to external environmental conditions, such as temperature, salinity, the presence of hard substrate and locally enhanced current regimes (De Mol et al., 2005; Dorschel et al., 2005; Foubert et al., 2007; Freiwald, 2002; Rüggeberg et al., 2007; White et al., 2005). In order to explain initial mound growth, this last hypothesis (external environmental conditons) is mostly preferred, although, hydrocarbon seepage cannot be excluded in some cases.

The first step in mound building (Fig. 1.6) is the colonisation of a hard substrate by the coral larvae, which will grow out to coral colonies. At the base of these colonies, mechanical erosion and bio-erosion create dead coral debris, which will provide new settling grounds for a new generation of corals. If coral growth exceeds the burial of the framework, by trapping sediment, mound growth will be initiated (Kenyon et al., 2003; Roberts et al., 2006). After this initial phase, coral mounds start to grow with relatively high vertical and horizontal growth rates, often from multiple nucleation sites. Consequently, high sediment accumulation rates can be expected compared with off-mound areas, varying between 0.067-0.5 mm yr^{-1} southwest of Ireland (Frank et al., 2005; Dorschel et al., 2007b; Kano et al., 2007) to 4.3-5 mm yr^{-1} for the Norwegian reefs (Lindberg et al., 2007).

When the external conditions change, cold-water coral reef growth decreases and can even disappear. The most dramatic changes occur when there is a shift from interglacial to glacial conditions as this reduces the water temperature and the current speed but increases the sediment supply. The cold-water coral reefs continue to collect sediment until they are completely buried and transformed into a fossil reef. When the conditions become again more suitable for coral growth (e.g. during an interglacial period), a new generation of corals can grow on top of these fossil reefs, building up a coral mound structure (Roberts et al., 2009). Several changes between cold and warm periods have occurred during the past 3.5 Ma in the northern hemisphere (Bartoli et al., 2005). Subsequently, most coral mounds represent several coral reef sequences which provide internal stability to the mound.

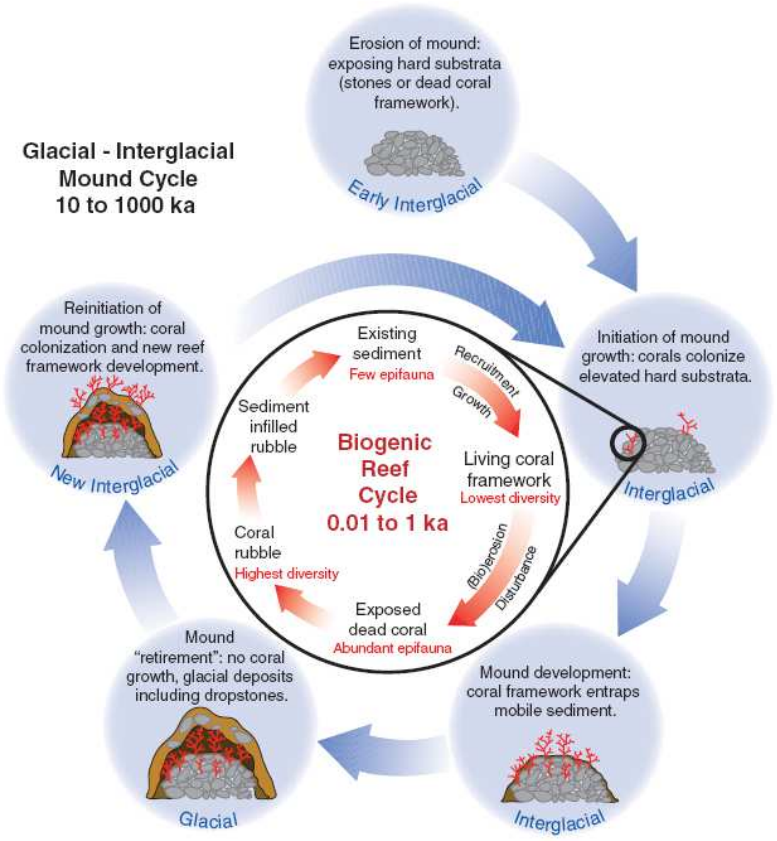

Fig. 1.6 *Schematic illustration showing the cyclic stages of carbonate mound growth (outer circle) and the biogenic reef cycle (inner circle) (Roberts et al., 2006).*

1.2.4 Diagenesis

Most cold-water coral mounds are influenced by diagenetic processes (e.g. Pirlet et al., 2010; Pirlet et al., 2011; Van der Land et al., 2010; Wehrmann et al., 2011). The term diagenesis encompasses all the processes which affect the sediments after deposition until the realms of incipient metamorphism at elevated temperatures and pressures (Pirlet, 2010). The first step is mostly sediment compaction which reduces the porosity and may result in the crushing or breaking of little bioclasts (Noé et al., 2006). Next, cementation can occur with sometimes even the formation of hardgrounds. The degree of cementation depends on the sediment composition and the near-seabed current velocity (Noé et al., 2006). In such conditions, scleractinian corals are generally dissolved, leaving moldic pores. More subtle processes can also have an impact such as the development of microporosity and changes in trace element and isotopic signatures (Tucker and Wright, 1990). The main driver for carbonate diagenesis in the surficial, marine environment is the microbial degradation of organic matter (Pirlet, 2010 and references therein). The biogeochemical processes associated with organic matter mineralisation affect the alkalinity and pH of the interstitial water and therefore steer carbonate dissolution and precipitation (Soetaert et al., 2007).

1.3 Oysters

Oysters can be found all over the world in marine or brackish habitats, generally in sheltered places. The various species have managed to adapt themselves to the different environments and biotopes of the world. However, salt is quasi-indispensable for oysters. Oysters are filter feeders, eating suspended plankton and particles. During feeding, they relax their single adductor muscle, allowing the two valves of the shell to open slightly. By pumping water through their bodies, gill cilia trap particles and funnel them towards the palps on which particles are sorted. Some particles, such as microalgae, are sent into the mouth; others, such as sediment, are usually rejected. They belong to the class of the Bivalvia in the phylum Mollusca. Oysters differ from other bivalves in having a highly irregular shell form, typically dictated by environmental constraints.

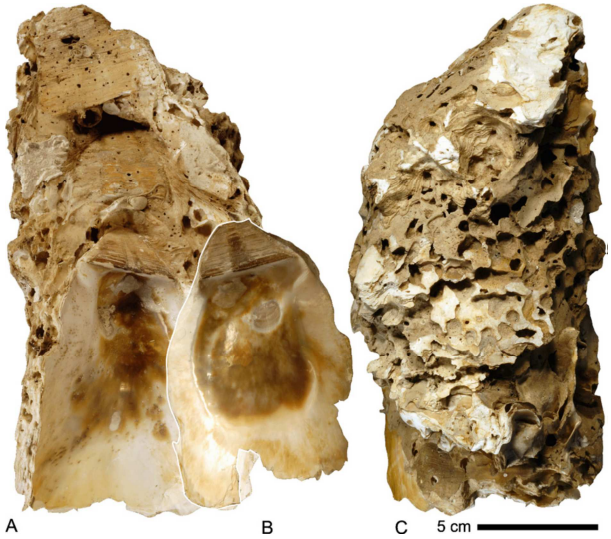

Fig. 1.7 *Stack of three* Neopycnodonte zibrowii*, close to 500 m water depth, Faial Channel (Azores): (A, B) interior of both valves and (C) exterior with distinct traces of boring hadromerid sponges (Wisshak et al., 2009a).*

Within this study, only the recently described deep-sea oyster *Neopycnodonte zibrowii* (Gofas, Salas and Taviani, 2009) will be discussed (Fig. 1.7). This species belongs to the superfamily Ostreoidea (Rafinesque, 1815) and the family of the Gryphaeidae (Vyalov, 1936). It has been first described by Wisshak et al. (2009a) from the Azores Archipelago where it thrives in water depths of 420 to > 500 m. They prefer vertical cliffs and underneath overhangs where they are encountered in clusters of up to several hundred individuals. The shell is relatively large (up to 20 cm), irregular in shape and inequivalve (left attached valve larger). It is characterised by a very unusual hinge line morphology: straight without a bulge of the resilium. They often grow on top of each other, in the same orientation, forming stacks that resemble dish piles. This is an effective way to optimise shell stability and size versus biomineralisation effort. The exterior of the oysters is often heavily bioeroded by microborers such as fungi and bacteria, as well as macroboring biota. Individuals reach an impressive lifespan in the order of several centuries, placing them among the longest-lived

molluscs known to date. Unlike short-lived, shallow-water oysters, *N. zibrowii* thrives under very stable environmental conditions with respect to temperature and salinity (Wisshak et al., 2009a).

1.4 Scope and framework

The discovery of large cold-water coral mound provinces along the European continental margin belongs to one of the most spectacular discoveries of the past decade (Henriet et al., 1998; Hovland et al., 1994; Kenyon et al., 2003; van Weering et al., 2003). Since then, these up to 350 m high hills became a hot topic within deep-water research resulting in many multidisciplinary studies (e.g. sedimentological, (micro)biological, palaeontological, geophysical, biochemical). At present, more than one thousand mounds have already been identified within different mound provinces along the European continental margin (Dorschel et al., 2005; Foubert et al., 2008; Foubert et al., 2007; Huvenne et al., 2007; Masson et al., 2003; Mienis et al., 2006; Wheeler et al., 2007; Wienberg et al., 2009). In 2005, IODP Expedition Leg 307 'Modern Carbonate Mounds: Porcupine Drilling' drilled for the first time through a coral mound (Challenger Mound, Porcupine Seabight) to unveil the origin and depositional processes within this sedimentary structure (IODP 307 Expedition Scientists, 2005). Although a few problems were tackled within this multidisciplinary study, a lot of questions still remain unanswered.

Two overarching questions have steered the present study:

- to what extent is the mound model, derived from the Irish margin studies and in particular from drilling Challenger Mound, truly representative for the recent mound phenomenon in the Atlantic realm,
- considering the generally inferred role of the MOW in the genesis and development of the cold-water coral mounds in Porcupine Basin, are carbonate mound provinces recurrent all along the track of the MOW from Gibraltar to Porcupine Seabight, or not?

Regarding the first question, there is a need for global studies to get a more general idea of mound growth and their trigger mechanisms. The recently discovered cold-water coral mounds along the Moroccan margin (Gulf of Cadiz) offered a prime opportunity to study the formation and development of coral mounds in a strongly contrasting setting. These mounds, much smaller than those on the Irish margin, might be considered to be in an initial stage of mound growth, which allows reconstructing a model for the early development of coral mounds. Additionally, the interpretation of the Morocco mounds as pristine juvenile mounds forms the rationale for a first attempt to approach the 3D architecture of a cold-water coral mound by combining visual observation techniques over the whole mound surface (2D) with sediment core analyses (the third dimension). In the senescent mounds of Porcupine Seabight, already partly in the burial stage, such areal analysis makes little sense

to approach the genuine 3D architecture of a mound, as the surface facies likely is no longer related to the mound growth phase. This 3D approach moreover allows to define more precisely locations for ground truthing by drilling, which is planned in the near future using the MeBo drill rig (MARUM – Germany).

A short overview of the different methodologies used during this research is given in chapter 2. Chapter 3 presents a detailed study of the present distribution of fossil cold-water corals on the Pen Duick Escarpment, and the growth and distribution of these corals in the past based on ROV observations and boxcore data. This distribution pattern will be compared with other mound areas such as the Porcupine Seabight and the margins of the Rockall Trough. Additionally, the role of cold-water coral rubble fields and the presence of carbonate slabs will be discussed. Based on these results, sediment cores were taken in three mounds, namely Alpha, Beta and Gamma Mound, on board the R/V Marion Dufresne in 2008. Chapter 4 shows a detailed study of these sediment cores using different techniques, e.g. X-ray computed tomography, magnetic susceptibility, X-ray fluorescence, grain-size analysis, end-member modelling, stable isotope analysis and U/Th dating. First, different CT facies were delineated and the amount of coral fragments was calculated. This allows to obtain more information about the internal structure of the mounds in three dimensions and the diagenetic processes. Next, different sediment contributors will be defined based on the end-member modelling analysis and linked with climate changes on the NW African continent. Finally, a model for the genesis and build-up of the cold-water coral mounds along the Moroccan margin is presented. This model will be compared with the existing models for the build-up of coral mounds SW of Ireland and along the Mauritanian margin.

To address the second question, there was no need for further surveying the European margin along the MOW track between Gibraltar and Galicia Bank, considering the density of observations already available. On these South and West Iberian margins, no significant mound province had been reported. The Renard Centre of Marine Geology (RCMG) hence focused on the Bay of Biscay margins in a sequence of cruises with R/V Belgica, which yearly alternated with cruises to the Morocco margin. Based on historical information (Le Danois, 1948), key areas were selected for detailed investigations. Multibeam and seismic mapping in combination with hydrologically steered ROV observations revealed large cold-water coral and oyster ecosystems within canyons along the French continental margin.

Chapter 5 is dedicated to the presence of cold-water corals in the Penmarc'h and Guilvinec Canyons in order to better understand their significance, distribution and environmental conditions. Chapter 6 presents the physical and oceanographic setting of the northern most and deepest occurrence of the *Neopycnodonte zibrowii* oysters

along the La Chapelle continental slope and within the Guilvinec Canyon. This will provide more insight in the habitat requirements of this recently described species.

Finally, chapter 7 summarises the conclusions of this thesis and will highlight some interesting future prospects in cold-water coral mound research.

1.5 Regional setting

1.5.1 Gulf of Cadiz

The Gulf of Cadiz is located west of the Strait of Gibraltar and is enclosed by the Iberian Peninsula and the Atlantic continental margin of Morocco (Fig. 1.8A). Water depths are varying between 200 m at the shelf edge and more than 4 km at the abyssal plain. The Gulf of Cadiz has a very complex geological setting due to the underlying boundary between the African and Eurasian plates and the westward motion of the Betic-Rifean Arc (Maldonado et al., 1999; Medialdea et al., 2009; Medialdea et al., 2004; Zitellini, 2009). The tectonic evolution of the Gulf of Cadiz comprises several phases of extension, convergence and strike-slip motions, starting with the European-African plate convergence from the Mid-Oligocene up to Late Miocene times (Maldonado et al., 1999; Medialdea et al., 2004). After culmination of compression in the Late Miocene, convergence along a NW-SE direction continued at slower rate until present. The westward drift of the front of the Gibraltar Arc during the Middle Miocene resulted in the development of an accretionary wedge. Due to increased subsidence during the Late Miocene, the Allochthonous Unit of the Gulf of Cadiz (olistostrome complex) was formed (Maldonado et al., 1999; Medialdea et al., 2004). This unit is covered with 0.2 to 2 km of Neogene sediments pierced by mud volcanoes, salt diapirs and fluid escape features (Medialdea et al., 2004; Somoza et al., 2003).

The study area, the Pen Duick Mound Province, is located 35 km offshore the north-western Moroccan margin (Fig. 1.8B) (Van Rensbergen et al., 2005). Extensional tectonics breaking up the Neogene sedimentary series in the subsurface resulted in topographic ridges bounded by fault escarpments (Flinch, 1993). One of these is the Pen Duick Escarpment (PDE), a steep fault escarpment that bounds the NW-SE oriented Renard Ridge toward the SW. The escarpment is a 6 km long, SSE-NNW oriented, 80 to 125 m high cliff with a southwest-facing slope of 8° to 12° (Van Rooij et al., 2011). 15 mounds were recognised on top of the escarpment (Foubert et al., 2008). This study will focus on three of these mounds: Alpha, Beta and Gamma Mound. Alpha and Beta Mound are located on the SE part of the escarpment, while Gamma Mound is located on the NW part. Alpha Mound is a 400 m long by 230 m wide NNW-SSE elongated mound with a maximum height of 30 m. The top of Alpha Mound is located in a water depth of 530 m. Beta Mound is a N-S elongated mound up to 40 m high, 450 m long to 280 m wide, and has two summits. The northernmost summit is located in a water depth of 520 m, the southernmost summit in a water depth of 515 m.

Gamma Mound has a more circular shape and is only 15 m high, 180 m wide and has a maximum length of 250 m. In addition, a small unnamed mound SE of Gamma Mound, with a diameter of 150 m and a height of 15 m, will be discussed.

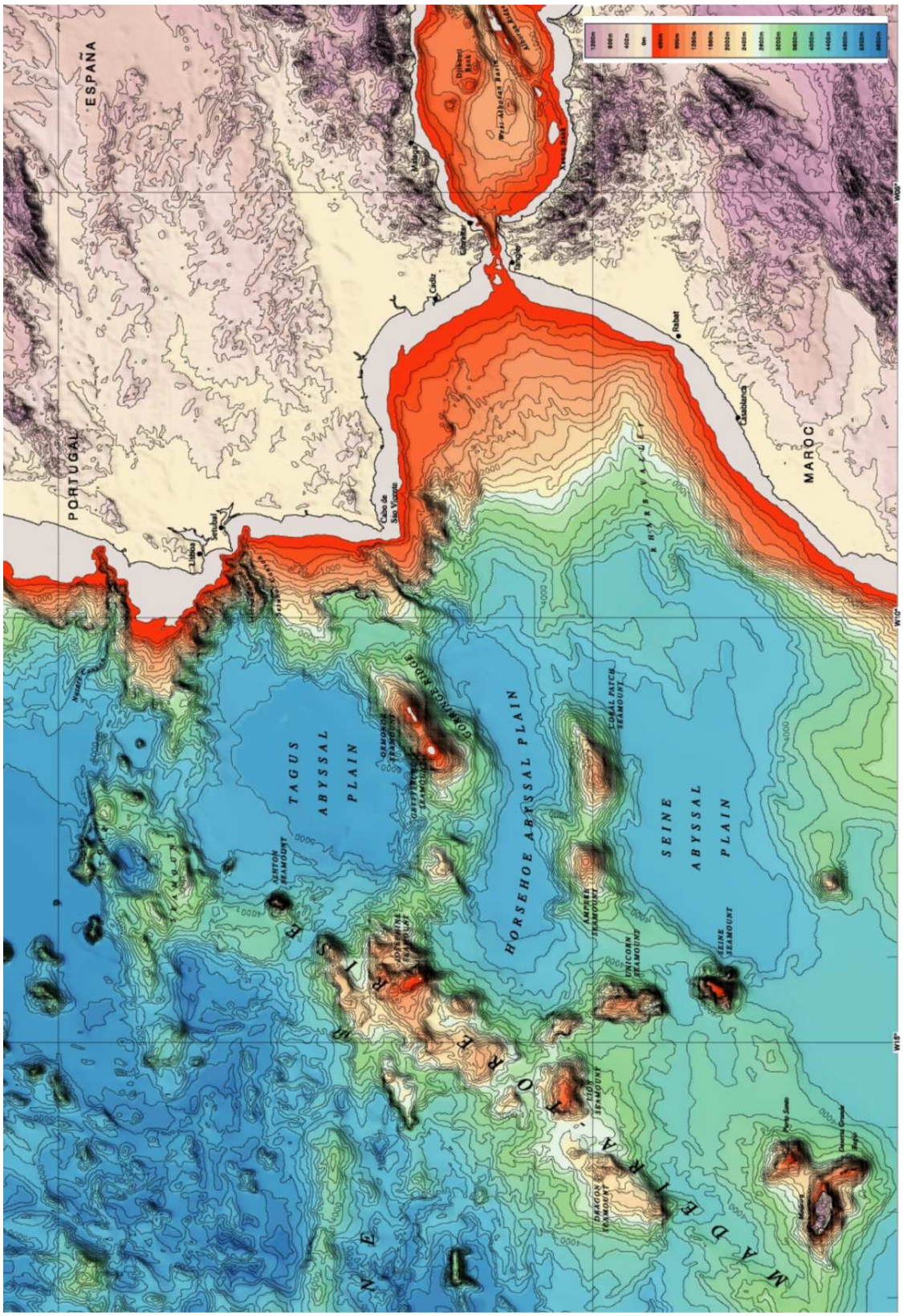

Fig. 1.8 *Bathymetric map of the Gulf of Cadiz (Sibuet et al., 2004).*

The hydrographic setting of the Gulf of Cadiz is controlled by the exchange of the Atlantic Inflow Water (AI) and the Mediterranean Outflow Water (MOW) through the Strait of Gibraltar (Hernández-Molina et al., 2006; Machin et al., 2006; Villanueva and Gutierrezmas, 1994). The AI is composed of the North Atlantic Superficial Water (NASW) down to 100 m and the North Atlantic Central Water (NACW) between 100 and 600 m water depth (Caralp, 1988; McCartney and Talley, 1982). The lower boundary of the NACW is characterised by a salinity minimum, which can be recognised in water depths of 300 m near the Strait of Gibraltar and 600 m in the rest of the Gulf of Cadiz (Machin et al., 2006). Below the NACW, the low-salinity Antarctic Intermediate Water (AAIW) and the high-salinity MOW are present until a water depth of 1500 m. After leaving the Strait of Gibraltar, the MOW splits into a Mediterranean Upper Core (MU), which flows north along the Spanish and Portuguese continental margins, and a Mediterranean Lower Core (ML), which follows a westward path with a small southern branch (Hernández-Molina et al., 2006; van Aken, 2000).

The temperature and salinity values around PDE correspond with the NACW, although below 600 m a decrease in temperature and a salinity minimum indicate the presence of the AAIW (Van Rooij et al., 2011). On top of the Renard Ridge, a temperature range of 10.7-11.8 °C, a salinity range of 35.56-35.65 and a potential density range of 27.15-27.25 kg m^{-3} are observed (Mienis et al., 2012). A semi-diurnal tidal cycle is observed with an average current speed of 8.8 cm s^{-1} with peaks up to 30 cm s^{-1}. At the plain below the escarpment the average current speed varies around 8 cm s^{-1} with peak current speeds up to 24 cm s^{-1} (Mienis et al., 2012; Van Rooij et al., 2011). The strongest currents (above 15 cm s^{-1}) have a NNE direction while the currents below 5 cm s^{-1} are directed to the NW. The residual currents have a NE direction (Mienis et al., 2012).

1.5.2 Bay of Biscay

The continental margin in the Bay of Biscay can be subdivided in five main geographic areas: the Celtic margin and Armorican margin in the north, and the Aquitaine margin, Cantabrian margin and Galician margin in the south (Fig. 1.9). The Armorican margin has an orientation of 140° with a relatively broad continental shelf, is up to 200 km wide, and has a steep slope with an average gradient between 2.86° and 5.15° (Lallemand and Sibuet, 1986; Le Suavé et al., 2000). The slope extends from a water depth of 200 m down to 4000 m. The morphology of the continental slope is characterised by spurs and canyons, organised in submarine drainage basins and feeding deep-sea fans during glacial times (Bourillet and Lericolais, 2003; Bourillet et al., 2003; Zaragosi et al., 2000).

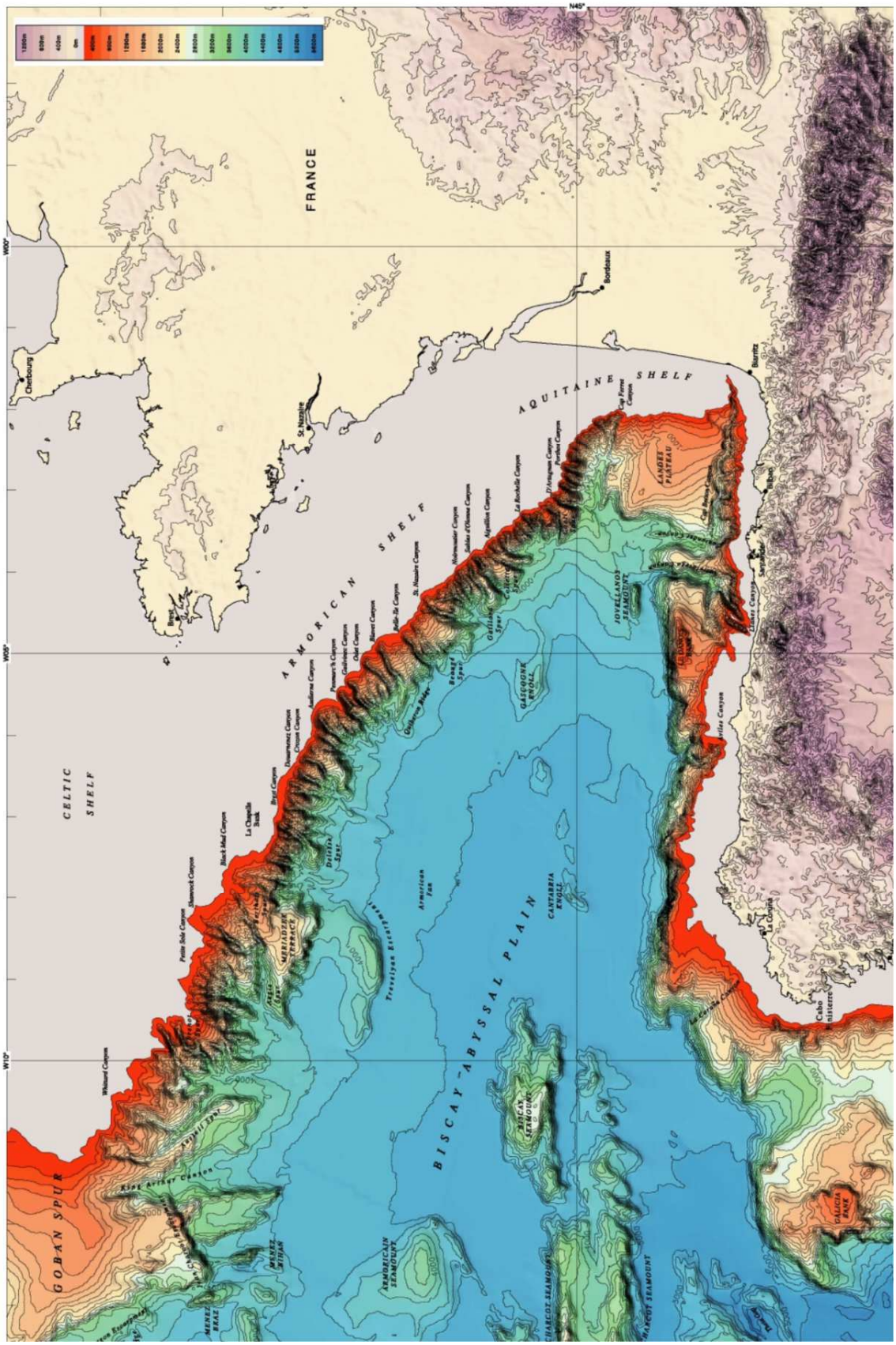

Fig. 1.9 *Bathymetric map of the Bay of Biscay (Sibuet et al., 2004).*

The water column stratification in the Bay of Biscay predominantly shows that water masses are of North Atlantic origin (Pollard et al., 1996). The uppermost water mass is the Eastern North Atlantic Central Water (ENACW) which extends down to water depths of 400-600 m. The ENACW is characterised by a cyclonic gyre with an average velocity of 4 $cm.s^{-1}$ (Pingree and Le Cann, 1989). Below a minimal density layer around 500 m water depth, corresponding to the lateral influence of the Sub Antarctic Intermediate Water (SAIW), the Mediterranean Outflow Water (MOW) is observed down to 1500 m water depth. Its circulation as a contour current is conditioned by seafloor irregularities and the Coriolis effect. MOW velocities have been measured in the Bay of Biscay at 8°W and 6°W with average values of 2-3 $cm\ s^{-1}$ (Pingree and Le Cann, 1989). Low salinity values observed on the Armorican continental slope may reflect a depletion of the MOW core (Van Aken, 2000). Between 1500 and 3000 m water depth, the North Atlantic Deep Water (NADW) is observed. It includes a core of Labrador Sea Water (LSW), recognised by a salinity minimum at 1800 to 2000 m, and the Iceland-Scotland Overflow Water (ISOW) which is identified by a small salinity maximum around 2600 m (González-Pola, 2006; McCartney, 1992; McCave et al., 2001; Pingree, 1973). Below the NADW, the Lower Deep Water (LDW) is identified (McCartney, 1992). A cyclonic recirculation cell over the Biscay Abyssal Plain is recognised with a characteristic poleward velocity near the continental margin of 1.2 (± 1.0) $cm.s^{-1}$ (Dickson et al., 1985; Paillet and Mercier, 1997).

Along the slopes of the Bay of Biscay strong, localised internal tides are reported, due to a combination of favourable water mass stratification, steep topography and strong barotrophic tidal currents (Huthnance, 1995; Pingree and Le Cann, 1989, 1990). These may be channelled and result in regions of locally increased flow, with mean values of about 14 cm/s or higher, and local circulations (Pingree and Le Cann, 1990). Internal tides are proposed to explain the enhanced levels of surface phytoplankton abundance (Holligan et al., 1985; Pingree and Griffiths, 1982).

Chapter 2

Methodology

2.1 Introduction

This chapter will give a short introduction to the various methodologies and techniques that were used throughout this research. The overview in this chapter is only limited to a description of the instrument and the basic principles. In the following research chapters, the specific material and methods sections give more insight in the detailed methods and available metadata used for each chapter, the sampling procedure and parameters and the sample processing. The research questions have been tackled using two different methodologies. On one hand video data has been analysed in order to visually investigate the seafloor while on the other hand a detailed analysis of sediment cores (e.g. boxcores and gravity cores) has been performed in order to have a look at the subseafloor.

2.2 Video data

2.2.1 ROV Genesis

In 2005, the Renard Centre of Marine Geology (RCMG) acquired a Remotely Operated Vehicle (ROV) called “Genesis”. It is a Sub-Atlantic Cherokee-type ROV with a Tethered Management System (TMS) and shipboard winch (Fig. 2.1). This winch hosts a reinforced cable of 1600 m which can bring the TMS and ROV to a safe depth prior to ROV launch, mostly 20-30 m above the seafloor. The ROV itself has a maximum tether of 200 m which can be controlled by the pilot in the ROV container. In total, five cameras and one still camera are installed on the ROV: one on the TMS (ROV launch & re-entry control), a backward looking camera within the ROV (for TMS re-entry and tether inspection), a camera on the ROV looking at the arm and tray, and two forward-looking black & white and colour cameras. An overlay on the screen with navigation control information can be added to any camera display. The ROV also contains a depth control, altimeter and forward-looking sonar for detection of seabed objects. The main sampling tool on the ROV is the controlled grab arm and a deployable tray in which samples can be stored. In addition, a CTD and a 5L Niskin bottle can be installed in order to know the water properties.

Positioning of the TMS and ROV is done through an IXSEA Global Acoustic Positioning System (GAPS). This GAPS system is a portable Ultra Short Base Line (USBL) system with integrated Inertial Navigation System (INS) and Global Positioning System (GPS). The GAPS is deployed at the side of the ship, about 1.5 m below the sea surface. Together with a transponder fixed on the TMS and one on the ROV, these components allow to visualise the position of the ship, TMS and ROV. Navigation data from the GAPS software is stored in raw format. During the deployments, the ship’s, TMS and ROV navigation is also recorded through the Ocean Floor Observation Protocol (OFOP) software (Huetten and Greinert, 2008).

During the ROV survey, the control is performed by the pilot, assisted by a co-pilot to navigate and a shipboard scientist to write down the observations and technical issues (Fig. 2.2). Propulsion of the ship remains diesel (rather than the diesel-electric option), which enables to handle the ship in a very controlled manner, even though dynamic positioning is not available on the R/V Belgica.

Fig. 2.1 *Picture of ROV Genesis.*

Fig. 2.2 *Picture of the control room.*

2.2.2 Processing & analysis

After the cruise the navigation data was edited to remove wrong data, smoothed to obtain an average track and splined for each second. Then the video was replayed and linked to the navigation file, based on date and time, in order to show all positions (ship, ROV and TMS) on a map. In a last step, detailed digitising of seafloor observations was made. Seafloor observation items were defined, based in first place on the different substrates and secondly on the different ecosystems.

Two different programs were used for processing and analysing the video data, namely ADELIE 1.8 (Ifremer) and OFOP 3.2.0c (J. Greinert). Both programs are post-processing tools for underwater vehicle data and actually give the same result, a facies interpretation map, although there are a few differences. ADELIE is developed especially for the Ifremer underwater vehicles (Nautile, ROV Victor 6000, Cyana, Scampi...) and is directly linked to a GIS system, namely ArcMap (ESRI). As ArcMap works with DBase files, it is necessary to transform the navigation files in the right format before they can be imported in ADELIE. On the other hand, OFOP works with ASCII-text files in order to allow maximum compatibility with other software. All the data can be easily imported into ArcGIS for further analysis.

2.3 Sediment cores

2.3.1 MD169 cruise

All gravity cores were obtained during the R/V Marion Dufresne 169 MiCROSYSTEMS cruise to the Gulf of Cadiz in July 2008 (Fig. 2.3) (Blamart et al., 2010; Van Rooij et al., 2011). This cruise was set out to investigate the objectives of the ESF EuroDIVERSITY MiCROSYSTEMS project (05_EDIV_FP083-MICROSYSTEMS), supplemented with additional shorter projects from European laboratories and institutes, as well as a small appendix to the previous MD168 AMOCINT cruise (Kissel et al., 2008).

The main objectives of the MD169 cruise were (1) biotope exploration and characterisation, and (2) microbial diversity census and evaluation of the functional link microbes-metazoans (Van Rooij *et al.*, 2008). The first objective focuses on the 3D spatial architecture and diversity of the microbial mound community and its possible role in slope stabilisation. In addition, present and past oceanic conditions were evaluated in combination with sedimentary dynamics variability in order to reveal the time frame of natural biodiversity changes. The second objective aims to investigate the microbial diversity census through biogeochemical approaches (biomarkers), molecular fingerprinting (DGGE, 16S rRNA), fluorescence in situ hybridization (FISH) and laboratory culture.

Fig. 2.3 *Picture of the R/V Marion Dufresne (left) and the gravity corer system (right).*

The coring sites were determined based on geophysical surveying (multibeam bathymetry and high-resolution reflection seismics) and ROV imagery obtained during the R/V Belgica CADIPOR III cruise in 2007. A total of five main site locations were identified: (1) Pen Duick mounds, (2) Conger cliff, (3) depression site at the foot of Pen Duick Escarpment, (4) palaeoceanographic reference sites, and (5) Mercator mud volcano. Every on-mound site was cored at least two times with one core for geochemistry and microbiology and a second core for sedimentology, palaeoceanography and chronostratigraphy. The on-mound sedimentology cores were cut in sections of 1.5 m and remained unopened.

2.3.2 X-ray computed tomography

X-ray computed tomography (CT) is a fast and non-destructive technique to obtain a 3D visualisation and characterisation of the sediment cores which allows to define different CT facies and quantify the amount of cold-water corals in the mounds. The first CT scanner, also known as the computed axial tomography (CAT) scanner, was built in the late 1960s and early 1970s by Cormack and Hounsfield (Hounsfield, 1973) based on the mathematical principle developed by Radon in the early 20th century (Radon, 1917). Basically a 3D object is reconstructed based on a set of 2D projections or radiographs taken from different angles by rotating the sample around a defined axis. CT was developed in medical sciences where it evolved from the traditional X-ray radiography. However, during the past decades it became clear that X-ray CT has a large potential for other applications, like geosciences: palaeontology, sedimentology, petrology, soil science and fluid-flow research (Cnudde et al., 2011; Cnudde et al., 2006).

The basic principle of all CT scanners is that the object is placed between an X-ray source and a detector (Fig. 2.4). The detector measures the attenuation (reduction in beam intensity) of the X-rays emitted by the source along multiple intersecting paths along the object. This X-ray transmission through an object is function of the composition, the density and the

thickness of the measured material. For each X-ray path, the total linear attenuation coefficient is the sum of the attenuation coefficients of each element in the path. The spatial resolution of the images depends on the magnification M (ratio of the distance between source and detector over the distance between source and sample), the focal spot size of the X-ray tube, the pixel size of the detector and physical phenomena like X-ray scattering and interaction between the detector pixels (Cnudde et al., 2006).

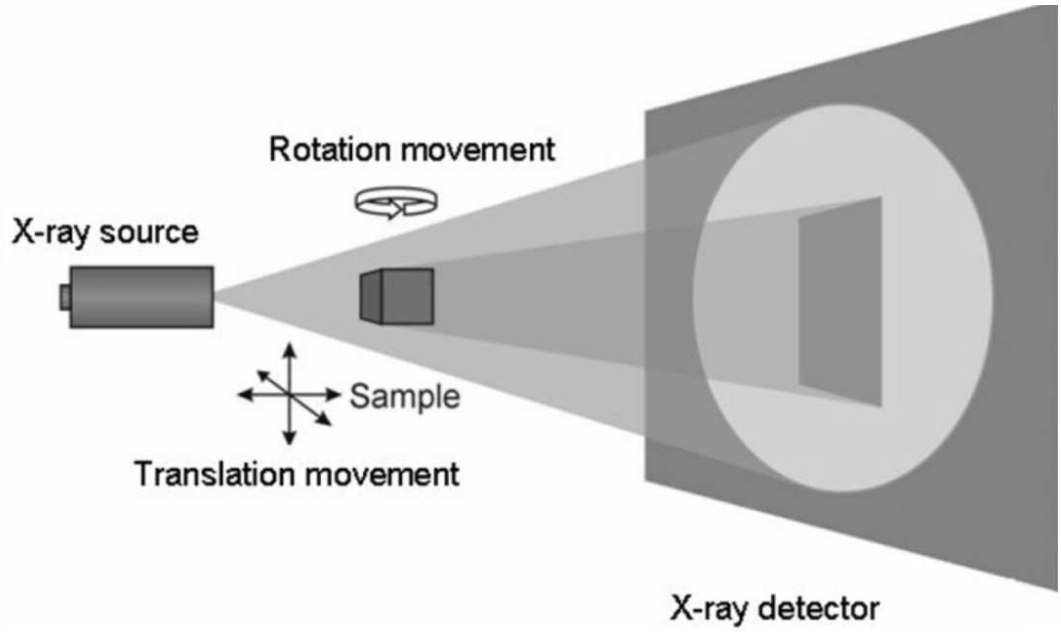

Fig. 2.4 *Schematic illustration of the basic set-up of an X-ray computed tomography scanner (courtesy UGCT, Ghent University, Belgium).*

Fig. 2.5 *Medical CT scanning of a sediment core at the Ghent University Hospital (Belgium).*

Medical CT scanners use a rotating detector-source system that revolves around the patient or object (Fig. 2.5). A helical scan path allows making full body CT-scans, with a spatial resolution up to 250 µm. The contrast and signal-to-noise-ratio of the CT slices is usually high due to the large and sensitive detector elements. Since the objects are positioned in the middle between source and detector, the magnification factor of the object is 2. These scanners are frequently applied to visualise the internal structure of rock material and in this case of unopened sediment cores from cold-water coral mounds. However, medical CT scanners are not optimised to study dense objects at high resolution. By using X-ray CT scanners with a small focal spot, higher resolutions can be obtained on small samples. In this case, micro-CT scanners (Fig. 2.6) can give a better solution with a spatial resolution down to 1 µm. These high-resolution images can give additional and more detailed information than the medical CT scans. One of the main differences with medical scanners is that for micro-CT the object is now placed on a rotation platform and the source-detector system remains at the same position. X-ray CT makes it possible to visualise the internal structure of complex objects, highlighting the difference in attenuation coefficients of the constituting elements. These attenuation coefficients are controlled by the density and the average atomic number of the scanned constituting elements. Medical CT scans were performed at the Ghent University Hospital (Belgium) in collaboration with Prof. Dr. P. Duyck. The micro-CT scans were carried out at the Centre for X-ray Tomography (UGCT, Ghent University, Belgium).

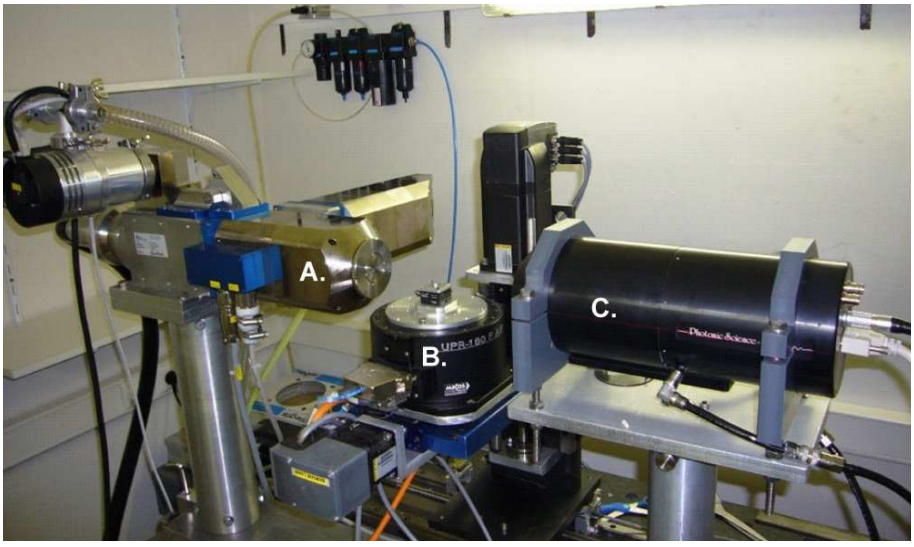

Fig. 2.6 *The set-up for micro-CT scanning at the Centre for X-ray Tomography (UGCT, Ghent University, Belgium) with (A) the X-ray source, (B) the sample on the rotation platform, and (C) the detector.*

Image reconstruction was performed using the Siemens software for the medical CT data and the Octopus software (UGCT, Ghent University, Belgium) for the micro-CT data. The interpretation of the obtained 3D CT data is an important challenge. For this interpretation visualisation alone is often not sufficient and quantitative 3D information is needed. The tomographic reconstruction process, which transforms a set of raw projections into a stack of cross-sections through the object providing a 3D volume for visualisation and analysis, is

very computer intensive. Processing and visualising of the images was carried out using the VGStudio MAX software package (Volume Graphics). This software allows to display the data in a 3D view as well as in three orthogonal slice image views. The data volume can be sliced in any required orientation to provide a detailed insight. For a detailed 3D analysis of the reconstructed volume Morpho+ (UGCT) can be used. It allows the determination of porosity and volume fraction, object identification, object parameterisation, object separation and visualisation.

2.3.3 XRF core logging

X-ray fluorescence (XRF) logging is a rapid and non-destructive technique in order to determine the chemical composition from aluminium to uranium of split sediment cores (Ca, Sr, Fe, Al, K, Ti, Si…). For example, the Ca/Fe ratio gives more insight in glacial/interglacial cycles while Fe/Al represents variations in the terrigeneous input. This technique was first developed at the Royal Netherlands Institute for Sea Research (NIOZ, Texel, The Netherlands) in 1988, resulting in a CORTEX scanner (Jansen et al., 1998) and later in an AVAATECH core scanner (Richter et al., 2006). It is based on the principle that the wavelength of emitted electromagnetic radiation is characteristic for each element and that the amplitude of the peak is proportional to the concentration (Fig. 2.7). This radiation is the result of a difference in energy between two shells due to the influence of incoming X-ray radiation, ejecting an electron from an inner shell and filling up the free space by an electron from an outer shell.

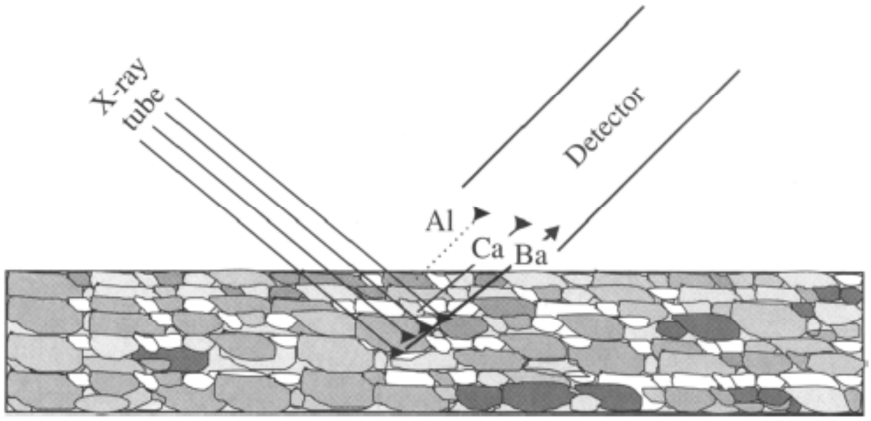

Fig. 2.7 *Simplified diagram showing the principle of XRF core logging (Richter et al., 2006).*

Both scanners have an identical instrument set-up (Richter et al., 2006). A prism is lowered onto the sediment surface with at one side the X-ray tube at an angle of 45° and on the other hand the detector, also installed at an angle of 45°. The variable optical system allows to determine independently the length (10 to 0.1 mm) and the width (15 to 2 mm) of the X-ray beam which optimises the measuring conditions and reduces the effects of e.g. bioturbation or laminations. The entire optical system is He-flushed for good light element

detection. Sample preparation includes flattening of the sediment surface to remove irregularities. Then, the sediment is covered with a thin foil highly transparent to X-rays to prevent the device being soiled and to prevent drying of the sample during long measurement times. A picture of the AVAATECH XRF core scanner used at the NIOZ is shown in figure 2.8.

Fig. 2.8 *Picture of the AVAATECH XRF core scanner at the Royal Netherlands Institute for Sea Research (NIOZ, Texel, The Netherlands).*

2.3.4 Magnetic susceptibility

The magnetic susceptibility determines the degree to which a material can be magnetised in an external magnetic field. It can be used as relative proxy for changes in sedimentary composition (e.g. diagenetic impact). Magnetic susceptibility, a dimensionless number, is reported in SI units with an accuracy typically of 5%.

The magnetic susceptibility of the sediment cores was determined at the Royal Netherlands Institute for Sea Research (NIOZ, Texel, The Netherlands) using a Bartington MS2E point sensor connected to the Bartington MS2 meter (Fig. 2.9). The MS2E sensor is designed to perform high resolution measurements along flat surfaces with a roughness less than 1 mm. The sensing surface is at the end of a ceramic tube, mounted on a metal enclosure which houses the electronic circuitry, and is protected by a thin aluminium oxide plate. The response area is 3.5 x 10.5 mm with a response depth of 50% at 1 mm and 10% at 3.5 mm. It operates at a frequency of 2 kHz. A complete measurement is accomplished in 1.3 seconds on 1.0 range. Temperature drift is less than $2 * 10^{-6}$ SI per 10 minutes after 5 minutes of

measurement. Susceptibility values in natural, marine sediment samples over an interval of only a few metres can range from a few tens to several thousands of 10^{-6} SI units.

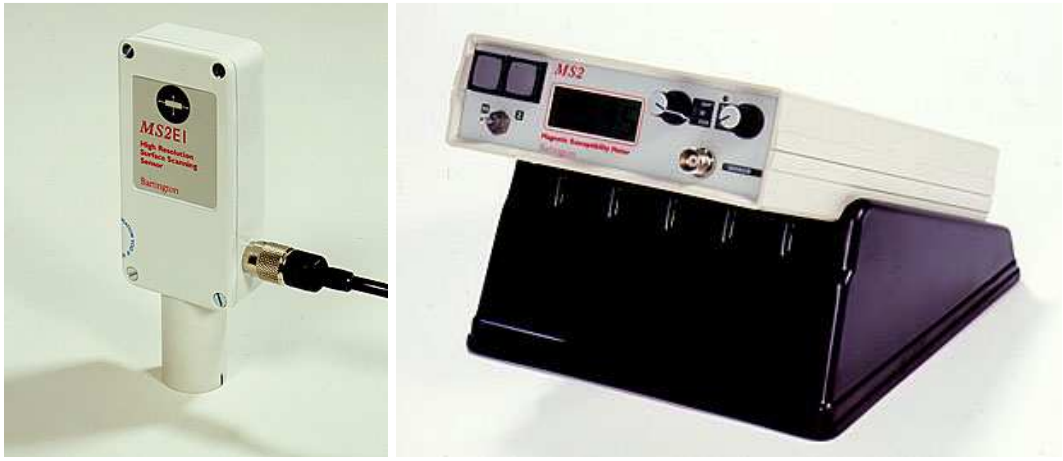

Fig. 2.9 *Picture of the Bartington MS2E sensor (left) and the MS2 meter (right).*

2.3.5 Grain-size analysis

Grain-size analysis allows to determine the mean grain-size, mode, skewness, kurtosis and sorting of a sediment sample. These analyses were performed using the Malvern Mastersizer 2000 of the Marine Biology Section (Ghent University, Belgium). This system measures particle sizes based on the technique of laser diffraction (Fig. 2.10). This technique is based on the principle that particles passing through a laser beam will scatter light at an angle that is directly related to their size. The diffraction angle is thereby assumed to be inversely related to the grain size. The observed scattering intensity is also dependent on particle sizes and diminishes, to a good approximation, in relation to the particle's cross-sectional area. Large particles therefore scatter light at narrow angles with high intensity, whereas small particles scatter at wider angles but with low intensity.

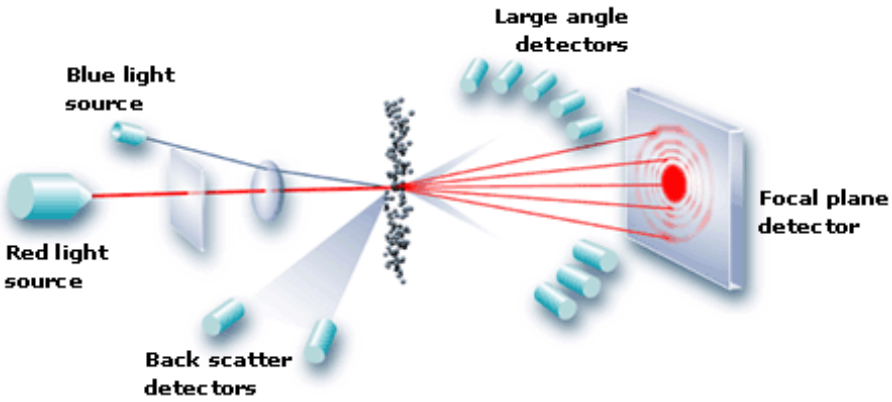

Fig. 2.10 *Basic principle of laser diffraction (source: Malvern Instruments).*

The goal of all particle-sizing techniques is to provide a single number that is indicative of the particle size. However, particles are three-dimensional objects for which at least three

parameters (length, width and height) are required in order to provide a complete description. Most sizing techniques assume that the material being measured is spherical and report the particle size as the diameter of the 'equivalent sphere' which would give the same response as the particle being measured. This assumption leads to an overestimation of the size of platy minerals, like clay-sized grains (McCave *et al.*, 2006). The size range accessible during the measurement is directly related to the angular range of the scattering measurement. Modern instruments make measurements from around 0.01 degrees through to 130 degrees, corresponding with grain sizes varying between 0.02 µm to 2 mm. The laser diffraction technique for grain-size analyses allows quick results with high resolution and high measurement precision.

Fig. 2.11 *Picture of a Malvern Mastersizer 2000.*

The Malvern Mastersizer instrument (Fig. 2.11) consists of a helium-neon gas laser source, which generates a beam of light with a fixed wavelength. The suspended particles pass through this beam, resulting in the diffraction of the beam at different angles according to the particle size. Next, the diffracted light is focussed by a lens onto a series of photosensitive detectors, which record the angular distribution of the scattered light. The transformation of laser diffraction data to grain-size frequency data is computed using the full Mie diffraction theory. This method allows to study a wide range of size spectra and expresses the data as volume percentages across this spectrum. The system was used in combination with an automated sample dispersion unit (Hydro 2000G).

Material properties	Measurement settings	Measurement time
Refraction index: 1.55	Pump speed: 2500 rpm	Sample: 15 s
Absorption: 0.1	Ultrasonification: 60 s	Background: 15 s

Table 2.1 *Standardised measurement settings of the Malvern Mastersizer 2000 at the Marine Biology Section (Ghent University, Belgium).*

All samples were analysed using the standard measurement settings of the Marine Biology Section (Table 2.1). The obscuration values were maintained between 10 to 20%. Each sample was measured once, although some random samples were measured twice in order to check the reproducibility of the measurements (i.e. instrument and operator precision).

2.3.6 End-member modelling

In a next step, the grain-size distributions were decomposed into elementary sub-populations in order to identify particular processes of sediment production, transport and/or deposition (Prins and Weltje, 1999; Weltje and Prins, 2003, 2007). Several methods have been developed over the years and can be subdivided in two major decomposition approaches: parametric versus non-parametric. The first method fits a number of statistical distribution functions of a predefined class to a sample's size-distribution while the second method defines an optimal set of elementary sub-populations based on the covariance structure of the particle-size dataset. A detailed overview of the different techniques is presented by Prins and Weltje (1999) and Weltje and Prins (2003). For sedimentological purposes non-parametric techniques show distinct advantages compared to the parametric methods (Weltje and Prins, 2007).

In collaboration with Dr. J.-B. Stuut (NIOZ, Texel, The Netherlands), the end-member modelling algorithm (EMMA), developed by Weltje (1997), was applied. As demonstrated by several studies in marine environments (Frenz et al., 2003; Holz et al., 2007; Prins et al., 2002; Prins and Weltje, 1999; Stuut et al., 2007; Thierens et al., 2010) it is a powerful method to obtain meaningful end-members. Such end-member is a physically meaningful and dataset-specific sub-population obtained by deconvoluting grain-size distributions. Each of these end-member size distributions represent an elementary sub-assemblage of grains that originated from statistically indistinguishable provenance and/or transport processes (Prins and Weltje, 1999; Weltje and Prins, 2003). The EMMA method consists of two modelling steps (Weltje, 1997; Weltje and Prins, 2007). A first step is to determine the appropriate amount of end-members by constrained weighted least-square estimation. This set of end-members results in the best approximation of the data and their degree of correlation is represented by the coefficient of approximation r^2. During the second step, the relative contribution of each end-member is calculated for each individual grain-size distribution by means of an iterative coordinate transformation procedure. In a next step, these end-members can be linked to specific sedimentological processes using additional analyses (e.g. X-ray diffraction, planktonic foraminifer assemblage, clay mineral assemblage, neodymium-strontium isotopes, thin-section petrography, cold-cathodoluminescence) (Stuut et al., 2007; Thierens et al., 2010; Weltje and Prins, 2003). This method has already been applied by Thierens et al. (2010) for the study of a cold-water coral mound in the Porcupine Seabight.

2.3.7 Stable carbon and oxygen isotope analysis

Stable carbon and oxygen isotope analysis of shells and skeletons of marine organisms is a well-known technique in palaeoceanographic studies and especially in marine palaeoclimatology. Naturally occurring oxygen is composed of three stable isotopes ^{16}O, ^{17}O and ^{18}O with ^{16}O being the most abundant. The isotope ratio $^{18}O/^{16}O$ can be used as palaeothermometer to reconstruct past climatic changes: glacial versus interglacial periods. During glacial periods, low $\delta^{18}O$ water is stored in ice sheets, resulting in a relatively high mean $\delta^{18}O$ value in the world's oceans. Organisms such as foraminifera which combine oxygen dissolved in the surrounding water with carbon and calcium to build their shells therefore incorporate the temperature-dependent ^{18}O to ^{16}O ratio. When these organisms die, they settle out on the sea bed, preserving a long and invaluable record of global climate change. However, important local effects in areas of high evaporation or low salinity due to freshwater input can influence the isotopic values of foraminifera. Carbon has two stable, naturally occurring istopes, ^{12}C and ^{13}C, of which ^{12}C is the most abundant. The isotope ratio $^{13}C/^{12}C$ reflects the carbon isotopic composition of the dissolved inorganic carbon (DIC) in seawater during calcite precipitation and can give more information about nutrient supply to the cold-water corals. Stable isotope abundances are expressed as the ratio of the two most abundant isotopes in the sample compared to the same ratio in an international standard, using the 'delta' (δ) notation. Because the differences in ratios between the sample and standard are very small, they are expressed as parts per thousand or 'per mil' (‰) deviation from the standard.

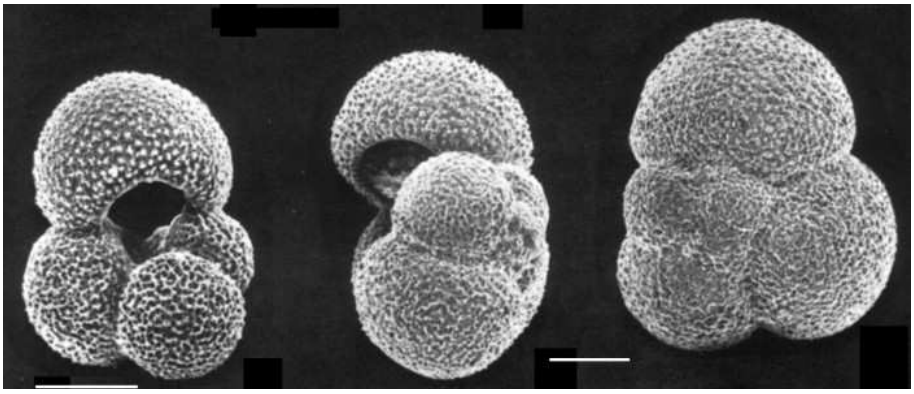

Fig. 2.12 *Microscopic pictures of Globigerina bulloides (image courtesy of the World Register of Marine Species).*

In this study, the planktonic foraminifera *Globigerina bulloides* (250-315 µm) was used (Fig. 2.12). *G. bulloides* has 2 to 2.5 whorls with 8 to 10 chambers (3-5 chambers in the last whorl) ending with a large umbilical aperture without lip. The chambers are spherical to slightly ovoid and increase slowly in size. The surface is rather rough with deep sutures and numerous spine collars. *G. bulloides* is mostly abundant in temperate to subpolar water masses in temperatures between 6 to 24°C. In order to minimise variability due to biological factors, it is important to select only one species with well-known ecological preferences from one size fraction (Ravelo and Hillaire-Marcel, 2007). The oxygen isotope composition of

a foraminiferal shell is linked to the temperature and the isotopic composition of the seawater during calcite precipitation. $\delta^{13}C$ will reflect changes in the $\delta^{13}C_{DIC}$ and the seawater carbon chemistry [CO_3^{2-}]. The stable isotope analyses were performed at the Laboratoire des Sciences du Climat et de l'Environnement (LSCE, Gif-sur-Yvette, France) in collaboration with Prof. Dr. D. Blamart.

2.3.8 U/Th dating

Finally, U/Th dating allows to determine the age of the cold-water coral fragments in the sediment cores and thus to obtain a reliable time framework of cold-water coral growth. U-series dating is based on the radioactive disequilibria between ^{238}U and its radioactive daughter products ^{234}U and ^{230}Th. It is a key tool in geochronology with different applications such as the reconstruction of sea level variations from tropical corals, calibration of the radiocarbon time scale, the determination of precise time scales of carbonate deposits (e.g. deep-water corals) and tracers of geochemical processes in the ocean (Adkins et al., 1998; Smith et al., 1997). The main aim of the U/Th dating technique within this study is to determine the age of the cold-water corals in order to obtain a reliable time framework.
U/Th dating of deep-sea corals is not similar to that of surface-dwelling corals (Cheng et al., 2000). First, deep-sea corals incorporate a significant amount of unsupported ^{230}Th during growth due to the higher ^{230}Th concentrations in deep ocean waters. A correction is needed for this effect which can have an influence on the precision and accuracy of the dating result. Secondly, diagenetic processes may affect the corals and thus the U/Th age. Nevertheless, the primary uranium concentrations (1-3 ppm) in cold-water corals are much higher than those of other biogenic deep-sea carbonates which make them ideal candidates for U-series dating (Cheng et al., 2000).

The U-series datings were performed at the Laboratoire des Sciences du Climat et de l'Environnement (LSCE, Gif-sur-Yvette, France) in collaboration with Dr. N. Frank. A detailed description of the preparation of the corals, the analytical procedures and the physical measurement routines is presented in Frank et al. (2005), Frank et al. (2004) and Douville et al. (2010). Prior to analysis, the coral fragments need to be physically and chemically cleaned to remove surface contamination. For this reason, only well-preserved cold-water coral fragments were selected without a ferromanganese coating and without traces of bioerosion. First, the outermost surface of the corals was carefully ground off, followed by a weak acid leach, ultrasound treatment, and several rinses with quartz distilled water and AR grade acetone. All samples were analysed by X-ray diffraction to verify the purity of the aragonite. Next, 100 to 400 mg of cleaned fragments were powdered, dissolved with HNO_3 and spiked with a mixed ^{233}U, ^{236}U and ^{229}Th solution. Finally, U and Th were extracted and purified, using a single UTEVA column, to achieve accurate measurements and to avoid matrix effects and isobaric interferences.

All samples were measured using inductively coupled plasma-quadrupole mass spectrometry (ICP-QMS). This technique reduces the chemical preparation time and analytical measurement time five to ten times compared to the ultra-high precision dating techniques, thermal ionisation mass spectrometry (TIMS) and multi-collector inductively coupled plasma mass spectrometry (MC-ICPMS). Similar U-series ages were obtained with both techniques; however, ICP-QMS has a lower analytical precision compared to TIMS. Nevertheless, the stability and the signal/noise ratio of ICP-QMS already reach 4‰ and 1% reproducibility for U and Th isotopic measurements, respectively (Douville et al., 2010).

Part 2

Gulf of Cadiz

Introduction

During an exploratory cruise of the R/V Belgica (CADIPOR) in May 2002 off Larache (Morocco), the El Arraiche mud volcano field has been discovered (Van Rensbergen et al., 2005) (Fig. 2A). The area consists of eight mud volcanoes in water depths between 200 and 700 m. Besides the giant mud volcanoes small mounds topping the ridges and structural heights were observed as well. Since then, the mounds became the topic of several multidisciplinary studies due to its unique setting. First, the area was further investigated in July 2002 on board the R/V Prof Logachev during Leg 2 of the TTR 12 cruise. The 2002 surveys yielded detailed multibeam bathymetry over a 700 km² study area, dense grids of high-resolution seismic data, deep-tow sub bottom profiles and side-scan sonar mosaics over the major structures. Selected video imagery lines, video guided grab samples, dredge samples, gravity cores and boxcores were collected for groundtruthing purposes (Van Rensbergen et al., 2005). In May 2004, a 9 m long Kasten core was recovered with the R/V Marion Dufresne (MD140 cruise) on top of one of the largest coral build-ups. The research continued in 2004 and 2005 with two campaigns on board of the R/V Pelagia and one cruise on the R/V Belgica (CADIPOR II) within the framework of the ESF EUROMARGINS MoundForce project (2003-2006). During these cruises additional multibeam data, high-resolution seismic lines, boxcores, piston cores, CTD data, seabed photography and video lines were obtained. Additionally, a BOBO and an ALBEX lander were deployed. In 2006, the area was further explored on board the R/V M.S. Merian by a team of IFM-GEOMAR (Kiel, Germany). Although the cruise mainly focused on the study of mud volcanoes, some sediment cores were retrieved in the coral mound area (Renard and Vernadsky ridges).

In January 2006, a new research project, called MiCROSYSTEMS, was funded by the European Science Foundation (ESF). This project aimed at investigating the microbial diversity and functionality in cold-water coral reef ecosystems, focusing on the Pen Duick mounds off Morocco. Within this framework, two cruises (R/V Pelagia in 2006 and R/V Belgica in 2007) were organised in order to obtain additional data to tackle the objectives in the MiCROSYSTEMS project, including ROV observations using ROV Genesis from Ghent University. Based on these ROV observations a cruise on board the R/V Marion Dufresne was planned in July 2008. In total, 19 cores were retrieved in the El Arraiche mud volcano field of which nine are located on the mounds on the Pen Duick Escarpment. A final cruise to the area was planned in 2009 on board of the R/V Belgica in order to obtain additional seismic profiles, ROV observations and boxcore samples.

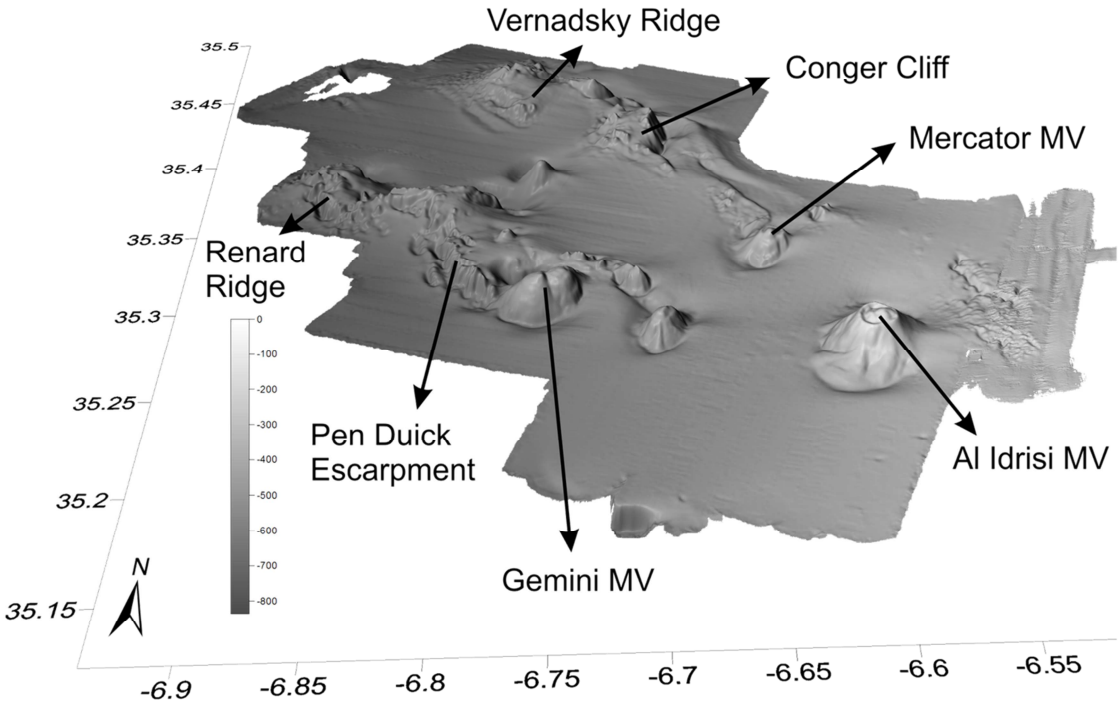

Fig. 2A *Bathymetric map of the El Arraiche mud volcano field with the mud volcanoes (MV) and geomorphological structures (after Foubert et al., 2008).*

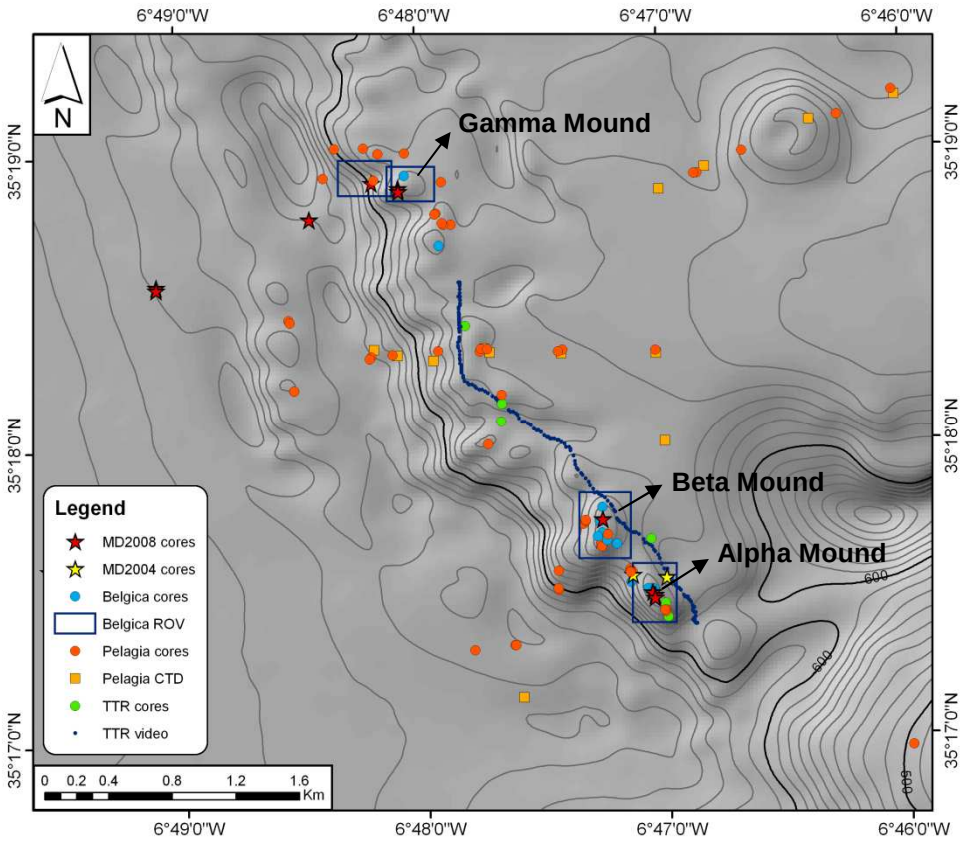

Fig. 2B *Overview of the available data on the Pen Duick Escarpment.*

During these ten years of intensive research in the El Arraiche mud volcano field, several results have been published. In the following short overview of available literature we will only focus on the cold-water coral mounds in the area. The first paper reporting the discovery of the coral mounds was published by Foubert et al. (2008). This paper discusses the co-occurrence of cold-water corals and carbonate mounds with mud volcanoes and active fluid seepage along the Moroccan margin. Additionally, a three-phase model for carbonate mound development has been proposed. Next, Wienberg et al. (2009) presented an overview of observations and findings on scleractinian reef-forming corals in the Gulf of Cadiz based upon reports, published data and new data. A further objective was to identify the temporal distribution of scleractinian cold-water corals in the Gulf of Cadiz during the past glacial-interglacial cycle and to relate their occurrence to climatic and oceanographic changes. The paper mainly focusses on the mud volcanoes in the southern Gulf of Cadiz, however a few results on the Pen Duick Escarpment were presented. In 2010, Wienberg et al. aimed to identify the main forcing factors triggering the development of cold-water coral ecosystems in the Gulf of Cadiz based on U-series datings. Maignien et al. (2011) described the methane-related geochemical processes in Alpha Mound, located at the Pen Duick Escarpment, as well as two reference locations off-mound and off-escarpment.

Within the framework of the ESF MiCROSYSTEMS project three additional papers on the Pen Duick mounds were published in 2011 and one in 2012. First, Van Rooij et al. (2011) presented the "MiCROSYSTEMS" approach, which included the development of an integrated view on the dynamic geological, biogeochemical and hydrographic environment within the vicinity of the Pen Duick mounds. Wehrmann et al. (2011) compared the non-methane influenced Gamma Mound with the methane influenced Alpha and Beta Mounds in order to evaluate the imprint of methane cycling on recent early diagenetic processes and the geological record. In Templer et al. (2011) the prokaryotic community and its activity and diversity is examined in Alpha and Beta Mound in order to assess whether such mounds are still biogeochemically active and represent an important sub-seafloor prokaryotic habitat. Finally, Pirlet et al. (2012) presented an in-depth study of the diagenetic features in the sediment of Alpha and Beta Mound. Despite their almost identical oceanographic and sedimentological settings, different assemblages of authigenic minerals are observed. Based on these assemblages a reconstruction of the diagenetic environment is made for both mounds. Additionally, the effect of lithification and brecciation processes on the biogeochemical environment is discussed.

Chapter 3

Distribution of fossil cold-water corals on the Pen Duick Escarpment

New manuscript, modified from:
De Mol, L., Larmagnat, S., Pirlet, H., de Haas, H., Mienis, F., Frank, N., Van Rooij, D., De Batist, M. & Henriet, J.-P. (in preparation). Distribution of fossil cold-water corals on the Pen Duick Escarpment (Gulf of Cadiz).
This chapter is partly published as De Mol, L., Hilàrio, A., Van Rooij, D. & Henriet, J.-P. (2011). Habitat mapping of a cold-water coral mound on Pen Duick Escarpment (Gulf of Cadiz). In: Harris, P.T. & Baker, E.K. (eds.). Seafloor geomorphology as Benthic Habitat: GeoHab Atlas of seafloor geomorphic features and benthic habitats. Elsevier Insights, 645-654.

Abstract

Three cold-water coral mounds on top of the Pen Duick Escarpment (PDE) were investigated, using video observations and boxcore samples. This paper reports a detailed study of the present distribution of fossil cold-water corals on PDE, the role of cold-water coral rubble fields, the presence of authigenic carbonate slabs, and the growth and distribution of the corals in the past. Video observations revealed four different seabed facies: (1) soft sediment, (2) soft sediment with a patchy distribution of sediment-clogged dead cold-water coral rubble, (3) dense cold-water coral rubble fields, and (4) outcropping hard substrate. Up to 40 m high cold-water coral mounds covered with fossil corals were observed in the Gulf of Cadiz, which is in contrast with the cold-water coral mounds on the Irish margin that are covered with a living coral cover. The mounds surfaces revealed a patchwork of facies due to a complex process of deposition, non-deposition and erosion, triggered by changes in bottom current strength and direction, and changes in the morphology of the escarpment. Bottom samples showed that Lophelia pertusa*,* Madrepora oculata *and* Dendrophyllia *sp. were the most common cold-water coral species. U/Th dating of the corals revealed that* L. pertusa *and* M. oculata *thrived in the Gulf of Cadiz during glacial periods, while* Dendrophyllia *sp. was able to survive after the Younger Dryas event.* Dendrophyllia *sp. will thus appear after the extinction of* L. pertusa *and* M. oculata*.*

3.1 Introduction

Cold-water corals are abundantly present along the NE Atlantic continental margin, creating small individual patches in canyons (De Mol et al., 2011b; Reveillaud et al., 2008; Tyler et al., 2009) and on seamounts (Duineveld et al., 2004), to large flourishing reefs on the slopes of the Norwegian margin (Fosså et al., 2005; Freiwald et al., 2002). Along the Irish continental margin (De Mol et al., 2002; Huvenne et al., 2007; Kenyon et al., 2003; Masson et al., 2003), the cold-water corals were able to build up mounds (up to 380 m high), mostly covered with a dense living coral cover (de Haas et al., 2009; Dorschel et al., 2009; Huvenne et al., 2005). In 2002, smaller fossil cold-water coral mounds (up to 60 m high) were discovered on the Moroccan margin in the southern Gulf of Cadiz (Foubert et al., 2008; Van Rensbergen et al., 2005).

Fossil cold-water corals in the Gulf of Cadiz were observed along the Spanish and Moroccan margins in water depths between 500 to 1000 m (Wienberg et al., 2009). They are mainly found on flanks of mud volcanoes, diapiric ridges, steep fault escarpments and mound structures. However, some findings are also reported from areas with no special topographic feature (Wienberg et al., 2009). In total, 20 mud volcanoes are already known to be covered by isolated coral patches and coral rubble (Pinheiro et al., 2003; Somoza et al., 2003). Besides these mud volcanoes, about 200 mound structures have been discovered in the southern Gulf of Cadiz on top of topographic highs (Foubert et al., 2008). These mounds occur either as single mounds or they are grouped in mound provinces. Within the El Arraiche mud volcano field (southern Gulf of Cadiz) four mound provinces were discovered during the R/V Belgica CADIPOR cruise in 2002, namely the Pen Duick Mound Province, the Renard Mound Province, the Vernadsky Mound Province, and the Al Idrisi Mound Province (Foubert et al., 2008). On these mounds, mostly fossil cold-water corals of glacial age were observed as isolated patches or as coral rubble. Present conditions are not suitable for cold-water coral growth in the Gulf of Cadiz, although during the past the environmental and oceanographic conditions must have changed in order to better suit the necessary conditions for corals to live (Foubert et al., 2008; Wienberg et al., 2009).

The presence of living cold-water corals is primarily controlled by strong topographically guided bottom currents and enhanced primary production, supplying food particles (particulate organic matter and/or zooplankton) to the scleractinian corals (Dorschel et al., 2007a; Duineveld et al., 2004; Eisele et al., 2011; Freiwald et al., 2004; Kiriakoulakis et al., 2004; Mienis et al., 2007; White and Dorschel, 2010; White et al., 2005; Wienberg et al., 2010). Additionally, cold-water corals, especially *L. pertusa*, prefer a certain temperature (4-12°C), salinity (31.7-38.8) and dissolved oxygen (4.3-7.2 ml l^{-1}) range of the water (Davies et al., 2008; Freiwald et al., 2004; Roberts et al., 2009). Recently, Dullo et al. (2008) discovered that living *L. pertusa* reefs occur within a potential density envelope of 27.35 to 27.65 kg m^{-3}

of the ambient sea water. Finally, scleractinian corals need a hard substrate to settle on, like boulders, ridges or banks (Rogers, 1990).

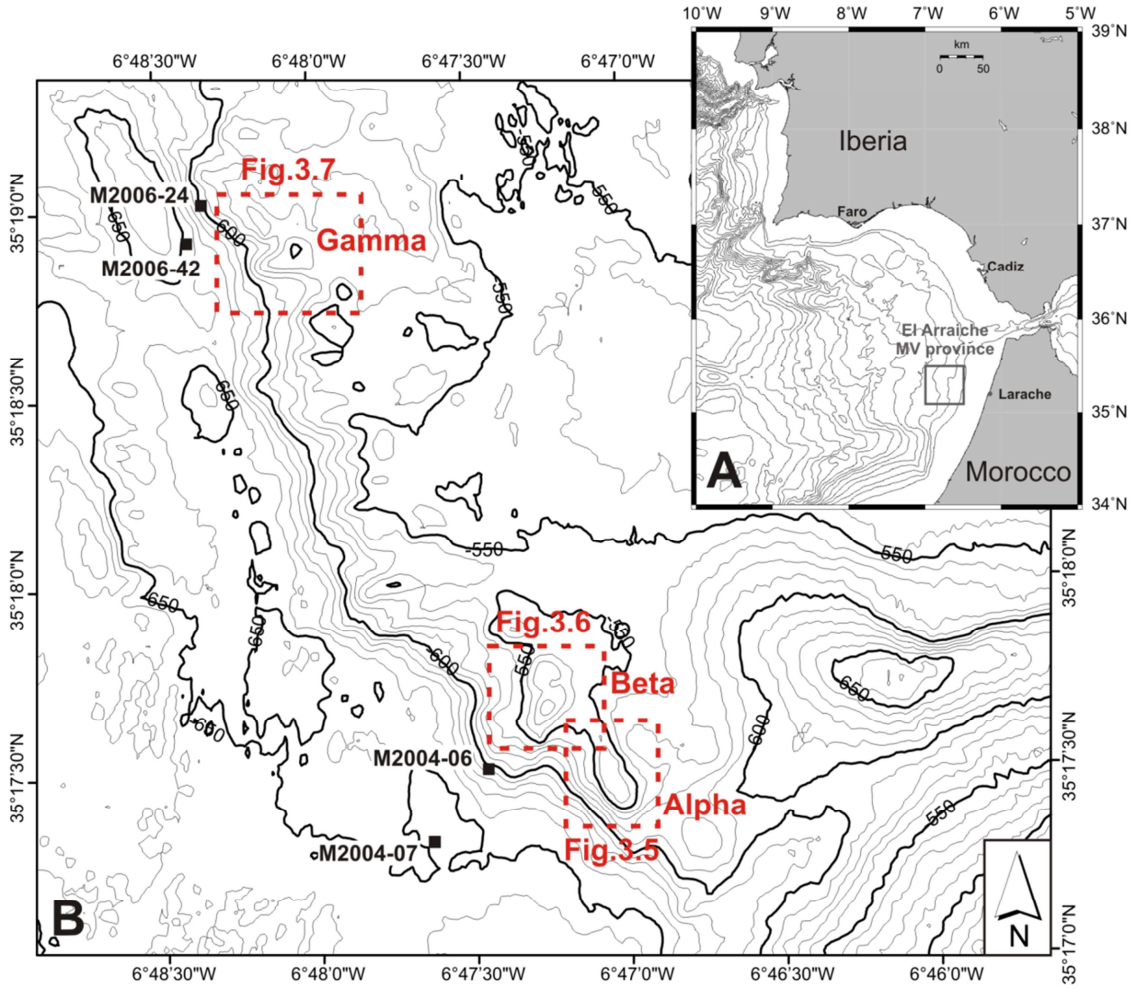

Fig. 3.1 *(A) Location of the study area in the Gulf of Cadiz along the Moroccan Atlantic continental margin, (B) a detailed bathymetric map of the Pen Duick Escarpment (contour lines every 10 m), with indication of the ROV survey zones (Fig. 3.5, 3.6 and 3.7) and off-mound boxcore samples (black square).*

This paper will compare three cold-water coral mounds, namely Alpha, Beta and Gamma Mound, and a smaller unnamed mound, located in the Pen Duick Mound Province (Fig. 3.1). This mound province hosts the largest mounds in the southern Gulf of Cadiz. The mounds are considered to be in an initial stage of mound growth which allows reconstructing a model for the early development of these mounds (Foubert et al., 2008; Van Rooij et al., 2011). Since the discovery of the Pen Duick mounds in 2002, several cruises have been dedicated to study in detail their structure and build-up. However, before making an integrated model, it is necessary to know the present situation on the mounds and what happened in the recent past by looking at sedimentological and biogeochemical processes at the surface and within the first centimetres of the mound sedimentary record. This study provides detailed insight in (1) the present distribution of fossil cold-water corals that are exposed at the seafloor, (2) the growth and distribution of these cold-water corals in the past, and (3) the comparison of this distribution pattern with other mound areas such as the

Porcupine Seabight and the margins of the Rockall Trough. Additionally, the role of cold-water coral rubble fields (e.g. composition, lithology and facies) will be discussed.

3.2 Material and methods

3.2.1 ROV observations

ROV observations (Table 3.1) were obtained with ROV Genesis of Ghent University (Belgium), using a forward-looking colour zoom and a black and white video camera. High-resolution still images of the seafloor were acquired using a digital Canon Powershot camera. The main sampling tool on the ROV is the remotely controlled manipulator and a deployable tray in which samples can be stored. A laser marker was added to the camera head for visualising scale (10 cm spacing). An accurate positioning of the TMS and ROV was obtained through an IXSEA Global Acoustic Positioning System (GAPS). This GAPS is a portable Ultra Short Base Line unit, allowing subsurface positioning with an accuracy of about 2-3 m. During the R/V Belgica 09/14b cruise, the ship, TMS and ROV navigation was recorded through OFOP (Ocean Floor Observation Protocol) (Huetten and Greinert, 2008). Afterwards all tapes of the dives were digitised in .avi and .mpeg format. Interpretation of the video data was performed with ADELIE 1.8 (Ifremer) for the R/V Belgica 07/13 cruise and with OFOP 3.2.0c for the R/V Belgica 09/14b cruise. Based on the observations, a number of facies characteristics for the study area were identified. Each facies was given a colour-code and was integrated into ArcGIS 9.2, resulting in a facies interpretation map.

Name	Location	Start track				End track			
		Latitude	*Longitude*	*Time*	*Depth*	*Latitude*	*Longitude*	*Time*	*Depth*
B07-06	Alpha Mound	35°17.4622' N	6°46.8638' W	13:51	572 m	35°17.4470' N	6°47.0059' W	15:00	541 m
B07-07	Beta Mound	35°17.6634' N	6°47.2088' W	09:18	543 m	35°17.7398' N	6°47.2648' W	09:59	524 m
B09-04	Alpha Mound	35°17.4686' N	6°47.0101' W	12:54	540 m	35°17.4916' N	6°47.0484' W	13:22	531 m
B09-05	Alpha Mound	35°17.3917' N	6°46.9904' W	07:01	570 m	35°17.5328' N	6°47.0902' W	07:40	530 m
B09-06	Beta Mound	35°17.6919' N	6°47.2491' W	08:13	512 m	35°17.7641' N	6°47.2538' W	10:22	480 m
B09-07	Beta Mound	35°17.7443' N	6°47.2566' W	07:05	526 m	35°17.7190' N	6°47.2733' W	08:26	520 m
B09-08	Beta Mound	35°17.7690' N	6°47.3077' W	10:01	533 m	35°17.5858' N	6°47.2975' W	11:24	548 m
B09-09	Gamma Mound	35°18.9082' N	6°48.0010' W	13:11	554 m	35°18.8717' N	6°48.0209' W	14:04	544 m
B09-10	Alpha Mound	35°17.5613' N	6°47.1292' W	15:36	552 m	35°17.4599' N	6°47.0265' W	15:58	530 m

Table 3.1 *Names, locations and operational data of the ROV Genesis dives. Time in UTC.*

3.2.2 Boxcore sampling

A total of 24 boxcores (Table 3.2) were retrieved during five cruises:, the R/V Pelagia M2004 (64PE229), M2005 (64PE237) and M2006 (64PE253) cruises and the R/V Belgica Cadipor III 07/13 and Pen Duick 09/14b cruises. Thirteen on-mound boxcores were collected from the top and flanks of the three coral mounds. Two additional on-mound boxcores are obtained a small mound SE of Gamma Mound. Nine off-mound boxcores were collected in the vicinity of the mounds, on the escarpment and at the plain (Table 3.2; Fig. 3.1, 3.5, 3.6 and 3.7). The

location of the boxcores during the R/V Belgica 07/13 and 09/14b cruises were based on the ROV observations.

From each boxcore, subsamples from different depths were taken for grain-size analyses (Table 3.3) with a Malvern Mastersizer 2000 (Marine Biology Section, Ghent University). The sediment was dried in a furnace at 60° for about 48 h. After subsampling 1 g of sediment, the carbonate fraction was removed by adding 75 ml of 10% acetic acid. This process was performed twice in order to remove all carbonate fragments. Afterwards, the sample was rinsed twice with distilled water, each time followed by a 24 h settling period. Finally, the sediment was transferred in a 15 ml tube together with 0.2% calgon (sodium hexametaphosphate) to prevent flocculation. Prior to analysis, the samples were rotated (20 rpm) for 24h. Afterwards, the results were processed with GRADISTAT (Blott and Pye, 2001) and the descriptive grain-size parameters were calculated using the Folk and Ward (1957) method.

Fourteen cold-water coral specimens (*L. pertusa* and *Dendrophyllia* sp.) from different boxcores and one specimen, collected during ROV dive B09-07, were sampled for U/Th dating (Table 3.4). The U-series measurements and age determination were carried out in the Laboratoire des Sciences du Climat et de l'Environnement (LSCE) in Gif-sur-Yvette using inductively coupled plasma source mass spectrometry (Thermo-Fisher X-Series). Preparation of corals, analytical procedures and physical measurement routines followed the detailed description by Frank et al. (2005), Frank et al. (2004) and Douville et al. (2010). The data is blank corrected and the HU1 standard is used to apply a bracketing technique to reduce internal drifts of the ICPMS as outlined by Douville et al. (2010). For *Dendrophyllia* sp. corals having highly elevated ^{232}Th concentrations the correction model for initial ^{230}Th from seawater is replaced by a correction for detritus ^{232}Th with an $(^{230}Th/^{232}Th)_{detritus}$ activity ratio of 1.0 ± 0.3 slightly higher than the mean crustal value of 0.75. However, the absolute value of those ages cannot be considered reliable given the uncertainty on the correction model applied, nevertheless the age clearly indicate a Holocene timing of the coral growth. All activity ratios are calculated using the half-lives of ^{238}U, ^{234}U, and ^{230}Th given by Cheng et al. (2000).

Biological subsampling was performed on boxcores B09-1401-bc, B09-1402-bc, B09-1404-bc, B09-1405-bc, B09-1406-bc and B09-1408-bc. In addition, 18 corals (*L. pertusa* and *Dendrophyllia* sp.) were sampled in situ using the ROV manipulator during dives B09-06 and B09-07 (both surveying the top of Beta Mound). Subsequently, some of these corals were used for the preparation of histological thin sections and SEM observations, performed by Stéphanie Larmagnat (Laval University, Québec, Canada). Both optical methods provide details of the histology, the micro-organismic contributions and the relationships between particles, living and non-living organic tissue in order to document the diversity of early diagenetic phenomena. The aim is to concentrate on the cold-water coral rubble fields and

their associated cryptic community (e.g. sponges). For this purpose, the samples were biologically fixed, applying a solution of glutaraldehyde, sodium cacodylate and sea water. The samples were fixed on board for 24 hours. Later the samples were transferred in multiple steps towards a storage solution of 70 % ethanol (respectively into 30, 50 and 70 %). For scanning electron microscopy (SEM, JEOL 840-A equipped with a NORAN light-elements energy dispersive analyser and low vacuum SEM, JEOL JSM6360LV), the samples were dried using the critical-point drying (CPD) method (collaboration R. Janvier, Laval University) and were kept in a dessicator. Prior to SEM observations, the samples were covered with a combination of gold and palladium to minimise charge effects. For light microscopy, the dehydrated samples were optionally stained in block portions with methylene blue and azur-II/methylene blue and embedded in LR White TM resin. Both stained and unstained samples were then cut into slices, 20 µm to 50 µm thick, using a Leica saw microtome.

	Cruise	Core number	Location	Latitude	Longitude	Depth (m)	Length (cm)
R/V Pelagia	M2004	M2004-02	Beta Mound	35°17.69' N	6°47.24' W	527	22
	64PE229	M2004-06	Slope escarpment	35°17.51' N	6°47.45' W	586	47
		M2004-07	Foot escarpment	35°17.32' N	6°47.63' W	641	46
		M2004-08	Beta Mound	35°17.74' N	6°47.33' W	529	31
	M2005	M2005-03	Alpha Mound	35°17.43' N	6°47.01' W	517	47
	64PE237	M2005-05C	Alpha Mound	35°17.56' N	6°47.15' W	533	37
		M2005-30	Mound	35°18.76' N	6°47.90' W	550	32
		M2005-31	Mound	35°18.79' N	6°47.93' W	559	27
	M2006	M2006-21	Plain	35°19.00' N	6°48.05' W	560	33
	64PE253	M2006-22	Plain	35°19.00' N	6°48.16' W	557	22
		M2006-23	Plain	35°19.02' N	6°48.22' W	557	31
		M2006-24	Slope escarpment	35°19.02' N	6°48.34' W	571	31
		M2006-39	Plain	35°18.90' N	6°47.90' W	560	48
		M2006-41	Slope escarpment	35°18.91' N	6°48.18' W	568	41
		M2006-42	Foot escarpment	35°18.92' N	6°48.39' W	637	35
R/V Belgica	CADIPOR III 07/13	B07-1304-bc	Beta Mound	35°23.696' N	6°47.264' W	524	70-83
	Pen Duick 09/14b	B09-1401-bc	Beta Mound	35°17.734' N	6°47.272' W	526	13
		B09-1402-bc	Beta Mound	35°17.783' N	6°47.260' W	528	5-20
		B09-1404-bc	Beta Mound	35°17.684' N	6°47.282' W	524	30
		B09-1405-bc	Gamma Mound	35°18.874' N	6°48.076' W	551	33
		B09-1406-bc	Alpha Mound	35°17.504' N	6°47.064' W	530	25-35
		B09-1407-bc	Alpha Mound	35°17.505' N	6°47.178' W	531	38-47
		B09-1408-bc	Alpha Mound	35°17.502' N	6°47.050' W	533	38
		B09-1409-bc	Alpha Mound	35°17.495' N	6°47.056' W	532	40

Table 3.2 *Location, water depth and recovery length of the studied boxcores.*

Area A	Location	Boxcore	Depth (cm)	Mode (µm)	Mean (µm)	Sorting	Skewness	Kurtosis
	Alpha Mound	M2005-03	5	6.06	6.30	2.72	-0.08	1.05
			20	9.98	7.61	3.15	-0.09	0.94
			30	12.67	8.21	3.35	-0.10	0.91
		B09-1406-bc	0	6.52	5.81	2.63	-0.15	1.06
		B09-1407-bc	0	7.85	7.18	2.41	-0.16	1.08
			25	11.27	7.04	3.25	-0.11	0.92
		B09-1408-bc	0	7.04	6.53	2.41	-0.16	1.09
			23	7.27	6.80	2.97	-0.08	0.97
		M2005-05C	3	6.36	6.34	2.38	-0.13	1.11
			10	5.92	6.17	2.66	-0.09	1.08
			20	6.27	7.25	2.99	-0.07	0.96
			28	14.11	8.61	3.26	-0.12	0.92
	Beta Mound	B09-1404-bc	0	6.34	6.05	2.76	-0.12	1.09
			15	10.30	6.63	3.18	-0.18	0.94
		M2004-02	3	6.12	6.45	2.62	-0.06	1.10
			15	7.08	6.72	2.96	-0.09	0.98
		B09-1401-bc	0	6.45	6.59	3.39	0.01	1.21
		M2004-08	5	6.54	6.80	2.92	-0.06	1.09
			13	12.16	8.75	3.43	-0.13	0.97
			20	12.77	8.29	3.27	-0.15	0.94
		B09-1402-bc	0	6.61	6.24	2.51	-0.13	1.10
	Slope escarpment	M2004-06	5	5.92	5.89	2.62	-0.10	1.08
			22	12.16	8.07	3.29	-0.10	0.92
	Foot escarpment	M2004-07	0	8.39	7.85	2.36	-0.16	1.09
			10	6.43	6.55	2.42	-0.10	1.10
			20	5.94	6.48	2.56	-0.06	1.07
			28	6.34	7.07	2.76	-0.07	1.03
Area B	**Location**	**Boxcore**	**Depth (cm)**	**Mode (µm)**	**Mean (µm)**	**Sorting**	**Skewness**	**Kurtosis**
	Mound	M2005-30	2	6.22	6.35	2.41	-0.11	1.11
			10	13.60	8.78	3.31	-0.13	0.94
			20	25.60	11.26	3.82	-0.30	0.91
			25	24.85	11.63	3.61	-0.31	0.91
		M2005-31	2	6.46	6.13	2.47	-0.14	1.10
			10	6.37	5.95	3.04	-0.10	1.03
			20	13.94	8.21	3.26	-0.15	0.92
	Gamma Mound	B09-1405-bc	0	7.12	6.62	2.39	-0.16	1.06
	Plain	M2006-39	0	6.82	6.53	2.40	-0.15	1.12
			10	5.97	6.10	2.60	-0.10	1.12
			20	6.14	6.50	3.08	-0.06	1.03
			30	6.75	7.51	3.32	-0.07	0.95
			40	10.11	8.12	3.30	-0.08	0.95
			45	18.79	9.98	3.33	-0.19	0.90
		M2006-21	0	6.73	6.64	2.40	-0.13	1.12
			10	5.99	6.19	2.81	-0.08	1.07
			20	7.09	7.24	3.18	-0.07	1.00
			30	12.38	8.08	3.38	-0.11	0.93
		M2006-22	0	7.05	6.65	2.37	-0.16	1.11
			5	6.24	6.19	2.44	-0.12	1.11
			10	6.32	6.03	2.66	-0.12	1.08
			15	10.23	6.89	3.33	-0.15	0.95
		M2006-23	0	6.53	6.26	2.48	-0.14	1.11
			5	7.52	7.64	3.36	-0.06	0.99
			10	11.87	8.51	3.46	-0.08	0.92
			20	14.24	8.33	3.37	-0.09	0.90
	Slope escarpment	M2006-24	0	6.29	6.05	2.51	-0.14	1.10
			10	10.74	7.04	3.47	-0.16	0.94
			20	11.42	7.89	3.42	-0.13	0.95
		M2006-41	0	6.76	6.34	2.47	-0.16	1.12
			10	6.30	5.88	2.92	-0.12	1.03
			20	11.98	8.11	3.48	-0.14	0.95
			25	14.99	8.97	3.62	-0.14	0.91
	Foot escarpment	M2006-42	0	6.80	6.50	2.49	-0.15	1.11
			10	6.95	5.89	3.13	-0.09	0.96
			20	11.76	7.67	3.49	-0.17	0.94
			30	10.90	6.71	3.26	-0.14	0.92

Table 3.3B *Results of the grain-size analyses, showing the statistical parameters (mode, mean, sorting, skewness and kurtosis).*

Boxcore	Depth (cm)	Coral species	[^{238}U] (ppm)	[^{232}Th] (ppb)	$^{234}U_M$ (‰)	(^{230}Th/^{238}U)	(^{230}Th/^{232}Th)	Age (ka)	$^{234}U_T$ (‰)	Corrected age * (ka)
B09-1401-bc	*0*	*Dendrophyllia sp.*	*5.065 ± 0.009*	*187.9 ± 0.3*	*142.8 ± 2.4*	*0.0341 ± 0.0008*	*2.8 ± 0.1*	*3.31 ± 0.08*	*144.2 ± 2.5*	*2.00 ± 0.50*
B09-1402-bc	*0*	*Dendrophyllia sp.*	*4.723 ± 0.007*	*85.5 ± 0.3*	*145.9 ± 1.8*	*0.0784 ± 0.0017*	*13.2 ± 0.3*	*7.73 ± 0.18*	*149.2 ± 2.0*	*7.10 ± 0.38*
B09-1404-bc	0	L. pertusa	3.789 ± 0.008	3.121 ± 0.011	129.1 ± 3.1	0.3548 ± 0.0040	1321 ± 16	40.9 ± 0.7	144.9 ± 3.8	No correction needed
B09-1405-bc	10	L. pertusa	3.352 ± 0.008	3.536 ± 0.008	142.2 ± 2.7	0.1853 ± 0.0029	537.6 ± 8.6	19.3 ± 0.4	150.2 ± 3.0	No correction needed
B09-1405-bc	15	L. pertusa	3.736 ± 0.007	1.614 ± 0.007	145.6 ± 3.0	0.1466 ± 0.0027	1038.3 ± 19.8	14.9 ± 0.3	151.9 ± 3.3	No correction needed
B09-1405-bc	30	L. pertusa	3.536 ± 0.006	0.665 ± 0.003	151.1 ± 2.7	0.1373 ± 0.0042	2244 ± 69	13.8 ± 0.5	157.1 ±3.1	No correction needed
B09-1406-bc	10	L. pertusa	3.421 ± 0.007	5.087 ± 0.024	147.4 ± 3.6	0.1236 ± 0.0056	255 ± 12	12.4 ± 0.6	152.7 ± 4.0	No correction needed
B09-1406-bc	15	L. pertusa	3.511 ± 0.008	0.875 ± 0.004	147.2 ± 1.7	0.1157 ± 0.0029	1419 ± 36	11.6 ± 0.3	152.1 ± 1.9	No correction needed
B09-1407-bc	*>10*	*Dendrophyllia sp.*	*4.728 ± 0.006*	*118.6 ± 0.2*	*144.5 ± 1.9*	*0.0773 ± 0.0009*	*9.4 ± 0.1*	*7.63 ± 0.10*	*147.7 ± 2.0*	*6.7 ± 0.40*
B09-1408-bc	0	L. pertusa	3.757 ± 0.004	0.204 ± 0.002	147.1 ± 2.3	0.1417 ± 0.0041	7959 ± 238	14.4 ± 0.5	153.2 ± 2.7	No correction needed
B09-1408-bc	38	L. pertusa	3.390 ± 0.007	1.191 ± 0.005	148.7 ± 2.9	0.1446 ± 0.0027	1259 ± 24	14.7 ± 0.3	155.0 ± 3.1	No correction needed
B09-1409-bc	20	L. pertusa	4.298 ± 0.008	4.959 ± 0.014	83.9 ± 3.3	0.9201 ± 0.0053	2439 ± 16	196 ± 5	146.0 ± 7.9	No correction needed
B09-07	*0*	*Dendrophyllia sp.*	*4.358 ± 0.004*	*0.539 ± 0.004*	*143.7 ± 2.2*	*0.0018 ± 0.0008*	*43.2 ± 19.9*	*0.17 ± 0.08*	*143.8 ± 2.2*	*0.16 ± 0.08*

Table 3.4 *Obtained results of the U-series datings according to depth and coral species, with the concentrations (ppm), isotopic ratios and ages (ka). * Corrected coral ages are based on the assumption that ^{232}Th indicates the presence of initial ^{230}Th from seawater with an (^{230}Th/^{232}Th)$_{seawater}$ activity ratio at t = 0 of 10±4 (Frank et al., 2004).*

3.3 Results

3.3.1 Facies description

Based on the sediment nature (e.g. soft sediment versus hard substrate) and the presence of fossil cold-water corals (e.g. patchy versus dense coral cover or no corals), four different facies were distinguished on the mounds.

Facies 1 corresponds to soft sediment (Fig. 3.2A-B), often bioturbated and mostly colonised by octocorals, including sea pens (Pennatulacea) and gorgonians (Gorgonacea). The latter ones form at certain locations dense bushes, which are in turn largely colonised by crinoids. Poriferans, sea urchins (Echinodermata, Echinoidea) and holothurians (Echinodermata, Holothuroidea) were also observed.

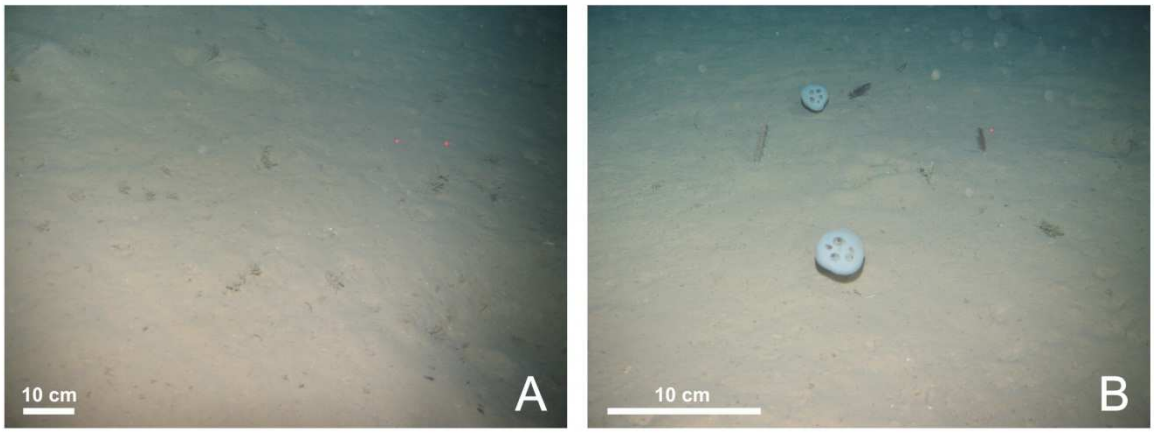

Fig. 3.2A-B *ROV images of facies 1: (A) soft sediment with indications of bioturbation at the sediment/water interface, and (B) soft sediment with* Hexactinnellida *sponges.*

Facies 2 is characterised by soft sediment with a patchy distribution of sediment-clogged dead cold-water coral fragments (< 75% dead cold-water corals) (Fig. 3.2C-F). These coral patches vary in size between a few centimetres up to patches of about 50 cm. The coral fragments are often colonised by crinoids.

Facies 3 is defined as thick (up to 60 cm) cold-water coral rubble fields (> 75% dead cold-water corals) (Fig. 3.2G-L), covering areas with a diameter of 10 to at least 50 m at the seafloor. Locally, these fields were covered with a very thin layer of soft sediment. This rubble facies had a characteristic three-dimensional fossil coral framework, mostly colonised by crinoids (Echinodermata, Crinoidea). Biota samples from boxcores and ROV dives documented the fauna associations inhabiting these dead cold-water coral fields. The fossil stony coral community was represented by the following species: *L. pertusa*, *M. oculata*, *Dendrophyllia alternata*, *Desmophyllum dianthus*, and possibly *Caryophyllia* sp.. For the living megafauna, Cnidaria were the most abundant. Along with the coral debris living

Porifera, living Echinodermata (uncategorised crinoids) and shells (brachiopods and uncategorised bivalves) were observed. Porifera occur as decimetre sized, massive forms (Fig. 3.2G), living on the seafloor but also as smaller (centimetre sized) forms living attached (e.g. encrusting sponge) to the dead coral skeleton debris (Fig. 3.2H; Fig. 3.3A; as white, yellow or orange masses). Brachiopods (e.g. *Terebratula* sp.), bivalves as well as crinoids were found attached (anchored) to dead coral skeletons (Fig. 3.3B). Meiofauna mainly corresponded to an encrusted community of bryozoans, serpulids worms and foraminifera (Fig. 3.4A-B). Planktonic foraminifera (Globigerinae family) and coccoliths were also present in the sediment (Fig. 3.4C). The coral skeletons often revealed signs of alteration such as dissolution holes or Fe/Mn oxide crusts (Fig. 3.3B) regardless of the scleractinian species. Macro-bioerosion occurred as small, regular, circular holes of 2 to 3 mm (Fig. 3.4D) and is due to excavating sponge activity (Beuck and Freiwald, 2005; Roberts et al., 2009). At a smaller scale, bioerosion by endolithic fungi was intensely affecting the living sponge *Haliclona* sp. (Fig. 3.4E) or infesting dead corals (e.g. with *Dendrophyllia* sp.; Fig. 3.4F). This fungal infestation (most likely *Dodgella* type) is very commonly documented in modern deep-water coral mounds in the Atlantic Ocean (Beuck and Freiwald, 2005; Freiwald and Wilson, 1998; Wisshak et al., 2005).

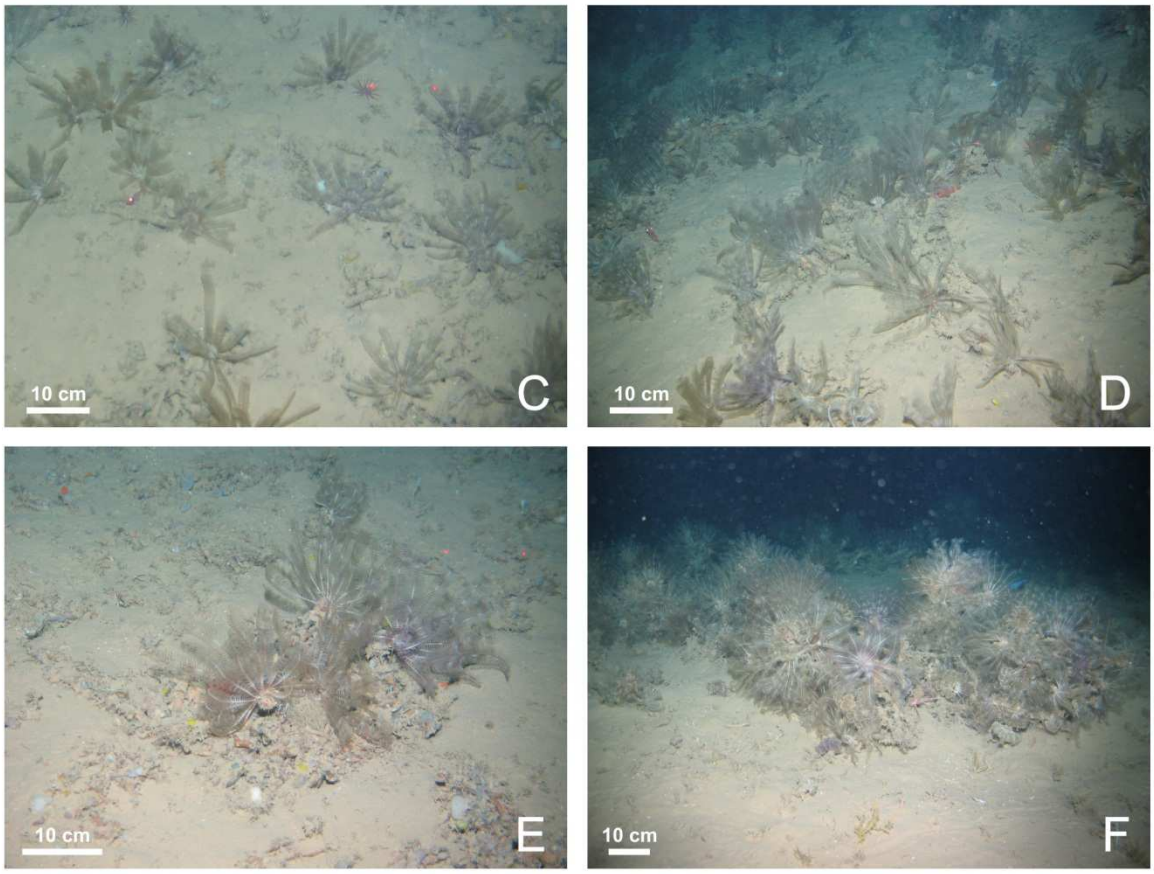

Fig. 3.2C-F *ROV images of facies 2: (C-D) soft sediment with a patchy distribution of coral rubble colonised by crinoids, (E) patchy distribution of sediment-clogged dead coral rubble fragments colonised by crinoids, (F) isolated coral rubble patch with a diameter of about 1 m.*

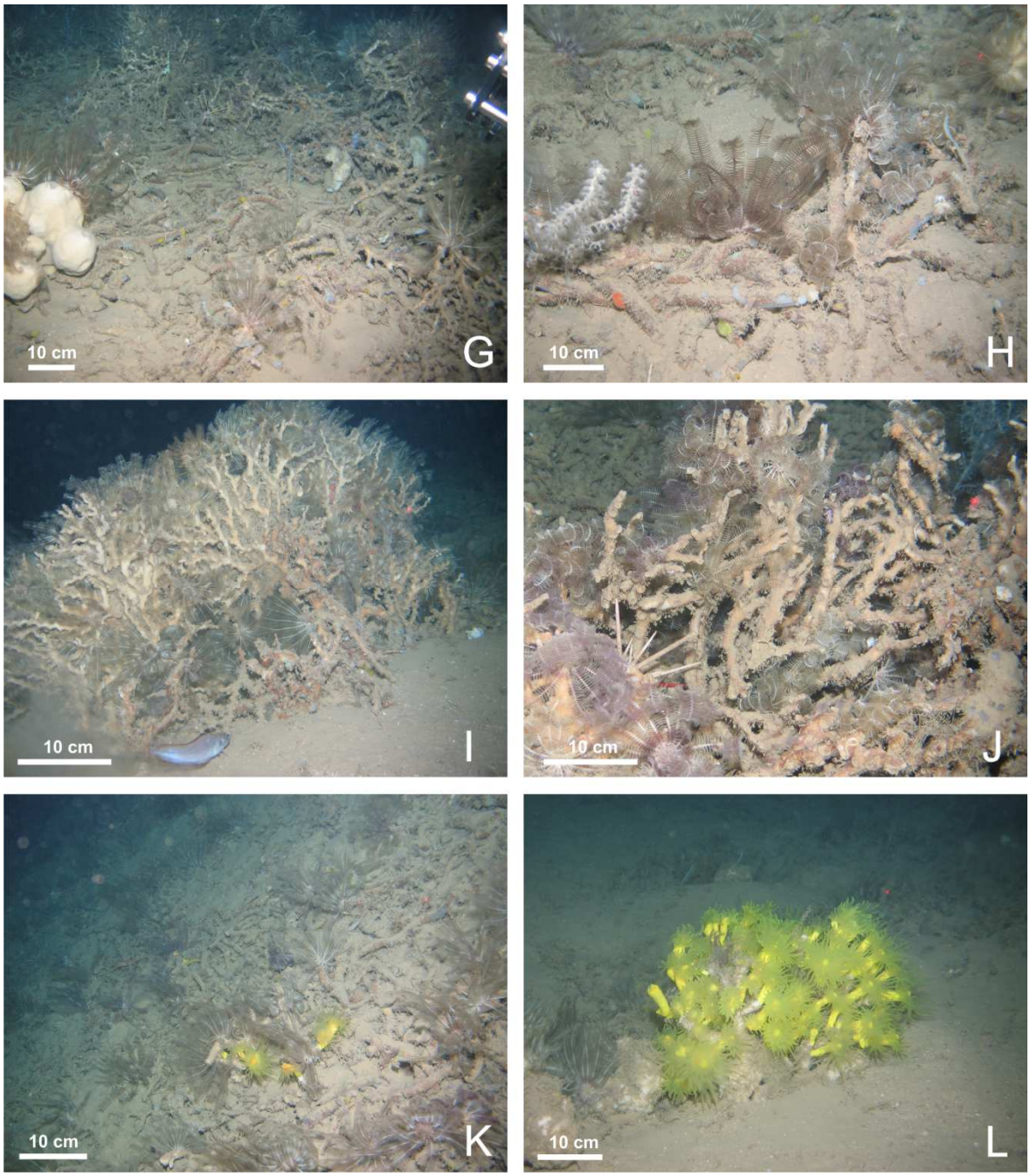

Fig. 3.2G-L *ROV images of facies 3: (G) dense cold-water coral rubble field mainly colonised by crinoids and sponges, (H) zoom on facies 3 illustrating that the coral fragments are covered with a very thin layer of soft sediment, (I) well preserved coral reef fragments (*Lophelia pertusa*) with heights up to 60 cm and also intensively colonised by crinoids, (J) detail of a big coral reef fragment with a sea-urchin and a high amount of crinoids, (K) cold-water coral rubble field with a few living* Dendrophyllia cornigera *on top, and (L) a living* Dendrophyllia cornigera.

Finally, facies 4 describes blocks of outcropping hard substrate, varying in size between 30 cm up to at least 1 m in diameter (Fig. 3.2M-N). At some places they can even reach heights of several decimetres. They are covered by a thin layer of soft sediment and colonised by crinoids, gorgonians and a few scattered sponges. On Alpha Mound, dead cold-water coral fragments were found attached to these rock slabs.

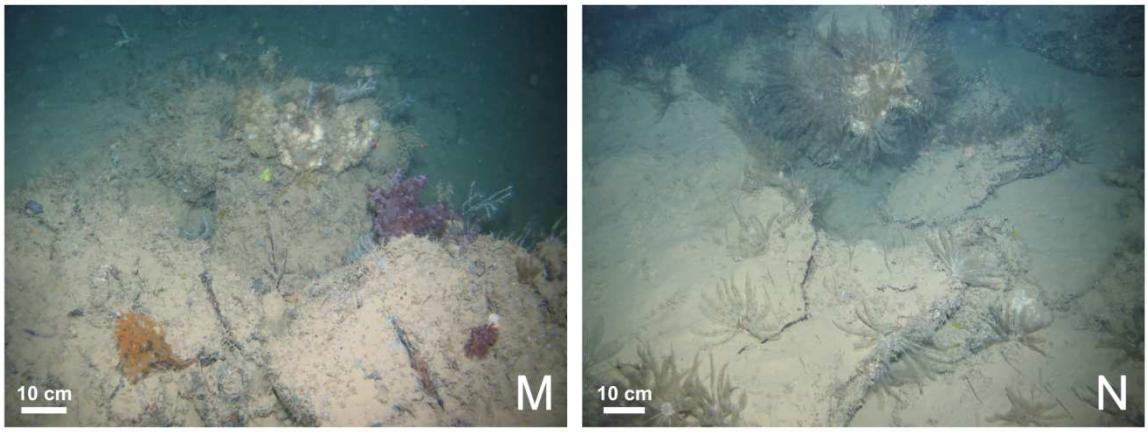

Fig. 3.2M-N *ROV images of facies 4: (M) rock slabs largely colonised by soft corals and sponges, and (N) rock slabs covered with a thin layer of soft sediment colonised by crinoids and sponges.*

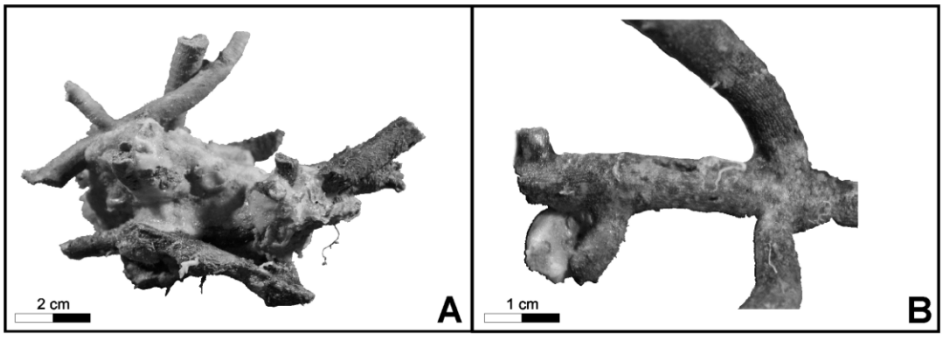

Fig. 3.3 *(A) Close association of dead scleractinian coral skeletons (*Dendrophyllia *sp.) with a demosponge. Coral skeletons are colonised by small scale epifaune such as polychaetes, hydroids and bryozoans (B).*

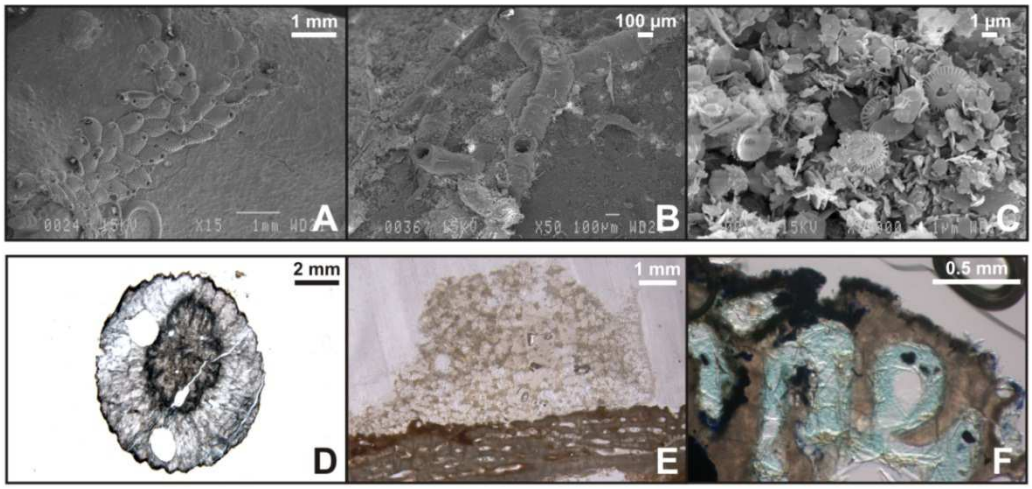

Fig. 3.4 *SEM micrographs (A-C) and microtome sections (D-F), obtained from samples of Beta Mound, with (A) encrusters community (bryozoans, serpulid worm tubes and foraminifera) living on a coral skeleton surface, (B) multi-generation of Polychaete worm tubes, (C) few coccoliths dispersed within the terrigenous mud trapped in the coral framework niches, (D)* L. pertusa *corallite showing circular holes within the sclerenchyme due to excavating sponge activity and fungal infestation and an opaque Fe/Mn coating on the outer surface, (E) small demosponges attached to a dead coral skeleton and borings affecting the coral outer surface resulting in infiltrated terrigenous mud (brown), and (F) scleractinian corallite showing fungal infestation which results in early post-mortem alteration of the corals.*

3.3.2 Facies distribution and sediment composition

Alpha Mound

On Alpha Mound, only three facies were present (Fig. 3.5). The southern and eastern flanks of the mound were largely covered by soft sediments (facies 1) whereas on the mound's summit and northern flank also scattered coral rubble (facies 2) was abundant. Blocks of hard substrate (facies 4) covered an area of 30 by 40 m on top of the mound as well as an area of 20 by 30 m on the northern flank. Also small outcrops of this hard substrate were observed on the southern flank.

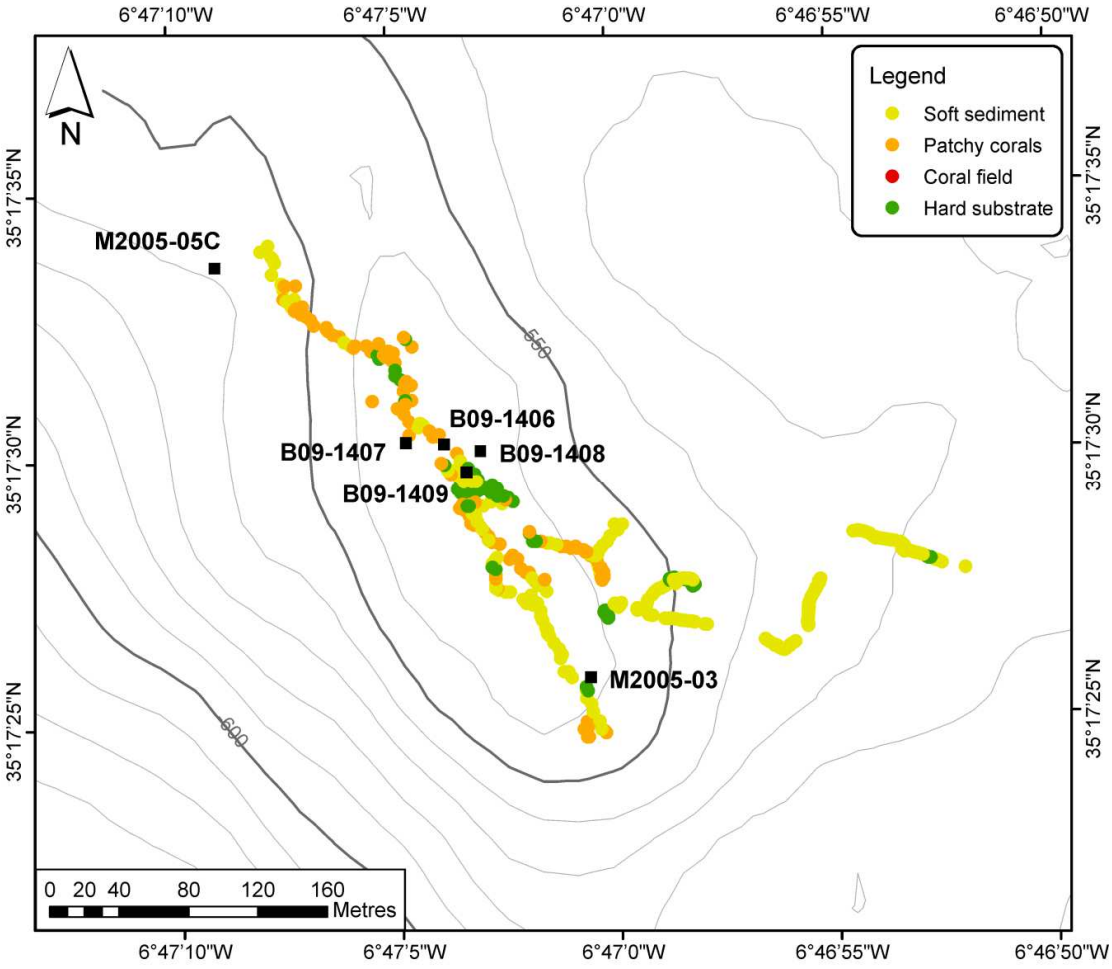

Fig. 3.5 *Facies interpretation map of Alpha Mound based on four ROV Genesis dives (contour interval 10 m). Boxcore samples are marked with black squares.*

All boxcores collected from the top of Alpha Mound (B09-1406-bc, B09-1407-bc, B09-1408-bc and B09-1409-bc) are composed of brownish to greyish silt and contain varying contents of coral fragments comprising mostly *Dendrophyllia* spp. and in a smaller amount *L. pertusa*, *M. oculata* and *Desmophyllum dianthus* (Fig. 3.5 and 3.8A). From a depth of 15 cm in boxcore B09-1409-bc, the first signs of dissolution of the corals are observed. Boxcore M2005-03 is located on the southern slope of Alpha Mound and is also characterised by

brownish to greyish silt with coral debris of *Dendrophyllia* spp. and *L. pertusa*. Finally, boxcore M2005-05C, which is located at the foot of Alpha Mound, consists again of brownish to greyish silt with a lot of coral fragments from a depth of 17 cm. Downcore, the size of the coral fragments decreases.

Beta Mound

The eastern flank of Beta Mound and the depression between its two summits (Fig. 3.6) was covered by soft sediments (facies 1). Scattered coral rubble (facies 2) was restricted to is northern and southern flanks merging into large accumulations of fossil coral framework (facies 3) as observed on the summits of Beta Mound and on its western flank. Finally, blocks of hard substrate (facies 4) occurred in a small area on the western flank in between the two summits.

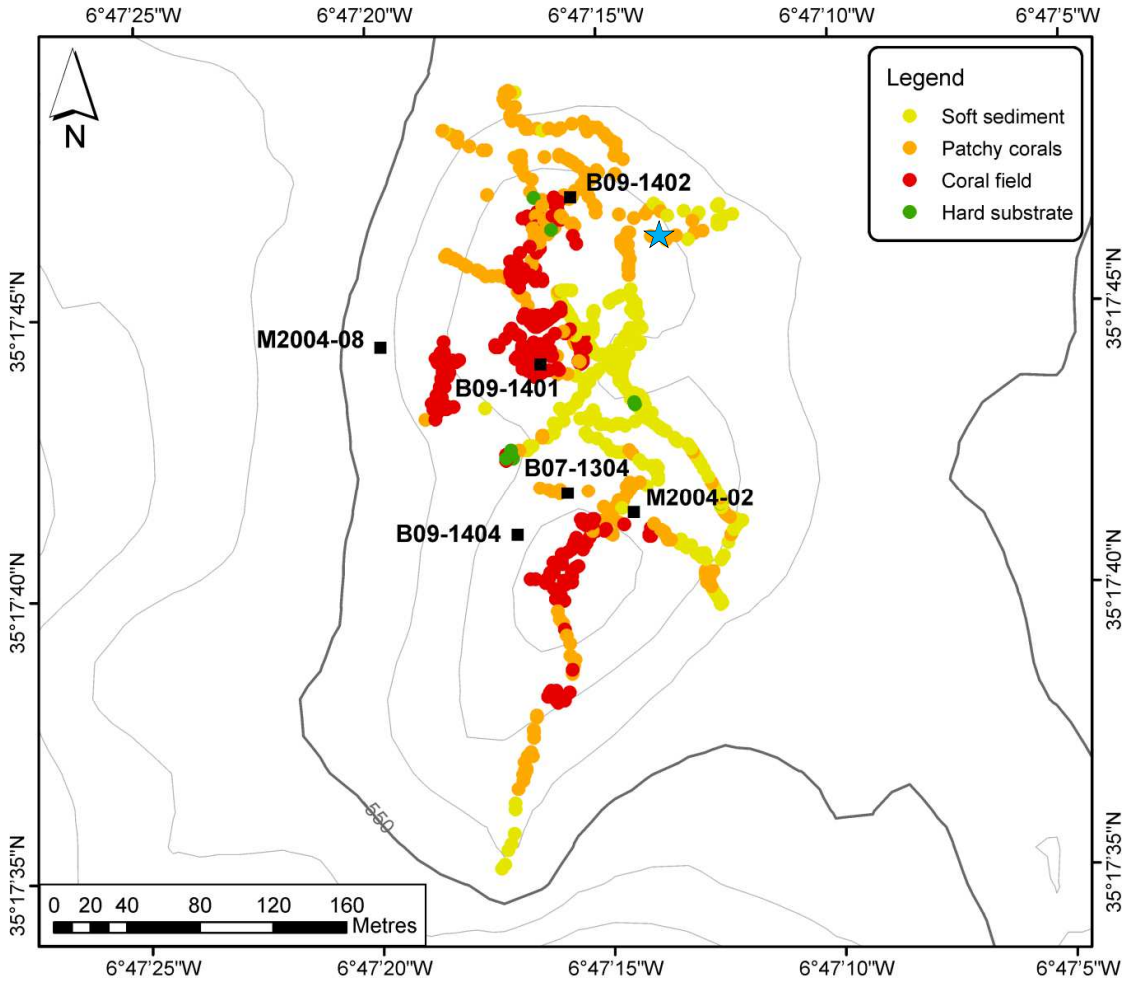

Fig. 3.6 *Facies interpretation map of Beta Mound based on four ROV Genesis dives (contour interval 10 m). Boxcore samples are marked with black squares. The location of the living* Dendrophyllia cornigera *is marked with the blue star.*

Boxcores B09-1401-bc and B09-1402-bc are located on the northern and southern flank, respectively, of the northernmost summit of Beta Mound (Fig. 3.6) and consists of brown silt with mostly *Dendrophyllia* spp. fragments (Fig. 3.8B). M2004-08 is located at the foot of the western slope of the northernmost summit of Beta Mound and consists of brownish to greyish silt with mainly *L. pertusa* coral debris. Boxcores B09-1404-bc, B07-1304-bc and M2004-02 are all located on the northern flank of the southernmost summit and are composed of brownish to greyish silt. They contain varying amounts of *Dendrophyllia* spp., *L. pertusa*, *M. oculata* and *Desmophyllum dianthus* fragments.

On all mounds, only dead cold-water corals were observed, except for one living coral thicket of *Dendrophyllia cornigera* on the eastern flank of the northernmost summit of Beta Mound (water depth of 528 m) (Fig. 3.2L and 3.6) and a few smaller ones on the eastern flank (De Mol et al., 2011a).

Gamma Mound

Unlike the other two mounds, the top of Gamma Mound (Fig. 7) was covered with soft sediment (facies 1) while on the flanks patches of coral fragments (facies 2) and even coral rubble fields (facies 3) were observed. The coral rubble fields vary in size between 10 and 45 m in diameter. However, the surface covered by these fields may be much bigger as it was not possible to delineate the edges of the different fields.

B09-1405-bc is located on the south-western flank of Gamma Mound (Fig. 3.7) and consists of brown to grey silt with big *L. pertusa* fragments (Fig. 3.8C). Boxcores M2005-30 and M2005-31 are located on the flanks of the small mound SE of Gamma Mound. They are both composed of brown to greyish brown silt with cm-sized coral fragments (*L. pertusa*, *M. oculata* and *Desmophyllum dianthus*) which are influenced by dissolution and/or bio-erosion.

Off-mound

All off-mound boxcores collected from the plain north (M2006-21, M2006-22 and M2006-23) and east (M2006-39) of Gamma Mound (Fig. 3.7) are composed of brownish to greyish silt (Fig. 3.8C). Only in boxcore M2006-23 dead coral fragments, mainly *M. oculata*, are observed throughout the entire core. Boxcores M2006-24, M2006-41 and M2004-06, all located on the slope of PDE (Fig. 3.1B and 3.7), consist of brown to grey silt. In all three cores cold-water coral fragments, mainly *L. pertusa*, are observed. In a smaller amount, fragments of *M. oculata* and *Dendrophyllia* spp. are noticed in boxcore M2006-24. Finally, two boxcores (M2006-42 and M2004-07) are obtained at the foot of the escarpment (Fig. 3.1B) and consist of brownish to greyish silt. Cm-sized coral debris is observed in boxcore M2006-42.

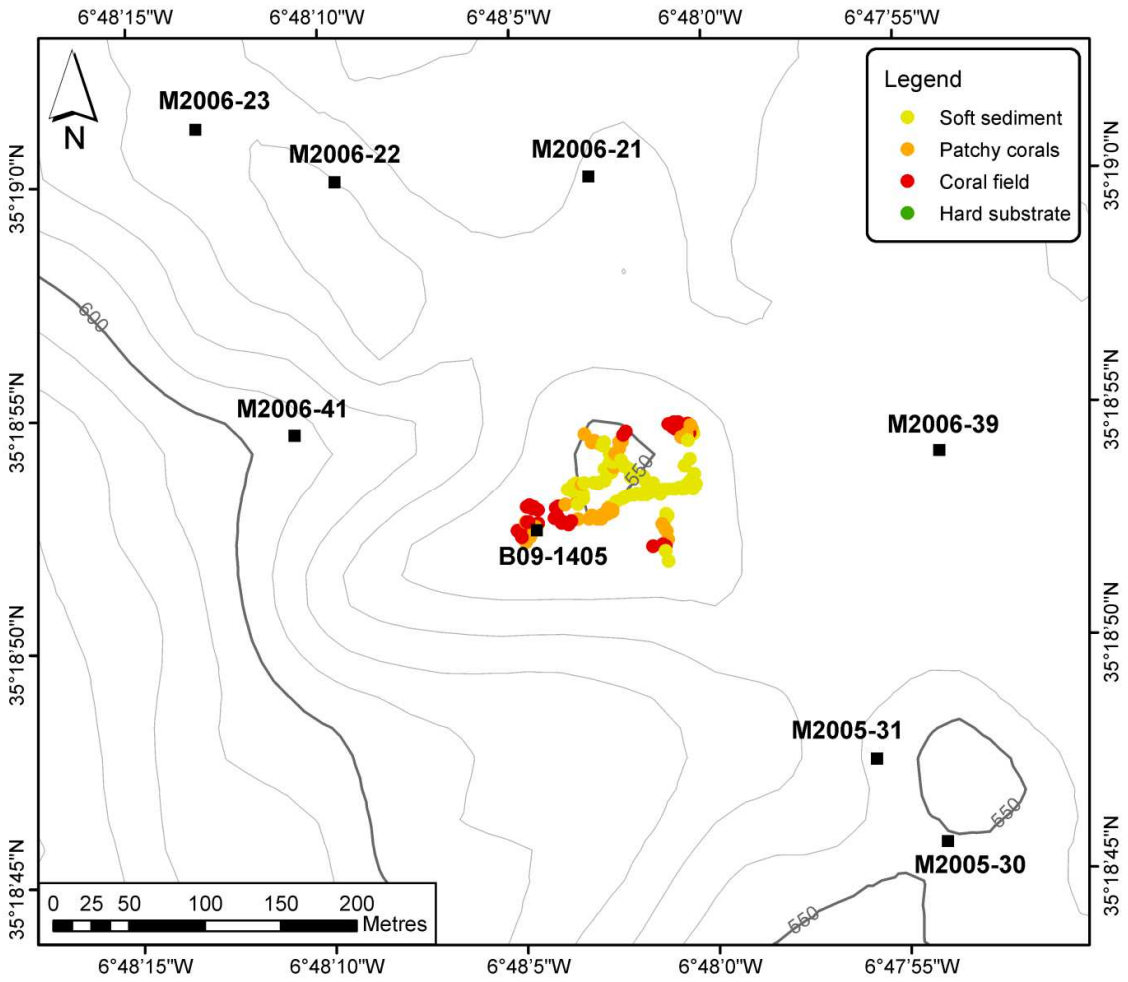

Fig. 3.7 *Facies interpretation map of Gamma Mound based on one ROV Genesis dive (contour interval 10 m). Boxcore samples are marked with black squares.*

3.3.3 U/Th datings

The U/Th datings (Table 3.4; Fig. 3.8) of the *L. pertusa* fragments resulted in ages varying between 11.6 ± 0.3 ka and 40.9 ± 0.7 ka with one outlier of 196 ± 5 ka. In contrast, the U/Th datings of the *Dendrophyllia* fragments resulted in much younger ages varying between 0.16 ± 0.08 ka and 7.1 ± 0.4 ka. Notably, there is an age reversal of 19.3 ± 0.4 ka of *L. pertusa* in boxcore B09-1405-bc around 10 cm while ages of 14.9 ± 0.3 ka and 13.8 ± 0.5 ka are measured at depths of 15 cm and 30 cm, respectively.

3.3.4 Grain-size analyses

In total 64 grain-size analyses were performed at different depths in the boxcores. Table 3.3 shows that the mean grain-size values remain constant for the uppermost 5-10 cm (about 6-7 µm) while below these depths much more scatter and variation is observed between the different areas/mounds and even between the boxcores located on the same mound. In general, the mode varies between 5.92 and 18.79 µm, corresponding with fine to medium

silt, with two extremes of 24.85 and 25.60 µm in boxcore M2005-30. Downcore slightly coarser sediment is present. All results show a poorly-sorted, symmetrical to fine-skewed, unimodal distribution. No difference is observed between the on-mound and off-mound boxcores as well as between the different facies types.

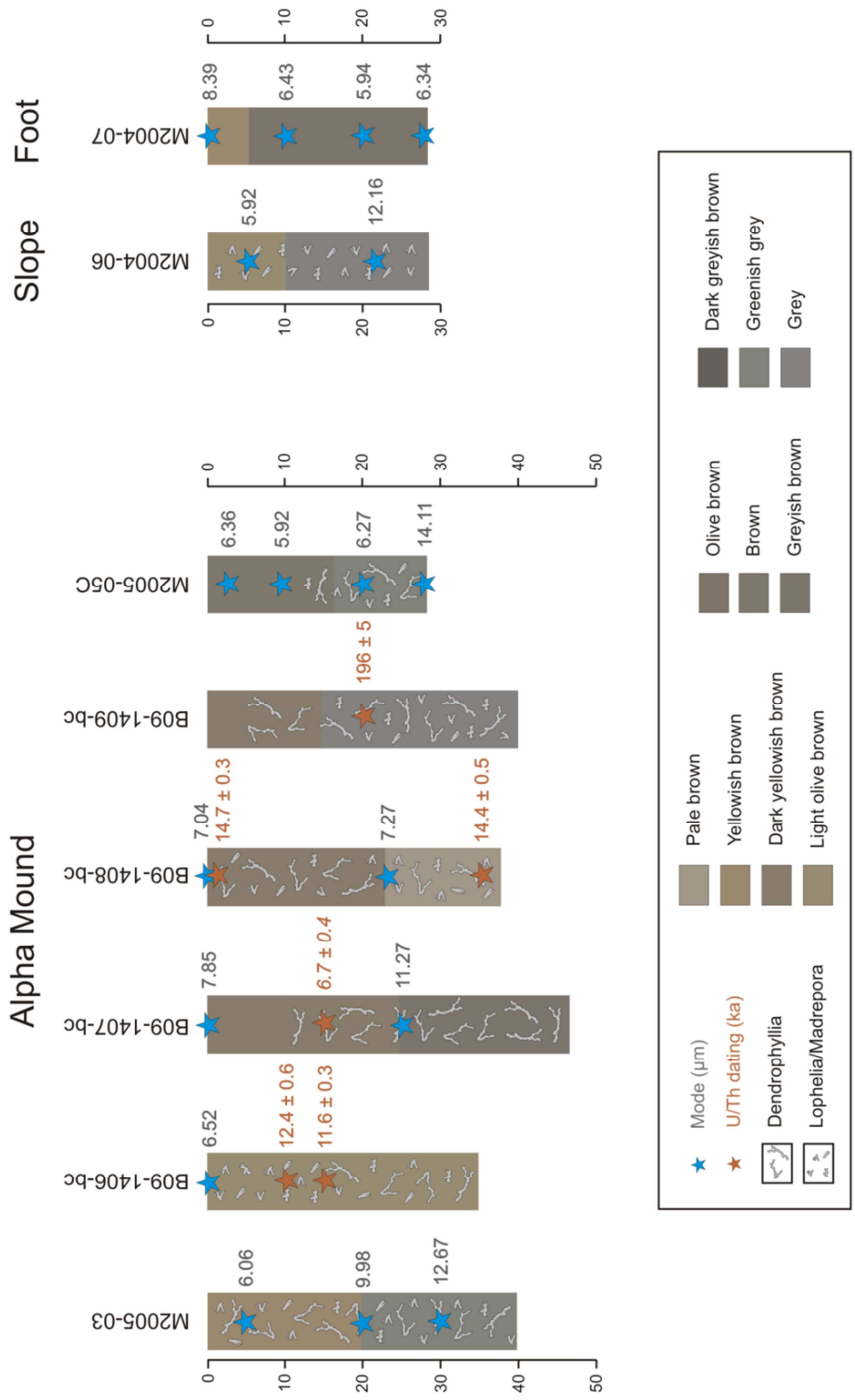

Fig. 3.8A *Description of the boxcores indicating the colour changes and the distribution of the different coral species within the boxcores. The boxcores are grouped per mound and the adjacent slope of Pen Duick Escarpment. The U-series datings are marked in red, the grain-size analysis results in blue.*

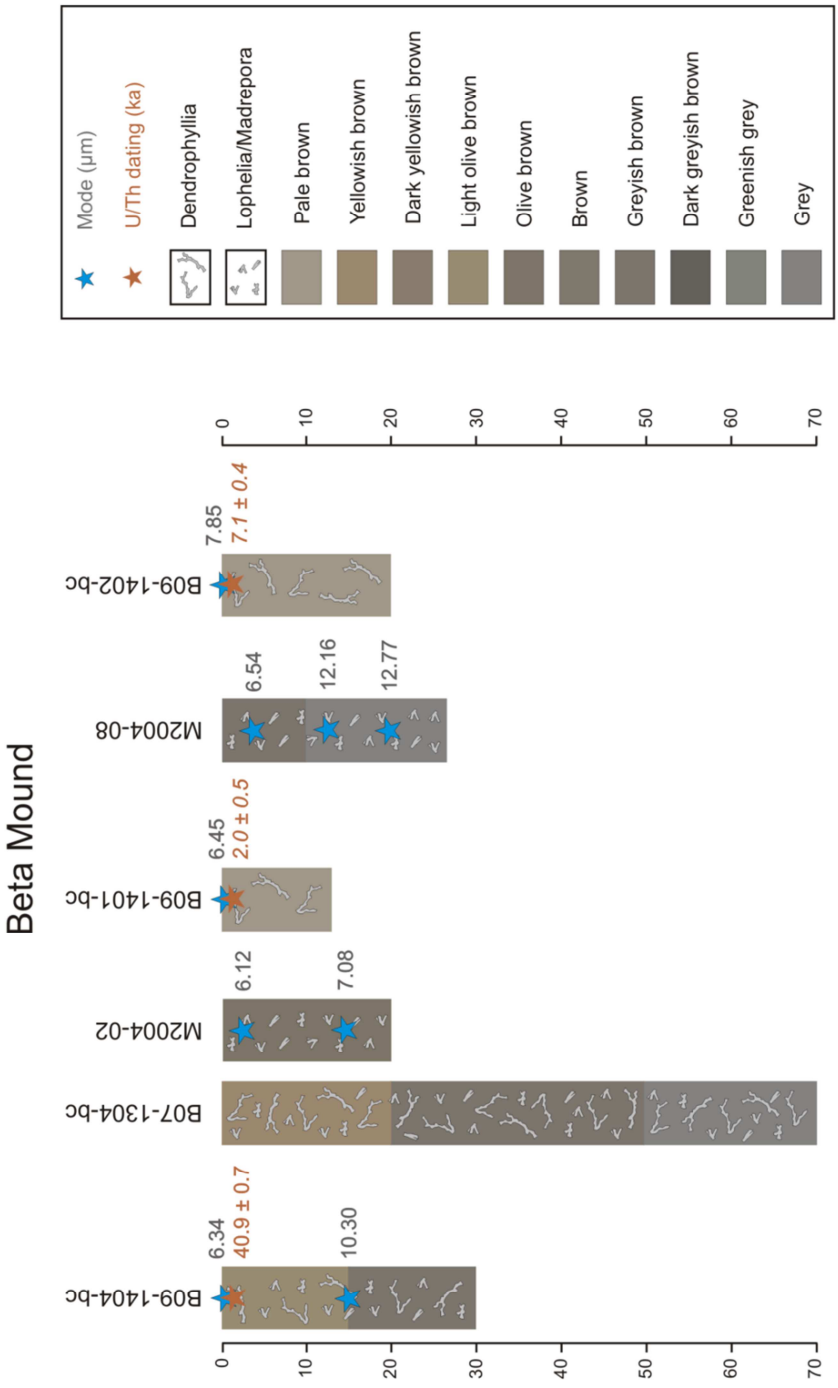

Fig. 3.8B *Description of the boxcores indicating the colour changes and the distribution of the different coral species within the boxcores. The boxcores are grouped per mound and the adjacent slope of Pen Duick Escarpment. The U-series datings are marked in red, the grain-size analysis results in blue.*

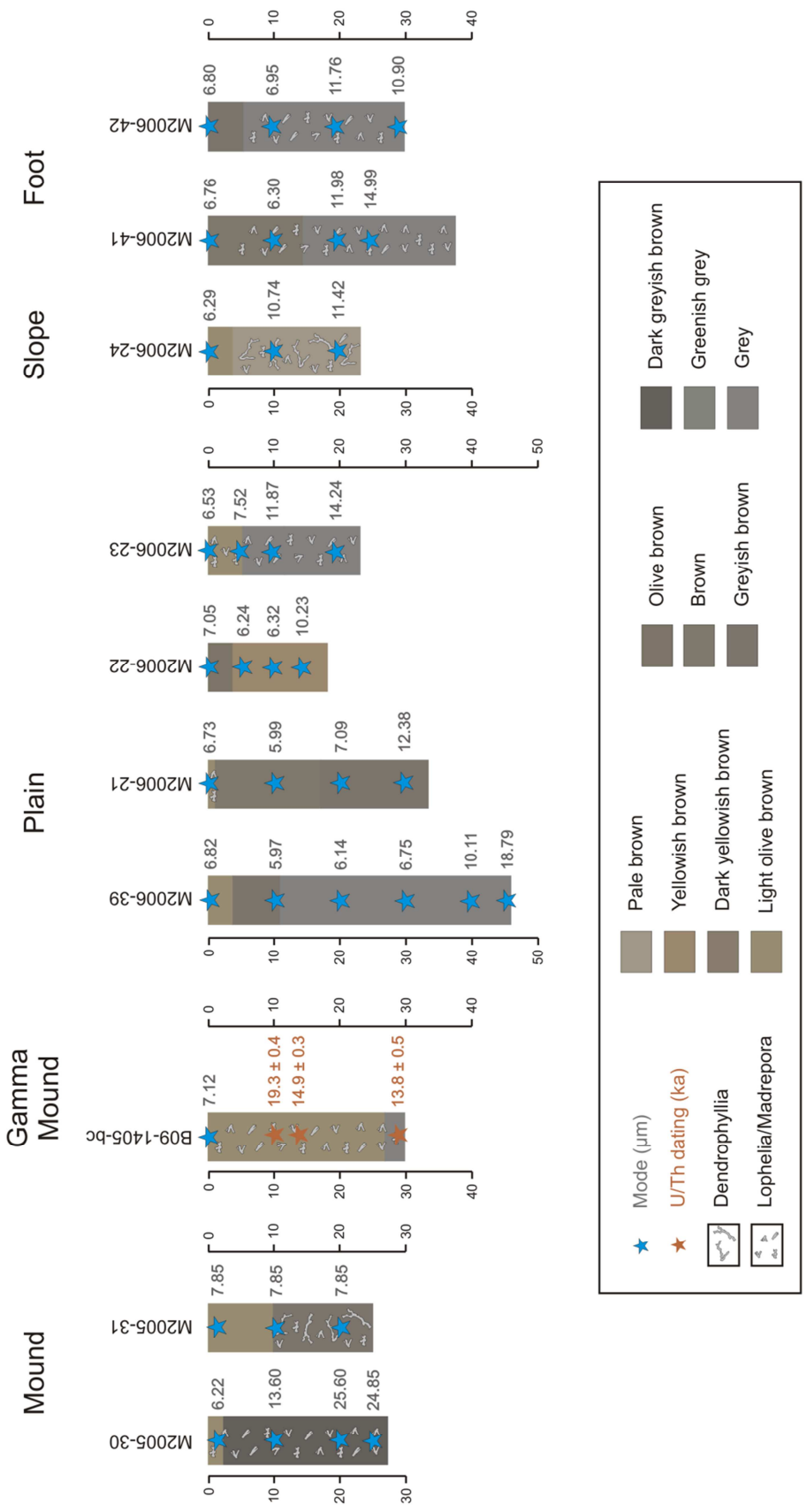

Fig. 3.8C *Description of the boxcores indicating the colour changes and the distribution of the different coral species within the boxcores. The boxcores are grouped per mound and the adjacent slope of Pen Duick Escarpment. The U-series datings are marked in red, the grain-size analysis results in blue.*

3.4 Discussion

3.4.1 Distribution of cold-water corals on PDE

Within the entire Gulf of Cadiz, mainly fossil cold-water corals (*L. pertusa*, *M. oculata* and *Dendrophyllia* sp.) are observed on mound structures, mud volcanoes and other topographic highs in the region (Foubert et al., 2008; Van Rooij et al., 2011; Wienberg et al., 2009, 2010). On the mound structures, a certain distribution pattern of these fossil corals can be expected, taking into account the preference of living corals for strong topographically guided bottom currents (Dorschel et al., 2007a; Freiwald et al., 2004; Mienis et al., 2007). Starting at the top of the mound, well-preserved bushes of coral skeleton will be present. While going down the flanks of the mound, the amount of broken coral fragments will increase, ending up at the base of the mound with only coral rubble. However, the presented ROV and boxcore data does not show a clear spatial trend in the distribution of fossil cold-water corals on the three mounds on PDE. The cold-water corals on Alpha and Beta Mound tend to prefer the north-western and western flank, respectively, and the top of the mound rather than the eastern flank (Fig. 3.5 and 3.6), while on Gamma Mound no cold-water corals, except for a few small patches, are present on top of the mound (Fig. 3.7). Instead, they occur on the flanks. This pattern corresponds with the presence of NE directed residual currents recorded on the PDE during long term near-bed hydrodynamic observations (Mienis et al., 2012). Although coral fragments are observed on the top and flanks of Alpha and Beta Mound, the coral rubble fields (facies 3) are absent on Alpha Mound while on Beta mound rubble fields are observed on the top and more patchy corals on the flanks. Linking the ROV observations with the boxcore data shows that at some locations (e.g. southern flank and top of Alpha Mound) the cold-water coral fragments are covered by a thin layer of sediment while at other locations the coral fragments are still exposed at the seabed. We suggest a process of deposition, non-deposition and erosion on the three mounds, due to local changes in bottom current strength and direction, in order to explain the diversity in distribution pattern on the mounds. The presence of coral rubble and rock slabs on the summits of Alpha and Beta Mound indicates that the present currents on the summits are relatively strong, resulting in non-deposition of sediments or even erosion. The same process is also reflected in the U/Th datings as at some locations corals with an age of about 14 ka are already buried while at other locations corals with the same age are exposed at the surface. In boxcore B09-1404-bc, located close to the top of Beta Mound, a coral with an age of 40.9 ± 0.7 ka is found at the surface, indicating erosion, a long period of non-deposition or a combination of both processes. This is confirmed by Mienis et al. (2012) who measured more vigorous current speeds on top of the escarpment compared to the plain below. The currents on the PDE are still high enough to resuspend fine grained particulate matter (> 100 µm) from the seabed, creating an up to 100 m thick bottom nepheloid layer (Mienis et al., 2012).

When studying the distribution of the different cold-water coral species in more detail, it is observed that *Dendrophyllia* sp. is mainly found on the south-eastern part of the escarpment (Alpha and Beta Mound) while on the north-western part (Gamma Mound) mainly *L. pertusa* and *M. oculata* are observed. This observation was also made by Foubert et al. (2008). Although there is a strong indication of a difference in coral species between the northern and southern areas on the escarpment, *L. pertusa* specimens were also found in some boxcore samples around Alpha and Beta Mound. This preference of coral species may be explained by the morphology of PDE (Fig. 3.1B). Several differences can be observed by comparing both ends of the escarpment. Firstly, there is a change in direction of the escarpment from NW-SE on the south-eastern end to NNW-SSE on the north-western end. Secondly, the NW part is located in deeper water depths than the SE part, and thirdly, the mounds are smaller and not elongated on the NW end. This might result in a difference in food supply, forced by local hydrodynamic conditions (Huvenne et al., 2002; Mienis et al., 2007). Changes in morphology along PDE explain not only the difference in coral species along the escarpment but also the difference in coral distribution pattern and can thus influence the process of deposition, non-deposition and erosion.

Cold-water corals on PDE are not only restricted to the cold-water coral mounds, but also occur along the slope of the escarpment as demonstrated by the presence of corals in nearly all boxcores. These corals can benefit from the strong currents at the top of the escarpment, where the largest coral cover is observed, and will allow the development of smaller coral specimens along the slope. Cold-water corals are not necessarily restricted to topographic highs but are also observed along steep canyon flanks in the Bay of Biscay (De Mol et al., 2011b; Reveillaud et al., 2008). However, it is uncertain whether the corals along the slope are found in situ. Another possibility is that the corals fell down the escarpment. Although the corals already show signs of disintegration and bio-erosion, they are found throughout all boxcores and do not differ much from the on-mound corals, suggesting that they are indeed in situ coral fragments. Although, this remains an assumption.

3.4.2 Growth and distribution of cold-water corals in the past

The U-series dating of nine *L. pertusa* specimens and four *Dendrophyllia* sp. specimens reveals that *Dendrophyllia* sp. continued to live for a short while in the Gulf of Cadiz during the Holocene, whereas *L. pertusa* only occurs during glacial periods (Fig. 3.9). This confirms the conclusions of Wienberg et al. (2009) and Wienberg et al. (2010), who state that, within the Gulf of Cadiz, *L. pertusa* seems to be restricted to the last glacial and prior glacial periods, when long-term stable conditions in terms of water temperature and current strength were present. In contrast to *L. pertusa*, dendrophylliid corals tend to be restricted to periods with relatively stable and warm conditions (Wienberg et al., 2009), and thus appears after the extinction of *L. pertusa* and *M. oculata*. In the present study, the U/Th datings show that *Dendrophyllia* sp. is able to live during the last 12 ka, however, to a lesser

extent than *L. pertusa* and *M. oculata* during glacial periods. This confirms that *Dendrophyllia* sp. is able to survive changing environmental conditions and that this species can adapt to warmer conditions with reduced bottom current strengths. However, at present only a few *Dendrophyllia* are still alive on PDE, indicating that during the Holocene the environmental conditions became less favourable for these corals. According to Voelker et al. (2006) changing environmental conditions at the end of the Younger Dryas caused a sudden decrease in current strength of the MOW. This change in current strength in combination with a decrease in productivity will result in less food supply and higher sedimentation rates, conditions which are not ideal for scleractinian corals to live. On PDE only poorly-sorted sediments with a fine to medium silt-size mode are observed which indicates at present a rather quiescent environment with low current speeds. Indeed, current velocities of 8-9 cm s^{-1} are measured on top of the Renard Ridge with occasionally peak current speeds up to 30 cm s^{-1} (Mienis et al., 2012; Van Rooij et al., 2011). In areas like the Rockall bank where the corals are alive, average current speeds of 10-20 cm s^{-1} are measured with daily peaks up to 45-60 cm s^{-1} (Mienis et al., 2007). A slight increase in grain-size is observed downcore most boxcores, suggesting higher currents in the past. The stronger currents during glacial periods in the southern Gulf of Cadiz might be the result of an enhancement of the lower Mediterranean branch (Llave et al., 2006; Voelker et al., 2006). The major extinction of *L. pertusa* and *M. oculata* at the end of the Younger Dryas can thus be explained by a sudden change in environmental conditions and current patterns, resulting in higher bottom-water temperatures and a decrease in bottom current strength.

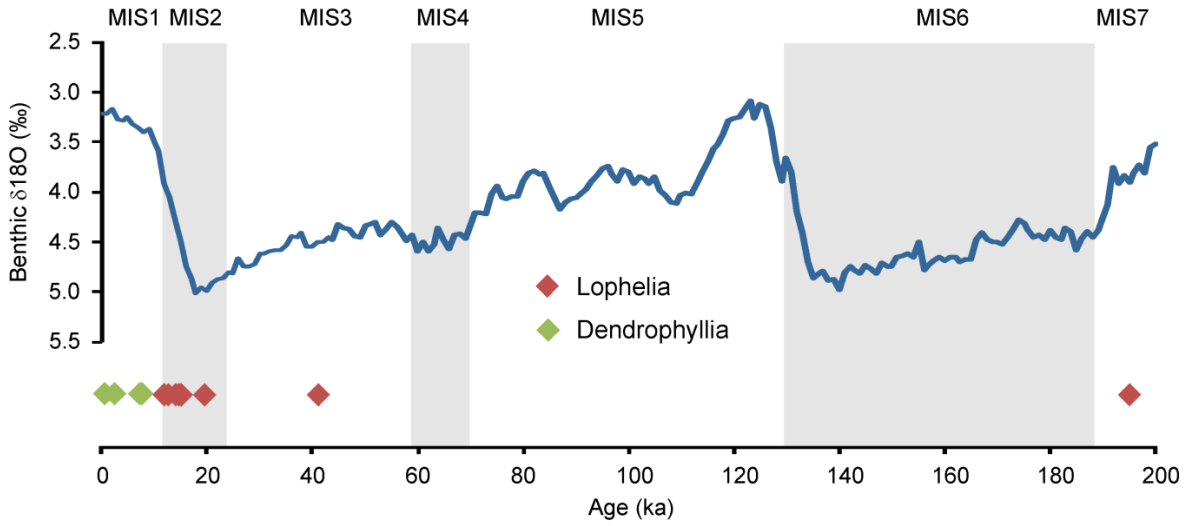

Fig. 3.9 *Results of the U/Th datings on the Pen Duick mounds cold-water corals, superimposed on the benthic $\delta^{18}O$ stack of Lisiecki and Raymo (2005).*

3.4.3 Role of cold-water coral rubble fields

The observed cold-water coral rubble fields (facies 3), corresponding with thick accumulations of fossil cold-water corals, create niches for micro-organisms to live and hide within the three-dimensional (open) coral framework and may play an important role in

creating high biodiversity in and around these coral fields. Even though no living cold-water corals are present, the dead coral framework can still create a habitat which is favourable to many other organisms, e.g. poriferans, crinoids, octocorals, crustaceans, fish (Bongiorni et al., 2010; De Mol et al., 2011a; Henry and Roberts, 2007; Jensen and Frederiksen, 1992; Raes and Vanreusel, 2005). The fauna associated with living *L. pertusa* colonies is in general poorer than on dead colonies (Mortensen et al., 1995) and even a more diverse fauna is found on dead corals (Jensen and Frederiksen, 1992) due to the sheltering function and higher habitat complexity of the three-dimensional coral framework (Mortensen et al., 1995). Therefore, the protection of deep-water corals and more specifically of dead cold-water corals can contribute to the maintenance of a high deep-sea biodiversity along continental margins (Bongiorni et al., 2010). Living corals are able to protect themselves against the settlement of sessile organisms by an increase in mucus production and selective sclerenchyme precipitation (Freiwald and Wilson, 1998). The slimy decay products of these associated sponges and other metazoans, observed on the coral framework elements, may play a significant role in sediment fixing, and thus burying the open framework, which was observed on top of Gamma Mound.

Microbial community distribution patterns are important in understanding cold-water mound development and preservation as a geological feature (Castanier et al., 1999; Henriet and Guidard, 2002; Neulinger et al., 2009). Microbes contribute to organic matter remineralisation processes that have a direct consequence on pH and alkalinity and, therefore, control both carbonate formation and preservation (Tribble, 1993). This has been documented for NE Atlantic cold-water coral mounds (Ferdelman et al., 2006; Pirlet et al., 2010; van der Land et al., 2010; Webster et al., 2009; Wehrmann et al., 2009) where microbes act as a major agent of cold-water coral reef initiation and subsequent mound geometry formation through early diagenetic mechanisms (e.g. early induration versus dissolution). Even though it has not yet been proven for PDE, microbial communities might play an important role in providing the initial relevant substrate (carbonate slabs) for coral communities to settle (Templer et al., 2011).

3.4.4 Presence of carbonate slabs

The outcropping hard substrate, observed on Alpha and Beta Mound, can be related to authigenic carbonate slabs (Fig. 3.10). These slabs were sampled by video-guided grab sampling near the northeast side of Beta Mound during the TTR12 cruise on board R/V Prof Logachev (Foubert et al., 2008) as well as by boxcoring on the southwest slope during the 2004 HERMES cruise on board R/V Pelagia (Depreiter, 2009). They consist of greyish to brownish lithified mud with variable inclusion of bioclasts (e.g. bivalve shells, coral and crinoid fragments, gastropods) and traces of bioerosion. In thin section, the slabs are mud-supported fossil-bearing micritic limestones (mudstones) to wackestones. They show variable carbonate mineralogy, although the mudstones mainly consist of dolomite and low-

Mg calcite while the wackestone mainly consist of low-Mg and high-Mg calcite with some dolomite. The $\delta^{18}O$ composition (2-5 ‰) indicates that the carbonates precipitated in equilibrium with seawater (Depreiter, 2009).

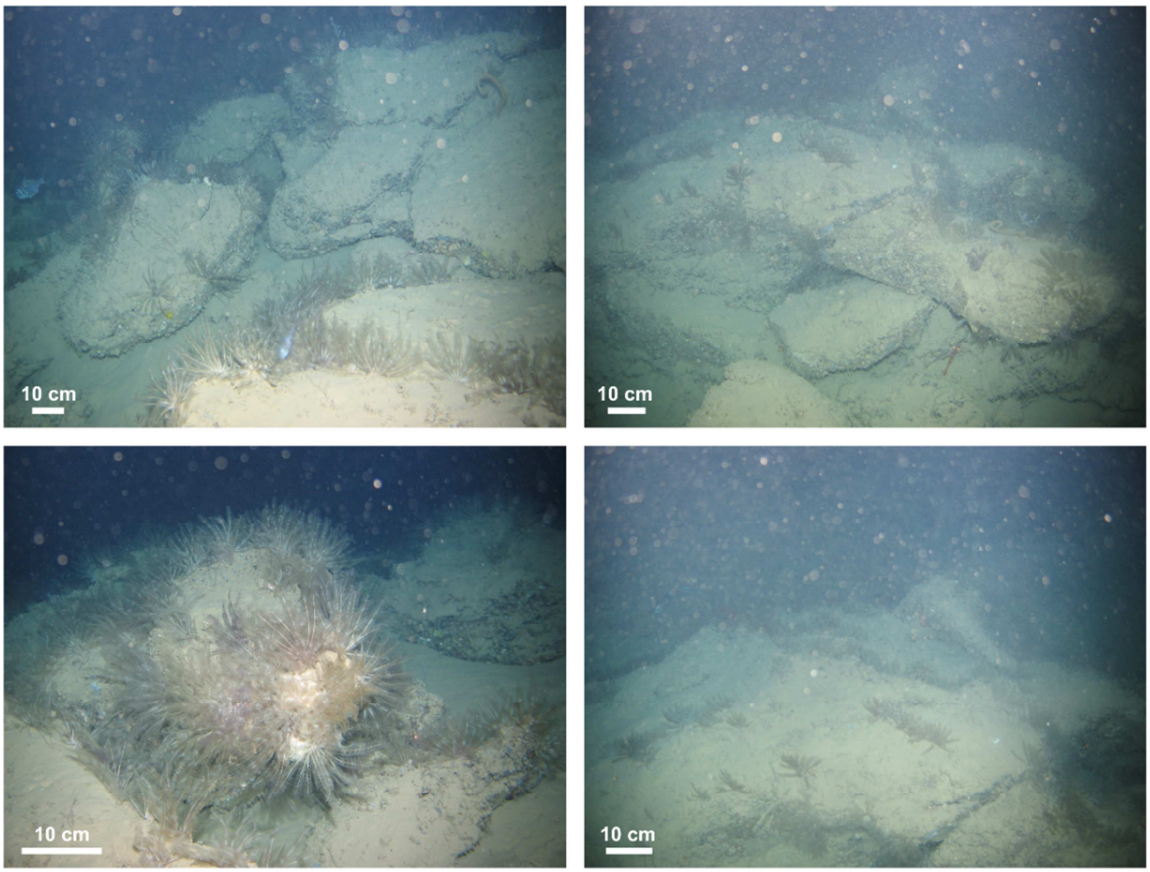

Fig. 3.10 *ROV images of the observed carbonate slabs on top of Alpha Mound.*

Several hypotheses can be proposed in order to explain the formation of carbonate slabs on top of a cold-water coral mound. However, further research, including intensive sampling of the carbonate slabs on different locations, is necessary in order to eliminate possible theories.

(1) Noé et al. (2006) already reported the presence of hardgrounds on the flanks and top of numerous carbonate mounds in the Porcupine Seabight and Rockall area off Ireland. A detailed study revealed that these hardgrounds are the result of early diagenetic lithification of pelagic foraminiferal-nannoplankton oozes with admixed benthic skeletal debris in a shallow subsurface realm. Intensified velocities of long-slope bottom currents favour the exhumation of the lithified carbonates, resulting in the presence of these hardgrounds at the surface. No indication for microbially mediated, methane-induced cementation was found (Noé et al., 2006). In contrast, results from bulk stable isotope analyses from the slabs on the Pen Duick mounds show $\delta^{13}C$ values in the range of -30 to -20‰, indicating the influence of methane (Depreiter, 2009).

(2) Pirlet et al. (2010) relates the formation of a lithified carbonate layer in Mound Perseverance (Porcupine Seabight) to aragonite dissolution. Excess calcium and bicarbonate diffuse upwards from sites where pyrite oxidation occurs. Reaching the seafloor, carbonate precipitates due to an increased pH and $CaCO_3$ saturation of the interstitial water. The appearance of the lithified carbonate layer at the sea bed can be attributed to increased currents (erosion) and/or a reduced sedimentation regime.

(3) A third process inducing carbonate formation is organomineralisation (Neuweiler et al., 1999; Noé et al., 2006), due to the close association of Porifera and scleractinian corals. Common in modern Atlantic deep-water environments (e.g. Sula ridge, offshore Norway, Freiwald et al., 1999), their intricate three-dimensional association (Fig. 3.7A) within cold-water coral rubble fields has a strong potential to drive an organomineralisation process (Trichet and Défarge, 1995). A process much like it has been documented in a modern tropical environment (Neuweiler et al., 2007) or ancient sponge-rich carbonate mounds (Desrochers et al., 2007; Neuweiler et al., 1999; Neuweiler et al., 2009). In such case, during suboxic cycling of organic matter, sponge-rich cryptic communities would provide both a suitable substrate and reactive fluids for authigenic carbonate formation. Within PDE, fluorescent dissolved organic matter (FDOM) patterns in pore-waters have been investigated (Larmagnat and Neuweiler, 2011). Although reactive FDOM fluids are locally present, no evidence of authigenic carbonate precipitation through induced and supported organomineralisation (ISOM) has been found yet.

(4) However, on the Pen Duick mounds the influence of methane cannot be excluded. Methane can play a major role in fluid seepage and thus in the formation of the carbonate slabs. According to Wehrmann et al. (2011) the mounds can be grouped in two areas based on their geochemical signatures. On one hand there is Alpha and Beta Mound, which are affected by a shallow sulphate-methane transition zone (SMTZ), and on the other hand Gamma Mound, where there is no influence of such shallow SMTZ in the upper 5 m. However, below 5 m, relatively high $\delta^{34}S$ values of the sedimentary pyrite in Gamma Mound suggest the upward diffusion of hydrogen sulfide from a SMTZ below (Pirlet, 2010). On PDE, Alpha and Beta Mound are two distinctive cases, affected by ascending hydrocarbon fluids that most likely have a deep thermogenic origin (Hensen et al., 2007; Maignien et al., 2011; Stadnitskaia et al., 2006; Wehrmann et al., 2011). The occurrence of methane is associated with a shallow position of the SMTZ (Maignien et al., 2011; Wehrmann et al., 2011). Based on DIC production and ^{13}C stable isotopes data, such SMTZ is interpreted as the result of microbial anaerobic oxidation of methane coupled with sulphate reduction (Boetius et al., 2000; Maignien et al., 2011; Wehrmann et al., 2011). Well documented in the literature of cold-seep settings (Luff and Wallmann, 2003; Luff et al., 2004), authigenic carbonates form through AOM-

derived dissolved inorganic carbon (DIC) precipitation. In addition, the presence of Gemini mud volcano can also play a role in this process. The south-eastern end of PDE is separated from its closest neighbouring mud volcano, namely Gemini mud volcano, by only a 1 km wide SW-NE moat feature (Van Rensbergen et al., 2005; Van Rooij et al., 2011). This mud volcano is one of the most active mud volcanoes in the area as indicated by little pelagic drape, a shallow sulphate reduction zone and high methane concentrations, as a result of fluid seepage and sediment extrusion (Van Rensbergen et al., 2005). In a gravity core on Alpha Mound (obtained during the TTR12 cruise in 2002) mud breccia and mud clasts were observed, indicating the influence of recent mud volcano activity (Foubert et al., 2008). These mud breccia and clasts show similar characteristics as those obtained from cores on Gemini mud volcano (Foubert et al., 2008; Van Rensbergen et al., 2005). However, no clear migration pathways are observed on seismic profiles (Van Rooij et al., 2011).

Such authigenic carbonates are not only observed on the Pen Duick Escarpment but also in other areas in the Gulf of Cadiz (Díaz-del-Río et al., 2003; León et al., 2006; León et al., 2007). Recently, Magalhães et al. (2012) presented a comprehensive overview and detailed characterisation of all the different types of methane-derived authigenic carbonates from the Gulf of Cadiz. Two main types were distinguished: dolomite dominated crusts, irregular massive forms and chimneys on one hand and aragonite dominated pavements and build-ups on the other hand. The dolomite-dominated samples result from cementation along fluid conduits inside the sedimentary column. In contrast, the aragonite-dominated samples represent precipitation of authigenic carbonates at the sediment-seawater interface or close to it, in a high alkalinity environment resulting from anaerobic oxidation of methane-rich fluids venting into sulphate-bearing pore waters. On the Pen Duick Escarpment, both types of authigenic carbonates were observed (Magalhães et al., 2012).

3.4.5 Comparison with other mound areas along the Atlantic Margin

Cold-water coral fragments are observed in all boxcores, suggesting that once large flourishing reefs have covered the mounds in the southern Gulf of Cadiz. U/Th datings revealed that these *L. pertusa* and *M. oculata* reefs preferred glacial times. More to the south, similar observations were made. On mounds along the Mauritanian margin, cold-water coral growth also mainly occurred during past glacial and interstadial climate periods (Eisele et al., 2011). During these cold periods the productivity increased due to upwelling and modified nutrient availability, creating a more suitable environment for cold-water corals (Frank et al., 2011). In contrast, more to the north along the NE Atlantic margin, fossil corals and coral rubble are mostly found in close association with still living cold-water corals, preferring interglacial periods to thrive, e.g. on the cold-water coral mounds in the Porcupine Seabight and along the margins of the Rockall Trough (Dorschel et al., 2005, 2007a; Foubert et al., 2005; Frank et al., 2009; Huvenne et al., 2005; Mienis et al., 2006;

Rüggeberg et al., 2007; van Weering et al., 2003; Wheeler et al., 2005). Glacial environmental conditions resulted in a reduction of cold-water corals north of 50°N (Frank et al., 2011). Subsequently, the coral mounds in the Gulf of Cadiz can be considered as a recent analogue of the mounds in the Porcupine Seabight and Rockall Trough during glacial times when there were no living corals.

The distribution pattern of the cold-water corals on Alpha and Beta Mound is coherent with the coral distribution observed in the Porcupine Seabight and the Rockall Trough. In these areas the highest and densest coral cover is found on the summit of the mounds, while on the flanks the coral abundance is decreasing and mainly coral debris and living coral patches are found (Dorschel et al., 2007a; Huvenne et al., 2005; van Weering et al., 2003; Wheeler et al., 2005). The distribution of the cold-water corals in these areas is controlled by locally enhanced currents and internal tides, providing food for the corals and preventing the settling of sediment (Kenyon et al., 2003; Mienis et al., 2007; White et al., 2005). An additional asymmetry is noted in the Porcupine Seabight related to the direction of the strongest bottom currents (Dorschel et al., 2007a). Nevertheless, comparing the grain-size distributions, differences are observed between the on-mound areas and the off-mound areas in the Porcupine Seabight and the Rockall Trough, while on PDE a homogeneous distribution in grain-size is present. The off-mound areas are typically covered by sandy deposits of ice-rafted material while on-mound areas, with a dense coral cover, mostly correspond with recent silty sediments (de Haas et al., 2009; Dorschel et al., 2007a; Mienis et al., 2009; Wheeler et al., 2011). According to Pirlet et al. (2011) and Thierens et al. (2010), this ice-rafted debris plays an important role in the mound development in the Porcupine Seabight. Within the Gulf of Cadiz there is no influence of this ice-rafted debris and thus no supply of coarse sediments which explains the presence of silty sediments with uniform grain-size value. The absence of ice-rafted debris can explain the difference in size and morphology between both mound areas. This basic difference in combination with a different hydrodynamic context (e.g. stronger bottom currents up north) is essential to understand both mound systems and their main differences.

3.5 Conclusions

ROV observations and boxcore analyses facilitate the first detailed mapping of three cold-water coral mounds (Alpha, Beta and Gamma Mound) on top of an escarpment in the southern Gulf of Cadiz. Hence, this allows studying the present distribution of fossil cold-water corals, the growth and distribution of these corals in the past, and the role of cold-water coral rubble fields.

Based on the sediment nature and the macrofaunal assemblages, four different facies were distinguished on the mounds. The coral distribution pattern is most likely the result of local variations in bottom current strength and direction, inducing local areas of deposition, non-

deposition and erosion. Additionally, this process is influenced by differences in the morphology of the escarpment between the SE and NW part. This explains the rather similar distribution pattern on Alpha and Beta Mound on one hand and Gamma Mound on the other hand. Remarkable is the preference of *L. pertusa* and *M. oculata* for the north-western part of PDE while *Dendrophyllia* sp. mostly occurs on the south-eastern end. Mainly fossil cold-water corals were found, except for a few living *Dendrophyllia* sp. specimens on the north-eastern flank of Beta Mound. U-series datings revealed that these *Dendrophyllia* sp. started to grow after the extinction of *L. pertusa* and *M. oculata*. This confirms that *Dendrophyllia* sp. prefers warmer conditions with reduced bottom currents while *L. pertusa* and *M. oculata* prefer colder environments. The observed cold-water coral fields can be considered as ideal hotspots for biodiversity. Although the cold-water corals are dead, creating open frameworks, they can still act as habitat for many other organisms.

Acknowledgements

The authors would like to thank the shipboard parties of the R/V Belgica 07/13 and 09/14 cruises and the R/V Pelagia 64PE229, 64PE237 and 64PE253 cruises for their help and nice cooperation during the cruises. This work was financially supported by the EC FP6 HERMES project “Hotspot Ecosystem Research on the Margins of European Seas” (GOCE-CT-2005-511234-1), the EC FP7 HERMIONE project “Hotspot Ecosystem Research and Man’s Impact on European Seas” (contract number 226354) and the ESF EuroDIVERSITY MiCROSYSTEMS project (05_EDIV_FP083-MICROSYSTEMS). We are grateful to Prof. Dr. M. Vincx (Marine Biology Section, Ghent University) for allowing us to use the Malvern Mastersizer 2000. S. Larmagnat acknowledges funds from the Natural sciences and Engineering Research Council of Canada (NSERC, SRO-project: Atlantic coral mounds). S. Larmagnat is grateful to R. Janvier (Interfaculty Histology Lab, Laval University) for the preparation of the CPD samples and to A. Ferland (Microanalysis-SEM Lab, Geology Department, Laval University) for his help with the SEM observations. The authors would like to thank the reviewers and H. de Stigter for their useful comments to improve the manuscript. L. De Mol acknowledges the support of the “Agency for Innovation by Science and Technology in Flanders (IWT)”.

Chapter 4

Glacial evolution and growth of cold-water coral mounds in the southern Gulf of Cadiz

Modified from:

De Mol, L., Pirlet, H., Van Rooij, D., Blamart, D., Cnudde, V., Stuut, J.-B., Duyck, P., De Batist, M. & Henriet, J.-P. (in preparation). Glacial evolution and growth of cold-water coral mounds in the southern Gulf of Cadiz. Sedimentology.

Abstract

In 2002, cold-water coral mounds were discovered on top of the Pen Duick Escarpment in the El Arraiche mud volcano field (southern Gulf of Cadiz). Gravity cores from three of these coral mounds were investigated using CT scanning, magnetic susceptibility, X-ray fluorescence, grain-size analysis, end-member modelling, stable carbon and oxygen isotope analysis, and U-series dating in order to reconstruct different phases of mound and coral growth, assess the impact of early diagenesis on the sedimentary record and to link these processes with specific palaeoenvironmental conditions. This study shows that diagenetic processes, like dissolution of carbonates, the formation of pyrite and carbonate precipitation, play an important role in mound build-up. However, we looked further and tried to unravel paleoenvironmental signals from the input of terrigenous sediment in a cold-water coral mound which is not significantly altered by diagenetic processes. The growth and evolution of the Pen Duick mounds are linked to climatic changes on the NW African continent. Lophelia pertusa *and* Madrepora oculata *are the dominant species within the mounds, indicating intense coral growth during glacial periods. Additionally, mound growth is also related to glacial times (mainly to Marine Isotopic Stages 2-4 and 8) due to the high input of aeolian dust during these periods. During interglacials coral growth is very limited and will result in slowing down or interrupting the mound building process.*

4.1 Introduction

Cold-water corals are widely distributed along the Northeast Atlantic margin (Freiwald et al., 2004; Freiwald and Roberts, 2005; Roberts et al., 2009), where they occur as patches and may even form reefs or large mound structures (Freiwald et al., 1999; Roberts et al., 2005). These mound structures can be up to 300 m high and are mostly covered by cold-water corals (living and/or dead). The best studied examples along the NE Atlantic margin can be found in the Porcupine Seabight (De Mol et al., 2002) and on the margins of the Rockall Trough (Kenyon et al., 2003; Masson et al., 2003). Within the Gulf of Cadiz submarine ridges and steep fault escarpments occur, which can favour the settlement of scleractinians and facilitate the build-up of cold-water coral mounds, if the appropriate environmental conditions are met (Foubert et al., 2008; Wienberg et al., 2009). One of these sites is the Pen Duick Escarpment (PDE), situated in the El Arraiche mud volcano field on the Moroccan continental margin (Van Rensbergen et al., 2005). Up to now, 15 cold-water coral mounds have been identified on top of this escarpment with an average elevation of 15 m (Foubert et al., 2008; Van Rooij et al., 2011). During the R/V Marion Dufresne 169 'MiCROSYSTEMS' cruise, gravity cores were obtained on three of these mounds for sedimentological and palaeoceanographic analyses in order to unveil the architectural framework of these cold-water coral build-ups. Compared to the mounds in the Porcupine Seabight and these on the margins of the Rockall Trough, the mounds on the PDE are much smaller in size, making them ideal to study the initial build-up and evolution of the mounds.

Two mechanisms have been proposed for the initiation of cold-water coral mounds: (1) the seepage of hydrocarbons (Henriet et al., 1998; Hovland et al., 1994) and (2) the influence of external environmental conditions like substrate, temperature, salinity, hydrographic regime, sedimentation and food availability (Carlier et al., 2009; Duineveld et al., 2007; Eisele et al., 2011; Mienis et al., 2007; Kiriakoulakis et al., 2007; White et al., 2005; Wienberg et al., 2009; Wienberg et al., 2010). Up till now, no decisive answer can be given about 'the' mechanism for mound build-up, however, most authors favour the second option as only a few cold-water coral habitats were found in the vicinity of cold seeps and fault zones (Henriet et al., 1998; Hovland et al., 1998; Hovland and Risk, 2003; Masson et al., 2003). Within the Gulf of Cadiz, a three-phase mound development model was proposed by Foubert et al. (2008). First, the cold-water corals start to colonise suitable substrates, followed by the build-up phase which is controlled by the interplay between sediments, currents and cold-water corals. Finally, this initial mound structure is affected by diagenetic processes under influence of fluid seepage. These diagenetic processes are further discussed in Pirlet et al. (2012) and Wehrmann et al. (2011).

This chapter presents the results of a detailed study of three sediment cores from three cold-water coral mounds on top of the PDE (Fig. 4.1). Medical CT facies characterisation combined with the quantification of coral fragments was used in order to obtain a general

overview of the internal structure of the coral mounds and reveal the processes (e.g. diagenetic and/or palaeoenvironmental) acting within the mounds. Additional micro-CT scanning was performed on a selection of subsamples, resulting in high-resolution images of these processes and products. The observed variations in grain-size and chemical composition are discussed in relation to the provenance of the terrigenous sediments from potential source areas on the adjacent continent. Considering the interpretation of the end-member modelling analysis, we postulate that changes in the ratios of the end-members reflect paleoclimatic variations in NW Africa. Finally, a general growth model is proposed for the cold-water coral mounds on the PDE and compared with other mound areas.

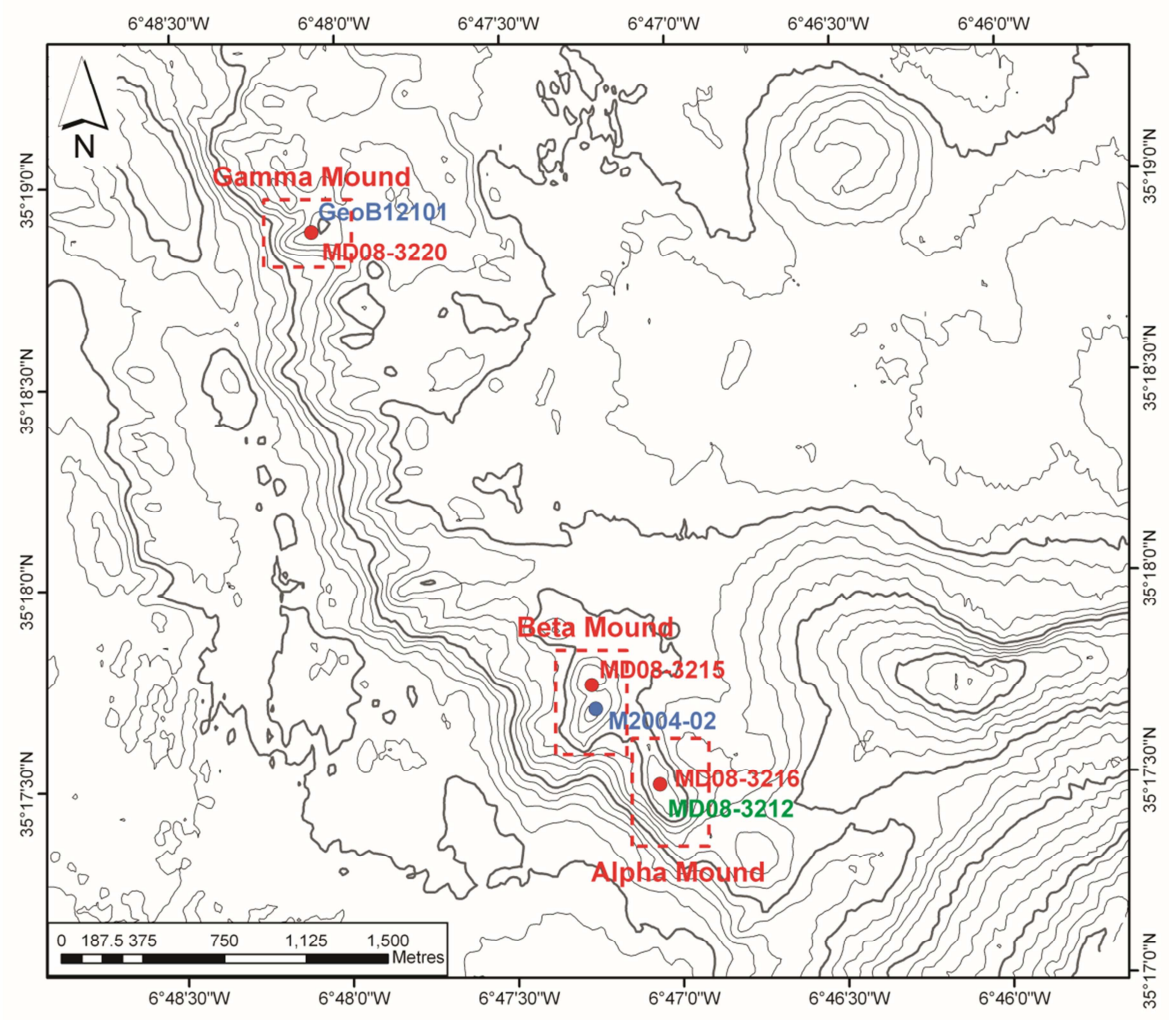

Fig. 4.1 *Detailed map of the Pen Duick Escarpment (contour lines every 10 m) with the locations of the gravity cores obtained on board the R/V Marion Dufresne in 2008 (red). The dating results of two additional cores (blue) from Wienberg et al. (2010) and one core (green) analysed by N. Frank (pers. comm.) were used to obtain a chronostratigraphic framework.*

4.2 Material and methods

All three gravity cores were obtained during the R/V Marion Dufresne 169 MiCROSYSTEMS cruise to the Gulf of Cadiz in July 2008 (Fig. 4.1; Table 4.1). The coring sites were determined

based on geophysical surveying (multibeam bathymetry, side-scan sonar imagery and high-resolution reflection seismic profiling) and ROV observations obtained during the R/V Belgica CADIPOR III cruise in 2007 (De Mol et al., 2011; Foubert et al., 2008; Van Rooij et al., 2011). The on-mound cores, which were obtained for sedimentological purposes, were cut in sections of 1.5 m.

Core number	Location	Latitude	Longitude	Depth (m)	Recovery (cm)
MD08-3215	Beta Mound	35°17.7405' N	6°47.2504' W	506	343
MD08-3216	Alpha Mound	35°17.4959' N	6°47.0581' W	515	445
MD08-3220	Gamma Mound	35°18.8727' N	6°48.0848' W	558	628

Table 4.1 *Location, water depth and core recovery of the studied cores, acquired during the R/V Marion Dufresne MD169 cruise.*

4.2.1 CT scanning

The sediment cores were scanned at the Ghent University Hospital (Belgium) with a Siemens medical CT scanner with an X-ray tube operating at 120 kV and an output of 100 mAs. Slices were taken every 3 mm with an overlap of 1 mm. The field of view was 150 mm.

Eleven micro-CT scans were carried out at the Centre for X-ray Tomography (UGCT, Ghent University, Belgium) on sediment from the coral cores which were sampled using 8 cm^3 sediment cubes (Table 4.2). The micro-CT subsamples were taken from specific intervals based on the visual description of the sediment cores. These high-resolution images can give additional and more detailed information than the medical CT scans. For example, very small cold-water coral fragments can be recognised as well as the preservation state and the impact of dissolution. For these samples, a scanner set-up consisting of a high power directional head as X-ray source and a Varian 2520V Paxscan X-ray detector was selected. This detector consists of 2000 x 1600 pixels with a pixel size of 127 µm by 127 µm. The samples were scanned at 130 kV with a thin Cu-filter in order to minimise beam hardening effects. In total, 800 projections were taken with each projection averaging two frames of 400 ms exposure time. To enhance image statistics, a pixel averaging of 2 x 2 pixels was used, reducing the resolution. The set-up of the micro-CT scanner is described in detail by Masschaele et al. (2007).

Image reconstruction was performed using the Siemens software for the medical CT data and the Octopus software (Vlassenbroeck et al., 2007b) for the micro-CT data. The raw projection data from the X-ray cameras were filtered by removing bright and dark spots. Subsequently they were normalised and regrouped in sinogram files which are finally used to calculate cross sections (Vlassenbroeck et al., 2007a). Processing and visualising of the images was carried out using the VGStudio MAX software package (Volume Graphics). This software allows to display the data in a 3D view as well as in three orthogonal slice image views. For a detailed 3D analysis of the reconstructed volume, the software package

Morpho+ was applied (Vlassenbroeck et al., 2007b; Brabant et al., 2011), developed at UGCT. It allows determination of porosity and volume fraction, object identification, object parameterisation, object separation, connectivity analysis and visualisation. In this study, the percentage of corals inside the sediment cores was quantified using the Morpho+ software. This analysis is based on differences in density which are reflected by variations in X-ray attenuation (grey value). A square box of 7 x 7 cm was selected as region of interest in order to avoid the influence of the plastic core liner. After loading the cropped slices in Morpho+, a dual thresholding technique was applied to select the areas corresponding with cold-water coral fragments. Next, the total and partial amount of cold-water coral fragments could be calculated as a volume percentage for each section and each slice.

Core number	Location	Depth (cm)	Corals (%)
MD08-3215	Beta Mound	68-70	7.8
		280-282	8.7
		309-311	11.5
MD08-3216	Alpha Mound	18-20	10.6
		144-146	5.8
		260-262	12.0
		365-367	6.0
		381-383	8.1
		414-416	9.0
MD08-3220	Gamma Mound	483-485	8.4
		578-580	9.5

Table 4.2 *Location, downcore depth and coral percentage of the micro-CT samples.*

4.2.2 Magnetic susceptibility

After CT scanning, the sediment cores were opened for further analysis. First, the cores were frozen for 36 hours at -20°C before opening them with a stone saw. The half cores were then cleaned under a shower to remove the sawdust. After 24 hours of defreezing, the cores were ready for the magnetic susceptibility measurements and XRF core scanning.

The magnetic susceptibility determines the degree to which a material can be magnetised in an external magnetic field. It can be used as relative proxy indicator for changes in composition that can be linked to palaeoclimate-controlled depositional processes. The magnetic susceptibility was measured at the Royal Netherlands Institute for Sea Research (Texel, The Netherlands) using a Bartington MS2E sensor connected to the Bartington MS2 meter. Once the cores were at room temperature, the magnetic susceptibility of the sediment was measured at 1 cm intervals. Before and after each measurement, the air was measured to be sure of a constant background value. If this was not the case, the sensor was calibrated and the sediment was measured again.

4.2.3 XRF measurements

The cores were analysed with an AVAATECH XRF core scanner (Royal NIOZ, The Netherlands), allowing to perform rapid non-destructive analyses of elements from aluminium to uranium, in concentrations from 100% down to ppm levels. This elemental analysis provides valuable information concerning the variability of sediment input (Ca/Fe and Fe counts), tracing fluctuations in the relative abundance of biogenic carbonate and terrigenous material (Richter et al., 2006; Zaragosi et al., 2006). Previous studies have demonstrated that this can provide a preliminary indication of glacial-interglacial cycles. Prior to the XRF analyses, all core surfaces needed to be cleaned in order to obtain a smooth sediment surface. After cleaning, the surface was covered with a neutral polypropylene film (100 µm) against desiccation and air bubbles between the sediment and film were removed. The core sections were measured at a sampling interval of 1 cm. First, the surface (1 cm^2) was irradiated with an energy of 10 kV (0.150 mA) during 30 s counting time, followed by a second run with an energy of 30 kV (0.500 mA) during 30 s counting time. The data was processed with the accompanying processing software WinAxilBatch. A visual quality control was carried out to eliminate erroneous data due to voids or cracks.

4.2.4 Grain-size analysis

All cores were sampled every 5 cm in order to perform grain-size analyses with a Malvern Mastersizer 2000 (Marine Biology Section, Ghent University). The sediment was dried in a furnace at 60° for about 48 h. After subsampling 1 g of sediment, the carbonate fraction was removed by adding 75 ml of 10% acetic acid. This process was performed twice in order to remove all carbonate fragments. Afterwards, the sample was rinsed twice with distilled water, each time followed by a 24 h settling period. Finally, the sediment was transferred in a 15 ml tube together with 0.2% calgon (sodium hexametaphosphate) to prevent flocculation. Prior to analysis, the samples were rotated (20 rpm) for 24 h. Afterwards, the results were processed with GRADISTAT (Blott and Pye, 2001) and the descriptive grain-size parameters were calculated using the Folk and Ward (1957) method.

4.2.5 End-member modelling

The end-member modelling algorithm (EMMA) by Weltje (1997) has been applied to the grain-size data in order to identify different sedimentary processes affecting the build-up of the mounds. It is a powerful approach to unmix the sediment into subpopulations that can subsequently be interpreted in terms of origin and/or transport pathways. A more detailed description of the method can be found in chapter 2 (section 2.2.6). In total, 255 samples (every 5 cm) were taken into account for the three mounds within a grain-size range of 0.3 to 130 µm. They were analysed all at once as this gives better results than splitting them up in three different models. The goodness-of-fit statistics indicate the adequacy of a model

with four end members (Fig. 4.2). Using this model 87% of the variance in the grain-size dataset is explained (r^2 = 0.87). A better fit can be obtained by increasing the number of end members, e.g. r^2 = 0.93 with five end members, however, this is not significant as the risk of modelling noise instead of signal becomes more likely.

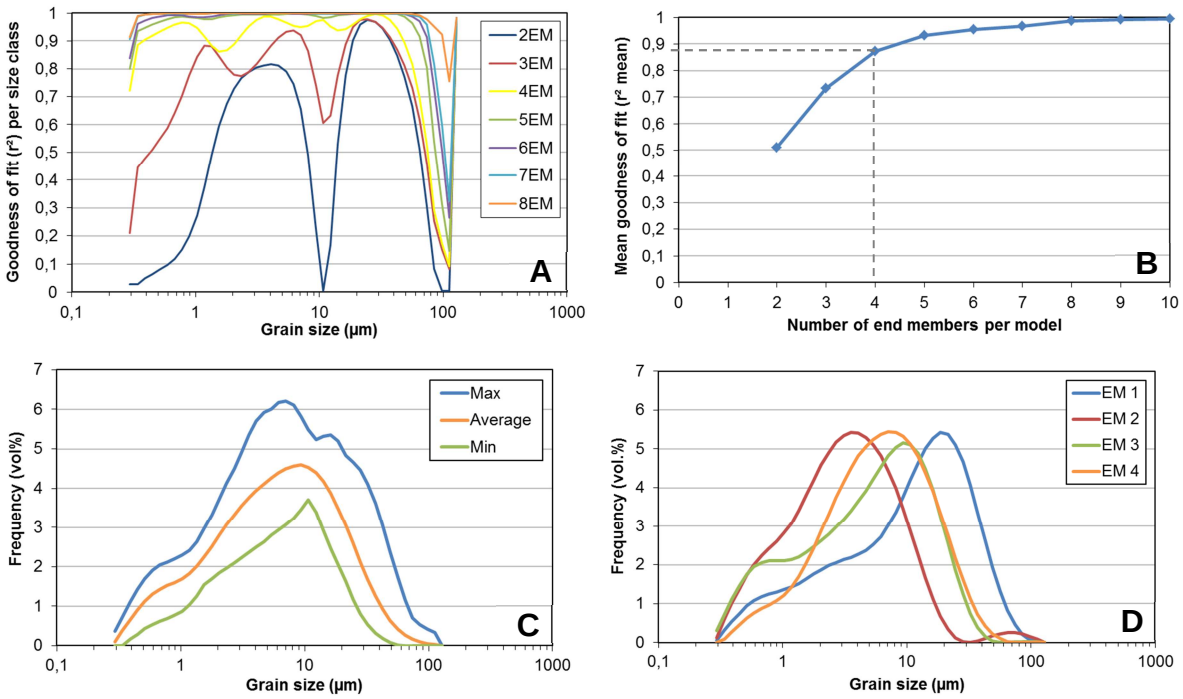

Fig. 4.2 *End-member modelling of the grain-size data: (A) goodness-of-fit statistics per size class for models with 2-8 end members, (B) overall mean goodness-of-fit (r^2) for models with 2-10 end members, (C) the minimum, average and maximum model using four end members, and (D) the individual grain-size distributions of the four end members (EM 1-4).*

4.2.6 X-ray diffraction analysis

X-ray diffraction (XRD) analyses were performed in order to obtain additional and independent information about the provenance and transport processes related to each end-member (Thierens et al., 2010). In total, 40 samples of bulk sediment from Alpha and Beta Mound were prepared for mineral identification and quantification using a Philips PW1830 diffractometer (K.U. Leuven - Belgium). These analyses were obtained within the framework of the PhD thesis of Dr. Hans Pirlet (RCMG - Ghent University - Belgium). The detailed preparation and analysis procedure is explained in Pirlet et al. (2012). In this study, the phase abundances (weight%) within the siliciclastic matrix after removal of the carbonate (calcite, dolomite and aragonite) and authigenic phases (gypsum and halite) will be presented, e.g. quartz, feldspars and clay. No XRD results are available for Gamma Mound due to planning constraints.

4.2.7 Stable isotope analysis

The stable carbon ($\delta^{13}C$) and oxygen ($\delta^{18}O$) isotope composition of the planktonic foraminifera *Globigerina bulloides* was measured at the Laboratoire des Sciences du Climat et de l'Environnement (LSCE, Gif-sur-Yvette, France). Samples were taken each 10 cm for all three sediment cores. About 10-15 foraminifera were selected in the size class from 250 to 315 µm and cleaned with methanol. All values are reported in per mil relative to the Pee Dee Belemnite (PDB) standard.

4.2.8 U/Th dating

In total, ten cold-water coral fragments were selected from Gamma Mound (MD08-3220) for U-series dating. Due to the bad condition of the cold-water coral fragments in the other sediment cores it was not possible to date any sample. In order to support relative dating based on the XRF measurements and the stable isotope analyses, additional U/Th datings from other sediment cores will be used. For Alpha Mound U-series dating results (Table 5.1) were provided by Dr. N. Frank (LSCE, Gif-sur-Yvette, France). The datings from Beta (M2004-02) and Gamma (GeoB 12101) Mound (Table 5.2) were taken from Wienberg et al. (2010). The U-series measurements and age determination of the MD08-3212 and MD08-3220 samples were carried out in the Laboratoire des Sciences du Climat et de l'Environnement (LSCE, Gif-sur-Yvette, France) using an inductively coupled plasma quadrupole mass spectrometer (ICP-QMS). Preparation of the corals, the analytical procedures and the physical measurement routines followed the detailed description by Frank et al. (2005), Frank et al. (2004) and Douville et al. (2010). The data is blank corrected and the HU1 standard is used to apply a bracketing technique to reduce internal drifts of the ICPMS as outlined by Douville et al. (2010). All activity ratios are calculated using the half-lives of ^{238}U, ^{234}U, and ^{230}Th given by Cheng et al. (2000).

4.3 Results

4.3.1 Medical CT

4.3.1.1 CT facies

In total, four different CT facies were delineated based on the quantity and appearance of cold-water corals, their preservation and the sediment matrix (Fig. 4.3). On one hand there are intervals with a relatively high amount of corals (5-24%) (Fig. 4.3A-D) and on the other hand zones with a rather low amount of corals or even no corals at all (0-2%) (Fig. 4.3E and 4.3F). In the first case two different facies can be distinguished: one facies (F1) with clearly recognisable, well preserved corals (5-24%) (Fig. 4.3A-C), and the second facies (F2) with crushed coral fragments (5-10%) (Fig. 4.3D). In both facies the corals are embedded in a

homogeneous matrix. In the second case with little or no cold-water corals, the facies (F3) can be described as a homogeneous matrix with bioturbations and/or cracks (Fig. 4.3E and 4.3F). Finally, the last facies (F4) is a combination of two facies (F1 and F2), namely a homogeneous matrix with an alternation between less and more preserved coral fragments (5-11%). In addition, it was also possible to identify different species of cold-water corals in the intervals with well-preserved corals: *Lophelia pertusa* (Fig. 4.3A), *Desmophyllum dianthus* (Fig. 4.3A), *Madrepora oculata* (Fig. 4.3B) and *Dendrophyllia* sp. (Fig. 4.3C). The solitary coral *Desmophyllum dianthus* will not be taken into account further on in this study as only a few specimens were observed within the cores.

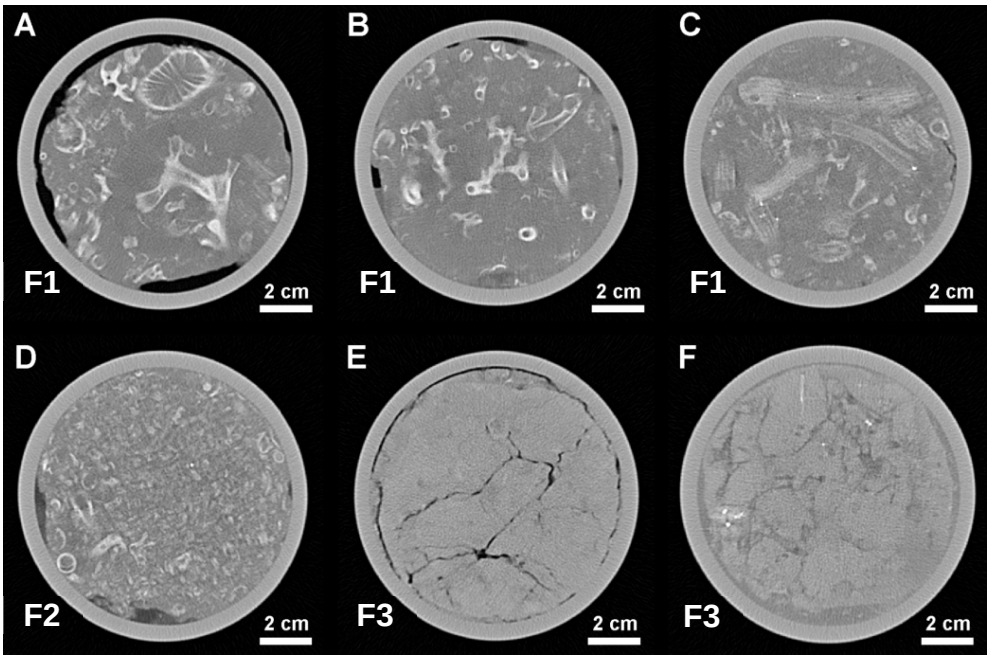

Fig. 4.3 *Overview of the different CT facies on sections perpendicular to the core length with (A) well preserved* Lophelia pertusa *fragments and one* Desmophyllum *specimen (facies F1), (B) well preserved* Madrepora oculata *corals (facies F1), (C) well preserved* Dendrophyllia *fragments (facies F1), (D) crushed cold-water coral fragments (facies F2), (E) homogeneous matrix with cracks (facies F3), and (F) homogeneous matrix with cracks and some framboidal pyrite (facies F3).*

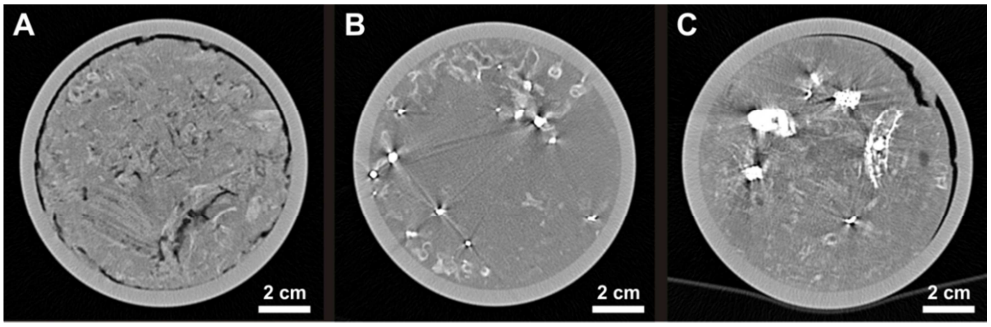

Fig. 4.4 *Expressions of early diagenetic processes within the mounds: (A) dissolution of the cold-water corals, (B) the formation of small pyrite crystals (white structures), and (C) the formation of large pyrite nodules (white structures) and the pyritisation of the cold-water coral fragments.*

At particular depths within the cores different stages of dissolution of the cold-water corals are observed (Fig. 4.4A). Some coral fragments are even completely dissolved, creating moldic pores within the sediment. Additionally, pyrite is observed, going from small (2-5 mm) scattered pyrite in the matrix (Fig. 4.4B) up to larger pyrite nodules of about 1-2 cm (Fig. 4.4C). Sporadically, some cold-water corals are pyritised or the pyrite is present within the coral fragments (Fig. 4.4C).

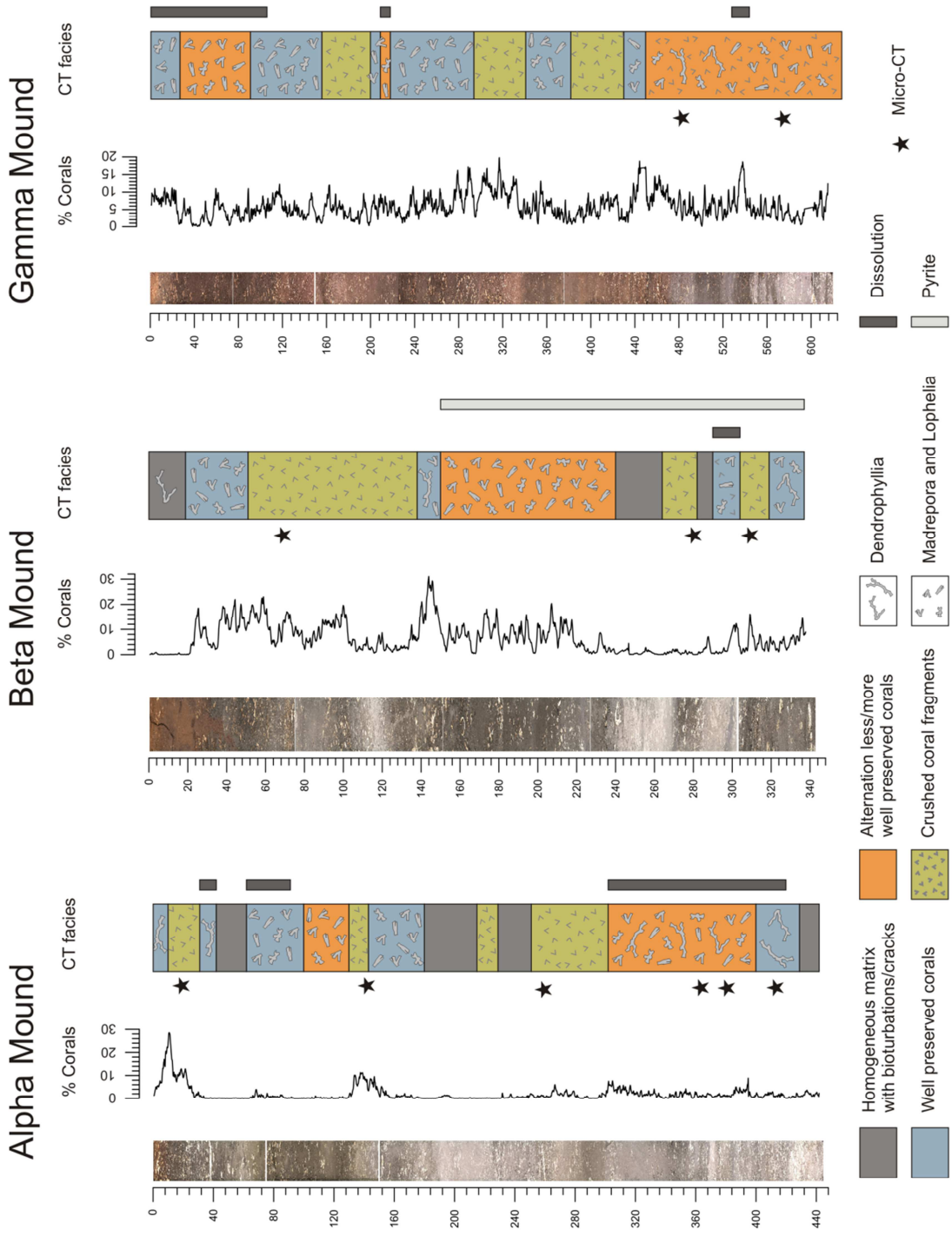

Fig. 4.5 *Overview of the CT facies analyses and the coral percentages for the three mounds. The black stars indicate the locations of the micro-CT samples (vertical scale: depth in centimetres).*

All cores show a variable vertical succession of the four different CT facies (Fig. 4.5). In Alpha and Beta Mounds, all four facies are observed while in Gamma Mound the homogeneous matrix is not present. This results, at least for Gamma Mound, in a continuous sequence of cold-water coral fragments throughout the core. Mostly *L. pertusa* and *M. oculata* are observed while *Dendrophyllia* sp. only occurs in a few intervals. Dissolution of these corals is observed in four intervals in Gamma Mound: 0-105, 209-218, 286-294 and 528-542 cm. In Beta Mound only between 290 and 304 cm dissolution occurs while in Alpha Mound dissolution is observed in almost the whole core. The formation of pyrite starts at a depth of 150 cm in Beta Mound while in the other two mounds no pyrite is observed on the medical CT images.

4.3.1.2 Cold-water coral quantification

Based on the Morpho+ analysis (Fig. 4.6), a clear difference can be noticed between the three cold-water coral mounds (Fig. 4.5). In general, a succession of the four CT facies is observed within the mounds, resulting in variations in coral percentage between 0 and 31% per slice. The intervals with well-preserved corals show average values between 5 and 24% coral fragments, while in the intervals with crushed coral fragments the average amount of corals varies between 5 and 10%. These latter values correspond with the average amount of corals in the interval with less and more well-preserved corals: 5-11%. Looking at the minimum and maximum average value within this interval, the amount of coral fragments varies between 0 and 20%. In the interval with only homogeneous matrix the average values vary between 0 and 2%, indicating no or only a few cold-water coral fragments.

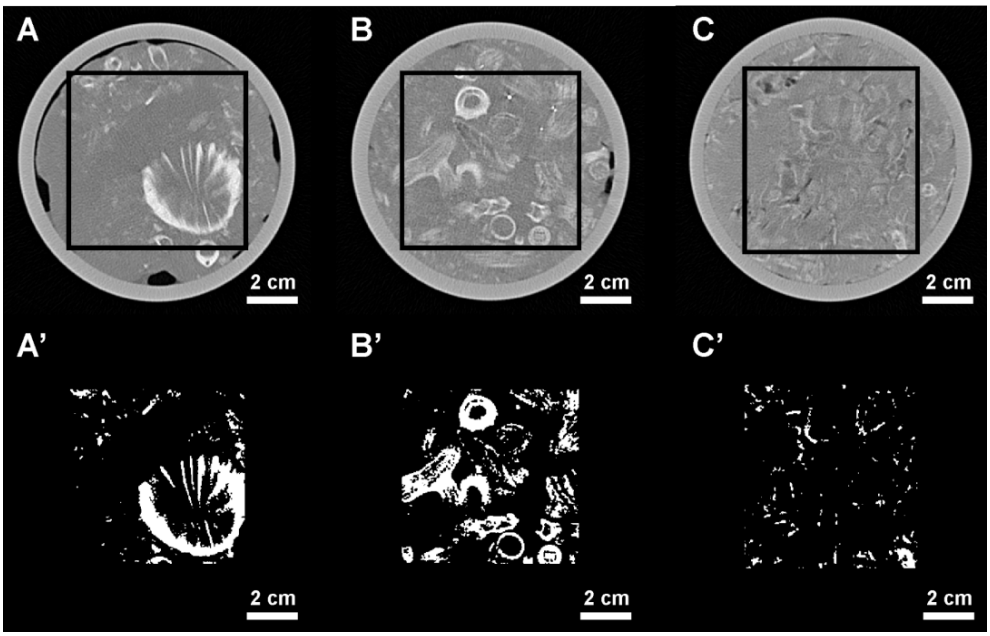

Fig. 4.6 *Examples of the "Morpho+" software analysis in order to demonstrate how the percentage of corals is obtained. The upper slices A, B and C are CT sections, the lower slices A', B' and C' represent the result of the Morpho+ analysis, based upon the 7x7 cm square boxes in each slice. Slices C-C' shows the possible discrepancy between true (C) and calculated coral content (C') due to dissolution processes (Alpha Mound).*

It seems that Alpha Mound has a low amount of cold-water coral fragments with average values between 0 and 2%, except for the intervals between 0-31 cm and 130-143 cm where average values of 10% and 7% respectively were measured. However, in this mound it is difficult to select the corals (Fig. 4.6C), due to a small difference in contrast between the corals and the surrounding matrix. Parts of the corals are heavily dissolved, due to the influence of diagenetic processes, and have already lost their primary density. This results in a small difference in attenuation coefficients and therefore also in the resulting grey values needed in Morpho+ to discriminate between the coral on one hand and the surrounding matrix on the other hand. Comparing the coral quantification data of Alpha Mound with the other two mounds creates a wrong impression. In Beta Mound, the average amount of cold-water corals varies between 4 and 24% for the coral-bearing intervals and between 0 and 2% for the intervals without coral fragments. The interval between 290 and 304 cm is influenced by dissolution which results in a significant underestimation of the real coral percentage. Most probably the corals within the intervals between 240 and 290 cm are also dissolved, resulting in very low coral percentages (1-2%). In Gamma Mound, only coral-bearing intervals are observed with an average amount of coral fragments between 4 and 12% and a maximum of 20%. Also in this mound dissolution is observed in several intervals (0-105 cm, 209-218 cm, 286-294 cm and 528-542 cm).

4.3.2 Micro-CT

The micro-CT subsamples were taken from intervals with crushed coral fragments (4 samples), areas with less preserved corals (4 samples) or well preserved corals (1 sample), or at the interface between these facies (2 samples) (Fig. 4.5). The first four samples (Fig. 4.7A, 4.7C, 4.7G and 4.7I) confirm that the medical CT facies described as crushed coral fragments indeed corresponds with crushed cold-water corals, although other biogenic fragments (e.g. molluscs) are also observed. Secondary porosity is observed in all four samples, especially in Alpha Mound at a depth of 260-262 cm (Fig. 4.7C). Mostly the small fragments start to dissolve first leaving small holes, however, some indications of dissolution of the larger coral fragments are also observed (Fig. 4.7A). In the intervals with an alternation between less and more preserved corals, a clear impact of dissolution is observed, especially in the two samples in Gamma Mound (Fig. 4.7J and 4.7K). On figure 4.7J we can still clearly recognise the cold-water coral, although there is a high influence of dissolution, while on figure 4.7K the influence of dissolution resulted in the almost complete disintegration of the coral. This latter disintegration is also observed in the interval with well-preserved corals (Fig. 4.7F). Although secondary porosity is only observed in certain intervals on the medical CT images, the micro-CT scans show that this secondary porosity is also present in other intervals. Additionally, the pyrite nodules in Beta Mound have also been visualised with the micro-CT scans (Fig. 4.7H).

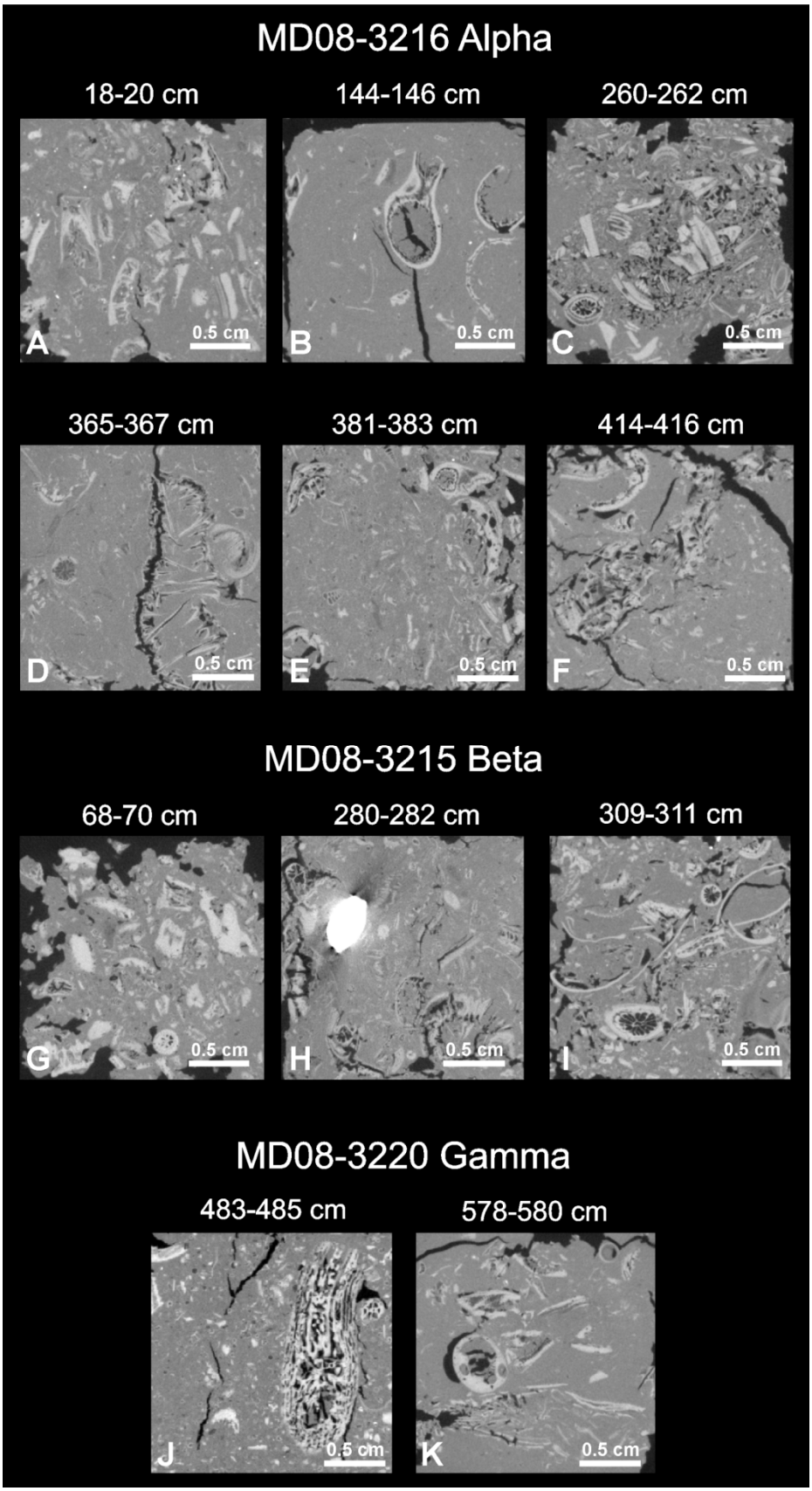

Fig. 4.7 *Overview of the micro-CT images at several depths within the sediment cores, indicating the effect of dissolution and the formation of pyrite.*

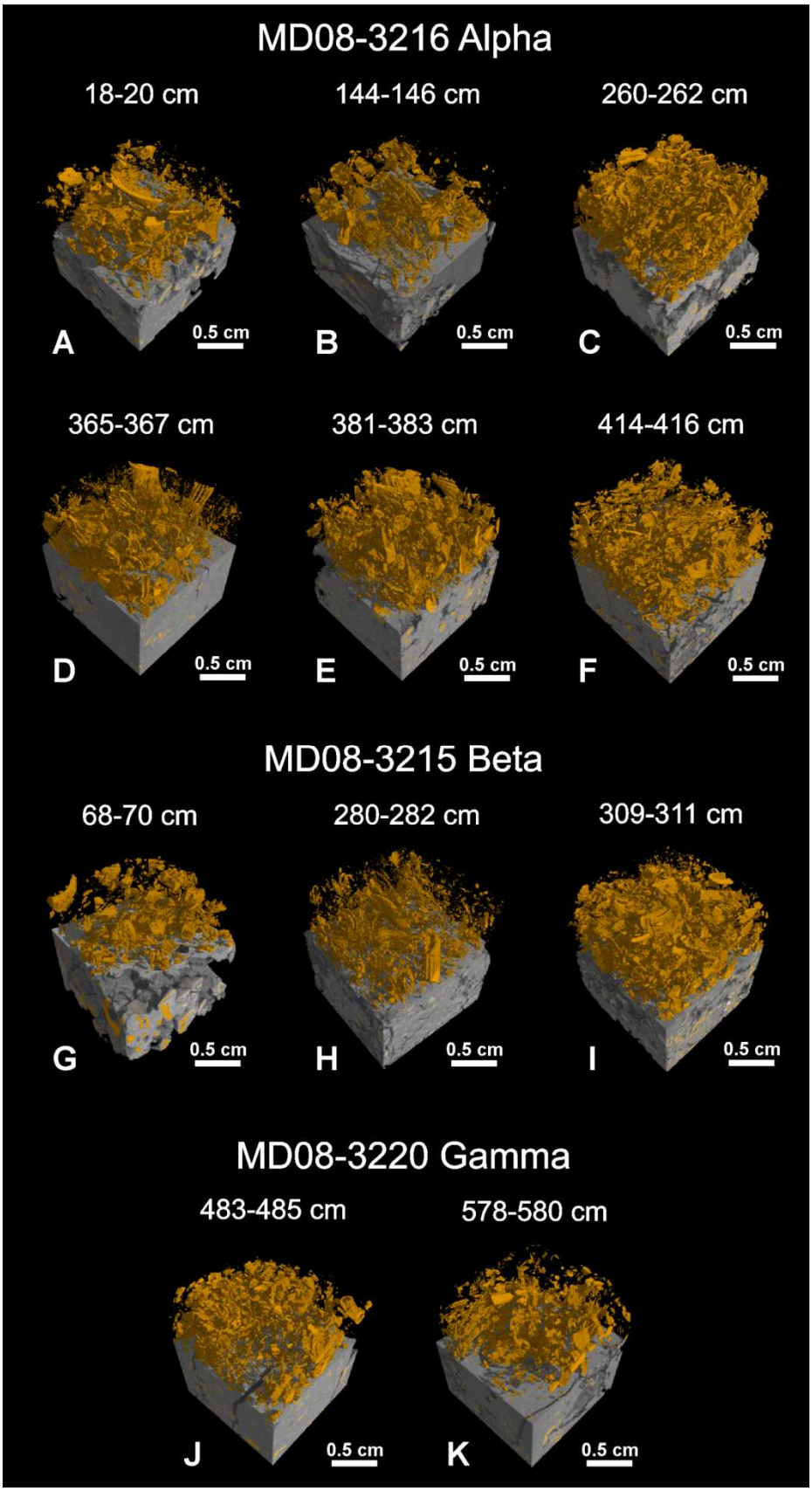

Fig. 4.8 *3D reconstructions of the micro-CT images at several depths within the sediment cores showing the variation in amount of corals and their preservation. The grey volume corresponds with the sediment, orange represents the cold-water coral fragments.*

Also for the micro-CT images, the amount of coral fragments were calculated within the different cubes, varying between 5.8 and 12.0 volume % (Table 4.2; Fig. 4.8). These average coral percentages seems to correspond with the average amount of corals for the different medical CT facies. However, slightly higher percentages are calculated due to the higher resolution of the micro-CT compared to the medical CT.

4.3.3 Magnetic susceptibility

The magnetic susceptibility measurements range from 0 to 40 x 10^{-5} SI units (Fig. 4.9), which are rather low values. In Alpha and Beta Mound the magnetic susceptibility drops sharply around the depth of 10 cm and 37 cm, respectively, towards values below 5 x 10^{-5} SI units. For Alpha Mound, values of about 10 x 10^{-5} SI units were measured in the uppermost centimetres while in Beta Mound the measurements range between 20 and 35 x 10^{-5} SI units. Within Gamma Mound, the magnetic susceptibility drops below 5 x 10^{-5} SI units at a depth of 470 cm. Above this depth, the measurements vary between 10 and 40 x 10^{-5} SI units and show a saw-tooth pattern around an average value of 22 x 10^{-5} SI units. Several drops in magnetic susceptibility are noticed around depths of 60, 78, 160, 255 and 300 cm. From a depth of 300 cm there is a slight decrease in magnetic susceptibility and the saw-tooth pattern becomes less pronounced.

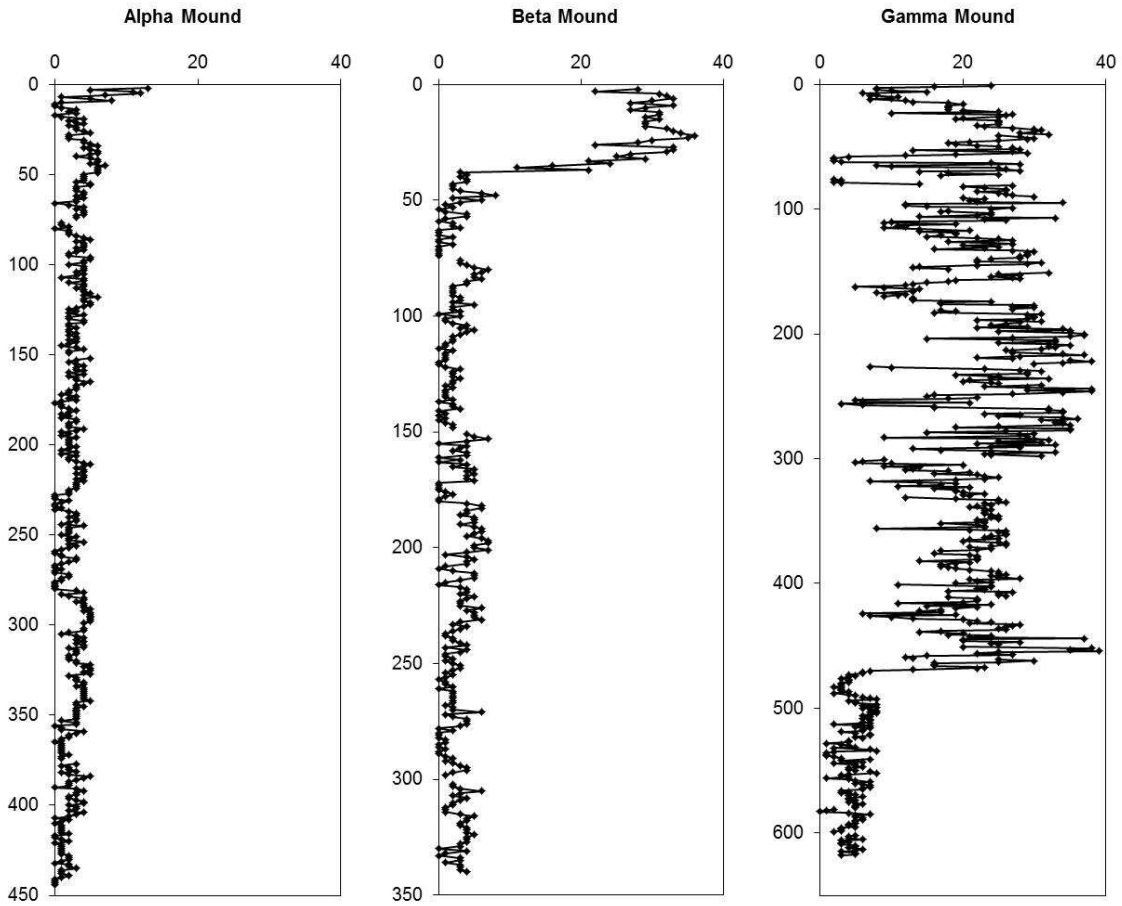

Fig. 4.9 *Magnetic susceptibility (vertical scale: depth in centimetres).*

4.3.4 XRF measurements

Several ratios (Ca/Fe, Fe/Al, Si/Al, Ti/Al, K/Al) and element intensities (Fe, Ti) were compared, however, only the Ca/Fe ratio and Fe intensity will be presented. They both show the clearest signal and are selected as a geochemical proxy for the input of terrestrial material. Within the three mounds the XRF Ca/Fe values vary mostly between 2 and 10 (Fig. 4.10). Within Alpha Mound, slightly higher values are measured between 160 to 280 cm and between 350 and 385 cm. From a depth of 400 cm, an increasing trend is observed with values between 10 and 20. In Beta Mound, higher values are noticed in three intervals: 40-75 cm, 230-265 cm and 280-320 cm. In Gamma Mound, slightly lower values are measured with an average value of 4 and a few intervals with increased values up to 10-12 (e.g. 160-200 cm, 280-340 cm, 440-490 cm and 540-625 cm). From a depth of 200 cm an increasing trend is present up till a depth of 340 cm. After this depth, the values drop again towards the average around 4. The high peaks that are often observed are most probably the result of the presence of cold-water coral fragments which can influence the XRF results due to their high Ca content (aragonite skeleton).

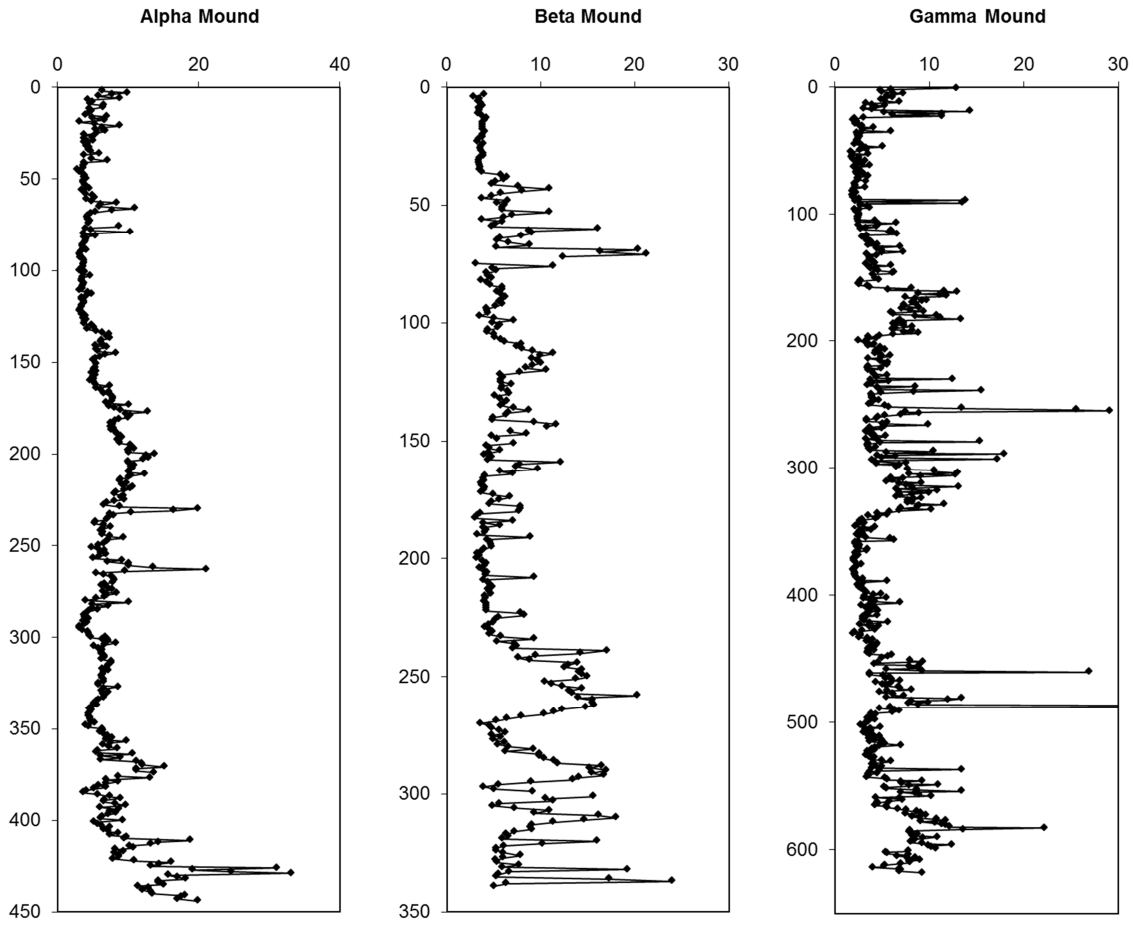

Fig. 4.10 *Variations in Ca/Fe ratio measured for each core (vertical scale: depth in centimetres).*

As the Ca/Fe ratio is influenced by the presence of the cold-water coral fragments in the sediment cores, the Fe intensity (counts per second, cps) will also be discussed separately in order to obtain an idea of the variations in terrigenous sediment input without the influence of calcite. However, the Fe intensity can be influenced by diagenetic processes which can result in wrong conclusions. Fe and Ti are closely related to each other in the terrigenous fraction, whereas Ti is inert to diagenetic processes (Richter et al., 2006). By comparing both intensities a good correlation is observed, indicating that the Fe signal is not disturbed. Additionally, in the plot of Fe versus S there is no relationship in the uppermost 470 cm of Gamma Mound while below this depth and in Alpha and Beta Mound a correlation is present. The coupled use of Fe, Ti and S can differentiate between a dominantly terrigenous supply of iron and distinct early diagenetic iron enrichments in oxidising and reducing environments (Richter et al., 2006). Here, the Fe intensity in Gamma Mound (< 470 cm) seems not to be disturbed by early diagenesis. The cps values were not converted to concentrations as we are interested in the relative changes in elemental composition rather than absolute values. Fe intensities are varying between 2500 and 52000 cps with an average of 22200 cps for Alpha Mound, 23190 cps for Beta Mound and 27314 cps for Gamma Mound. All cycles show a typical saw-tooth like pattern.

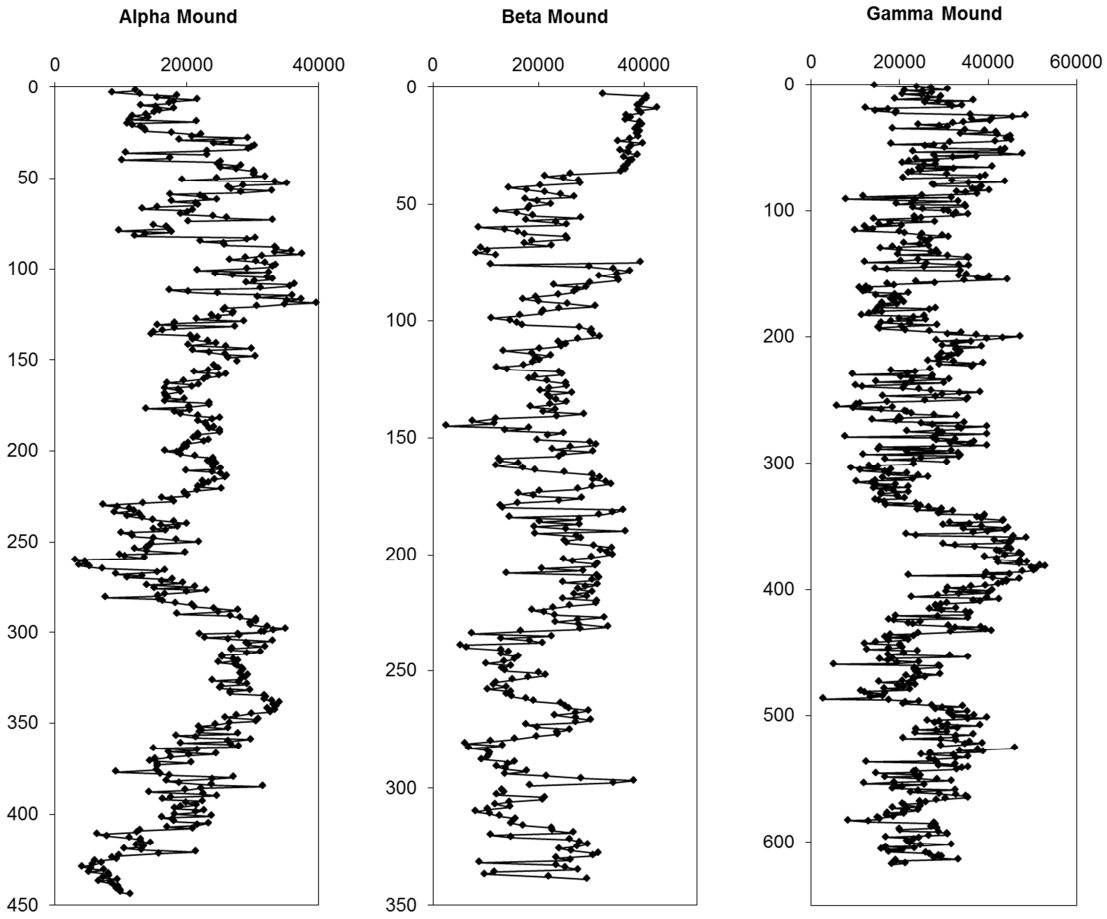

Fig. 4.11 *Fluctuations in Fe counts measured for each core (vertical scale: depth in centimetres).*

In Alpha Mound a general increasing trend is observed between 0 and 120 cm depth from 8700 cps to 40000 cps with a small drop between 60 and 85 cm. From a depth of 120 cm up to 230 cm the Fe intensities remain rather constant with values around 20000 cps. Below 230 cm the Fe count rates drop to lower values to reach a minimum value of 3000 cps at a depth of 260 cm. A second increasing trend is observed between 260 and 300 cm with Fe intensities up to 35000 cps, followed by a decrease to 4000 cps at a depth of 430 cm. In the upper 30 cm from Beta Mound the Fe counts are slightly decreasing from 40500 cps to 37000 cps. Between 30 and 70 cm a decreasing trend is observed from 37000 cps to 9000 cps, followed by a second decreasing trend between 70 and 100 cm (39500 to 11000 cps) and a third one between 100 and 120 cm (32000 to 12000 cps). Between 120 and 230 cm the Fe intensities are slightly increasing with a few small drops around depths of 145, 160 and 180 cm. From a depth of 230 cm alternating intervals with values around 13000 cps on one hand (230-260 cm and 280-315 cm) and 25000 cps on the other hand (260-280 cm, 295-300 cm and 315-340 cm) are observed. While in Alpha and Beta Mound the Fe intensities reach maximum values of 39665 and 42558 cps, respectively, the Fe count rates in Gamma Mound show a maximum of 52868 cps. The uppermost 25 cm of the core is characterised by a small increase in Fe count rates, followed by a general decreasing trend from 48000 to 10000 cps between 25 and 115 cm. Next, the Fe intensities increase again up to 44000 cps at a depth of 155 cm. Here, the count rates drop to values between 10000 and 28000 cps for the next 45 cm. Between 200-260 cm and 260-330 cm, two general decreasing trends are observed from 47000 to 6000 cps and 40000 to 10000 cps, respectively. From 330 cm up to 380 cm the values increase again until the maximum value of 52868 cps. This maximum count rate is followed by two general decreasing trends which are separated by a sudden increase to 40000 cps at a depth of 490 cm.

4.3.5 Grain-size analyses

The mode of the particles is fluctuating between 5 and 25 µm (Fig. 4.12). In Alpha Mound three intervals can be distinguished, 40-140 cm, 175-280 cm and 280-440 cm, each characterised by fining upward and modes close to 10 µm. At the top of each interval, a sudden increase in mode is observed. Between 0 and 40 cm and between 140 and 175 cm higher modes are observed, varying between 10 and 15 µm. In the lowermost interval, three peaks with a slightly higher mode are present at depths of 310, 390 and 415 cm. Beta Mound shows the highest mode values, especially between 140 and 250 cm with values varying between 10 and 25 µm. This latter value is reached around a depth of 190 cm. Above and below this interval modes are observed around 10 µm, except for the first 70 cm of the core. From 30 to 70 cm, again values between 10 and 20 µm were measured while a sudden drop is observed around 30 cm with only modes between 5 and 10 µm for the uppermost part. Gamma Mound can be divided in six intervals. From the bottom of the core until 500 cm the mode is fluctuating between 10 and 20 µm with a small fining upward trend. This interval is followed by a rather stable mode around 10 µm with a small peak of 17 µm at a

depth of 450 cm. Next, a coarsening upward trend is observed between 160 and 330 cm with values between 10 and 17 µm, followed by a sudden drop in grain-size below 10 µm between 120 and 160 cm. Then, again higher modes are observed around 12 µm up till a depth of 80 cm where after a small drop, a coarsening upward trend is observed up to 15 µm at the top of the mound. For all three mounds a positive correlation is observed with the amount of corals, measured on the medical CT scans. With increasing amount of corals the grain-size values become coarser.

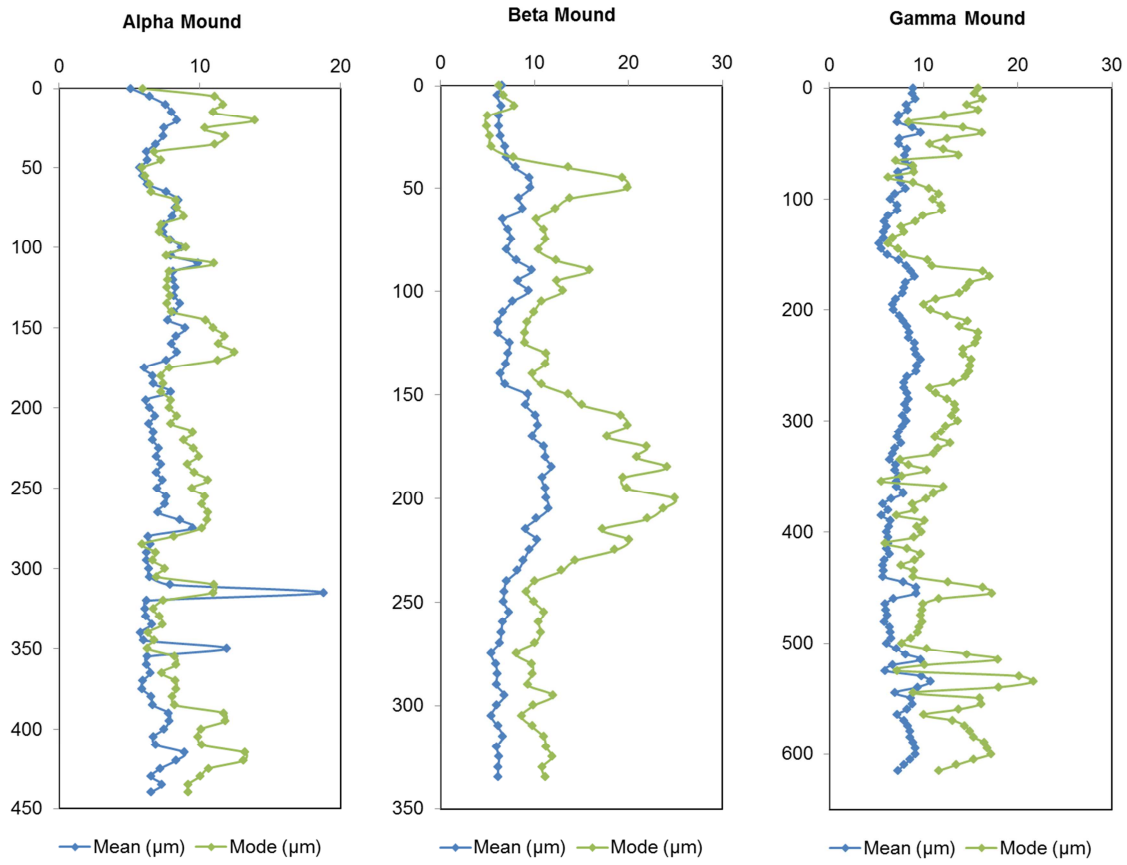

Fig. 4.12 *Grain-size analysis results showing variations in the mean (µm) and mode (µm) (vertical scale: depth in centimetres).*

4.3.6 End-member modelling

The four end-members all have a clearly different and dominant modal size (Fig. 4.13). EM 1 represents a poorly sorted, very fine skewed, mesokurtic distribution with a modal size of 20 µm, corresponding with medium silt. EM 2 is also a poorly sorted, mesokurtic distribution but is more symmetric. The modal size belongs to the very fine silt fraction (ca. 4 µm). EM 3 is poorly sorted, fine skewed and platykurtic in shape with a modal size of 10 µm (fine silt). Finally, EM 4 is again a poorly sorted, fine skewed distribution with a mesokurtic shape. The grain-size mode is around 8 µm, also in the fine silt fraction. Although all end-members are poorly sorted, EM 1 and EM 3 are overall better sorted than EM 2 and EM4.

Taking into account a minimum abundance of 10 %, only 6 % of the samples can be reproduced by only one end-member while in 27 % of the samples, all four end-members are present. However, most of the samples (46 %) can be explained by a combination of three end-members. The four end-members are found semi-continuously, each occurring in a minimum of 54 % of all samples (minimum 10 % contribution). EM 4 is even observed in 95 % of all samples with an average proportion of 38 %. EM 1, 3 and 4 are the dominant end-members in 28 %, 31 % and 34 % of the samples, respectively, with average contributions of 49 %, 50 % and 62 %, respectively. EM 2 is only dominant in 7 % of the samples with an average proportion of 36 %.

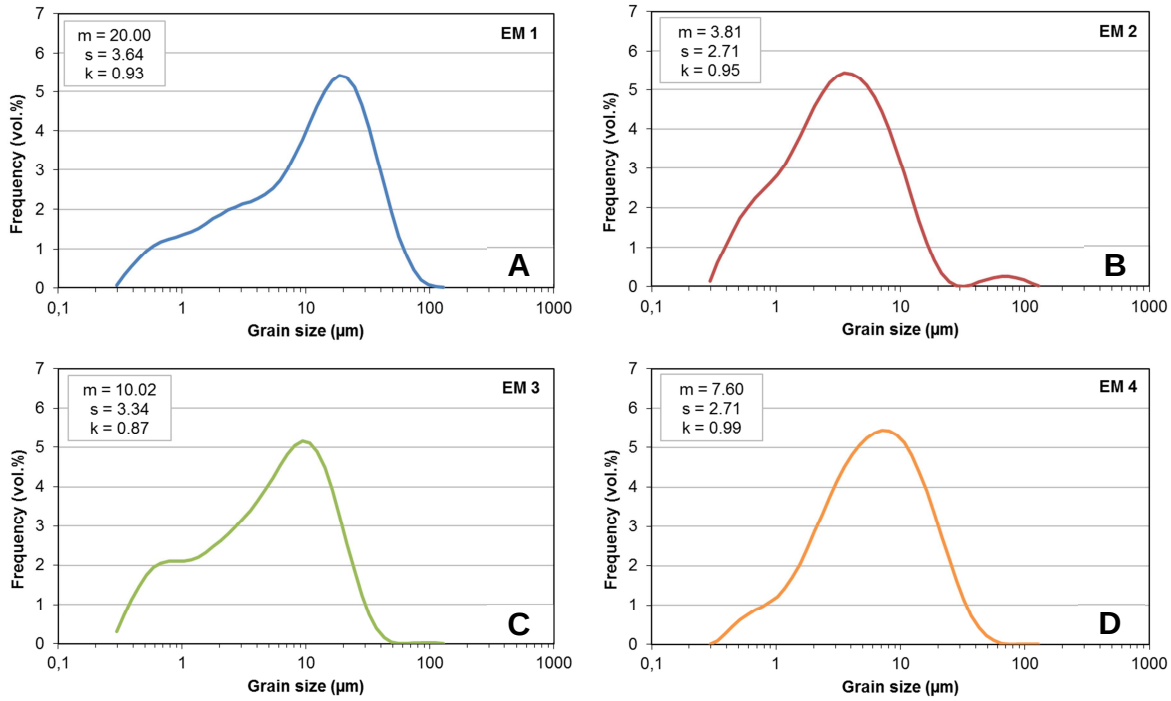

Fig. 4.13 *Grain-size distributions for the four end-members (EM 1-4) observed in the three Pen Duick mounds, with m = mode, s = sorting and k = kurtosis.*

In Alpha Mound, EM 1 can be found in dominating proportions from 145 to 175 cm and from 385 to 405 cm (Fig. 4.14). EM 3 is only dominant in the lowermost part of the core between 405 and 440 cm while EM 2 is not observed as dominant end-member. The most common end-member, as mentioned above, is EM 4 (40-145 cm and 285-350 cm). Within three intervals, 0-40 cm, 175-285 cm and 350-385 cm, it is not possible to determine one dominant end-member as they are all fluctuating around an average contribution of about 20%. The top of Beta Mound is dominated by EM 4 until a depth of 40 cm. Below this depth, an alternation of EM 1 (40-64 cm, 85-105 cm and 145-235 cm) and EM 3 (65-85 cm, 105-145 cm and 235-335 cm) as dominant end-member is observed. Within Gamma Mound, more variation is observed in the dominant end-members. The upper- and lowermost part of the core (0-30 cm and 550-615 cm) is characterised by the dominance of EM 1. Additional influence of EM 4 is observed from 30 to 60 cm and from 205 to 230 cm. In between these intervals EM 3 (95-120 cm, 165-205 cm and 415-495 cm) and EM 4 (60-95 cm, 120-165 cm,

230-320 cm and 495-550 cm) are alternating as dominant end-members. Between 320 and 415 cm depth, no specific end-member is dominant.

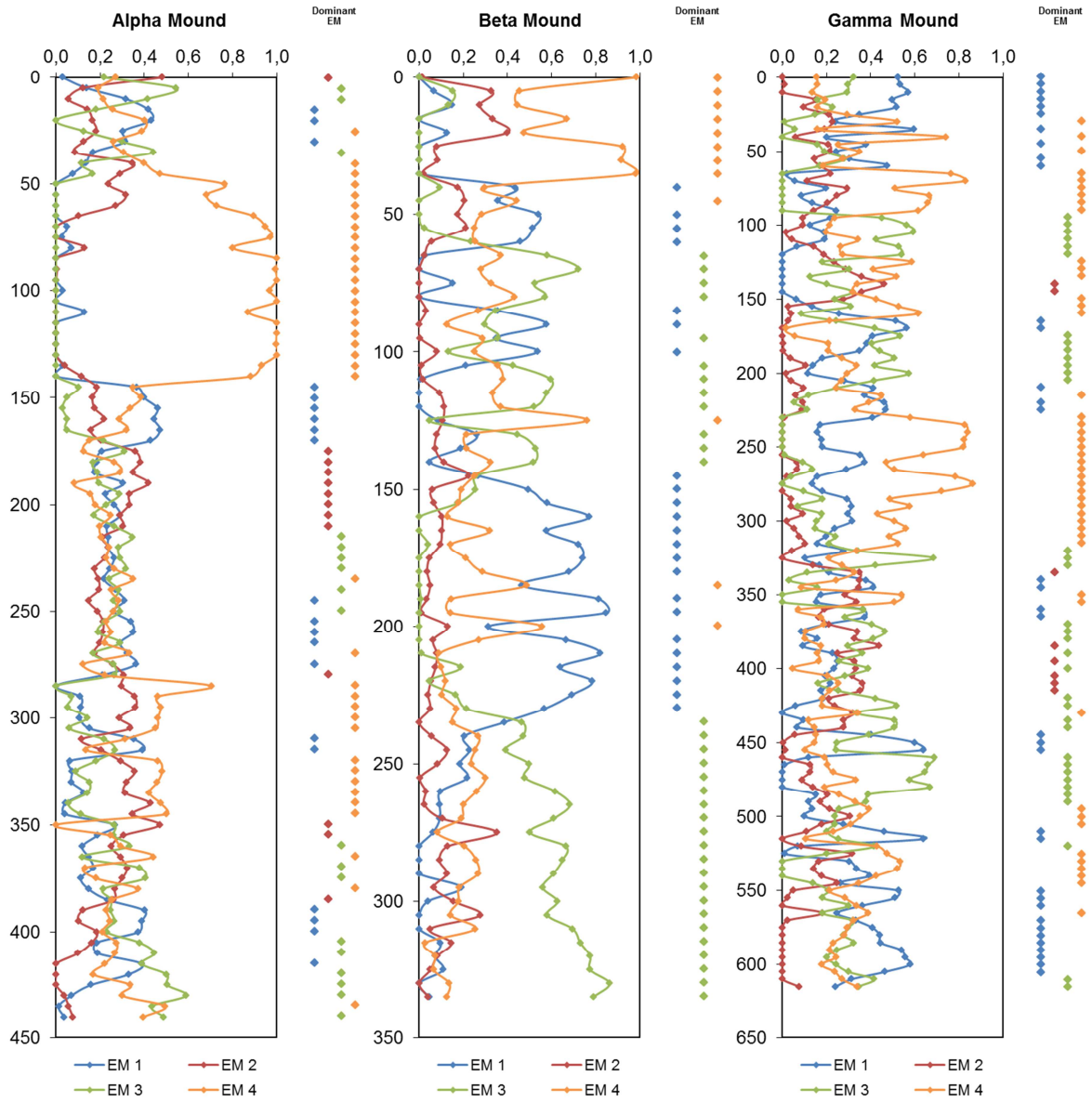

Fig. 4.14 *Relative abundance of the four end members for each mound with an indication of the dominant end member for each sample (vertical scale: depth in centimetres).*

4.3.7 XRD analyses

The total siliciclastic matrix makes only 38 wt.% and 41 wt.%, respectively, of the total matrix sediment in Alpha and Beta Mound (Fig. 4.15 and 4.16). This total matrix sediment is mostly dominated by carbonate minerals (calcite, dolomite and aragonite), as demonstrated by Pirlet et al. (2012). In Alpha Mound (Fig. 4.15), the siliciclastic matrix increases until a depth of 120 cm (52 wt.%), followed by a decrease until 260 cm (26 wt.%). Afterwards, the percentage increases again up to a depth of 340 cm (48 wt.%). A sudden decrease to 27 wt.% is observed around 370 cm. In Beta Mound (Fig. 4.16), the siliciclastic matrix decreases

from 46 wt.% at the surface until 33 wt.% around 110 cm. Next, an increase up to 59 wt.% is measured up to 59 wt.% (180 cm), followed by a decrease to 26 wt.%. In this latter interval a peak of 47 wt.% is present at a depth of 320 cm.

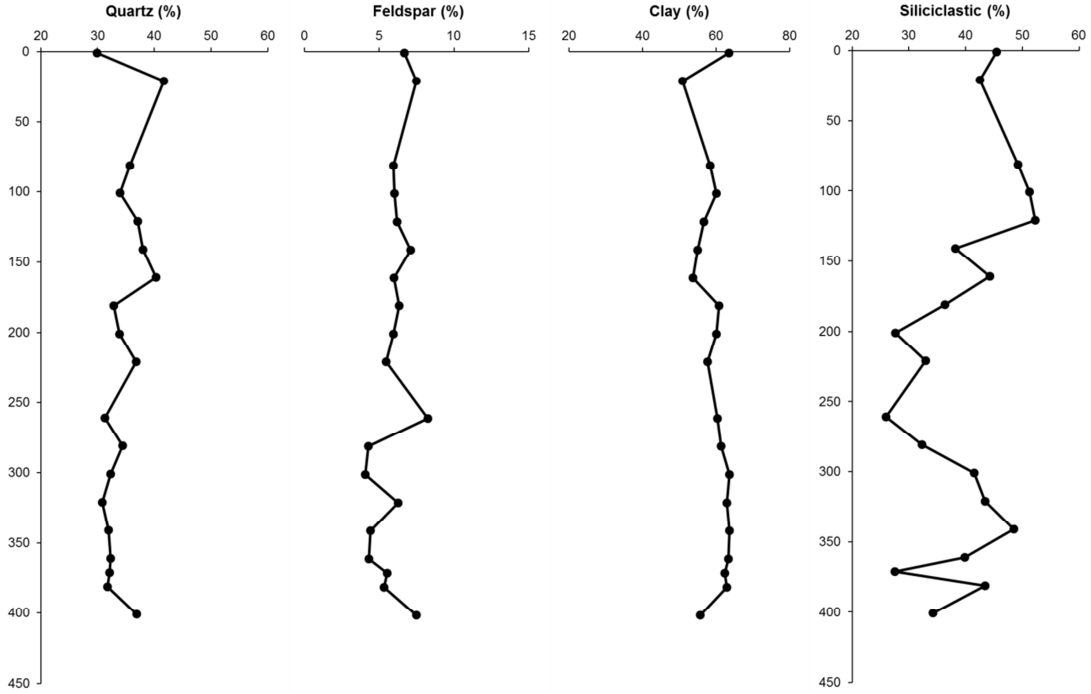

Fig. 4.15 *X-ray diffraction data of the siliciclastic matrix fraction of Alpha Mound (MD08-3216) (vertical scale: depth in centimetres).*

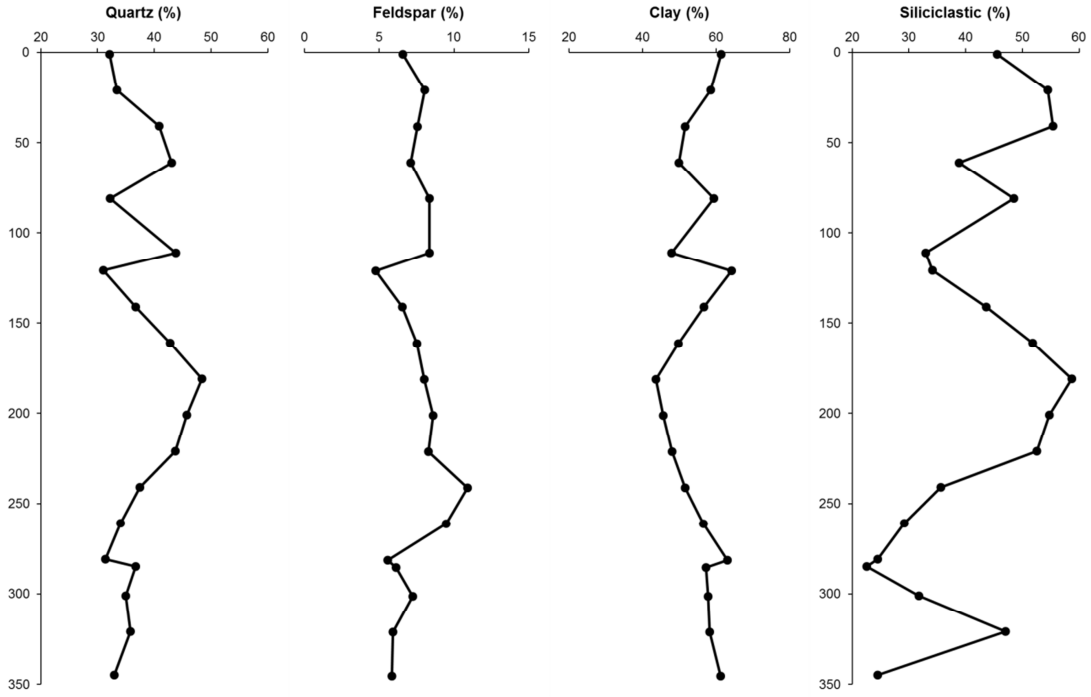

Fig. 4.16 *X-ray diffraction data of the siliciclastic matrix fraction of Beta Mound (MD08-3215) (vertical scale: depth in centimetres).*

Within the siliciclastic matrix (Fig. 4.15 and 4.16), clay minerals are the most abundant, varying between 50 and 64 wt.% in Alpha Mound (mean: 60 wt.%) and between 43 and 64 wt.% in Beta Mound (mean: 55 wt.%). Quartz makes 35 and 38 wt.%, respectively, of the siliciclastic fraction, whereas feldspars only occur in minor quantities (4-11 wt.%).

4.3.8 Stable isotope analyses

Figures 4.17, 4.18 and 4.19 show the results of the $\delta^{13}C$ and $\delta^{18}O$ isotope analyses from Alpha, Beta and Gamma Mound. Except for the surface sample and one sample at a depth of 265 cm in Beta Mound, all samples in the three mounds are depleted in ^{13}C and enriched in ^{18}O with respect to the PDB standard. In Alpha Mound, the $\delta^{18}O$ and $\delta^{13}C$ values show opposite trends. Between 0 and 230 cm the $\delta^{18}O$ values increase from 0.21 to 2.90 ‰, followed by a decrease until 1.67 ‰. The $\delta^{13}C$ values show first a decrease from -1.17 ‰ at the surface towards -10.75 ‰ around the depth of 230 cm, followed by an increase towards -2.26 ‰. In the first interval a small drop to -7.52 ‰ is observed around 60 cm. In Beta Mound, the first 20 cm correspond with low $\delta^{18}O$ values around 0 ‰. From this depth onwards the values vary around an average of 1.07 ‰ with peaks at 50 cm (1.91 ‰), 100 cm (1.91 ‰), 270 cm (2.22 ‰) and 300 cm (2.39 ‰). A negative peak of -0.51 ‰ is observed at the depth of 265 cm. Also the $\delta^{13}C$ values remain rather constant (average: 1.75 ‰) with a slight downcore increase. Two peaks of -12.1 ‰ and -9.5 ‰ are measured at depths of 265 and 300 cm, respectively. In Gamma Mound, the first 340 cm represent rather constant $\delta^{18}O$ values with an average of 0.74 ‰, although slightly higher values are observed in the first 80 cm (average: 0.95 ‰). At the depth of 340 cm the $\delta^{18}O$ values suddenly increase with a maximum value of 2.07 ‰ around 370 cm. Between 370 and 490 cm a decrease is observed to $\delta^{18}O$ values of 0.56 ‰, followed by an increase up to 1.80 ‰. The $\delta^{13}C$ values are varying between -0.60 and -1.50 ‰ until the depth of 510 cm. From this depth on, a decreasing trend is observed with a minimum value of -3.16 ‰ around the depth of 600 cm.

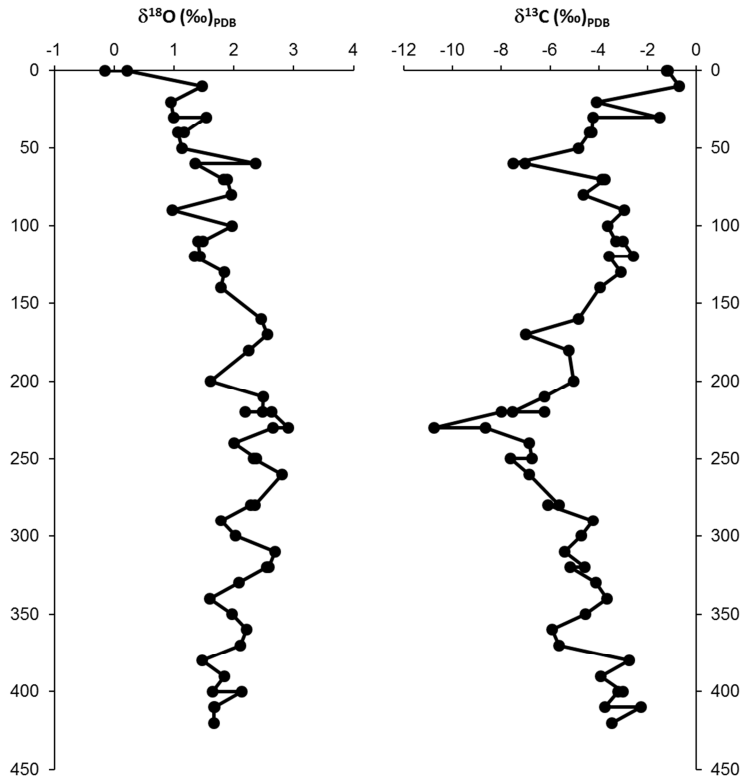

Fig. 4.17 *The $\delta^{18}0$ and $\delta^{13}C$ results measured on the planktonic foraminifera* G. bulloides *from Alpha Mound (vertical scale: depth in centimetres).*

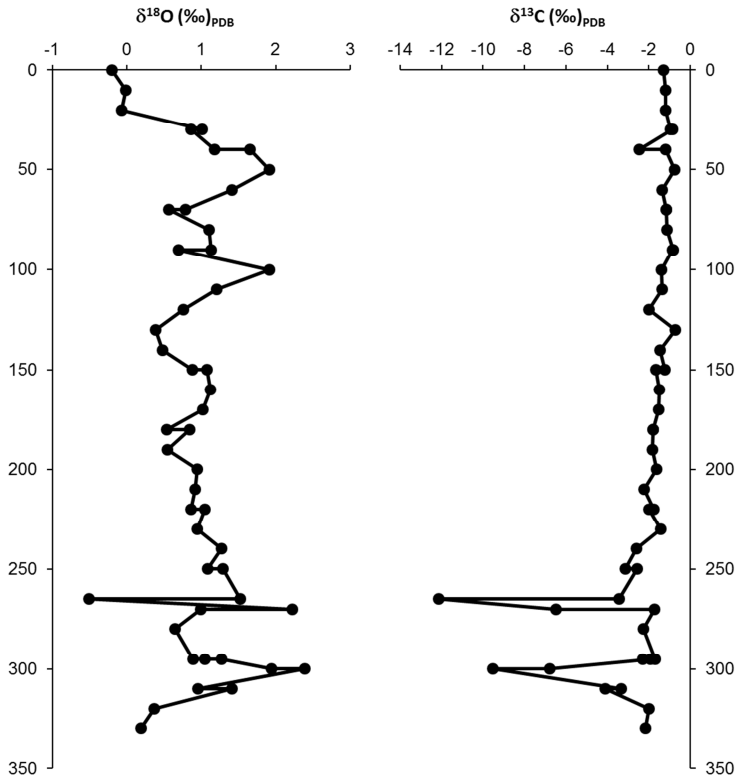

Fig. 4.18 *The $\delta^{18}0$ and $\delta^{13}C$ results measured on the planktonic foraminifera* G. bulloides *from Beta Mound (vertical scale: depth in centimetres).*

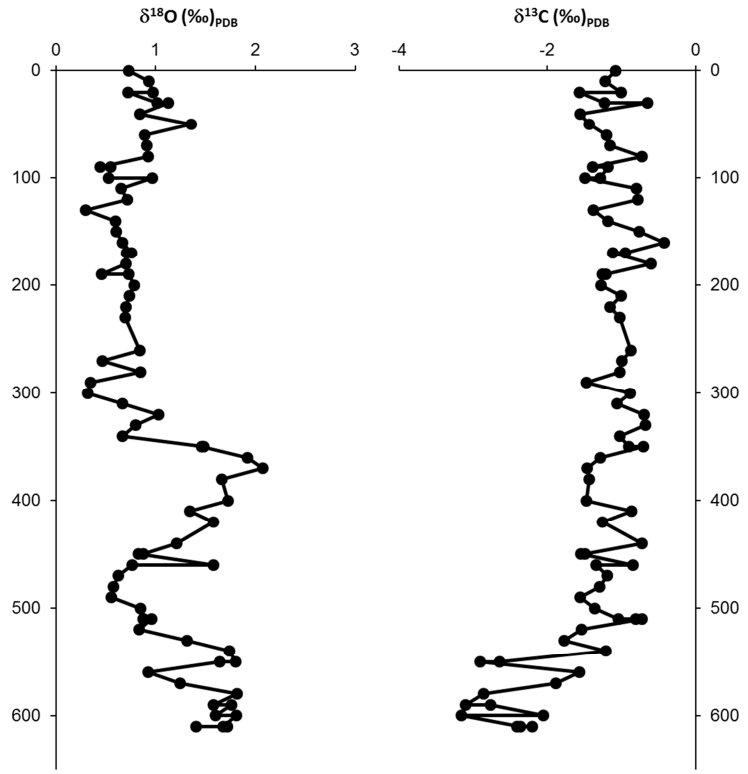

Fig. 4.19 *The $\delta^{18}0$ and $\delta^{13}C$ results measured on the planktonic foraminifera* G. bulloides *from Gamma Mound (vertical scale: depth in centimetres).*

4.3.9 U/Th datings

Calculated U-series ages from the three mounds range between 3.34 ka and 430.76 ka (Table 4.3, 4.4 and 4.5; Fig. 4.20). Within Gamma Mound, only four datings out of ten can be considered as reliable (Table 4.5). The other cold-water coral fragments show excess or loss of ^{234}U, indicating U-series open system behaviour. Most cold-water coral fragments (75%) belong to glacial periods, e.g. marine isotope stages (MIS) 2 to 12. However, a few exceptions have been observed. The *Dendrophyllia* sp. fragments all belong to the Holocene (MIS 1), starting with the first appearance around 11 ka. Additionally, three *M. oculata* specimens are related to interglacial periods: at 55-60 cm depth in Alpha Mound (311 ka – MIS 9), at 49 cm depth in Beta Mound (9.15 ka – MIS 1) and at 363 cm depth in Beta Mound (242 ka – MIS 7). However, taking into account the error on the U-series age, this latter sample can be most probably related to MIS 8.

Core number	Location	Depth (cm)	Age (ka)	Error (ka)	Coral species	Period
MD08-3212	Alpha Mound	0-5	3.42	0.44	*Dendrophyllia* sp.	MIS1
		5-10	11.10	0.23	*Dendrophyllia* sp.	MIS1
		10-17	6.97	0.19	*Dendrophyllia* sp.	MIS1
		17-25	14.30	0.69	Unknown	MIS2
		25-30	364.40	23.08	*M. oculata*	MIS10
		30-35	3.34	0.68	*Dendrophyllia* sp.	MIS1
		35-40	34.90	0.92	*M. oculata*	MIS3
		40-45	35.10	1.40	*M. oculata*	MIS3
		45-50	156.60	3.30	*M. oculata*	MIS6
		50-55	282.00	4.00	*M. oculata*	MIS8
		55-60	311.00	16.00	*M. oculata*	MIS9

Table 4.3 *Results of the U/Th datings of core MD08-3212 on Alpha Mound (MIS = Marine Isotope Stage).*

Core number	Location	Depth (cm)	Age (ka)	Error (ka)	Coral species	Period
M2004-02	Beta Mound	49	9.15	0.71	*M. oculata*	MIS1
		85	19.36	0.54	*L. pertusa*	MIS2
		105	19.87	0.52	*L. pertusa*	MIS2
		141	21.37	0.42	*L. pertusa*	MIS2
		147	22.75	0.26	*L. pertusa*	MIS2
		176	24.03	0.26	*L. pertusa*	MIS2
		247	34.90	0.43	*L. pertusa*	MIS3
		273	36.27	0.43	*M. oculata*	MIS3
		313	142.08	1.92	*L. pertusa*	MIS6
		343	175.01	2.79	*L. pertusa*	MIS6
		363	242.07	8.35	*M. oculata*	MIS7
		403	262.80	7.46	*L. pertusa*	MIS8
GeoB 12101	Gamma Mound	451	430.76	56.55	*M. oculata*	MIS12

Table 4.4 *Results of the U/Th datings on Beta and Gamma Mound (MIS = Marine Isotope Stage) taken from Wienberg et al. (2010).*

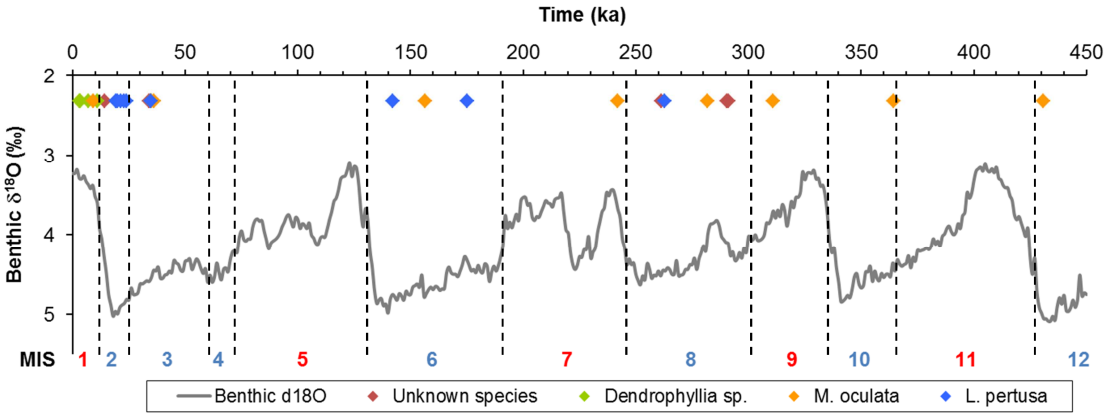

Fig. 4.20 *U/Th dating results from cold-water coral fragments (*Lophelia pertusa*,* Madrepora oculata *and* Dendrophyllia *sp.) superimposed on the benthic* $\delta^{18}O$ *stack of Lisiecki and Raymo (2005). The marine isotope stages (MIS) are marked in red for interglacial periods and in blue for glacial periods.*

Depth (cm)	[^{238}U]	[^{232}Th]	$\delta^{234}U_m$	$^{230}Th/^{238}U$	($^{230}Th/^{232}Th$)	Age (ka)	$\delta^{234}U_{(0)}$ (‰)	Corrected age (ka)	Period
2	3.137±0.005	2.171±0.009	109.7±2.0	0.27203±0.00093	1167±4	30.561±0.19	119.6±2.2	*(30.334 ± 0.28)*	
24	3.779±0.007	0.952±0.001	132.9±1.3	0.30527±0.00053	3593±6	34.066±0.12	146.3±1.5	33.985 ± 0.15	MIS3
116	4.310±0.008	1.703±0.003	142.0±2.0	0.61230±0.00153	4610±11	82.205±0.53	179.1±2.6	*(82.081 ± 0.58)*	
120	3.113±0.010	1.103±0.003	117.5±2.4	0.77791±0.00256	6513±21	125.990±1.32	167.7±3.5	*(125.878 ± 1.37)*	
170	3.382±0.006	14.618±0.045	66.9±1.0	0.98825±0.00328	679±2	262.888±4.78	140.0±3.0	261.525 ± 5.28	MIS8
205	3.139±0.006	7.591±0.017	66.6±1.2	1.01151±0.00225	1243±3	291.185±5.01	151.3±3.5	290.427 ± 5.28	MIS8
216	3.299±0.006	4.624±0.005	68.6±1.3	1.03993±0.00121	2202±3	333.316±5.68	175.9±4.5	*(332.884 ± 5.83)*	
261	2.847±0.006	0.431±0.001	64.2±1.2	1.00866±0.00142	19767±28	291.294±3.87	146.2±3.1	291.244 ± 3.89	MIS8
281	2.631±0.004	1.068±0.001	70.5±1.1	1.04325±0.00204	7631±15	335.183±6.82	181.8±4.5	*(335.057 ± 6.86)*	
546	2.709±0.007	7.124±0.040	51.3±1.9	1.05437±0.00564	1191±6	465.590±51.84	190.9±28.8	*(464.844 ± 51.82)*	

Table 4.5 *Results of the U/Th datings of core MD08-3220 on Gamma Mound (MIS = Marine Isotope Stage). The age results between brackets indicate excess or loss of ^{234}U and hence U-series open system behaviour.*

4.4 Discussion

4.4.1 Diagenetic processes within the Pen Duick mounds

The Pen Duick mounds are intensively influenced by early diagenetic processes (Maignien et al., 2011; Pirlet et al., 2012; Wehrmann et al., 2011), as also demonstrated by the magnetic susceptibility which suddenly drops at the shallow depth of 10 and 37 cm in Alpha and Beta Mound, respectively (Fig. 4.9). This decline in magnetic susceptibility can be explained by the consumption of iron-(oxyhydr)oxides and the pyritisation of detrital iron-bearing minerals during bacterial sulphate reduction (Bloemendal et al., 1992; Hayashida et al., 2007; Karlin and Levi, 1983). A similar effect is also documented in cold-water coral mounds in the Porcupine Seabight (Foubert et al., 2007). In Gamma Mound, this type of diagenesis only starts at a depth of 470 cm (Fig. 4.9). In Gamma Mound no apparent influence of shallow anaerobic oxidation of methane is observed in the uppermost 5 m compared to Alpha and Beta Mound. The brown colour of the sediment, the low amount of iron sulphides and the extremely low $\delta^{34}S$ values indicate that bacterial sulphate reduction is largely outcompeted by dissimilatory iron reduction (Pirlet, 2010). Below 470 cm, the relatively high $\delta^{34}S$ values of the sedimentary pyrite reveal upward diffusion of hydrogen sulphide from a sulphate-methane transition zone (SMTZ), inducing the bad preservation of cold-water coral fragments and calcite and dolomite precipitation (Pirlet, 2010). Although Gamma Mound seems to be less affected by diagenetic processes, other processes are influencing the mound such as the mineralisation of deposited organic matter (Wehrmann et al., 2011). This indicates that although their close proximity and similar sedimentary setting a different diagenetic impact is observed between the three mounds.

The importance of diagenetic processes is confirmed by the CT images which show evidence of the dissolution of the cold-water coral fragments and the formation of pyrite (Pirlet et al., 2012; Wehrmann et al., 2011). This latter process is discussed in detailed in Pirlet et al. (2012) showing the presence of two different pyrite morphologies with framboidal pyrite in Alpha Mound and euhedral pyrite in Beta Mound. These different pyrite morphologies are most probably related to fluctuations of a shallow SMTZ in combination with anaerobic oxidation of methane (Pirlet et al., 2012).

The dissolution of the aragonite of the cold-water coral fragments is observed in all three mounds. Although this effect seems to be limited to certain intervals on the medical CT images, the micro-CT scanning shows that it has a much larger impact (Fig. 4.5). Dissolution plays an important role within the mound, although the impact and intensity can change throughout the mound. Microbial sulphate reduction and consequent reactions can lead to either precipitation or dissolution of calcium carbonate, depending on the degree of openness of the system and the amount of reactive iron in the sediment (Ferdelman et al., 2006; Sanders, 2003; Wehrmann et al., 2009). Dissolution creates secondary porosity which

can be either filled up again with the matrix sediments or remain unaffected. Wehrmann et al. (2011) proposed three mechanisms to explain coral dissolution: (1) anaerobic methanotrophy (earlier suggested by Foubert et al. (2008)), (2) hydrogen sulphide/pyrite oxidation, and (3) dissolution by H_2S-titration. This latter mechanism is most likely the best option, although the second mechanism cannot be excluded (Wehrmann et al., 2011).

Pirlet et al. (2012) showed the presence of several lithified layers due to carbonate precipitation in Alpha (162-255 cm, 367-375 cm and 419-445 cm) and Beta (101-120 cm, 234-268 cm and 281-300 cm) Mound, illustrating the importance of early diagenesis in the stabilisation of the mounds. However, comparing these intervals with the grain-size data, which is independent of any diagenetic influence, the lithified layers correspond with small changes in grain-size (0-5 µm). This suggests that the early diagenesis within the cold-water coral mounds is not only determined by the position of the SMTZ but also by the composition of the original, unaffected sediment.

The influence of diagenesis is also observed in the carbon isotopic signatures of the planktonic foraminifera in Alpha and Beta Mound (Fig. 4.17 and 4.18). In Beta Mound, two spikes are observed in the $\delta^{13}C$ signature: at 265 cm and 300 cm depth (Fig. 4.18). Similar anomalies are present in the $\delta^{18}O$ signature, indicating the influence of a post-depositional contamination, e.g. diagenetic alteration (Hill et al., 2003). In Alpha Mound, negative carbon isotopic values are observed throughout the whole core reaching a minimum value of -10.75 ‰ at a depth of 230 cm (Fig. 4.17). Additionally, slightly increased values are observed in the oxygen isotopic signature, which are typically altered due to the presence of authigenic carbonate (Hill et al., 2003). This might also indicate post-depositional alteration in Alpha Mound, most probably caused by the imprint of the isotope composition of the authigenic high-Mg calcite that formed in close vicinity of a SMTZ (Wehrmann et al., 2011).

4.4.2 Cold-water coral growth on Pen Duick Escarpment

Cold-water corals are observed through the whole mound body, however, the species and the amount of coral fragments is temporally variable. The variation in cold-water coral species throughout the sediment cores indicates the dominance of *L. pertusa* and *M. oculata* over *Dendrophyllia* sp. (Fig. 4.4). In Alpha and Beta Mound *Dendrophyllia* sp. is observed in the uppermost part of the mound (0-40 cm) and below a depth of 300 cm while in Gamma Mound *Dendrophyllia* sp. only occurs between 480 and 530 cm. In Beta Mound a few *Dendrophyllia* sp. specimens are also present between 140 and 145 cm. *L. pertusa* and *M. oculata* are able to form bush-like colonies, preferably under cold and stable conditions (Wienberg et al., 2009; Wienberg et al., 2010). In contrast, *Dendrophyllia* sp. forms small colonies under warm conditions and is thus most probably not co-occurring with *L. pertusa* and *M. oculata* (Wienberg et al., 2009). As the three mounds on the PDE are mainly built up of the latter two cold-water coral species, mound growth in the Gulf of Cadiz can be mostly

assigned to glacial periods. This is confirmed by the U/Th datings where 75% of all dated cold-water coral fragments belong to glacial times (Fig. 4.20). Even 88% is reached when only looking to the *L. pertusa* and *M. oculata* specimens. Cold-water coral growth is mainly observed during MIS 2, 3, 6 and 8. All *Dendrophyllia* sp. coral fragments belong to the Holocene (MIS 1), corresponding with interglacial conditions.

Striking differences are observed in the U-series dating between the three mounds. For example, in Alpha Mound coral ages of 280 ka are already reached at a depth of 50 cm while in Beta Mound this age occurs around the depth of 400 cm and in Gamma Mound around 200 cm. As already mentioned in the previous section (4.4.1) Alpha and Beta Mound have been diagenetically altered, which can have a big impact on the dating results (N. Frank, pers. comm.). Isotopic systems are more sensitive to diagenetic change than is any petrographic or general geochemical parameter (Chen et al., 1991; Zhu et al., 1993). However, no general correction technique has yet been developed for diagenetically altered fossil corals (Scholz et al., 2004). This diagenetic alteration results in older apparent ages due to elevated $\delta^{234}U$ concentrations and excess ^{230}Th. A fundamental principle of U/Th dating is that corals incorporate substantial seawater uranium and negligible thorium into their aragonite skeletons during growth, and remain subsequently closed to uranium and thorium loss or gain (Broecker et al., 1963). Several processes can disturb this closed system such as the decay of dissolved uranium, due to leaching and dissolution of carbonate, and α-recoil mobilisation of uranium daughters (Thompson et al., 2003). Excess ^{234}Th and ^{230}Th can be gained by the growth of secondary minerals and cements, and the aqueous transport of fine carbonate particles. These source materials have relatively high U concentrations, are finely divided and are in close contact with or intermingled with coral aragonite (Thompson et al., 2003). Both, dissolution of carbonate and the growth of secondary minerals have been observed in Alpha and Beta Mound (Pirlet et al., 2012).

4.4.3 Characterising sediment contributors

Based on the EMMA, four significant end-members (EM 1-4) were determined. Next, these end-members enable the characterisation of “EM-dominated lithofacies” which can in turn be related to different sedimentary processes, e.g. sediment source and transport pathway.

Aeolian dust from the Sahara and Sahel regions plays an important role along the northwest African coast (Fig. 4.21). At present, 130 to 700 million tons per year of dust is transported to the subtropical and tropical Atlantic (Marticorena and Bergametti, 1996; Schütz et al., 1981; Swap et al., 1996), corresponding with one third of the global aeolian dust input to the world ocean (Duce et al., 1991). Aeolian sediments deposited in the deep sea close to the continent are in general coarser grained than hemipelagic sediments. Several studies show that terrigenous sediments with mean grain-sizes > 6 µm can be attributed to aeolian transport while mean grain-size < 6 µm represent hemipelagic transport (Prins et al., 2000;

Ratmeyer et al., 1999; Sarnthein et al., 1981). Present-day grain-size distributions from dust samples along the NW African coast have mean modal size from about 8 to 42 µm (Stuut et al., 2005). However, terrigenous sediments are not only transported by wind but also river input can play a role along the continental margin (Holz et al., 2004; Holz et al., 2007). The total discharge by northwest African rivers is estimated at 110 million tons per year (Hillier, 1995).

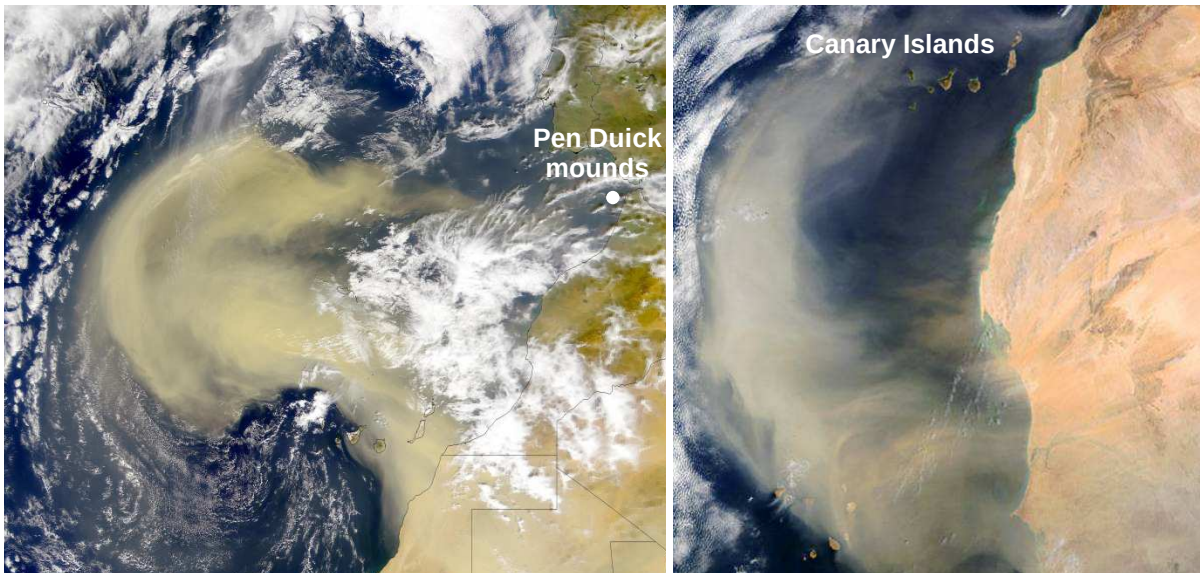

Fig. 4.21 *Examples of recent Saharan dust releases to the Atlantic Ocean along the NW African continental margin (source: http://www.nasa.gov).*

Hence, the three coarsest end-members (EM 1, 3 and 4) are interpreted as aeolian dust input. EM 1 has a mean modal size of 20 µm and is defined as coarse aeolian dust whereas EM 3 and EM 4, with mean modal sizes of 10 and 7.8 µm respectively, are defined as fine aeolian dust. The last end-member, EM 2, with a mean modal size of 3.8 µm is correlated to hemipelagic sediments. This hemipelagic mud is derived from continental runoff and is settled out of suspension from nepheloid layers (Stuut et al., 2002). Comparable EMMA results were obtained by several studies along the NW African margin (e.g. Holz et al., 2007; Stuut et al., 2005; Wienberg et al., 2010).

Three end-members (EM 2, 3 and 4) have mean modal sizes smaller than 10 µm, inducing cohesive particle behaviour (McCave and Hall, 2006). These sediments will be transported and deposited as aggregates, particles bound together by biological and/or physical processes. Hydrodynamic inferences from aggregates are not straight-forward as they behave hydraulically equivalent to the coarser, non-cohesive grains (Chang et al., 2007). However, aggregate-rich deposits do suggest a relatively quiescent environment, as aggregate break-up in more energetic conditions would significantly suppress the deposition of fines (McCave and Hall, 2006). Additionally, only poorly sorted sediment is observed which is another indication for a low impact of bottom current activity. Sediment sorting occurs principally during resuspension and deposition by processes of aggregate breakup

(McCave and Hall, 2006), unless a sediment preserving agent exists. The presence of a dense, stabilising coral framework can significantly promote accumulation of very fine sediment (Thierens et al., 2010). Although higher bottom current activity has occurred on PDE, the impact of these currents on sediment transport and deposition of fine sediment is difficult to trace using EMMA. However, several arguments, e.g. poorly sorted material and a dense coral framework, favour a low impact.

Aeolian dust is widely recognised as a potential major player and recorder of environmental change (Stuut et al., 2005). Subsequently, the wind strength and total aeolian input can be calculated (Fig. 4.21), knowing that three out of four end-members are of aeolian origin. The EM1/(EM1+EM3+EM4) ratio (coarse vs fine aeolian dust ratio) is considered as a measure for the relative wind intensity (Stuut et al., 2002), while the proportion of the aeolian end-members (1-EM2) represents changes in continental aridity. In all three cores, at least 50% of the sediment input for each sample can be explained by the contribution of aeolian dust. On average more than 80% and even 90% in Beta Mound is related to this aeolian input.

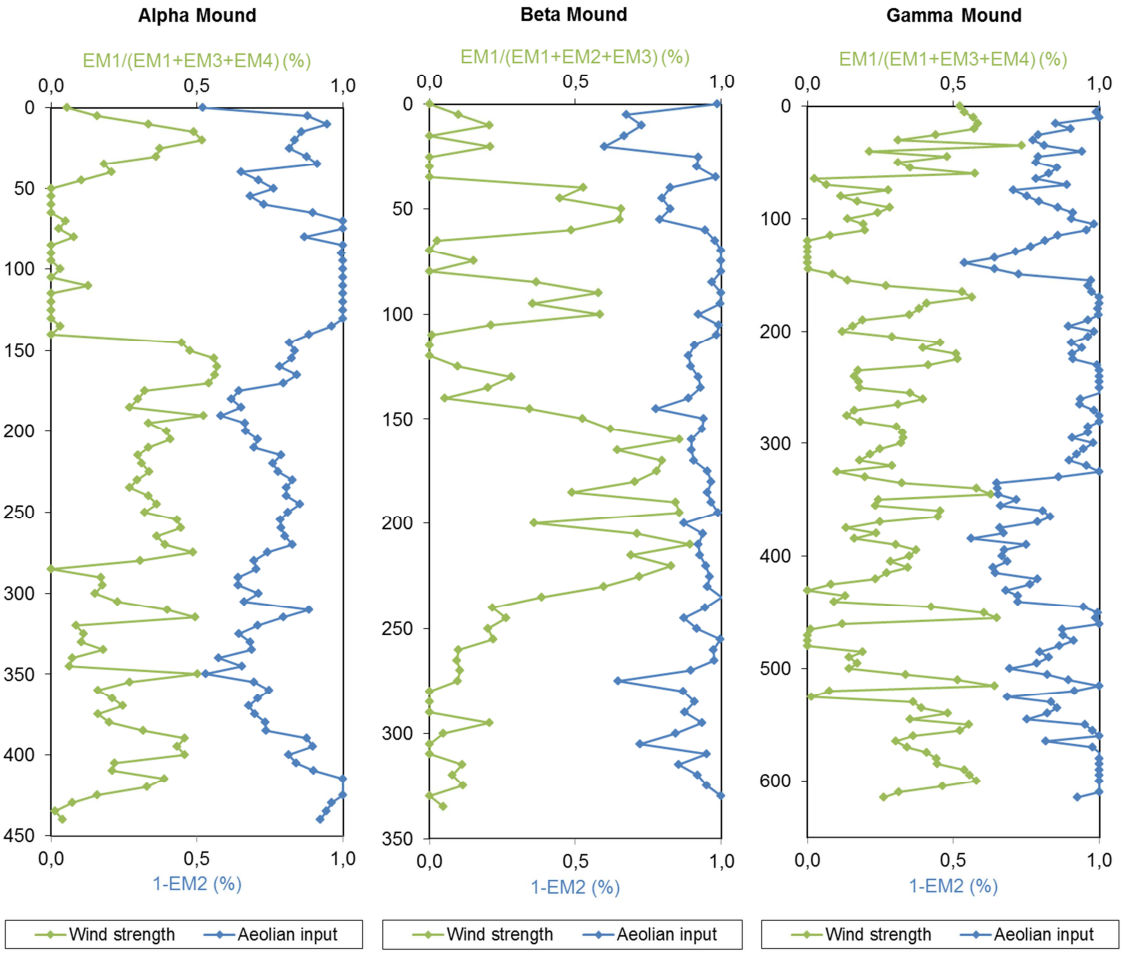

Fig. 4.22 *Variations in wind strength and aeolian dust input based on the EMMA (vertical scale: depth in centimetres).*

4.4.4 Link between mound growth and NW African climate

Within this section, we will mainly focus on Gamma Mound in order to reveal the evolution of the Pen Duick mounds related to paleoenvironment (Fig. 4.23). The significant impact of diagenesis starts at a depth of 470 cm while in Alpha and Beta Mound the influence of diagenetic processes is already observed close to the surface (10 and 37 cm, respectively). This impact is reflected in the CT analyses, magnetic susceptibility measurements, stable isotope analyses and U/Th datings (as described in sections 4.4.1 and 4.4.2). The terrigenous fraction of marine sediment records reflects the input of material produced on and discharged from continents, which is directly related to climate conditions in the hinterland (Holz et al., 2007). Many factors, such as wind intensity, direction, and seasonality, as well as vegetation cover, terrestrial weathering intensity, and balance between aeolian and fluvial transport, affect the composition of this terrestrial material along the NW African continental margin (Cole et al., 2009). At present, northwest Africa is dominated by two climate systems, separated by the Saharan desert belt (Nicholson, 2000). The climate north of 20-24°N is dominated by the North Atlantic and Mediterranean winter rains while south of this, summer monsoonal rains play a major role in subtropical African climate (Knippertz et al., 2003). During the past, paleoclimatic changes on the African continent appear to have been a complex alternation of wet and dry periods with abrupt transitions (deMenocal et al., 2000; Gasse, 2000).

The observed growth pattern in Gamma Mound can be explained by changes in climatic conditions on the NW African continent (Fig. 4.23). Cold-water coral growth on the Pen Duick mounds is restricted to glacial periods, as shown in chapter 3 and section 4.4.2. Additionally, based on the core analyses, we can conclude that also mound growth can be assigned to glacial conditions, mainly during MIS 8 and MIS 2-4 (Fig. 4.23). These glacial periods are characterised by enhanced wind intensity and a reduced vegetation cover due to a more arid climate on the NW African continent (Sarnthein, 1978; Stein, 1985; Zühlsdorff et al., 2007) (Fig. 4.24A). This results in an increase in dust erosion and transport (Moreno et al., 2001; Stein, 1985), which is reflected in the end-member modelling analyses and in the enhanced Fe supply (Fig. 4.23). Fe supply is associated with hematite and can be linked with increased aeolian input (Rogerson et al., 2006). During periods of enhanced dust input, the primary production increases due to the supply of iron and manganese in combination with locally intense upwelling, which results in enhanced food availability for the cold-water corals (Boyd et al., 2000; De Jong et al., 2007; Wienberg et al., 2010). These strong upwelling conditions can be related to migrations of the Azores Front towards the Gulf of Cadiz (Rogerson et al., 2004). Not only on top of the escarpment but also at the foot, the influence of aeolian input during glacial times is recorded (De Jonge, 2010).

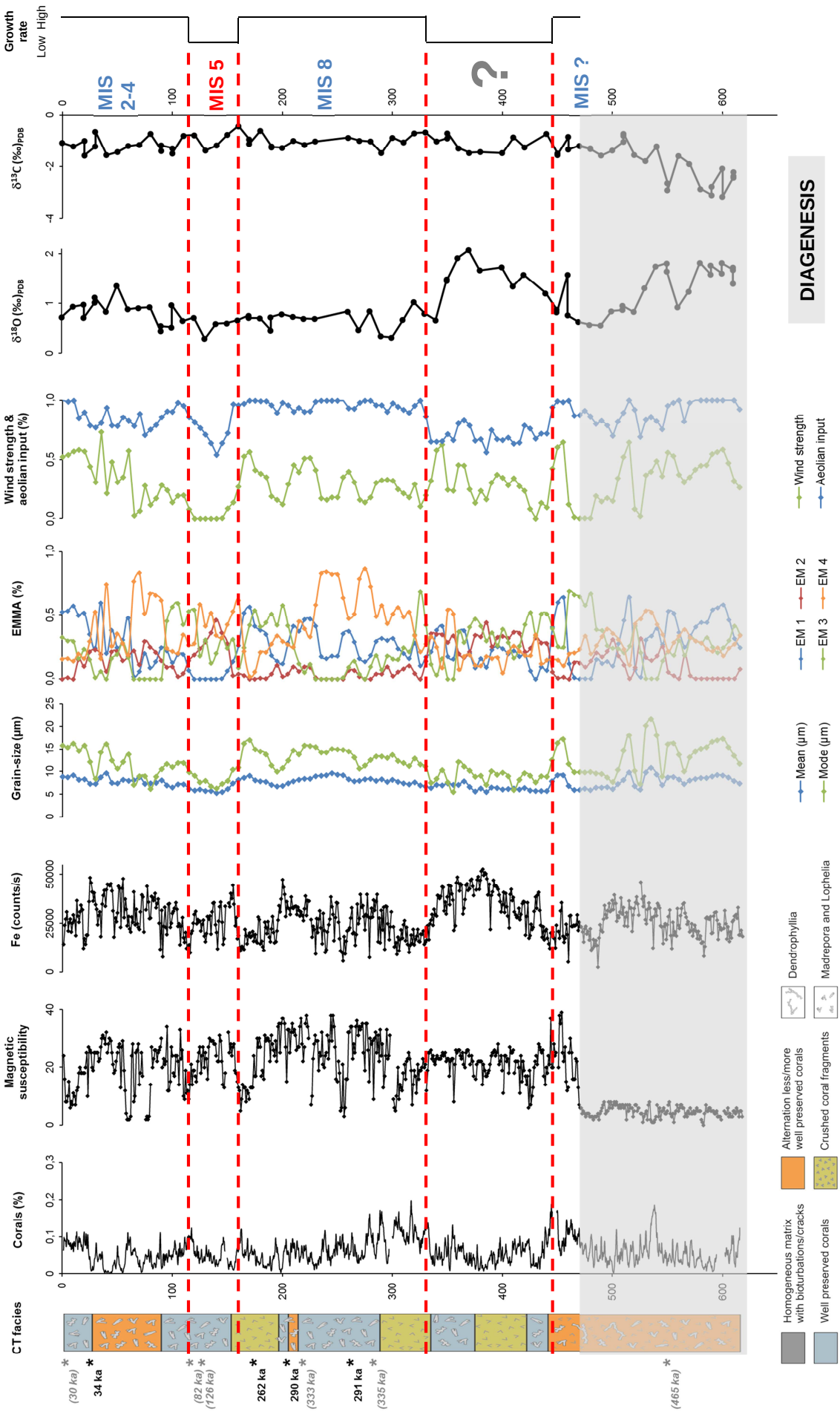
Growth rate
Low High
MIS 2-4
MIS 5
MIS 8
?
MIS ?
δ13C (‰)PDB
δ18O (‰)PDB
Wind strength & aeolian input (%)
EMMA (%)
Grain-size (µm)
Fe (counts/s)
Magnetic susceptibility
Corals (%)
CT facies
DIAGENESIS
Wind strength
Aeolian input
EM 1
EM 2
EM 3
EM 4
Mean (µm)
Mode (µm)
Dendrophyllia
Madrepora and Lophelia
Alternation less/more well preserved corals
Crushed coral fragments
Homogeneous matrix with bioturbations/cracks
Well preserved corals
(30 ka)
34 ka
(82 ka)
(126 ka)
262 ka
290 ka
(333 ka)
291 ka
(335 ka)
(465 ka)

(Left) Fig. 4.23 *Results of the core analyses on Gamma Mound, indicating different mound growth periods (dashed red lines). MIS = Marine Isotope Stage (blue = glacial, red = interglacial).*

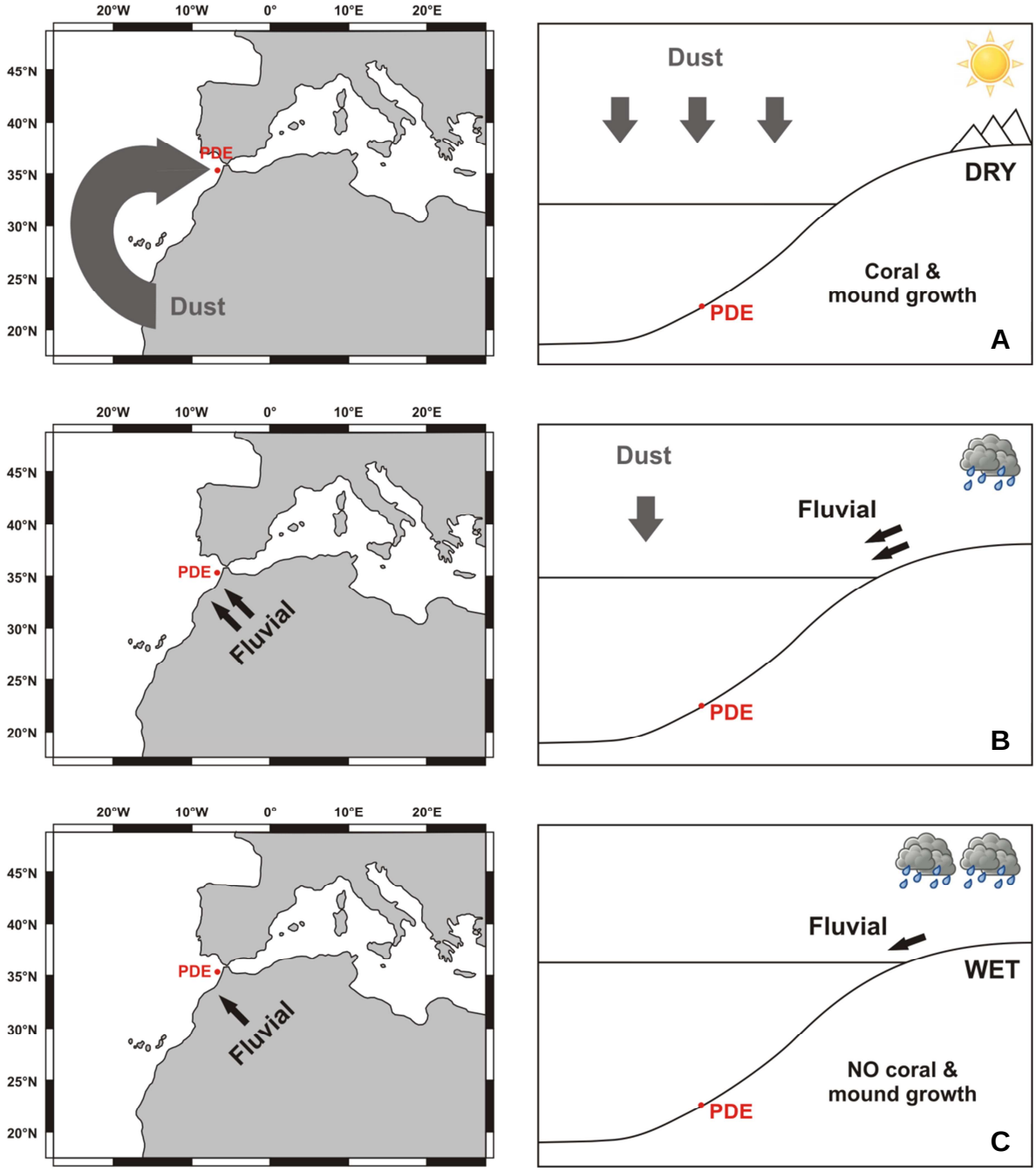

Fig. 4.24 *Evolution and growth of the cold-water coral mounds on the Pen Duick Escarpment (PDE) related to NW African climate changes: (A) during glacial periods, (B) during glacial/interglacial transitions, and (C) during interglacial periods.*

In contrast, interglacial periods show much wetter conditions (Fig. 4.24C). During these humid periods, the Saharan desert region was nearly completely vegetated (Jolly et al., 1998) with numerous lakes (Gasse, 2000; Hoelzmann et al., 1998). In combination with a decrease in wind stress, only minor amounts of dust were supplied to the outer shelf and the continental slope (deMenocal et al., 2000; Sarnthein et al., 1981). During humid to arid

climatic transitions (Fig. 4.24B), the fluvial sediment supply across the shelf edge to the deep sea increased and probably continued during the warm stages (Stein, 1985). Fluvial input along the Moroccan margin is provided by rivers draining the Atlas Mountains. For example, the drainage basin of the Sebou river covers an area of 40.000 km² and is responsible for very strong erosion (929 $t.km^{-2}.a^{-1}$) during periods with a scarce plant cover and relatively frequent precipitations (Snoussi et al., 1990), such as glacial/interglacial transitions. On the PDE, mound growth is very limited during interglacials, which will possibly result in slowing down or interrupting the mound building process.

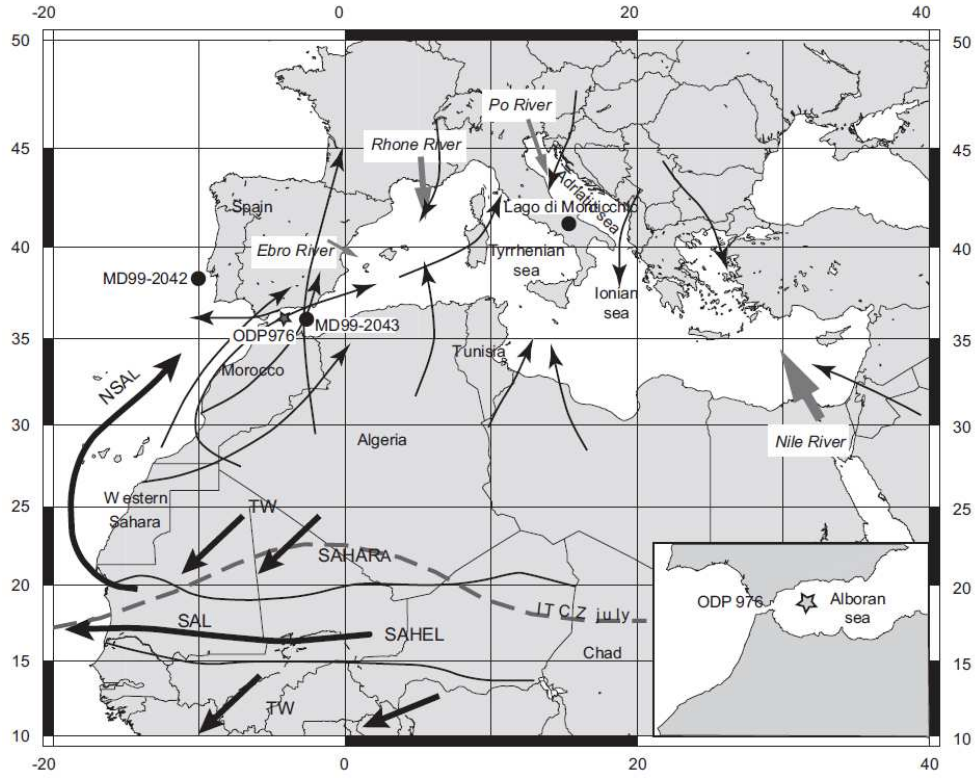

Fig. 4.25 *Map showing the main wind trajectories (black arrows) and river supply (grey arrows) in the Mediterranean area. SAL: Saharan air layer, TW: northeast trade winds, NSAL: northern branch of the SAL, ITCZ July: position of the Inter-Tropical Convergence Zone in July (Bout-Roumazeilles et al., 2007).*

The source area and transport pattern of the dust towards the Gulf of Cadiz can be derived from studies in the Mediterranean Sea and more specifically from the dust input in the Alboran Sea (at the other side of the Gibraltar Strait) (Fig. 4.25). The African continent is influenced by intensified NE trade winds during glacial periods, although these trade winds cannot explain the input of dust along the Moroccan margin (NW of the African continent). The major source area of aeolian dust towards the western Mediterranean Sea is predominantly from the southwest (Morocco/NW Algeria) during interglacial periods and from the southern Saharan/Sahelian region during glacial times (Weldeab et al., 2003). Based on pollen and clay mineral-specific features, Bout-Roumazeilles et al. (2007) defines western Morocco as the dominant source of wind-blown particles during glacial periods. However, further mineralogical research is necessary to determine the exact source area for

dust input on the PDE. This dust is mainly transported towards the Gulf of Cadiz by the northern branch of the Saharan air layer (NSAL) as well as by smaller wind trajectories from southern Morocco (Fig. 4.25).

Within Gamma Mound, five different growth periods have been recognised (Fig. 4.23). The lowermost interval between 445 and 470 cm can be defined as a glacial stage, probably MIS 10 or 12, however, no dating results are available. This interval is characterised by high aeolian input, high wind intensity, higher grain-sizes and increased magnetic susceptibility, indicating cold environmental conditions. Next, between 330 and 445 cm depth, an interval is determined which cannot be related to a glacial or an interglacial event. Compared to the previous and following phase, the dust input decreases and the fluvial input (EM 2) increases, indicating interglacial conditions. However, the stable oxygen isotopic values increase as well as the Fe supply, pointing towards a glacial environment. U-series datings of the coral fragments can give an answer to this question which will allow to explain these contradictory observations. MIS 8 represents the largest interval (155-330 cm) and thus corresponds with a long period of coral and mound growth on the PDE. This interval shows a dust input of almost 100%, high wind intensities, rather high grain-sizes and high magnetic susceptibility values; all indicators for glacial times. This is confirmed by the U/Th datings: 262, 290 and 291 ka. MIS 8 starts with thriving cold-water coral growth which gradually decreases towards the end of the interval. In the North Atlantic, glacial periods are characterised by high concentrations of magnetic minerals while interglacial periods have low magnetic mineral concentrations (Robinson, 1986). During the following phase (115-155 cm), the aeolian input as well as the wind strength suddenly decreases and the influence of fluvial discharge (represented by EM 2) becomes more important. This might suggest an interglacial period, most probably MIS 5. However, the magnetic susceptibility and the Fe counts are relatively high compared to glacial periods. Cheggour et al. (2005) showed that continental runoff is a major contributor of Fe supply to the estuaries and thus the continental shelf. The amounts of Fe are high in all the studied estuaries, including the Sebou river, along the Moroccan coast (Cheggour et al., 2005 and references therein) which can explain the high Fe counts during interglacial intervals on the PDE. The last growth phase can be linked with MIS 2-4 and is represented in the core from 0 to 115 cm. This interval is characterised by a high input of aeolian dust (at least 78%), high Fe counts, increasing wind intensity and increasing grain-sizes. All these observations indicate glacial environmental conditions which is confirmed by U-series datings of the cold-water coral fragments (14, 19 and 34 ka).

During the past, there was not always a constant mound building process but hiatuses might be expected due to paleoenvironmental changes, e.g. dust input, fluvial input, wind intensity and direction, oceanographic circulation patterns (Foubert and Henriet, 2009; Kano et al., 2007; Mienis et al., 2009). During these hiatuses, dead cold-water corals are exposed at the seabed for a much longer amount of time, which can result in disintegration and/or bio-

erosion of the coral fragments. This latter process, mostly by sponges and fungi, is the key process in the formation of coral rubble (Roberts et al., 2009). This coral rubble can then provide a substratum for renewed coral settlement, starting a new phase in reef forming and thus a next phase in the mound building process. Hiatuses are not only linked with interglacial periods on the Pen Duick mounds. For example, MIS 6 is missing in Gamma Mound while cold-water coral fragments of this period are observed in Alpha and Beta Mound. These differences can occur due to local hydrodynamic and bottom current variations (McCave and Hall, 2006), as also described in chapter 3. The presence of *Dendrophyllia* sp. fragments at the top of Alpha and Beta Mound can be linked with the most recent African Humid Period (MIS 1). This wet period occurred roughly between about 9 and 6 ka (Ritchie et al., 1985), although several marine records indicate a more extended duration of the wettest part from about 14.5 to 5.5 ka (Gasse, 2000; deMenocal et al., 2000). Remarkable is the presence of *Dedrophyllia* sp. fragments in the lower part of all three mounds (Fig. 4.5), indicating another period of warmer conditions. However, U-series dating of these coral fragments was not possible due to their bad preservation state under influence of diagenetic processes. For this reason, it was only possible to date a few *L. pertusa* and *M. oculata* fragments, which are linked to glacial environmental conditions. These results can give a wrong impression of glacial/interglacial mound growth due to a methodological restriction. Hence, this indicates that mound growth can continue during interglacials, although with a reduced growth rate. However, at this moment, it is not possible to trace this within the sediment cores.

The Pen Duick mounds show a similar growth pattern as the large coral mounds off Ireland and off Mauritania: all mounds are characterised by a periodic growth with intervals containing coral bearing sediments and marked by numerous hiatuses that represent periods without cold-water coral growth on the mounds. However, one of the major differences is the type of sediment. While the terrigenous fraction in the Porcupine mounds is built up of ice-rafted debris, mainly linked to the development of the British-Irish Ice Sheet (Thierens et al., 2012), the terrigenous fraction of the mounds on the PDE consist of aeolian dust derived from the NW African continent. Hence, the terrigenous component of mound growth is not restricted to a certain type of sediment source but a large input of terrigenous sediment is more important in order to stimulate vertical growth. Additionally, suitable conditions for cold-water coral growth are necessary. Surface water productivity is one of the most prominent local forcings for cold-water coral growth and mound growth off Ireland and off Mauritania (Eisele et al., 2011; Thierens et al., submitted). Planktonic foraminifera assemblages show signs of enhanced productivity during the last glacial, caused by frontal upwelling, in a sediment core NW of the Pen Duick Escarpment (Wienberg et al., 2010). However, further research on the Pen Duick mounds is necessary in order to reveal the role of surface water productivity on cold-water coral growth in the southern Gulf of Cadiz.

4.5 Conclusions

The Pen Duick mounds are largely impacted by diagenetic alteration such as dissolution of carbonates, the formation of pyrite and the formation of lithified layers. However, in Gamma Mound the significant impact of these diagenetic processes only start at a depth of 470 cm which makes it a suitable mound to study the build-up of the mounds. Cold-water coral fragments are observed throughout the whole core but species and amount of corals vary. *L. pertusa* and *M. oculata* are the dominant framework building species although some *Dendrophyllia* sp. fragments are also observed. 88 % of the U-series dating results of the first two species belong to glacial times while *Dendrophyllia* sp. prefers warmer conditions during interglacial periods such as the Holocene (MIS 1). The growth and evolution of cold-water coral mounds on the Pen Duick Escarpment is related to climatic changes on the NW African continent. During glacial periods, a more arid climate results in increased wind intensity and a scarce plant cover, providing high dust input in the NE Atlantic Ocean. Aeolian dust is transported to the southern Gulf of Cadiz by the northern branch of the Saharan air layer and some additional smaller wind trajectories from southern Morocco. This dust input not only favours cold-water coral growth but also mound growth as on average more than 80 % of the terrigenous fraction of the mound sediments consists of this aeolian dust. Mound growth can be mainly assigned to MIS 8 and MIS 2-4 for Gamma Mound, although MIS 6 is also represented in Alpha and Beta Mound. During interglacial periods, the on land climate becomes more humid which will increase the supply of fluvial material towards the continental shelf. During these periods, mound growth is slowed down or even interrupted, creating hiatuses. However, the presence of *Dendrophyllia* sp. fragments in the deeper part of the mounds indicates possible mound growth during interglacial periods. Due to the bad preservation of the coral fragments it is not possible to date these fragments and thus to trace coral and mound growth during past interglacial periods on the Pen Duick mounds.

Acknowledgements

The authors would like to thank the shipboard party of the R/V Marion Dufresne 169 cruise for their help and nice cooperation. We especially want to thank IPEV, Y. Balut and H. Leau for the logistic and operational support for the coring facilities. The MD169 MiCROSYSTEMS cruise was financially supported by the CNRS-EDD. B. Delay (Scientific Board) and N. Gibelin (International Relations) are warmly thanked for their active contribution to this project. This work was financially supported by the ESF EuroDIVERSITY MiCROSYSTEMS project (05_EDIV_FP083-MICROSYSTEMS), the EC FP6 HERMES project “Hotspot Ecosystem Research on the Margins of European Seas” (GOCE-CT-2005-511234-1) and the EC FP7 HERMIONE project “Hotspot Ecosystem Research and Man’s Impact on European Seas” (contract number 226354). A part of the study was performed within the ESF Short Term Visit Grant Scheme in between the EuroDIVERSITY and EuroDEEP projects at the Royal Netherlands Institute for Sea Research (NIOZ). R. Gielis, H. de Haas, C. van der Land and F.

Mienis are thanked for their help with the core opening, XRF analyses and MS measurements. L. De Mol wishes to acknowledge the Centre for X-ray Tomography (UGCT) and the Ghent University Hospital, especially H. Houbrechts, for the use of their facilities and knowledge regarding CT imagery. M. Boone and J. Dewanckele are thanked for their help with the different CT visualisation software packages. We are grateful to Prof. Dr. M. Vincx (Marine Biology Section, Ghent University) for allowing us to use the Malvern Mastersizer 2000. L. De Mol is funded by the "Agency for Innovation by Science and Technology in Flanders (IWT)".

Part 3

Bay of Biscay

Introduction

Cold-water coral research in the Bay of Biscay started already in the 19th century. The first cruise along the French coasts was conducted by Audouin and Milne Edwards in 1830 (Le Danois, 1948). From the year 1870 onwards also deep-sea research campaigns were organised (Reveillaud et al., 2008). In 1922, Joubin produced a map of the cold-water coral reef occurrences in the NE Atlantic based on 70 cold-water coral reef reports. Massive cold-water coral reefs were described, mainly of *Lophelia pertusa* and *Madrepora oculata*. During the following years, mainly the zoologist Le Danois focussed on the area which ended up in 1948 with the publication "Les profondeurs de la mer: trente ans de recherches sur la faune sous-marine au large des côtes de France". He defined the species *Lophelia pertusa* and *Madrepora oculata* as the two main reef forming species. Additionally, he described the presence of the yellow coral *Dendrophyllia cornigera*. Five important coral reef sites were reported along the margins of the Bay of Biscay: the "Massif du Banc de la Chapelle", the "Massif de la Grande Vasière", the "Massif coral jaune du Banc Le Danois", the "Massif Galicien de l'Est", and the "Massif Galicien de l'Ouest" (Fig. 3A).

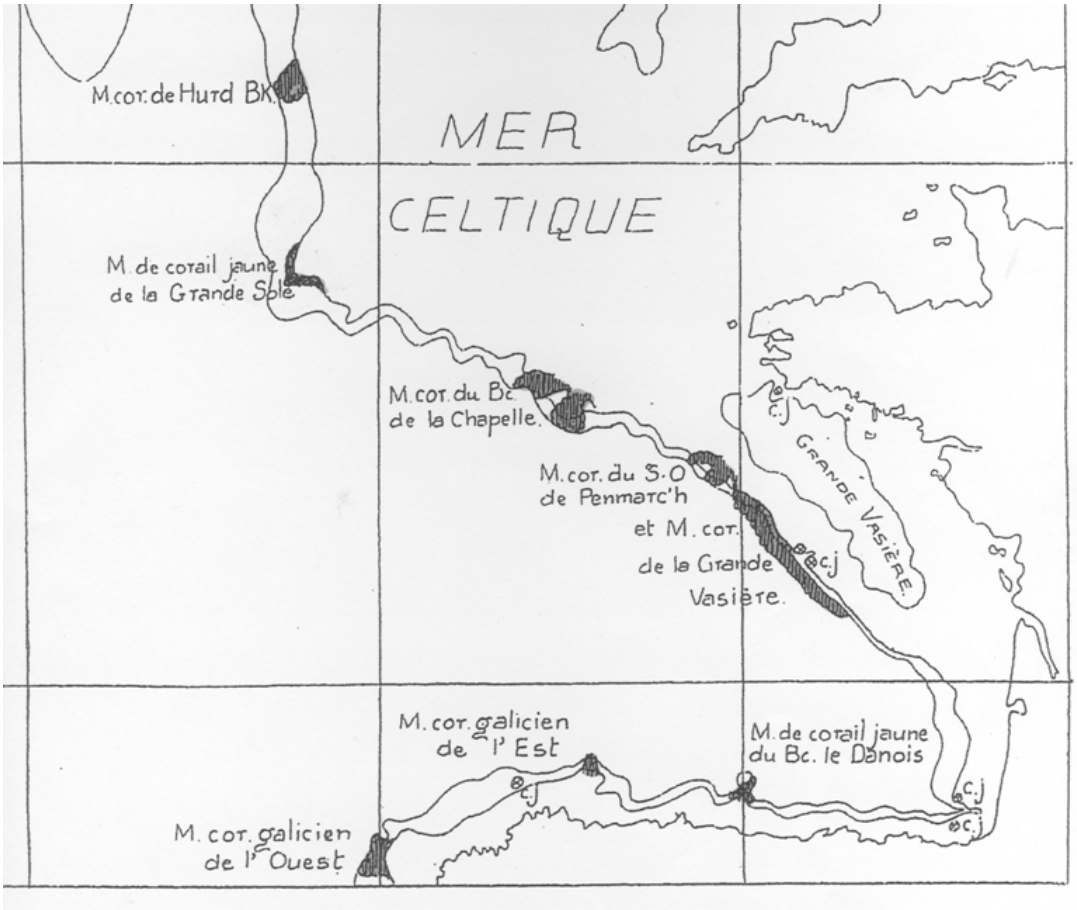

Fig. 3A *Overview of the cold-water coral locations defined by Le Danois (1948) in the Bay of Biscay.*

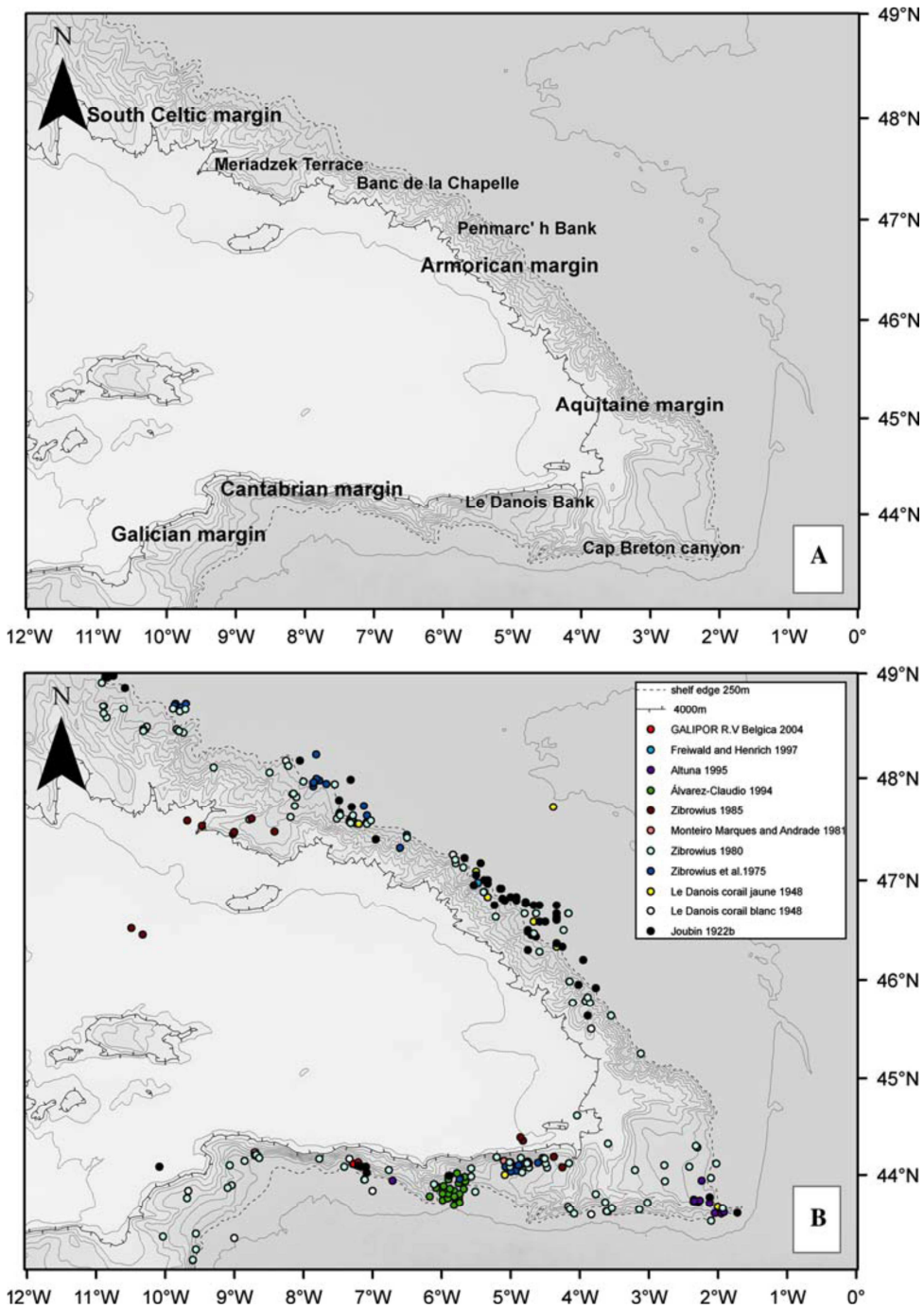

Fig. 3B *(A) The continental margin of the Bay of Biscay with the geographic names. The shelf edge is on average at 250 m (dashed line) and the foot of the continental margin is at 4000 m water depth (crossed line). Spacing of contour lines is 500 m. (B) Findings of cold-water scleractinians cluster along the continental margin in the Bay of Biscay (Reveillaud et al., 2008).*

During the following 30 years, the Bay of Biscay only received occasional attention, however, Zibrowius et al. (1975) reported eight scleractinian species and described numerous stations with cold-water coral reefs in the NE Atlantic (Reveillaud et al., 2008). The research continued from 1972 to 1981 in the framework of the French BIOGAS (Biology Gascogne) program (Laubier and Monniot, 1985; Zibrowius, 1985). Next, a French-Spanish project (1987-1990) focussed on the Cap Breton canyon (SE Biscay margin) (Altuna, 1994; Altuna,

1995). Additional stations were sampled in 1987 in a small area of the Cantabrian margin (Álvarez-Claudio, 1994). In total, Álvarez-Claudio (1994) reported 1100 cold-water coral specimens in a depth range from 50 to 1347 m, belonging to 15 scleractinian species and five families. After 10 years of no research in the Bay of Biscay, the canyon heads near the Banc de la Chapelle and the Penmarc'h Bank have been revisited during the R/V Victor Hensen VH-97 cruise in 1997 (Reveillaud et al., 2008). In the shallow part mainly *Caryophyllia smithii* corals were observed while in the deeper part dead colonies of *Lophelia pertusa*, *Madrepora oculata* and *Desmophyllum dianthus* were present. No living scleractinians were encountered, except for a few living colonies of *Dendrophyllia cornigera* near the outer Penmarc'h Bank (Reveillaud et al., 2008). A more extended overview of the historical campaigns and the evolution of the knowledge on scleractinians in the Bay of Biscay is presented in Reveillaud et al. (2008) (Fig. 3B).

After again a few years of only occasional research interest, the RCMG started in 2004 to revisit several locations in the Bay of Biscay where Le Danois (1948) had earlier described thriving coral colonies (Fig. 3A). The first cruise onboard the R/V Belgica (the GALIPOR cruise) was set out in 2004 in order to investigate the Cantabrian and Galician margins. Extensive zones of dead coral rubble was observed on the shelf margin which is in contrast with the earlier described thriving coral colonies by Le Danois (1948). In 2006, a second cruise was organised to the Banc de la Chapelle (north Armorican margin), followed by two R/V Belgica cruises in 2008 and 2010 to the Penmarc'h and Guilvinec canyons (south Armorican margin). These latter two cruises followed a rigorous, integrated exploration protocol comprising high-resolution multibeam coverage, subsequent high-resolution seismic data acquisition, CTD profiling to characterise the water masses in the canyon, and finally targeted exploratory ROV dives and boxcoring. The R/V Belgica cruises all frame within the EU FP6 HERMES and the EU FP7 HERMIONE projects which aim to investigate ecosystems at critical sites on Europe's deep-ocean margin. Data from the R/V Belgica cruises in 2006 and 2008 will be discussed in the following two chapters.

Besides the Belgian interest in cold-water coral ecosystems along the continental margin in the Bay of Biscay, also the interest of French institutes raised. This led to the organisation of two cruises BobGEO (2010) and BobECO (2011) within the framework of the European CoralFISH project (2008-2012). This project aims to study the interactions between corals and fisheries, and to provide information needed for a better management of these ecosystems, especially classification criteria to protect zones according to international conventions. The BobGEO cruise dealt with high-resolution mapping of three zones characterising canyons and interfluves in the Bay of Biscay where corals have already been collected. The BobECO cruise aimed to reveal the high-resolution spatial structure of communities occurring in coral ecosystems, the occurrence of deep-sea fishes and the impact of fisheries. In order to better prepare this cruise the results of the R/V Belgica cruises were used to define the target areas.

Chapter 5

Cold-water coral habitats in the Penmarc'h and Guilvinec Canyons: Deep-water vs shallow-water settings

Published as:
De Mol, L., Van Rooij, D., Pirlet, H., Greinert, J., Frank, N., Quemmerais, F. & Henriet, J.-P. (2011). Cold-water coral habitats in the Penmarc'h and Guilvinec Canyons (Bay of Biscay): Deep-water versus shallow-water settings. Marine Geology 282, 40-52.

Abstract

In 1948, Le Danois reported for the first time the occurrence of living cold-water coral reefs, the so-called "massifs coralliens", along the European Atlantic continental margin. In 2008, a cruise with R/V Belgica was set out to re-investigate these cold-water corals in the Penmarc'h and Guilvinec Canyons along the Gascogne margin of the Bay of Biscay. During this cruise, an area of 560 km^2 was studied using multibeam swath bathymetry, CTD casts, ROV observations and USBL-guided boxcoring. Based on the multibeam data and the ROV video imagery, two different cold-water coral reef settings were distinguished. In water depths ranging from 260 to 350 m, mini mounds up to 5 m high, covered by dead cold-water coral rubble, were observed. In between these mounds, soft sediment with a patchy distribution of gravel was recognised. The second setting (350-950 m) features hard substrates with cracks, spurs, cliffs and overhangs. In water depths of 700 to 950 m, both living and dead cold-water corals occur. Occasionally, they form dense coral patches with a diameter of about 10-60 m, characterised by mostly stacked dead coral rubble and a few living specimens. U/Th datings indicate a shift in cold-water coral growth after the Late Glacial Maximum (about 11.5 ka BP) from shallow to deep-water settings. The living cold-water corals from the deeper area occur in a water density (sigma-theta) of 27.35 – 27.55 $kg.m^{-3}$, suggested to be a prerequisite for the growth and distribution of cold-water coral reefs along the northern Atlantic margin. In contrast, the dead cold-water coral fragments in the shallow area occur in a density range of 27.15-27.20 $kg.m^{-3}$ which is slightly outside the density range where living cold-water corals normally occur. The presented data suggest that this prerequisite is also valid for coral growth in the deeper canyons (>350 m) in the Bay of Biscay.

5.1 Introduction

Cold-water corals are widespread along the European Atlantic continental margin (Freiwald and Roberts, 2005; Freiwald et al., 2004; Roberts et al., 2006, 2009). Previous studies have already revealed a large amount of information about the distribution, significance and environmental setting of these ecosystems along the Norwegian margin (Fosså et al., 2005; Freiwald et al., 2002; Hovland et al., 1998; Lindberg and Mienert, 2005; Mortensen et al., 1995), and the continental margin off Ireland and the UK (De Mol et al., 2002; Dorschel et al., 2007a; Huvenne et al., 2007; Kenyon et al., 2003; Masson et al., 2003; Mienis et al., 2007; Roberts et al., 2006; Van Weering et al., 2003; Wheeler et al., 2007). Cold-water corals are able to form habitats which vary in size from small patches (few metres in size) to large reef structures covering several kilometres (Freiwald et al., 1999; Roberts et al., 2005). In the Porcupine Seabight and Rockall Trough giant cold-water mounds up to 300 m high were observed (De Mol et al., 2002; Kenyon et al., 2003; Wheeler et al., 2007; Van Weering et al., 2003). In contrast to these well studied areas, coral occurrences within the Bay of Biscay, and more specifically the Armorican margin, are less investigated (Reveillaud et al., 2008).

The occurrence of cold-water corals in the Bay of Biscay was already reported by Joubin (1922) and Le Danois (1948). The latter study mainly observed the presence of living *Madrepora oculata* and *Lophelia pertusa*, mostly occurring in a patchy distribution but at some locations able to form a dense coral field with a maximum height of 2 m. Afterwards these cold-water corals were also reported at different locations in the Bay of Biscay by Altuna (1995), Alvarez-Claudio (1994), Zibrowius (1980, 1985) and Zibrowius et al. (1975). In 1997, two areas along the north Atlantic margin in the Bay of Biscay were revisited by Freiwald and Henrich (1997), namely the Penmarc'h Bank and the Banc de la Chapelle, 160 km northwest of Penmarc'h Bank. On the Banc de la Chapelle, only dead colonies of *L. pertusa*, *M. oculata* and *Desmophyllum dianthus* were found in water depths of 340 to 790 m. Further south, on the Penmarc'h Bank living colonies of *Dendrophyllia cornigera* were observed (Reveillaud et al., 2008). The same authors also observed *Caryophyllia smithii* specimens which yielded calibrated U/Th ages of the end of the last glacial period (11-14 ka BP) (Schröder-Ritzrau et al., 2005). In 2008, Reveillaud et al. presented an overview of the cold-water coral distribution and diversity in the Bay of Biscay based on historical reports and more recent (pre-2008) data. However, it is still not known to which extent the available information represents the actual distribution of cold-water corals in the Bay of Biscay.

Cold-water corals occur in temperatures ranging between 4° and 12°C. This temperature zone corresponds with water depths between ~50 and 1000 m at high latitudes and up to 4000 m at low latitudes (Freiwald et al., 2004). Besides temperature several other environmental factors favour coral settlement and growth: hard substrates (e.g., boulders, moraine ridges, flanks of oceanic banks, seamounts, sedimentary mounds; Dodge and Vaisnys, 1977; Rogers, 1990), strong topographically guided bottom currents (Freiwald et al.,

2004), nutrient-rich waters containing labile organic matter (Kiriakoulakis et al., 2004) and zooplankton (Freiwald et al., 2004), and the depth of the aragonite saturation horizon (Davies et al., 2008). Due to the presence of these conditions along the continental slope in the Bay of Biscay, this area is a potential habitat for cold-water coral ecosystems (Hall-Spencer et al., 2007; Reveillaud et al., 2008). The numerous canyons cutting the slope of the Bay of Biscay (Bourillet et al., 2003, 2006b; Le Suavé et al., 2000; Zaragosi et al., 2006) funnel sediment and labile organic matter from the continental shelf (~200 m) to the abyssal plain (~4000 m) (Freiwald et al., 2004). An additional major food source is provided by nutrient-rich waters (Freiwald et al., 2004). Recently, Dullo et al. (2008) discovered that water density also plays an important role in the distribution of cold-water corals. Along a transect stretching from 51 to 70°N (~3000 km), living cold-water corals (*L. pertusa*) occur within a narrow density (sigma-theta) range of σ_Θ = 27.35 to 27.65 kg m^{-3}, independent from the surrounding water masses.

The data presented in this paper were collected during the BiSCOSYSTEMS cruise on board of the R/V Belgica from 25 May to 7 June 2008 within the framework of the EC FP6 IP HERMES and the ESF EuroDIVERSITY MiCROSYSTEMS projects (Fig. 5.1). The main aim of the study was (1) to revisit one of the cold-water coral locations described by Le Danois (1948) in order to better understand their significance, distribution and environmental conditions, and (2) to test the hypothesis that cold-water corals only occur within the potential density range described by Dullo et al. (2008), also south of 51°N.

5.2 Material and methods

5.2.1 Multibeam echosounding

The multibeam echosounder used during the BiSCOSYSTEMS cruise is a Kongsberg Simrad EM1002 system, installed permanently on the R/V Belgica. The EM1002 has up to 111 receiver beams of 2° (across track) x 3.3° (along track) width. The high-resolution depth data was obtained with a nominal frequency of 95 kHz and a ping-rate of 4 to 6 Hz. Survey speed was between 4 and 6 knots depending on water depth and wave conditions. In total, an area of 560 km² along the Armorican margin was mapped in water depths between 160 m and 1000 m (Fig. 5.1B).

The bathymetric information of the recorded files was extracted as xyz-data with the open source MB-Systems software (Caress and Chayes, 1995). Next, data editing occurred in the IVS Fledermaus software package resulting in a digital terrain model (DTM) with a 5-m grid resolution.

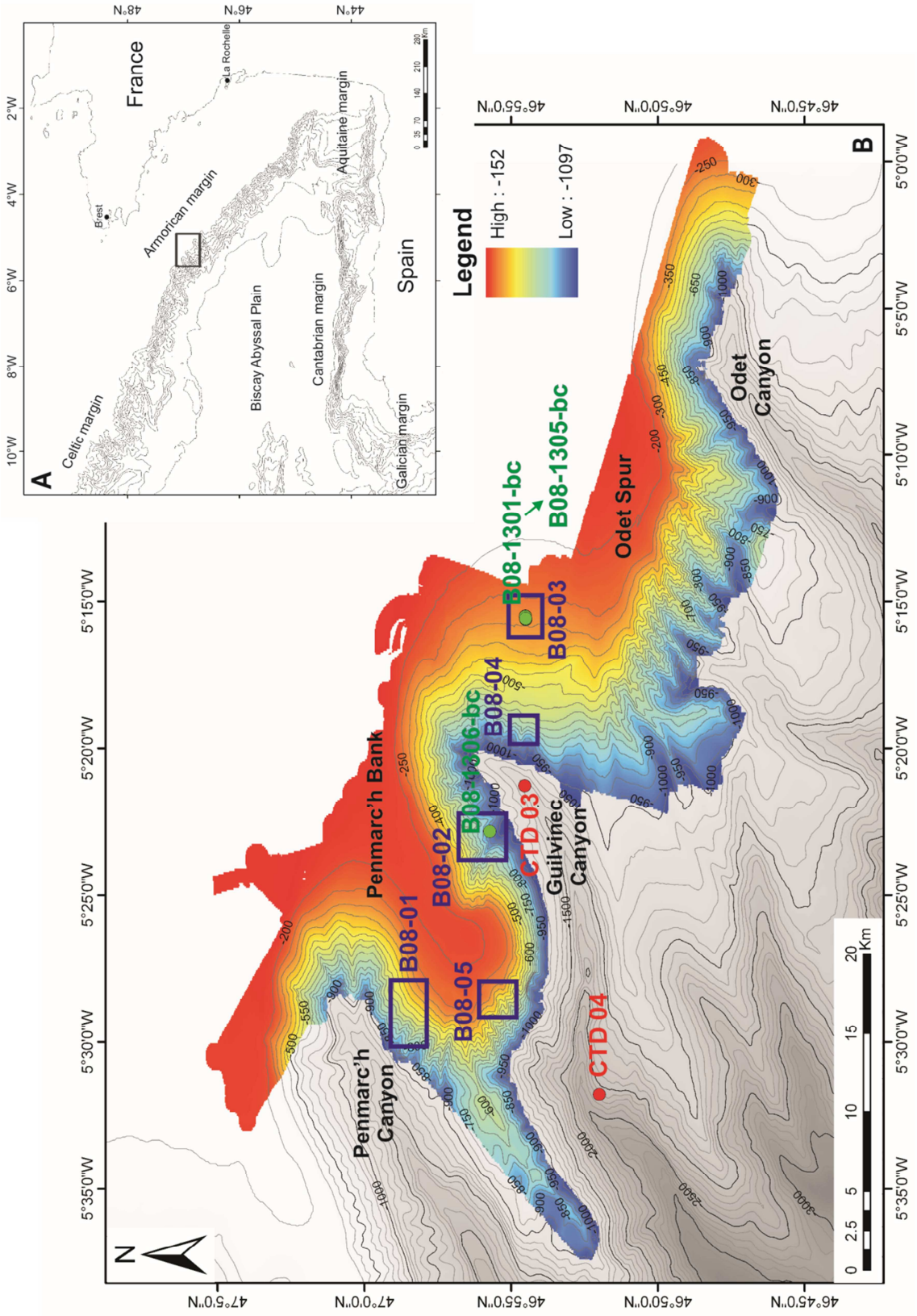

Fig. 5.1 *(A) Location of the study area along the French Atlantic continental margin (GEBCO bathymetry, contour lines every 500 m), (B) Detail of the study area with EM1002 bathymetry (contour lines every 50 m) and the location of the CTD casts (red), ROV dives (blue) and boxcores (green), collected during the R/V Belgica BiSCOSYSTEMS cruise (2008). As background a bathymetric map of IFREMER (Normand and Mazé, 2000) is used (contour lines every 100 m).*

5.2.2 CTD measurements

Two CTD casts (CTD 03: 46°51.990'N/5°31.768'W at 1450 m water depth and CTD 04: 46°54.536'N/5°21.262'W at 1250 m water depth) were obtained in the Guilvinec Canyon using a SBE Seacat 19 in order to gain insight into the local water mass stratification and to calibrate the EM1002 echosounder for sound velocity. The raw data were binned at 1 m using the SBE Data Processing software (version 7.18c).

5.2.3 ROV observations

The Remotely Operated Vehicle (ROV) 'Genesis' from Ghent University is a Sub-Atlantic Cherokee-type ROV with an operational survey depth down to 1600 m. Imagery was obtained from one forward-looking colour camera, recorded with and without a navigational overlay. High-resolution still images were obtained from a Canon Powershot camera. Two parallel laser beams with a distance of 10 cm were used as a scale during seabed observations. The ROV positioning was obtained using the USBL (Ultra Short Base Line) IXSEA GAPS positioning system. This allowed subsurface positioning with an accuracy of about 2-3 m. The processing and interpretation of the dives was performed using OFOP (Ocean Floor Observation Protocol) version 3.2.0c (Huetten and Greinert, 2008). Based on the observations, a number of facies characteristic for the study area were identified. Each facies was given a colour-code and integrated into ArcGIS 9.1, resulting in a facies interpretation map.

5.2.4 Sedimentological analyses of boxcore samples

Boxcores were taken at different locations within the Guilvinec Canyon. For each boxcore, subsamples from different depths (mostly one sample from the surface and one from the bottom) and/or subcores (if possible) were taken for sedimentological analysis. Each subcore was sampled every 5 cm. The location of boxcores B08-1305-bc and B08-1306-bc was accurately determined by using the GAPS USBL system.

Subsamples were analysed for grain-size distribution with a Malvern Mastersizer 2000 (Marine Biology Section, Ghent University). First, the sediment was dried in a furnace at 60° for about 48h. After subsampling 1 cm^3 of sediment, the carbonate fraction was removed by adding 75 ml of 10% acetic acid (CH_3COOH). This process was performed twice in order to remove all carbonate fragments. Afterwards, the sample was rinsed twice with distilled water, each time followed by a 24 h settling period. Finally, the sediment was transferred in a 15 ml centrifuge tube together with 0.2% calgon (sodium hexametaphosphate, $(NaPO_3)_6$). Prior to analysis, the samples were rotated (20 rpm) for 24h. Afterwards, the results were processed with GRADISTAT (Blott and Pye, 2001) and the mean grain-sizes were calculated using the Folk and Ward (1957) method.

Six cold-water coral specimens (*L. pertusa*) from the surface of different boxcores (B08-1301-bc, B08-1305-bc and B08-1306-bc) were sampled for U/Th dating. The U-series measurements and age determination were carried out in the Laboratoire des Sciences du Climat et de l'Environnement (LSCE) in Gif-sur-Yvette using inductively coupled plasma source mass spectrometry (Thermo-Fisher X-Series). Preparation of corals, analytical procedures and physical measurement routines followed the detailed description by Frank et al. (2004, 2005) and Douville et al. (2010).

5.3 Results

5.3.1 Environmental setting of the canyons and spurs

5.3.1.1 Geomorphology

The morphology of the canyon head and SE flank of the Penmarc'h Canyon, the Guilvinec Canyon and the NW flank and canyon head of the Odet Canyon was studied in detail using multibeam mapping (Fig. 5.1B). These canyons are orientated in a NE-SW direction and are separated by two spurs: the Penmarc'h Bank and the Odet Spur.

The Penmarc'h Canyon is a slightly asymmetric V-shaped canyon with a maximum width of 10 km. The SE flank has an average slope of 10° and is incised by WNW-ESE orientated gullies with average slopes varying between 9-14° (Fig. 5.1B).

The Guilvinec Canyon is an asymmetric V-shaped canyon with a maximum width of 16 km. The NW slope has an average slope of 8° whereas the SE slope is characterised by an average slope of 6°. The total length of the canyon from the canyon head until the abyssal plain is about 33 km and the maximum incision depth is 2 km. The slopes flanking the canyons show ENE-WSW orientated gullies on the SE flanks with an average slope of 8-11° and NW-SE orientated gullies on the NW flanks with an average slope of 10°. The width of the gullies varies between 600 and 1000 m.

The Odet Canyon is also an asymmetric V-shaped canyon with a maximum width of 9 km. The NW flank of the Odet Canyon has a constant average slope of about 11°, compared to the SE flank where an abrupt change in slope occurs around 1000 m water depth. The NW slope of the Odet Canyon shows NW-SE orientated gullies with an average slope of 8-12°.

The Penmarc'h Bank is a narrow spur with a minimum width of 4 km which goes up to 10 km close to the canyon heads. In contrast the Odet Spur has a maximum width of 14 km. Along both spurs, NE-SW orientated gullies occur with an average slope of 8-13°. In the shallow area on the western part of the Odet Spur between 200 and 300 m water depth, small mounds were observed with a diameter of approximately 100 m and a height of 5 to 10 m.

5.3.1.2 Hydrography

The stratification of the water masses does not change significantly over the study area (Fig. 5.2). The CTD casts show the presence of a seasonal thermocline down to 50 m water depth. A salinity minimum (35.58 psu) is observed at 550 m, separating the overlying Eastern North Atlantic Central Water (ENACW) from the Mediterranean Outflow Water (MOW), which has its salinity maximum (35.76 psu) at about 1000 m. Below, the T/S (temperature versus salinity) profile gradually follows the 27.75 $kg.m^{-3}$ potential density gradient towards the Labrador Sea Water (LSW) and North Atlantic Deep Water (NADW), as shown in González-Pola (2006) and Van Rooij et al. (2010a).

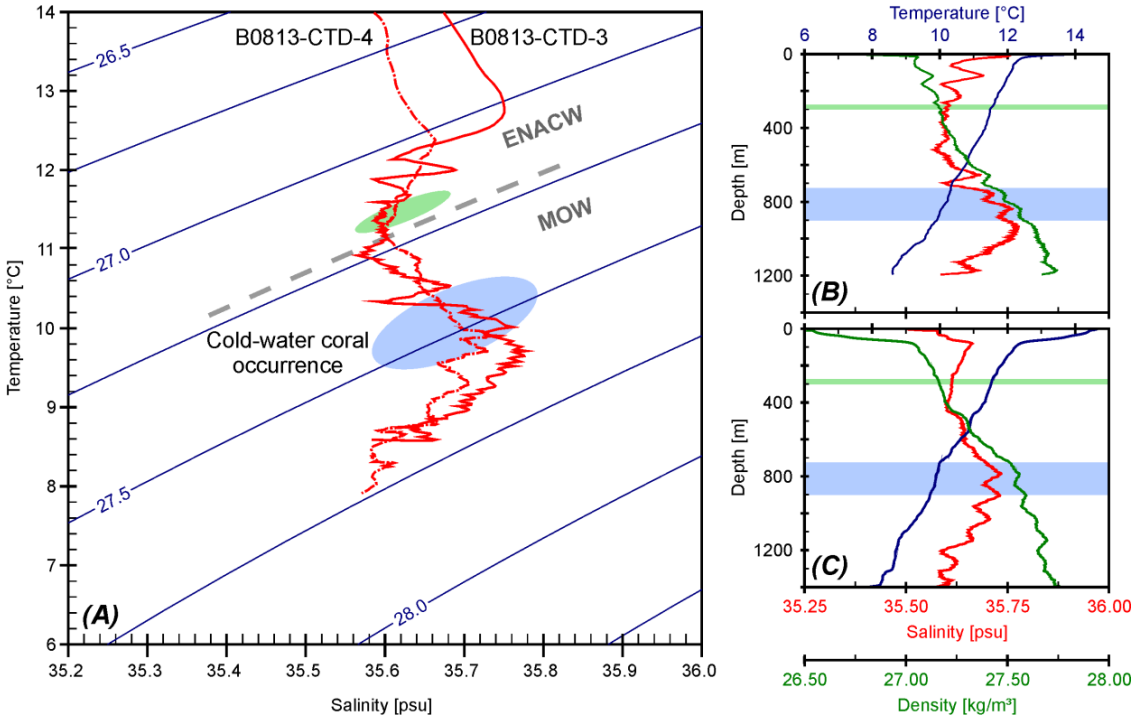

Fig. 5.2 *Hydrographic data of the Guilvinec Canyon. (A) Temperature/salinity plot for both CTD casts, with indication of the boundary (dashed grey line) between the Eastern North Atlantic Central Water (ENACW) and the Mediterranean Outflow Water (MOW). The estimated occurrence envelope of the shallow-water (green) and deep-water (blue) cold-water corals in the Penmarc'h and Guilvinec Canyons is based on the ROV observations, plotted on the CTD data of respectively (B) cast B0813-CTD-3 and (C) cast B0813-CTD-4.*

5.3.2 Shallow-water coral rubble fields on Odet Spur

Mini mounds were observed on the multibeam echosounder data on Odet Spur in water depths of 260 to 350 m. The gentle slope features an average gradient of 3-4° (Fig. 5.1B). ROV observations (Table 5.1) allowed to distinguish four different facies: (1) rippled soft sediment with a patchy distribution of dead cold-water corals (Fig. 5.3A), (2) rippled seabed with biogenic debris and a patchy distribution of dead cold-water corals, (3) rippled soft

sediment covered with gravel or small pebbles (Fig. 5.3B), and (4) a dense cold-water coral rubble coverage, dominated by *L. pertusa* and/or *M. oculata* (Fig. 5.3C and Fig. 5.3D).

Name	Area	Start track		End track	
		Time	Depth	Time	Depth
B08-01	South flank of Penmarc'h canyon	13:16:02	385 m	16:47:44	699 m
B08-02	North flank of Guilvinec canyon	11:24:46	712 m	15:46:00	900 m
B08-03	South flank of Guilvinec canyon: small mounds/ridges on the top	12:29:41	278 m	14:05:25	289 m
B08-04	Spur, south flank of Guilvinec canyon	15:51:10	676 m	16:38:51	691 m
B08-05	North flank of Guilvinec canyon	11:17:00	305 m	14:27:53	529 m

Table 5.1 *Names, locations and operational data of the ROV Genesis dives. Time in UTC.*

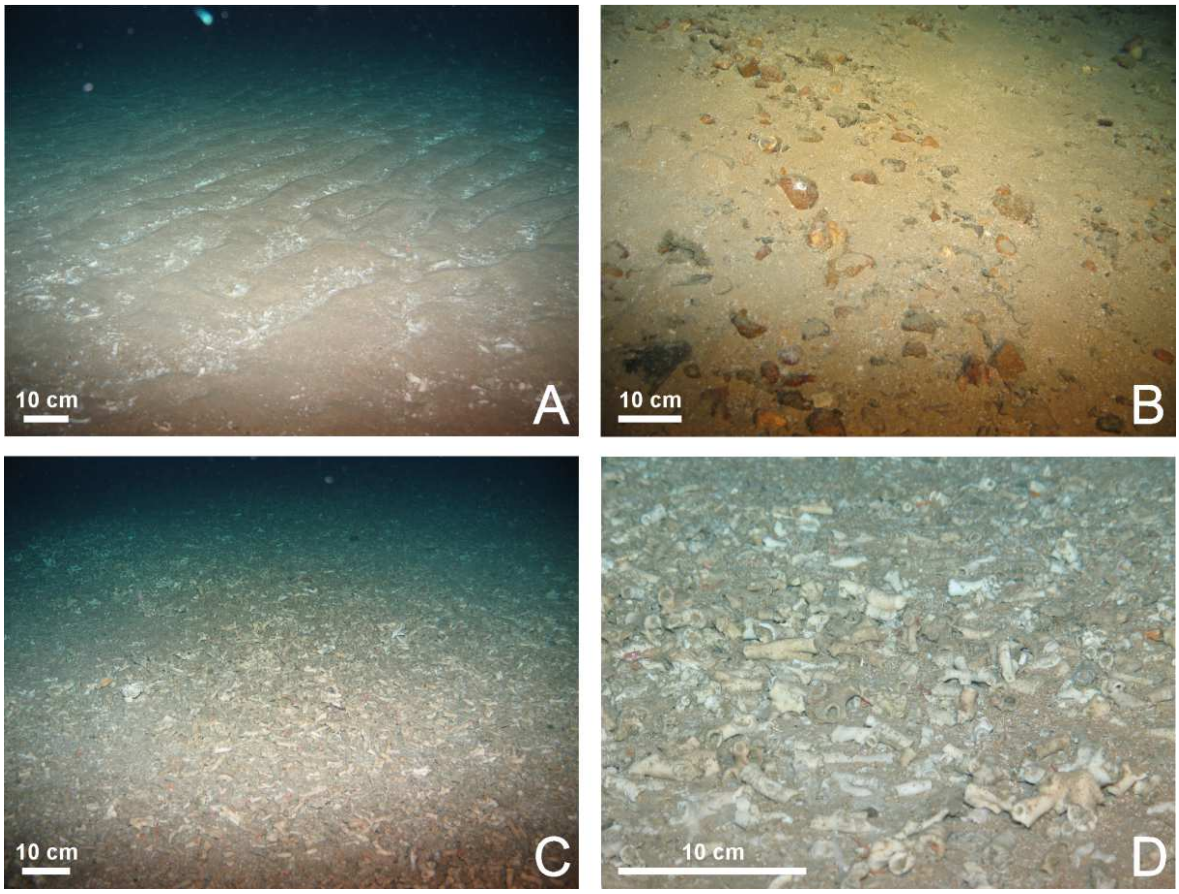

Fig. 5.3 *ROV images from the shallow-water setting (ROV dive B08-03): (A) rippled seabed with a patchy distribution of cold-water corals, (B) coarse sand with a high amount of gravel, (C) the dense cold-water coral rubble coverage on top of the small mounds, and (D) zoom in this coral rubble facies with predominantly* Lophelia pertusa.

Figure 5.4A shows that the small mounds are covered by dead cold-water coral rubble. At the base of the mounds and in between them, an alternation of rippled soft sediment with a patchy distribution of dead cold-water corals and/or biogenic debris, and rippled soft sediment with gravel-sized particles was observed (Fig. 5.3A and Fig. 5.3B). The coral rubble consists of crushed coral fragments (Fig. 5.3C and Fig. 5.3D) and nearly no visible living

fauna. The size of the coral rubble fields varies between 20 to 80 m. The undulatory N-S to NNW-SSE orientated sand ripples appear with wavelengths between 5 and 10 cm and have heights of about 3-5 cm.

Core number	Latitude	Longitude	Water Depth	Recovery
B08-1301-bc	46°54.514' N	5°15.489' W	285 m	31 cm
B08-1302-bc	46°54.499' N	5°15.602' W	290 m	17 cm
B08-1303-bc	46°54.511' N	5°15.504' W	285 m	20 cm
B08-1304-bc	46°54.498' N	5°15.587' W	288 m	5 cm
B08-1305-bc	46°54.501' N	5°15.577' W	288 m	14 cm
B08-1306-bc	46°55.723' N	5°22.828' W	866 m	10-15 cm

Table 5.2 *Location, water depth and recovery length of the studied boxcores.*

Boxcore samples were taken along the track of ROV dive B08-03 resulting in two different lithofacies (Table 5.2; Fig. 5.4B). Lithofacies 1 is characterised by olive brown to olive grey poorly-sorted, fine to medium sand with mean grain-sizes varying between 215 µm and 305 µm. Within this facies in boxcore B08-1302-bc fine laminations are observed between olive brown and olive grey sand. In contrast, a clear colour change is observed in boxcore B08-1305-bc at a depth of 5 cm. In boxcore B08-1303-bc, on top of a mini mound (Fig. 5.4A), only a very thin layer of lithofacies 1 is observed. The surface of all boxcores is covered with coarse biogenic debris and several *L. pertusa* fragments (1-4 cm), up to 5 cm depth. At the surface of boxcore B08-1303 also large gravel fragments (up to 7 cm) were observed. Lithofacies 2 is characterised by olive grey very poorly to poorly-sorted, medium silt with grain-sizes varying between 8.9 µm and 12.6 µm. Within this unit black sediment spots, supposedly caused by reducing geochemical conditions, were observed. In boxcore B08-1303-bc a few sand lenses occur between 5 and 10 cm depth. Boxcore B08-1304-bc had a penetration of only 5 cm (no subcoring). It consists of olive grey, well sorted sand (lithofacies 1) with coarse biogenic debris and robust coral fragments of *L. pertusa* (several cm).

Shallow water setting			Deep-water setting		
Sample name	**Age (ka)**	**Error (ka)**	**Sample name**	**Age (ka)**	**Error (ka)**
B08-1301-bc	7.35	0.45	B08-1306-bc A	1.32	0.52
B08-1305-bc A	7.78	0.71	B08-1306-bc B	1.21	0.13
B08-1305-bc A	9.07	0.25	B08-1306-bc C	2.27	0.30
B08-03 B	8.89	0.31			
B08-03 C	1.41	0.17			

Table 5.3 *Overview of the U-series datings in the shallow water setting (left) and the deep-water setting (right).*

In addition, several coral fragments were dated using U-series: two coral fragments (*L. pertusa*) were collected during ROV dive B08-03, one coral fragment (*L. pertusa*) in boxcore B08-1301-bc and two coral fragments in B08-1305-bc. The resulting ages after correction are shown in Table 5.3.

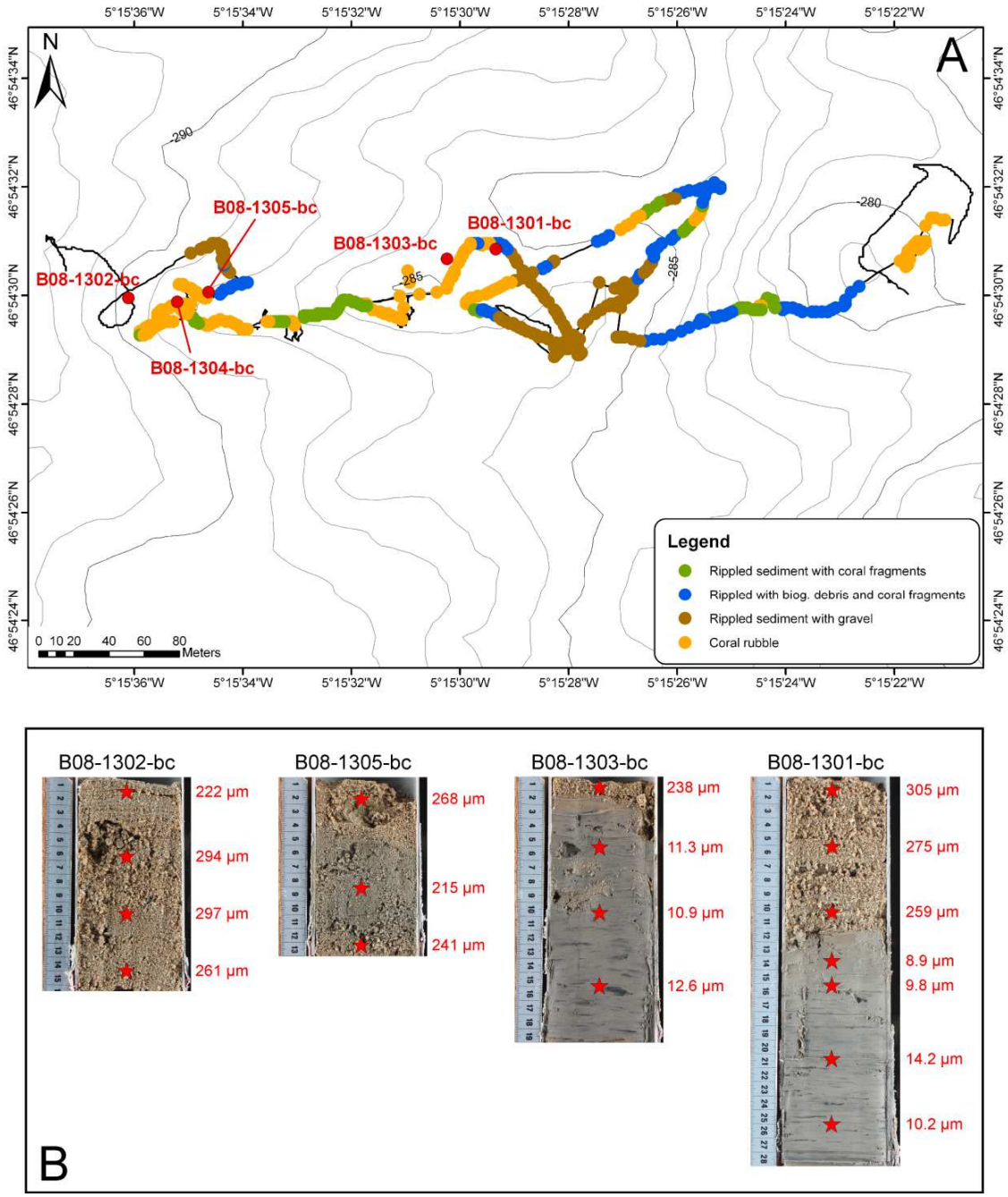

Fig. 5.4 *(A) Facies interpretation map of the shallow-water dive B08-03 on the southeastern flank of the Guilvinec Canyon in water depths between 278 and 289 m. (B) Photographs of the obtained boxcores in the shallow water area with the locations and mean grain-size values.*

5.3.3 Deep-water corals in the Penmarc'h and Guilvinec Canyons

The second setting features cold-water corals observed in the Penmarc'h and Guilvinec Canyons in water depths of 700 to 900 m. Both living and dead coral specimens occur, predominantly *M. oculata*. In total, eleven different facies were defined during four ROV dives (Table 5.1). Facies 1 and 2 correspond to respectively even (Fig. 5.5A) and rippled soft sediment with at some locations intense bioturbation. Facies 3 and 4 correspond to respectively even and rippled soft sediment covered with a patchy distribution of cold-water

corals (mostly *M. oculata*) (Fig. 5.5B). Living as well as dead species occur. Soft sediment with a cover of biogenic debris was defined as facies 5 (Fig. 5.5C). No ripple marks were observed. Facies 6 and 7 are characterised by respectively even and rippled soft sediment covered with biogenic debris and a patchy distribution of cold-water corals (dead and living *M. oculata*). Next, facies 8 consists of soft sediment with gravel (Fig. 5.5D). The gravel fragments reach sizes up to 10 cm. Facies 9 corresponds with outcropping hard substratum (Fig. 5.5E and Fig. 5.5F), colonised by living cold-water corals (*M. oculata*) and sponges. At some locations, cracks filled with soft sediment were observed (Fig. 5.5G and Fig. 5.5H). Finally, facies 10 and 11 relate to the cold-water coral coverage. Facies 10 is characterised by a dense coverage of coral rubble (Fig. 5.6A) whereas facies 11 also features living species of *M. oculata* and *L. pertusa* on top of the coral rubble, creating dense coral fields (Fig. 5.6B, Fig. 5.6C and Fig. 5.6D). Facies 11 often coincides with a very rough seafloor and big boulders (20 cm up to 1 m). Boxcore B08-1306-bc was taken within this facies which delivered three coral pieces for U-series dating (Table 5.3). Grain-size analysis reveals very poorly sorted fine sand with a mean grain-size of 81 µm.

Four ROV dives were undertaken. Dive B08-01 is located on the SE flank of the Penmarc'h Canyon in water depths of 385 to 750 m. During this dive, an E-W downslope transect was made with an average slope gradient of 8-10°. A large part of the track consists of soft sediment with gravel (facies 8). At a water depth of 530 m the gravel disappears and strongly bioturbated soft sediment (facies 1) remains until a water depth of 720 m (Fig. 5.5A). Below 720 m, the first cold-water corals (facies 3) (*L. pertusa* and *M. oculata*), with a size of 10-20 cm width and about 15 cm high, appear on boulders with a diameter of 25 cm. Except for one living *M. oculata*, all corals are dead.

Dive B08-02 on the NW flank of the Guilvinec Canyon has a U-shaped track starting with a first transect southwards from the NE flank of a gully at 712 m water depth and ending with a second transect on the SW flank of that gully. The slope of this part features an average gradient of 11°. During this dive many different facies were observed (Fig. 5.7). In the uppermost part of the slope, between 700 and 900 m, soft sediment alternates with coral fields which vary in diameter between 10 and 60 m (Fig. 5.6B). The soft sediment is sometimes covered with biogenic debris (Fig. 5.5C), gravel (Fig. 5.5D) and/or a patchy distribution of cold-water corals, mostly *M. oculata*. Also big boulders with a diameter up to 1 m were observed, colonised with living cold-water corals (*M. oculata*) and *Hexadella sp.* sponges (Fig. 5.6E and Fig. 5.6F). Between 800 and 900 m, asymmetric N-S orientated sand ripples appear with wavelengths between 10 and 20 cm and with heights of about 5 cm. Below 900 m water depth, mostly hard substratum (Fig. 5.5E and Fig. 5.5F) occurs with a patchy distribution of living cold-water corals (*M. oculata*). NW-SE orientated cracks of 5 cm up to 40 cm occur in this area, and are filled with (rippled) soft sediment (Fig. 5.5G and Fig. 5.5H). At several locations, the rather smoothly sloping seabed is interrupted by the presence of small banks (Fig. 5.6G) or cliffs (Fig. 5.6H). Between 700 and 750 m water depth,

these escarpments have an E-W orientation, while the deeper ones reveal a S-N or SSW-NNE orientation. The banks are generally few decimetres in height and thus much smaller than the cliffs, which vary in height between 2 and 4 m. At three locations, the escarpments are colonised by *M. oculata* corals and *Neopycnodonte zibrowii* oysters, which are discussed in more detail in Van Rooij et al. (2010a).

Dive B08-04 is located on a small spur with dimensions of 200 by 400 m on the SE flank of the Guilvinec Canyon in water depths of 675 to 700 m. Only one facies was recognised: a dense cold-water coral coverage with dead and living species, predominantly *M. oculata* (Fig. 5.6C and Fig. 5.6D). The living species grow on the dead coral rubble, which is built up by chunky coral fragments up to 40 cm high.

Finally, dive B08-05 investigated the southern shoulder of a gully south of the spur that separates the Penmarc'h Canyon from the Guilvinec Canyon. The track follows a southern to western course between 300 and 750 m water depth with an overall slope gradient of 8-10°. This track does not show many different facies. Between 300 and 450 m a rippled seafloor with regionally some biogenic debris and/or gravel was observed. The straight to gently undulatory SSE-NNW orientated sand ripples have a wavelength between 10 and 15 cm. The area between 450 and 730 m is characterised by soft sediment with bioturbations and a zone of low-relief rippled seabed. Close to a water depth of 480 m, some small escarpments are present. At 735 m, the gently dipping seafloor is interrupted by a 4 m high WSW-ENE escarpment, colonised by *M. oculata* cold-water corals and *Neopycnodonte zibrowii* oysters (Van Rooij et al., 2010a).

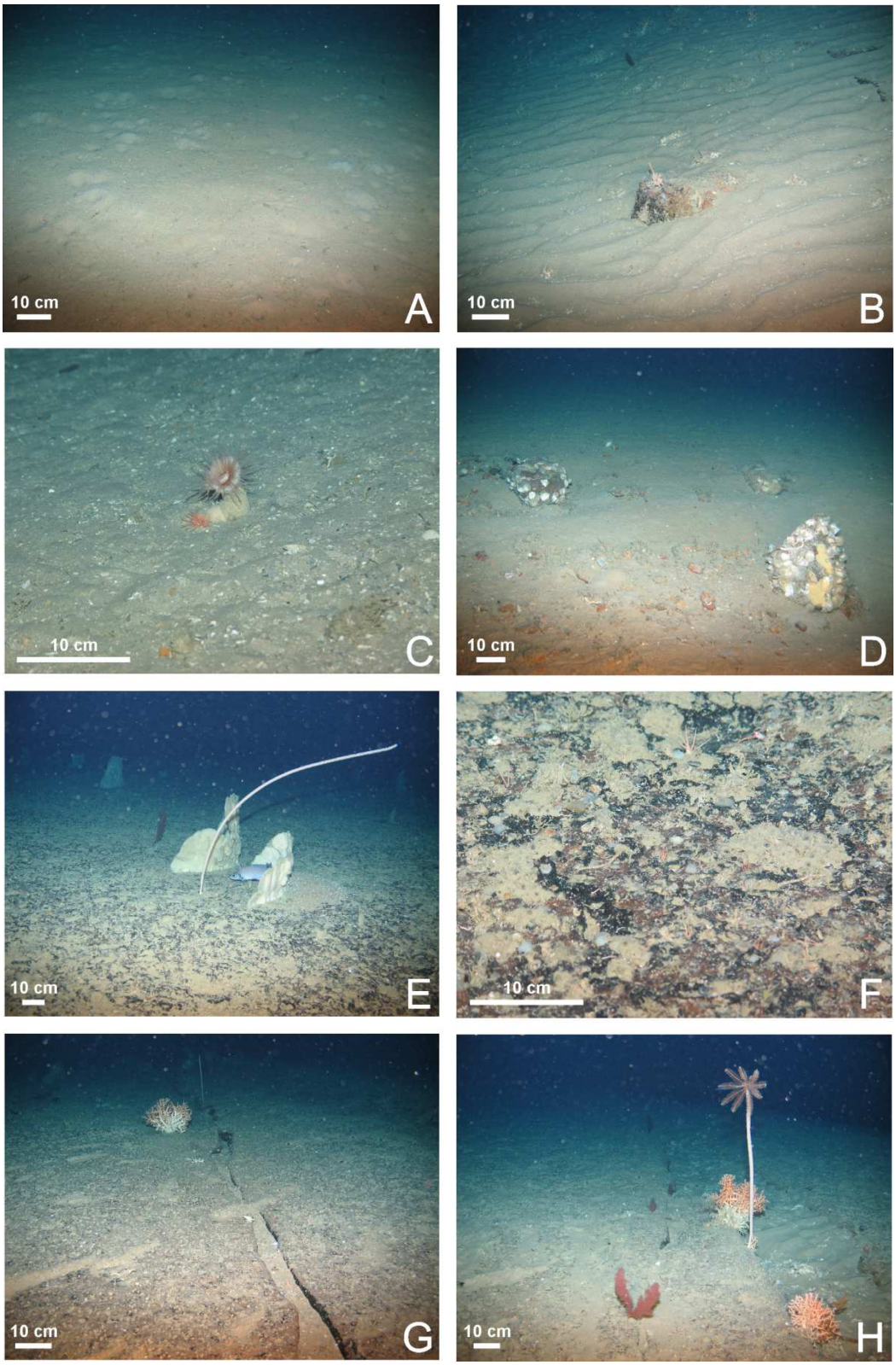

Fig. 5.5 *ROV stills imagery highlighting the most important facies and associated fauna in the deep-water setting: (A) soft sediment with bioturbations; (B) rippled soft sediment with gravel; (C) a seabed covered with biogenic debris; (D) soft sediment with a patchy distribution of gravel; (E) hard substrate with a patchy distribution of cold-water corals, sponges and a sea urchin; (F) zoom on the hard substrate; (G) hard substrate with a large crack and one* Madrepora oculata *species; (H) hard substrate with a crack filled up with rippled soft sediment, colonised by a crinoid and a few living* Madrepora oculata *corals.*

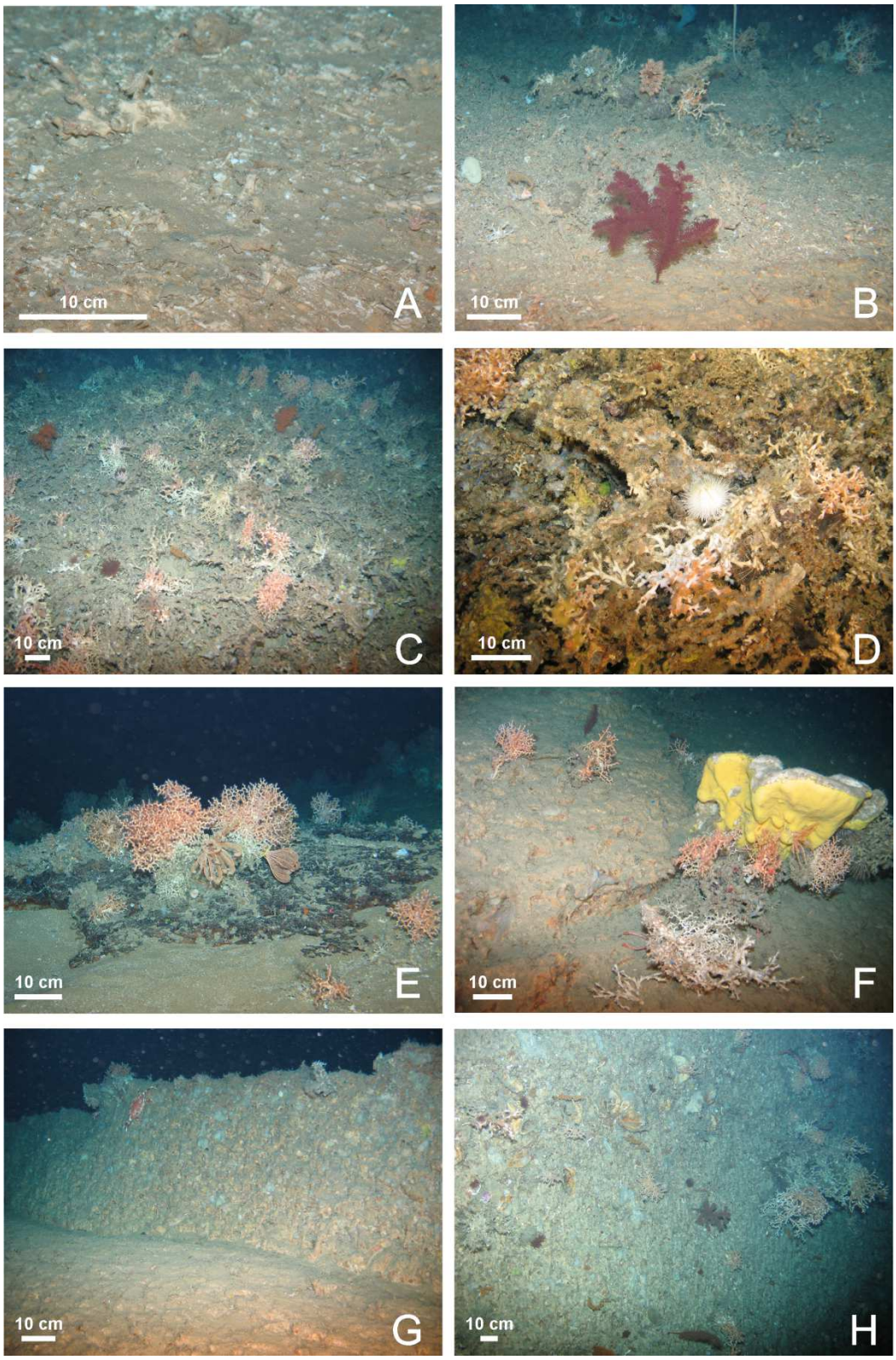

Fig. 5.6 *ROV stills imagery highlighting the different types of cold-water coral occurrences in the deep-water coral setting: (A) rippled seabed with coral rubble and biogenic debris; (B) example of a coral field with living and dead coral species; (C) a dense cold-water coral coverage with both living and dead species; (D) detailed zoom on the facies mentioned in A; (E) outcropping hard substratum with a few living coral species (*Madrepora oculata*) and Gorgonians; (F) outcropping hard substratum with the sponges* Geodia *sp. and* Topsentia *sp., and again living and dead* Madrepora oculata *specimens; (G) a small bank with a height of 50 cm colonised by oysters and a few living coral species; (H) a vertical cliff colonised with oysters and living* Madrepora oculata*.*

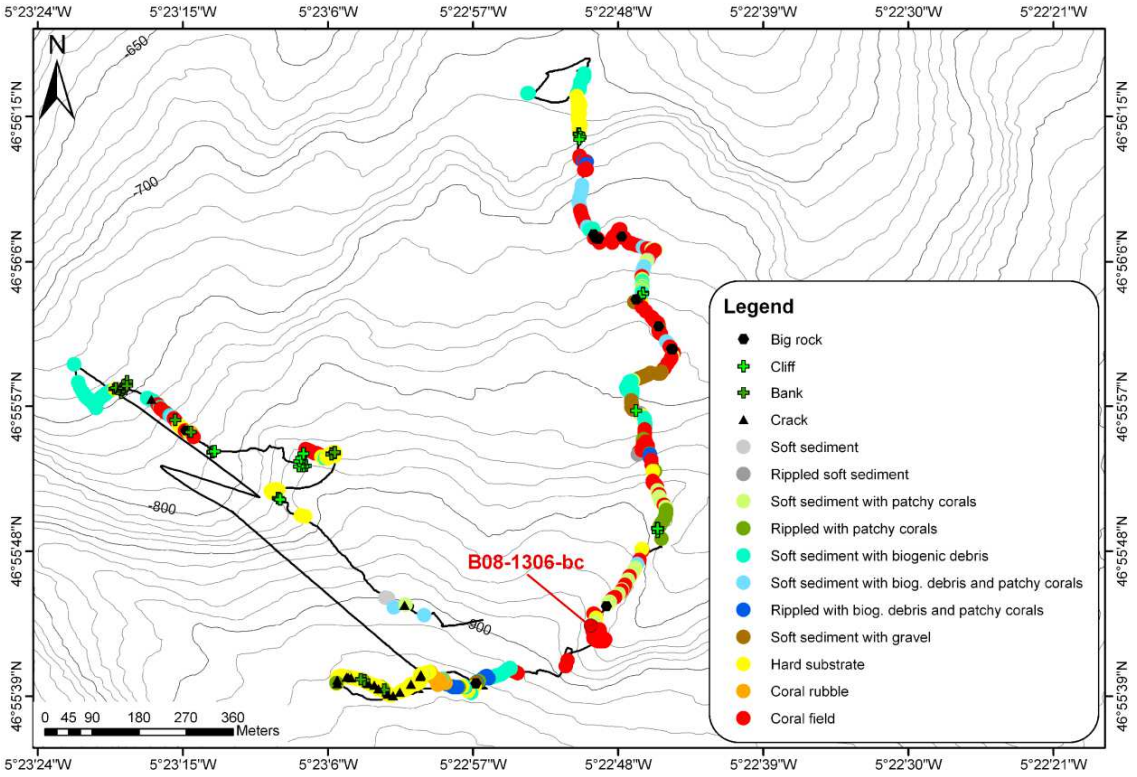

Fig. 5.7 *Facies interpretation map of ROV dive B08-02 on the northwestern flank of the Guilvinec Canyon in water depths of 712 to 900 m.*

5.4 Discussion

5.4.1 Canyons as cold-water coral habitats

For the first time a cold-water coral habitat is mapped in detail within a canyon setting in the Bay of Biscay. Although deep-sea canyons may provide suitable environmental conditions for cold-water corals to grow, resulting deep-water habitats have not yet been described in detail. Canyons are transport ways of organic matter from the continental shelf down to the abyssal plain (Canals et al., 2006; Freiwald et al., 2004). During most of the ROV dives described here, an intense marine snow was observed, composed of suspended particulate material, ideal nutrients for scleractinians. In addition, the cold-water corals occur just above, in case of the shallow water setting, and just beneath, in case of the deep-water setting, the physical boundary between the Eastern North Atlantic Central Water (ENACW) and the Mediterranean Outflow Water (MOW) (Fig. 5.2). As De Stigter et al. (2007) already demonstrated, the mixing of both water masses results in enhanced suspended material thus favouring the feeding of scleractinians. Moreover, the observations of ripple marks on the seabed, within the upper zone of the MOW, indicate the presence of an E-W bottom current with a speed around 10 to 40 $cm.s^{-1}$ (Stow et al., 2009). This elevated bottom current is beneficial for coral growth as it delivers nutrients to the polyps. Additionally, the asymmetry of the sand ripples shows a sediment transport direction away from the shelf edge into the canyon axis. Similar observations were made by Cunningham et al. (2005) in

the canyons on the Celtic Margin between Goban Spur and Brenot Spur. Apart from the flow velocity of the MOW, the bottom currents may be enhanced by strong internal tides (White, 2007). Next to a favourable oceanographic environment, the sedimentological environment of deep-sea canyons provides hard substrates for living cold-water corals to settle on. Indeed, during the ROV dives, corals were observed on cliffs, outcropping hard substratum and on the numerous boulders which are scattered on the seabed. The dives also revealed a preferential erosion of the western flank of the canyons while the eastern flank is draped with soft sediment. This is attributed to the strong E-W bottom currents. The western slope will act as an obstacle for these enhanced currents intensifying the easterly bottom currents through isopycnal doming, which results in erosion (Hernandez-Molina et al., 2003; Iorga and Lozier, 1999; Van Rooij et al., 2010a). Hence, the constant reworking by downslope (turbiditic) and alongslope (contouritic) current processes (Arzola et al., 2008; Bourillet et al., 2006b; Cunningham et al., 2005; Pingree and Le Cann, 1989; Toucanne et al., 2009) which occur along this slope will play an important role in the shaping of habitats suitable for coral settlement. This study indicates that canyons are perfectly suited for coral growth due to the food availability, strong bottom currents and the presence of hard substratum. More coral habitats might be discovered in a similar setting in the future.

5.4.2 Mini mounds on Odet Spur

The shallow area, located in water depths between 278 and 289 m, revealed a dense coverage of dead cold-water coral fragments on top of mini mounds and small ridges (Fig. 5.4A). Within the boxcores, cold-water coral fragments were only found in the uppermost 5 cm which suggests that these mini mounds were present before the settling of the cold-water corals. The fact that the boxcores only show a thin sand cover (1.5 cm) on top of the mini mound while at the base of the mound the sand cover increases to 11 cm, these mini mounds and ridges are probably the result of selective erosion of the clayey substrate due to strong bottom currents during interglacials and interstadials, as observed by Øvrebø et al. (2006) offshore Ireland. This observation highlights the importance of an elevated topography which acts as a template for coral settlement (Freiwald et al., 2004; Roberts et al., 2006). The lack of coral fragments deeper in the sediment of the mini mounds is a fundamental difference with the giant coral mounds observed along the Irish margin which are completely constructed by corals (Kano et al., 2007). In that aspect, the mini mounds on Odet Spur reveal strong similarities with the Darwin mounds in the northern Rockall Trough. The size of the coral topped Darwin mounds is similar (height: 5 m / diameter: 75 m) but they are located in a deeper water depth (1000 m). Coring revealed that corals are not a major contributor to mound building (Masson et al., 2003). The Moira mounds in the Porcupine Seabight which are characterised by diameters of 30-50 m and heights up to 5 m (Foubert et al., 2005; Wheeler et al., 2005) might also serve as an analogue for the mounds observed on Odet Spur.

5.4.3 Time and distribution of coral growth

The dating of the cold-water corals using U-series reveals that coral growth in the study area started at the beginning of the Holocene. The older age of the corals in the shallow (7.4-9.1 ka) compared to the deeper setting (1.2-2.3 ka) indicates a migration of the coral habitats towards greater water depths. Moreover, the fact that the corals observed in the shallow water setting are heavily bio-eroded and disintegrated, demonstrates that they are already exposed on the seabed for a significant amount of time. In contrast, the corals in the deeper setting are much better preserved suggesting a younger age for these species. The cause of the downslope migration of the corals is still uncertain. However, the changing sea level, influencing labile organic matter fluxes (Hall and McCave, 1998), and the rising temperatures, might have forced corals to deeper water depths, where they found better live conditions. A more dramatic hypothesis is that the shallow coral reefs were destroyed by bottom trawling since the shallower area is subject to intense fishing activity (Bourillet et al., 2006a). According to Hily et al. (2008), a great change has been observed in the benthic communities in the northern part of the Bay of Biscay since the 1960s due to bottom trawling. Bottom trawling could also explain the age difference between sample B08-03 C, with an age of 1.41 ± 0.17 ka, and the other samples with ages over 7 ka (Table 5.3). Due to the reworking effect of trawling, most of the coral reefs are turned upside down. However, no trawl marks were observed within the shallow water area during the ROV dive.

On a more regional scale, the U-series datings of the corals confirm a climate-driven influence. Since the Late Glacial Maximum (about 11.5 ka BP), extended living cold-water coral reefs appear along the European margin between 50° and 70° N (Frank et al., 2009). In contrast, during glacial times, the cold-water corals were only able to survive in the relatively more temperate Atlantic below 50° N (Frank et al., in press). At present, only scarce coral occurrences are observed south of 50°N (Reveillaud et al., 2008; Wienberg et al., 2009), which is also confirmed by the results presented in this paper. The northern part of the Bay of Biscay, and more specifically the Armorican margin, can be seen as a transition zone between the eastern temperate Atlantic and the eastern North Atlantic between 50° and 70° N. This might explain why no successive mound growth occurred in the Bay of Biscay, resulting in the build up of giant coral mounds as discovered in the Porcupine Seabight (De Mol et al., 2002; Dorschel et al., 2007a; Henriet et al., 1998; Huvenne et al., 2007, 2009; Wheeler et al., 2005) and the Rockall Trough (De Haas et al., 2009; Kenyon et al., 2003; Mienis et al., 2006; Van Weering et al., 2003).

5.4.4 Relation between potential density and cold-water coral occurrence

The results of the present study may add to the theory of Dullo et al. (2008) who concluded that the potential density (σ_Θ = sigma-theta), where cold-water corals are able to live and migrate along the Norwegian margin and in the Porcupine Seabight, needs to be between

27.35 and 27.65 kg.m^{-3}. The deeper canyon setting, where living cold-water corals have been observed, is located in this density range (27.35 and 27.55 kg.m^{-3}) (Fig. 5.2) and thus supports the results of Dullo et al. (2008). In contrast, the dead shallow water corals fall within a density range of 27.15-27.20 kg.m^{-3} which is slightly outside the density range where living cold-water corals normally occur. This finding demonstrates that the density range of 27.35 and 27.65 kg.m^{-3} is also valid for the living cold-water corals in the Bay of Biscay. In addition, our results confirm that this density range is not only applicable for dense living *L. pertusa* reefs but also accounts in this setting for living *M. oculata* species.

5.5 Conclusions

Cold-water coral habitats along the Gascogne margin in the Bay of Biscay, earlier reported by Le Danois in 1948, were investigated. The R/V Belgica BiSCOSYSTEMS cruise was set out to better understand the significance and distribution of these cold-water coral ecosystems and the environmental controls on their living habitat.

The main conclusions are:

- Deep-sea canyons such as the Penmarc'h and Guilvinec Canyons are suitable habitats for the settlement of cold-water corals (*M. oculata* and *L. pertusa*).
- Two cold-water coral settings were distinguished within the canyons: a shallow setting in water depths of 280-290 m with only dead coral rubble (mostly *L. pertusa*) and a deep-water setting (700-920 m) with mostly living *M. oculata* species on top of coral rubble. The occurrence of the mini mounds at ~280 m water depth is an unusually shallow water depth compared to most other cold-water coral (reef) occurrences along the NE Atlantic margin.
- The Bay of Biscay can be considered as a transition zone between the temperate Atlantic (below 50°N) and the cold north-eastern Atlantic between 50° and 70°N. After the Late Glacial Maximum, cold-water corals started to grow along the Armorican margin but migrated likely during the mid-Holocene to deeper water depths.
- The density range of 27.35 to 27.65 kg.m^{-3} (Dullo et al., 2008) is also valid for the living cold-water corals (mostly *M. oculata*) in the Bay of Biscay, which makes it a good prerequisite for the distribution and growth of living cold-water corals along the northeast Atlantic margin. It can be used as a predictive tool in order to discover more cold-water coral habitats along the European continental margin.

Acknowledgements

The shipboard scientific party wants to thank the captain and crew of R/V Belgica for their tremendous efforts and the fine cooperation during this campaign. This work was financially supported by the the ESF EuroDIVERSITY project MiCROSYSTEMS "Microbial diversity and

functionality in cold-water coral reef ecosystems" and the EC FP6 project HERMES (GOCE-CT-2005-511234-1) "Hotspot Ecosystem Research on the Margins of European Seas", which will be continued during the FP7 HERMIONE project (contract number 226354) "Hotspot Ecosystem Research and Man's Impact On European Seas". We are grateful to Prof. Dr. M. Vincx (Marine Biology Department, Ghent University) for allowing us to use the Malvern Mastersizer 2000. E. Sallé and C. Noury from LSCE are kindly acknowledged for their help with respect to U series sample preparation and dating. L. De Mol acknowledges the support of the "Institute for the Promotion of Innovation through Science and Technology in Flanders (IWT-Vlaanderen)". H. Pirlet and D. Van Rooij are funded through respectively an FWO-Flanders PhD and post-doctoral fellowship.

Chapter 6

Environmental setting of deep-water oysters

Published as:
Van Rooij, D., De Mol, L., Le Guilloux, E., Wisshak, M., Huvenne, V.A.I., Moeremans, R. & Henriet, J.-P. (2010). Environmental setting of deep-water oysters in the Bay of Biscay. Deep-Sea Research I 57 (12), 1561-1572. (L. De Mol was responsible for the video data interpretation and assisted in the writing of the manuscript.)

Abstract

We report the northernmost and deepest known occurrence of deep-water pycnodontine oysters, based on two surveys along the French Atlantic continental margin to the La Chapelle continental slope (2006) and the Guilvinec Canyon (2008). The combined use of multibeam bathymetry, seismic profiling, CTD casts and a remotely operated vehicle (ROV) made it possible to describe the physical habitat and to assess the oceanographic control for the recently described species Neopycnodonte zibrowii*. These oysters have been observed in vivo in depths from 540 to 846 m, colonising overhanging banks or escarpments protruding from steep canyon flanks. Especially in the Bay of Biscay, such physical habitats may only be observed within canyons, where they are created by both long-term turbiditic and contouritic processes. Frequent observations of sand ripples on the seabed indicate the presence of a steady, but enhanced bottom current of about 40 cm* s^{-1}*. The occurrence of oysters also coincides with the interface between the Eastern North Atlantic Water and the Mediterranean Outflow Water. A combination of this water mass mixing, internal tide generation and a strong primary surface productivity may generate an enhanced nutrient flux, which is funnelled through the canyon. When the ideal environmental conditions are met, up to 100 individuals per* m^2 *may be observed. These deep-water oysters require a vertical habitat, which is often incompatible with the requirements of other sessile organisms, and are only sparsely distributed along the continental margins. The discovery of these giant oyster banks illustrates the rich biodiversity of deep-sea canyons and their underestimation as true ecosystem hotspots.*

6.1 Introduction

Ocean margins are dynamic environments that host valuable deep-water benthic ecosystems. Along the Eastern Atlantic margin from Morocco to Norway, several 'deep-water ecosystem hotspots', associated with a complex interplay of oceanography, geology and seabed morphology, have been identified (Weaver and Gunn, 2009). One of these hotspots is represented by canyon ecosystems, which often feature cold-water coral reefs (Arzola et al., 2008; Canals et al., 2006; De Mol et al., 2011b; de Stigter et al., 2007; Dorschel et al., 2009; Palanques et al., 2009). The main ecosystem driver within canyons involves a careful balance of the hydrodynamic environment controlling sediment and nutrient supply (Dorschel et al., 2009; Mienis et al., 2007; Roberts et al., 2006). As such, canyons play a critical role since they are the most important mechanism of focussed nutrient input into the deep marine environment (Canals et al., 2006; de Stigter et al., 2007; Duineveld et al., 2001; Palanques et al., 2009). Moreover, due to frequent incisions during glacial sea-level lowstands (Bourillet et al., 2006b; Toucanne et al., 2009; Zaragosi et al., 2000), the eroded canyon flanks may offer an environment that promotes the settling of sessile organisms, which profit from the enhanced nutrient flux. Already in the late 19th and the mid-20th century fisheries research had demonstrated the presence of cold-water corals and associated species in the vicinity of the canyons in the northern Bay of Biscay (Reveillaud et al., 2008). Sporadically, scientists and fishermen also reported dead or sub-fossil oyster specimens from this part of the margin (Le Danois, 1948; Reveillaud et al., 2008), which was not given the appropriate attention at that time.

Although oysters are commonly referred to as typical shallow-water and occasionally reef-forming molluscs, a number of samples have also been recovered from the deeper realm (Wisshak et al., 2009a). The deep-water oyster, *Neopycnodonte zibrowii* formally described only recently in Wisshak et al. (2009a) based on submersible observations and sampling of live specimens in the Azores Archipelago between 2002 and 2007. Further isolated records of this species stem from steep open slopes such as the Gorringe Bank off Portugal (Auzende et al., 1984), south of Madeira (Hoernle et al., 2001) and in the Central Mediterranean Sea, where they occur as prominent (sub-) fossil oyster banks (Gofas et al., 2007). This 'living fossil' oyster is most unusual with respect to its habitat, size, geochemical signature and its particularly pronounced centennial longevity (Wisshak et al., 2009a, b). It stands in strong contrast to all other extant oyster species, such as *Neopycnodonte cochlear* (Poli, 1791), which are relatively short-lived. The smaller (4-5 cm) *N. cochlear* was reported by Le Danois (1948) on the upper slope of the Bay of Biscay (200-500 m). It is usually associated with hard substrates and in certain places colonises *Dendrophyllia cornigera* (Lamarck, 1816) coral reefs (Le Danois, 1948). *Neopycnodonte cochlear* certainly has the largest distribution worldwide, both in ancient (Videt and Neraudeau, 2003) and modern environments (Harry, 1981). The recently described *Neopycnodonte zibrowii* can be regarded as a distinct deep-sea relative of *N. cochlear* with specific adaptations allowing it to thrive in upper bathyal

depths. Most recently, Delongueville and Sciallet (2009), reinvestigated two unusually large specimens sampled alive from the Bay of Biscay margin and previously identified as *N. cochlear* (Delongueville and Sciallet, 1999). These can now be attributed to *N. zibrowii*.

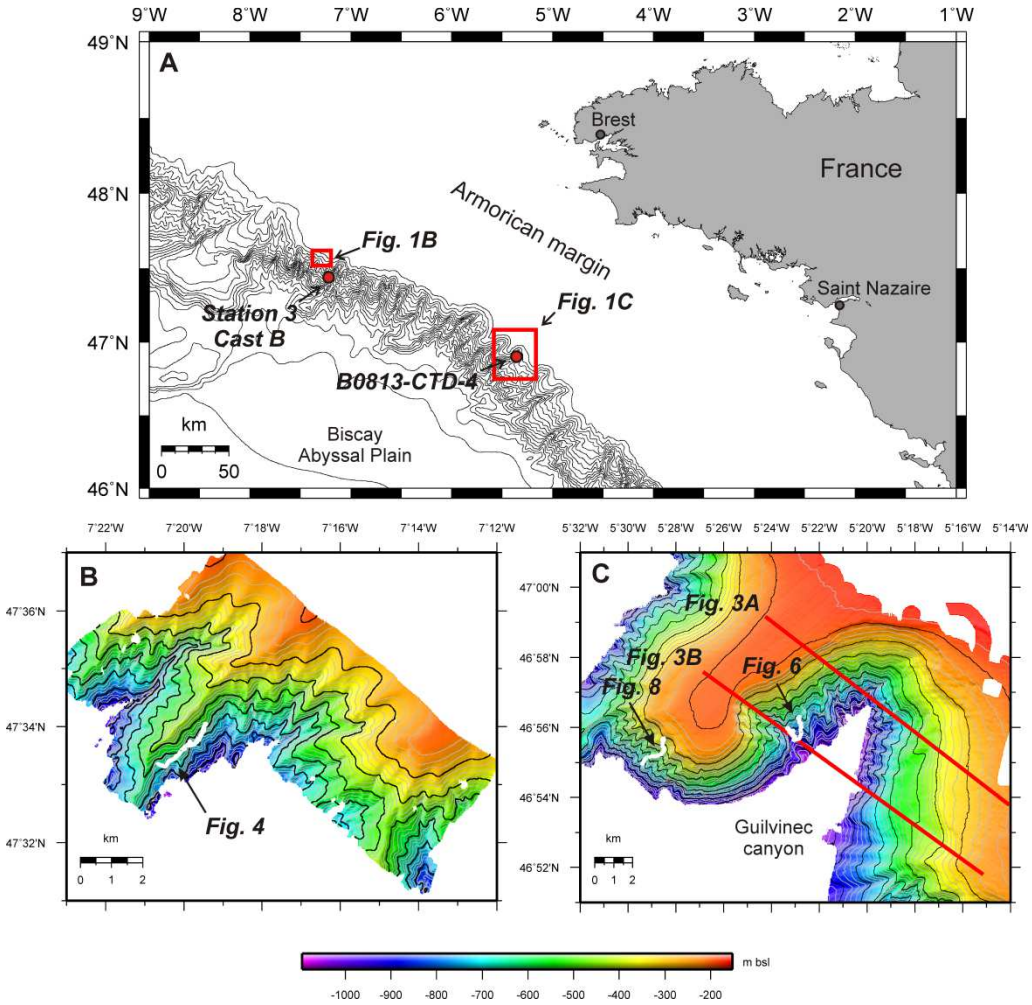

Fig. 6.1 *(A) Location of the study areas along the French Atlantic continental margin (GEBCO bathymetry, contour lines every 250 m), with indication of the CTD locations (Table 6.2), (B) Detail of the La Chapelle slope area with EM1002 bathymetry (contour spacing 25 m) and the location of ROV dive B06-02 (white), and (C) Detail of the Guilvinec Canyon area with EM1002 bathymetry (contour spacing 25 m), with the location of seismic profiles (red) and ROV dives B08-02 and B08-05 (white).*

In this paper, we describe the physical and oceanographic setting of the northernmost and deepest occurrence of *Neopycnodonte zibrowii* oysters within two canyons along the French Atlantic margin (Fig. 6.1). Seabed observations with the Remotely Operated Vehicle (ROV) *Genesis* resulted in the discovery of giant deep-water oyster banks and cliffs at depths between 540 to 846 m. These observations were performed with R/V *Belgica* during the HERMES Geo cruise in June 2006 (La Chapelle continental slope) and the BiSCOSYSTEMS cruise in June 2008 (Guilvinec Canyon). Although no samples could be acquired for morphological or molecular taxonomy, the observed spatial distribution of the molluscs in relation to the slope morphology, and local hydrographic regime, provides an insight in the habitat requirements of this recently described species.

6.2 Material and methods

The data collected for this study was acquired during two R/V *Belgica* expeditions in the Bay of Biscay. A first campaign, HERMES Geo, focussed during a period of 3 days in June 2006 on the La Chapelle continental slope (Fig. 6.1B). In June 2008, the BiSCOSYSTEMS cruise surveyed the vicinity of the Guilvinec Canyon (Fig. 6.1C). During both cruises a geophysical survey (multibeam bathymetry and seismic profiling) and CTD profiling (Fig. 6.2) preceded the ROV observations.

6.2.1 Geophysical survey

Initial swath bathymetry coverage of both study areas was obtained using the R/V *Belgica* hull-mounted SIMRAD EM-1002 multibeam echosounder. On the La Chapelle continental slope, an area of 72 km² was mapped at water depths ranging from 200 to 950 m (Fig. 6.1B) and processed using the IFREMER CARAIBES software. In 2008, an area of 584 km² was mapped around the Guilvinec Canyon at water depths ranging from 180 to 1000 m (Fig. 6.1C). The 2008 dataset was processed using the MB-Systems and IVS Fledermaus software. Both datasets were gridded to a cell measuring 20 by 20 m and visualised using GMT version 4.2 (Wessel and Smith, 1991).

In order to obtain insights into the sedimentary processes and the thickness of the sediment cover, single channel seismic profiles were acquired using a SIG sparker source at a velocity of 3 knots (Figs. 6.1C and 6.3). The source was triggered every 3 s, reaching 500 J energy. The vertical resolution of the profiles varied between 1 to 2 m. A basic processing (band-pass filtering, automatic gain control) was applied using the PROMAX software.

6.2.2 Water mass characterisation

At both sites, information regarding the water mass stratification was obtained using a SEACAT SBE 19 CTD down to water depths of about 1400 m (Table 6.1). The raw data was binned at 1 m using SBE Data Processing (version 7.16a). The obtained temperature (°C), salinity and derived potential density (sigma-thèta, kg/m^3) were used to identify the water masses and to indicate the relationship between deep-water oyster occurrence and hydrography. The zig-zag pattern observed below 800 m in the salinity and density curves of cast B0813-CTD-4, may be due to a defective CTD pump, and should be considered with caution.

Name	Date	Location	Latitude	Longitude	Depth
Station 3 cast B	1 june 2006	La Chapelle slope	47°25.00' N	7°16.00' W	1396 m
B0813-CTD-4	4 june 2008	Guilvinec Canyon	46°54.53' N	5°21.26' W	1404 m

Table 6.1 *Metadata of the CTD casts.*

6.2.3 ROV observations

The ROV observations (Table 6.2) were performed using Ghent University's ROV *Genesis*, a Sub Atlantic Cherokee type ROV with a Tethered Management System (TMS) allowing investigations down to 1400 m water depth. The underwater positioning was obtained using an IXSEA GAPS USBL system, allowing an accuracy in the order of 2 m. Seafloor observations were made by means of a forward-looking colour zoom and black & white video camera, assisted by > 250 Watt Q-LED illumination. Laser markers were added to the camera head for scale (10 cm spacing). High-resolution images were acquired at irregular intervals using a digital Canon Powershot stills camera. Unfortunately, due to a defect during the June 2006 campaign, images had to be derived from video capture instead of the stills camera. The processing and interpretation of dive B06-02 was performed in an ArcGIS environment, expanded with the Adélie extension for ArcGIS 9.0 developed at IFREMER. Dives B08-02 and B08-05 were interpreted using OFOP (Ocean Floor Observation Protocol) version 3.2.0c (Huetten and Greinert, 2008) and integrated into ArcGIS. For the purpose of this paper, the ROV data were only interpreted with respect to the occurrence of *Neopycnodonte zibrowii* and the different substrates. A more detailed study on the distribution, diversity and habitat settings of cold-water corals within the Guilvinec Canyon was performed by De Mol et al. (2011b).

Dive	Location	Start track			End track			*Oyster depth*
		Coordinates	*Time*	*Depth*	*Coordinates*	*Time*	*Depth*	
B06-02	La Chapelle slope	47°33.34' N 7°20.69' W	08:31	587 m	47°34.07' N 7°19.44' W	15:25	557 m	540-680 m
B08-02	NW flank Guilvinec Canyon	46°56.27' N 5°22.89' W	11:24	712 m	46°55.72' N 5°22.90' W	09:59	524 m	720-846 m
B08-05	W flank Guilvinec Canyon	46°55.68' N 5°28.52' W	11:17	305 m	46°55.16' N 5°29.00' W	15:58	530 m	737-740 m

Table 6.2 *Metadata of the ROV Genesis dive tracks.*

6.3 Results

6.3.1 Environmental setting

6.3.1.1 Hydrography

The CTD casts show a similar water mass stratification in both study areas (Fig. 6.2). The seasonal thermocline is recognised down to 50 m water depth (Figs. 6.2B-C). A salinity minimum (± 35.58) at about 550 m separates the upper Eastern North Atlantic Water (ENAW) from the saline Mediterranean Outflow Water (MOW), which has its salinity maximum (± 35.76) at about 1000 m. Below, the T/S profile gradually follows the 27.75 kg/m^3 potential density gradient towards the LSW and NADW.

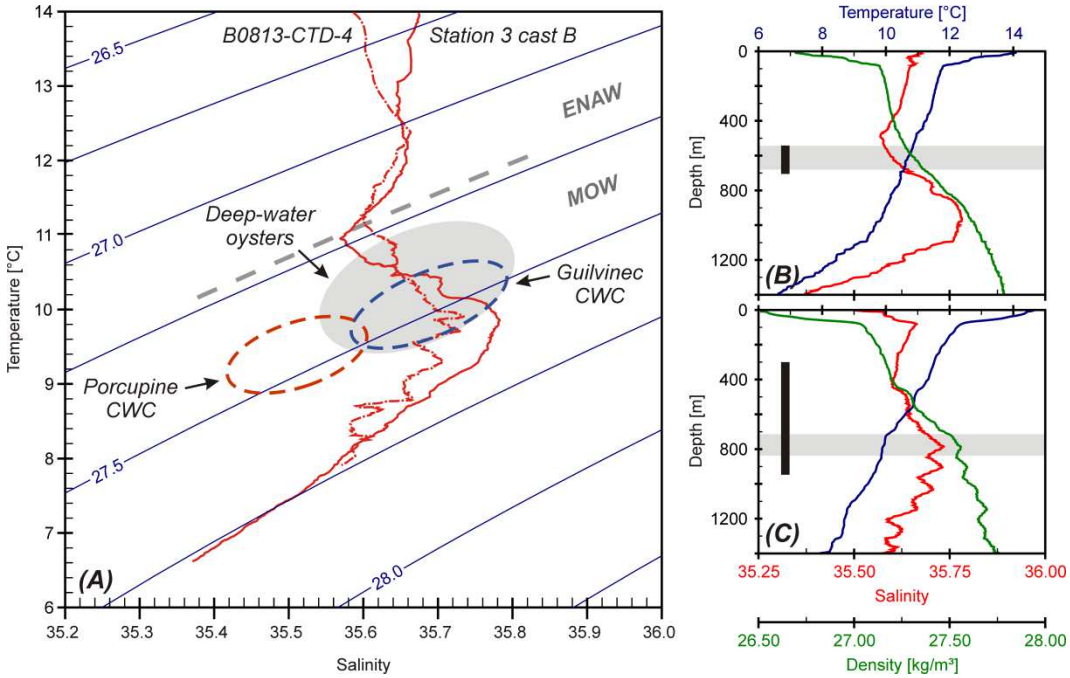

Fig. 6.2 *Hydrographic data of the two study areas. (A) Temperature/salinity plot for both CTD casts (Table 6.2), with indication of the boundary (dashed grey line) between the Eastern North Atlantic Water (ENAW) and the Mediterranean Outflow Water (MOW). The red and blue dashed envelopes refer to the occurrence of cold-water coral (CWC) reefs in respectively the Porcupine Seabight (Dullo et al., 2008) and within the Guilvinec Canyon (De Mol et al., 2011b). The estimated occurrence envelope of deep-water oysters in the Bay of Biscay is based on the ROV observations (Table 6.1), plotted on the CTD data of, respectively, (B) cast "Station 3 cast B" and (C) cast "B0813-CTD-4" in full grey. Here, the black vertical bars indicate the corresponding depth range of ROV observations.*

6.3.1.2 Geomorphology

This study was carried out around a prominent spur on the La Chapelle continental slope, flanked by deep canyons and thalweg channels in water depths from 150 to 1100 m (Fig. 6.1B). The spur has a main NE-SW orientation and an average inclination of 2°. The slopes flanking the spur show a 'herringbone' pattern of WNW-ESE orientated gullies on the western slope (13-15°) and NNW-SSE orientated gullies on the eastern slope (16°).

The Armorican margin near the Guilvinec Canyon is characterised by a heavily incised slope with NE-SW oriented canyons and spurs (Fig. 6.1). The Guilvinec Canyon is 14 km wide and bound to the northwest by the Penmarc'h Spur. The main part of this spur is relatively flat (0-2°) until 250 m water depth. Here, the gradient towards the Guilvinec Canyon is rather abrupt (10°), especially along its relatively steep northern to north-western flanks (30-40°). This flank contains about 4 large dendritic gully systems with a NNW-SSE orientation. In contrast, the eastern flank of the canyon is much smoother (and less incised) with slope gradients ranging from 5 to maximum 20°. This asymmetry is also observed on the seismic profiles (Figs. 6.1C and 6.3). Figure 3b shows a seismic profile through the largest (1 km wide) and steepest (17-35°) gully, which was also examined during ROV dive B08-02 (Fig. 6.1C). Exclusively on the SE flank, a large (200-400 ms TWT) sigmoidal depositional sequence

can be observed which explains the smoother slope texture. A comparison with other regional seismic stratigraphic studies (Bourillet et al., 2003; Paquet et al., 2010) suggests that this sequence may be correlated with the Pliocene to Pleistocene Little Sole Formation. On the other hand, almost the entire NW flank is covered with diffraction hyperbolae, suggesting erosive steep slopes, irregular topography or outcropping hard substratum. Along the south-western tip of the spur, six more gullies can be observed within the prolongation of the spur's axis. These gullies are approximately 400-500 m wide and have a gradient between 10 to 25°.

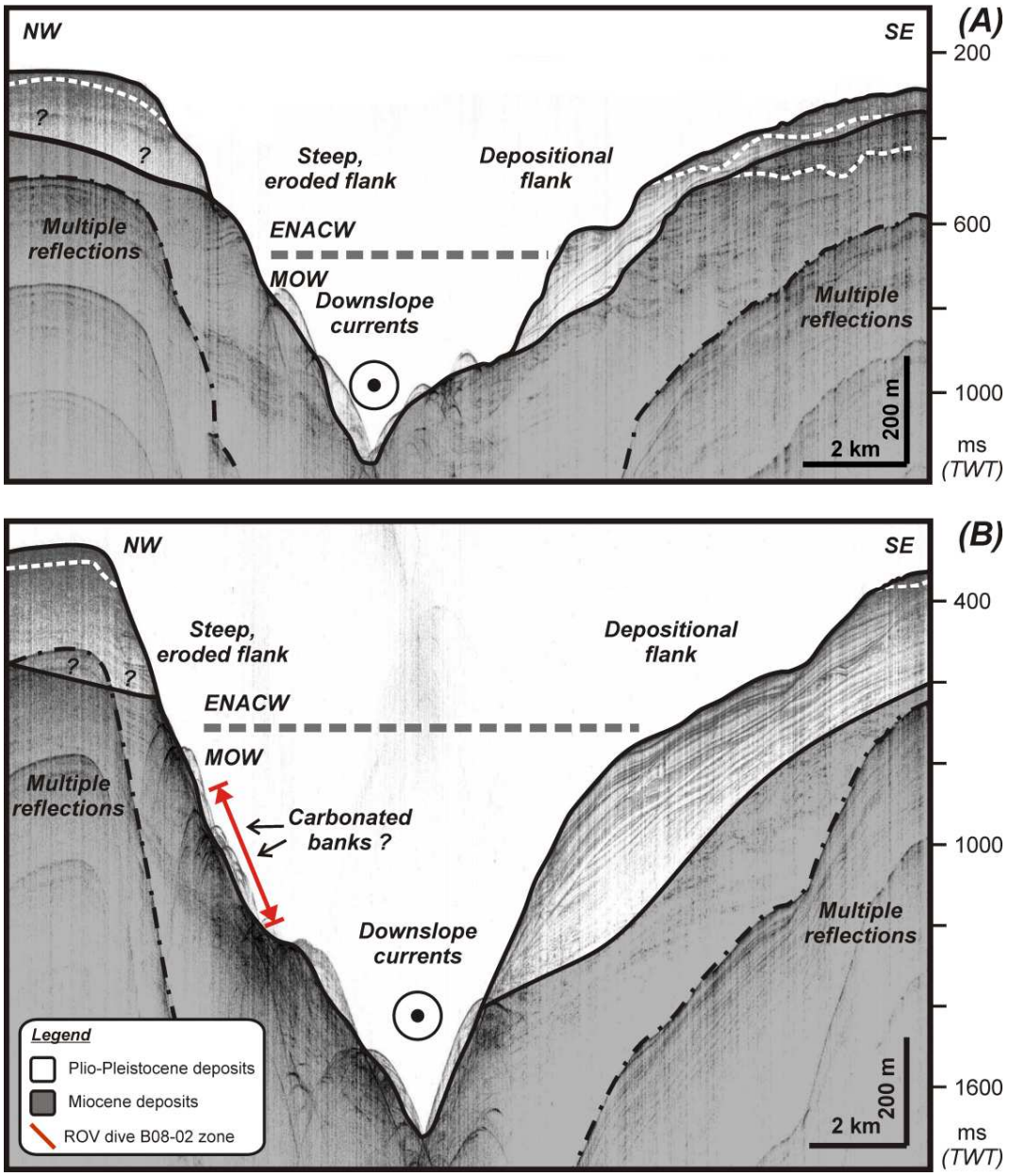

Fig. 6.3 *Seismic profiles Ga080605 (A) and Ga080604 (B), illustrating the seismic stratigraphy and thickness of the sedimentary cover across the Guilvinec Canyon (Fig. 6.1C). Note the asymmetry of canyon morphology and the difference between the sedimentary processes on both flanks. The white dashed lines indicate additional unconformities within the main sequences. These figures have a 10-fold vertical exaggeration.*

6.3.2 ROV observations

6.3.2.1 Dive B06-02: La Chapelle continental slope

Dive B06-02 followed a SW-NE, 2800-m-long track over the eastern flank of a prominent spur, parallel to its elongation, and crossing several of the steep NNW-SSE orientated gullies (Figs. 1b and 4). The main observations were carried out on the central gully between 7°20'00"W and 7°19'40"W, allowing a more comprehensive view on the gully environment (Fig. 6.4).

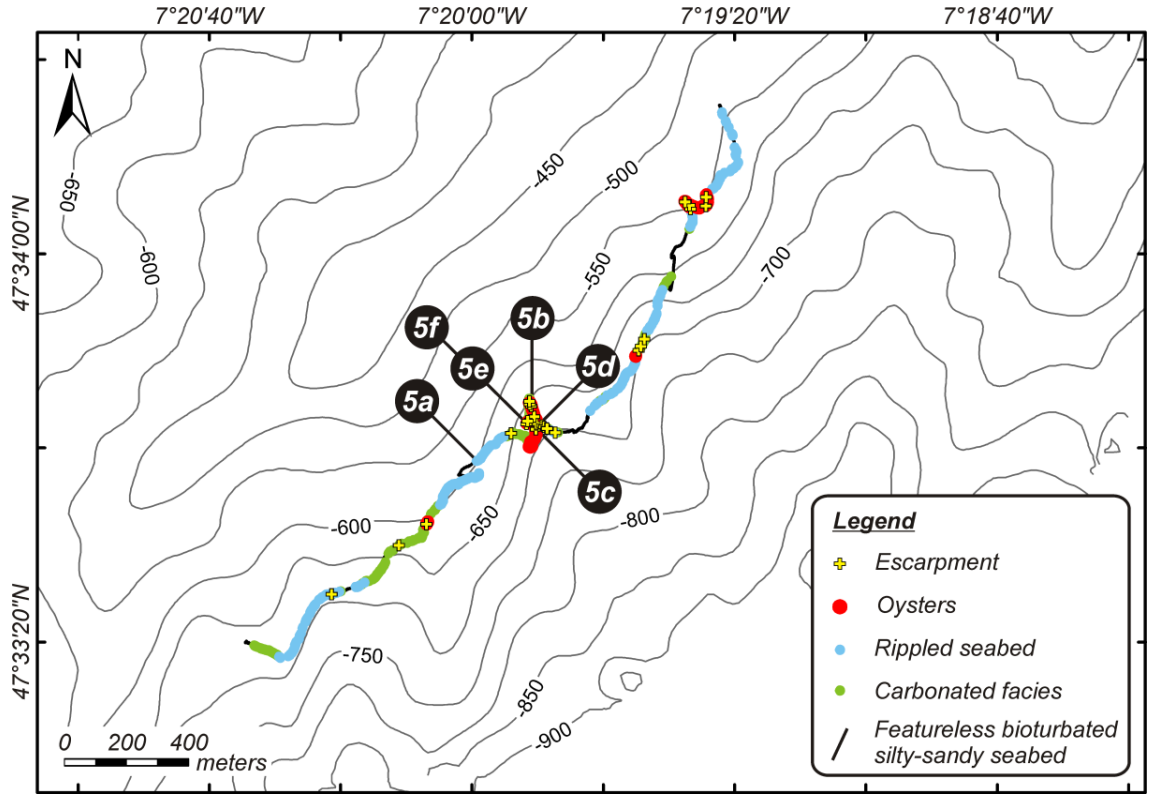

Fig. 6.4 *ROV dive B06-02 track superimposed on the R/V Belgica EM1002 bathymetry (contour lines every 50 m) with indication of the recognised lithologies, seabed features and the location of the imagery shown in Fig. 6.5.*

More than half (57 %) of the observed seafloor showed sandy bioturbated sediments with ripple marks on the relatively flat gully shoulders (Figs. 6.4 and 6.5A). These relatively straight NW-SE oriented sand ripples have wavelengths of approximately 10-20 cm and are less than 10 cm high. On other locations outside the gully axis, a frequent (25%) enigmatic pale-coloured facies was observed featuring decimetric to metric blocks or knolls inferred to be carbonated material (Fig. 6.5B). No recent sediment cover was observed and yellow *Hexadella* sp. sponges were noticed frequently on top of these blocks. Protruding banks with a thickness ranging from 10 to 30 cm were observed regularly (16%), especially on the steep slopes within the central part between 620 and 680 m (Figs. 6.4 and 6.5C-D). They form steps down to the central gully thalweg along a NNE-SSW to NW-SE orientation (Fig. 6.4). In total, 20 laterally variable banks were encountered over 60 m depth. Towards the centre of

the gully they disappear into a large N-S oriented escarpment between 630 and 650 m water depth (Fig. 6.5F). Based on our observations, this escarpment cliff is at least 10 m high. At the base of this cliff and the larger banks above, accumulated debris provides settling sites for sessile organisms, whilst the escarpment and the larger protruding banks are sporadically colonised by medium to dense communities of giant (10-15 cm) *Neopycnodonte zibrowii* oysters (Figs. 5d-e), forming a 3D assemblage with occasional dead cold-water corals (*Lophelia pertusa*). The oysters only occur in high densities (up to 100 individuals per m²) near the centre of the gully between 620 and 680 m depth, but were also observed in a similar setting at 4 other locations between 540 and 680 m (Fig. 6.4). Most typically, at the side of the gully, they only occur underneath overhangs with a width of at least 10-15 cm (Fig. 6.5D). Only nine of the observed overhangs were large enough to offer sufficient space for closely-stacked, suspended shells with a medium density of about 30 individuals per m² (Fig. 6.5E). Near the escarpment, they form a high-density vertical pavement (Fig. 6.5F). Many oyster individuals are still articulated and alive, or, where the free right valve is detached, show the non-degraded and locally still dark-coloured endostracum indicating that they had died only recently (Fig. 6.5E).

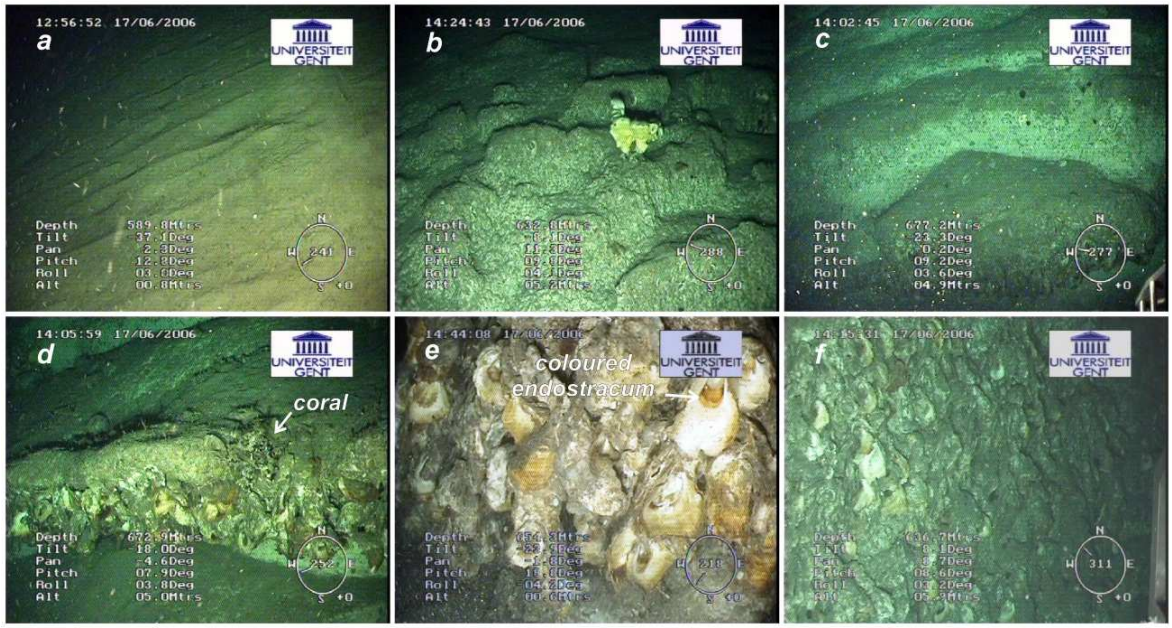

Fig. 6.5 *Video-derived images of oyster assemblages and facies recognised during dive B06-02 (Fig. 6.4). Each image bears depth information and orientation. (A) NW-SE straight sand ripples, (B) carbonate knolls with* Hexadella *sp. sponge, (C) carbonate banks in a series of steps, (D) overhanging carbonate bank with (low-density) oyster community attached below the bank, in association with a dead cold-water coral, (E) close-up of a probably living (high density) deep-water oyster community, (F) steep oyster cliff, note the altitude of the ROV (5.3 m above sea floor).*

6.3.2.2 Dive B08-02: North-western flank of Guilvinec Canyon

Dive B08-02 provided 3700 m of seafloor observations along a U-shaped track starting with the first stretch southwards from the NE flank of a gully at 700 m water depth and ending with a second stretch parallel to the gully axis (Figs. 6.1C and 6.6).

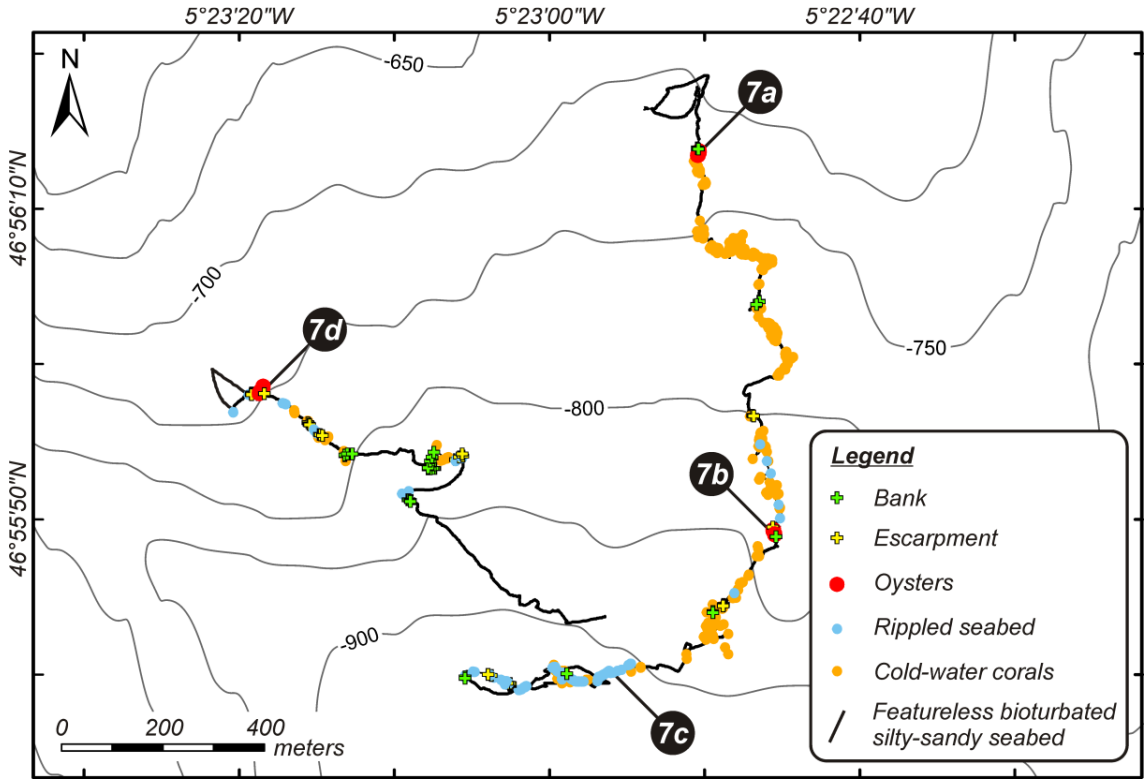

Fig. 6.6 *ROV dive B08-02 track superimposed on the R/V Belgica EM1002 bathymetry (contour lines every 50 m) with indication of the recognised lithologies, seabed features and the location of the stills imagery shown in Fig. 6.7.*

Along the main part of the dive track, a featureless bioturbated sandy seafloor was observed (Fig. 6.6). Nevertheless, the eastern part of the track revealed the presence of abundant yellow *Hexadella* sp. sponges, live *Madrepora oculata* patches and fossil *Lophelia pertusa* debris. Between 800 and 950 m, a rippled seabed was encountered in 10% of the frames. Especially below 900 m, straight and sometimes sinuous N-S oriented low-relief sand ripples were observed with wavelengths ranging between 10-20 cm and heights of approximately 5 cm (Figs. 6.6 and 6.7C). Sporadically (less than 5% of observations), the rather smoothly sloping seabed was interrupted by small banks or escarpments (Figs. 6.6 and 6.7A-B). These escarpments are long "ruptures" in the seabed, showing consolidated substrates and have an E-W orientation between 700 and 750 m, while those located deeper than 750 m are usually orientated in a S-N or SSW-NNE direction. Generally, the banks are up to tens of centimetres thick, while the heights of the escarpments range between 2 to 4 m. At only three out of nine locations (Figs. 6.6 and 6.7A-C), the escarpments were colonised by *N. zibrowii* oysters and, in lesser degree, by *M. oculata.* The relative abundance of *N. zibrowii*

on these escarpments is rather low, with 10 to 30 individuals per m² (Figs. 6.7A-B). Only on the leeward side of a 1-m-high W-E overhanging escarpment (at 744 m depth) was a community of up to100 individuals per m² observed. Here, the top 40 cm underneath the edge is colonised.

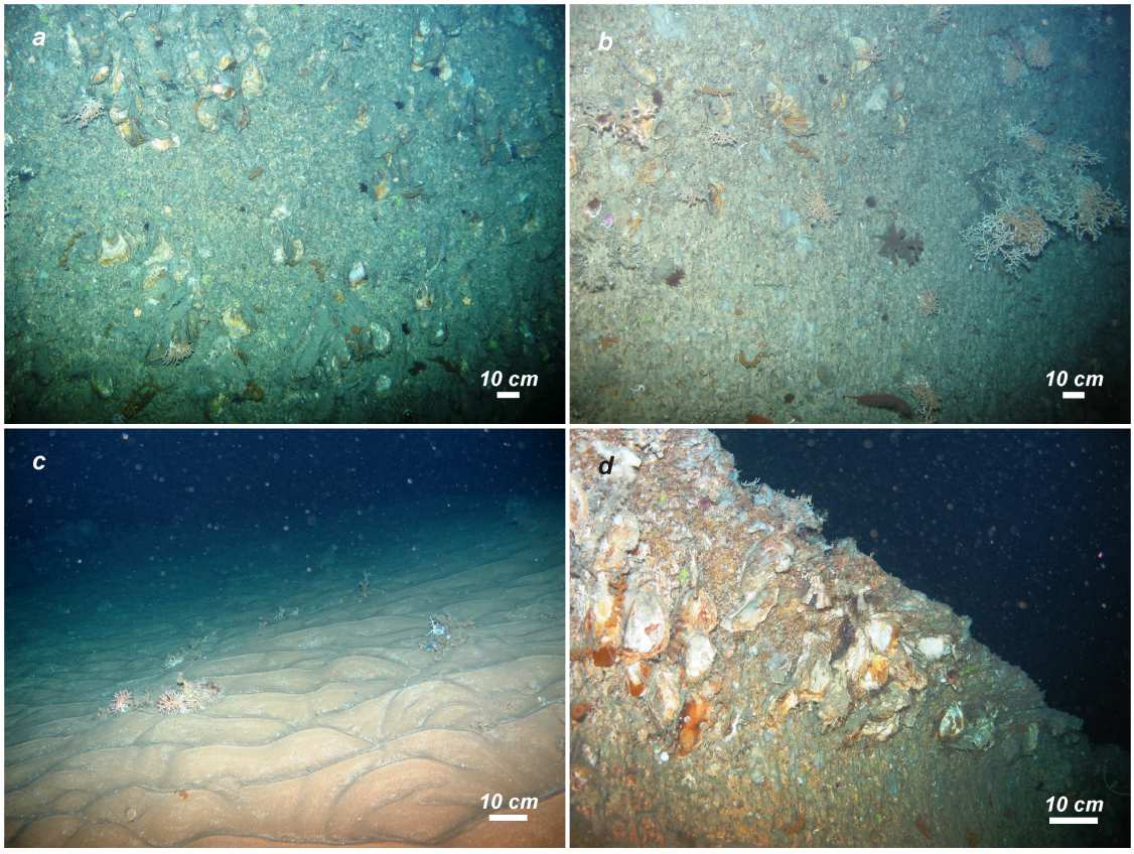

Fig. 6.7 *Stills images of oyster assemblages and facies recognised during dive B08-02 (Fig. 6.6). (A) E-W escarpment (± 3 m high) with frequent oyster colonization, (B), S-N oriented escarpment with a mixed solitary oyster and cold-water coral community (*Lophelia pertusa *and the black corals* Parantipathes *sp.,* Stichopathes *sp.,* Trissopathes *sp.), (C) sinuous S-N oriented sand ripples with sparse live solitary* Madrepora oculata*, and (D) leeward side of a W-E outcropping and overhanging rock (± 1 m high), colonised by deep-water oysters.*

6.3.2.3 Dive B08-05: Western flank of Guilvinec Canyon

Dive B08-05 investigated the southern shoulder of a gully south of the spur that separates the Guilvinec from the Penmarc'h Canyon (Figs. 6.1C and 6.8). The 3100 m long track followed a southward course, later on turning to the west, covering a depth range between 300 and 750 m.

Between 300 and 450 m, about 37% of the gently dipping slope is characterised by the presence of straight to gently sinuous sand ripples with a wavelength between 10 to 15 cm and a general SSE-NNW orientation (Fig. 6.9A). Sometimes coarser sand was observed in between the ripples. From 450 to 730 m, a relatively flat and bioturbated silty to sandy seafloor is observed with some small escarpments near 480 m and a low-relief rippled

seabed (Fig. 6.8). Only at the very end of Dive B08-05, the gentle slope is abruptly interrupted by a large, laterally continuous 4-m-high WSW-ENE rocky escarpment at 735 m. The first meter of this escarpment is a 50 cm deep overhanging cliff underneath which a thriving community of *N. zibrowii* oysters (Figs. 6.9B-C). Figure 6.9D shows the typical high-density assemblage of *N. zibrowii,* in which individuals seem to have grown on top of each other. Their size reaches 10 cm on the smallest axis and 15 cm on the largest axis. The density is estimated at 63 individuals per m². Both the oysters and the occasional corals are hanging upside down, concentrated near the most overhanging end of the cliff.

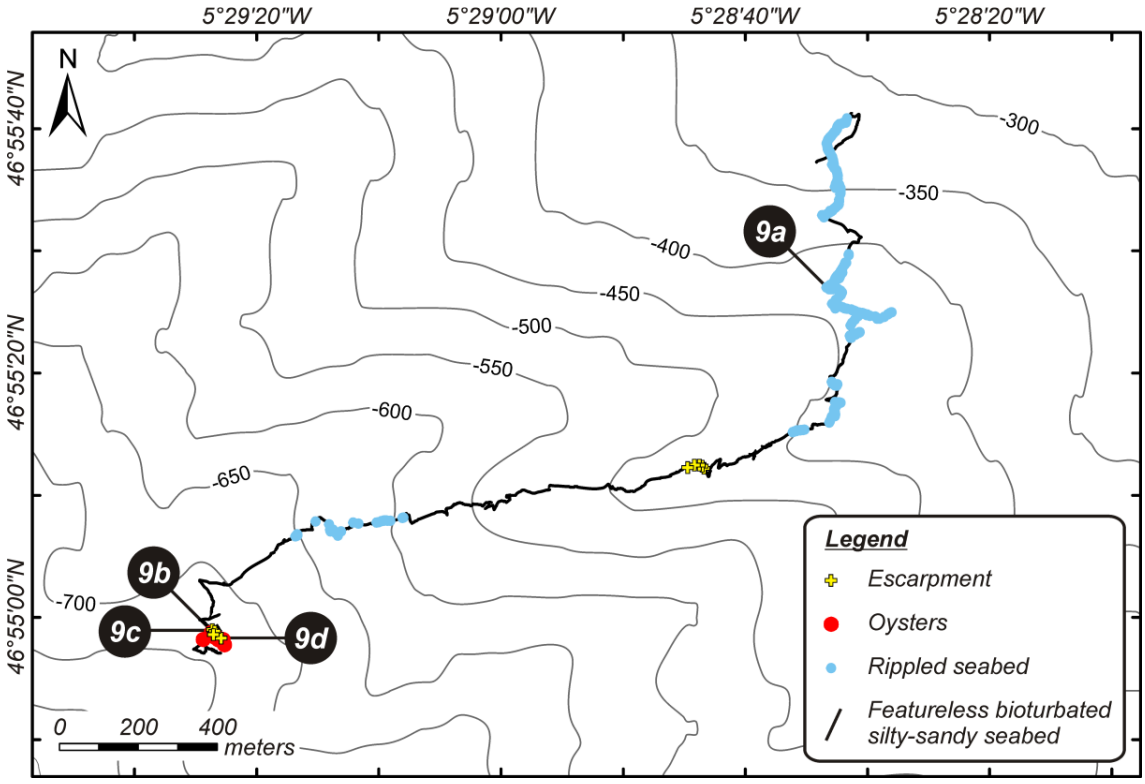

Fig. 6.8 *ROV dive B08-05 track superimposed on the R/V Belgica EM1002 bathymetry (contour lines every 50 m) with indication of the recognised lithologies, seabed features and the location of the stills imagery shown in Fig. 6.9.*

6.4 Discussion

Compared to the previously known occurrences of *Neopycnodonte zibrowii* (Wisshak et al., 2009a,b), these present observations in the Bay of Biscay expand the bathymetric range of this species from 350 to 846 metres. The habitat in which these giant deep-water oysters are thriving is dependent on specific conditions, both topographic and environmental. The main part of the discussion is based on the observations made during ROV dive B06-02 along the La Chapelle continental margin, since it provided the best overview of the occurrence of *N. zibrowii* in relation with its environment (Fig. 6.10).

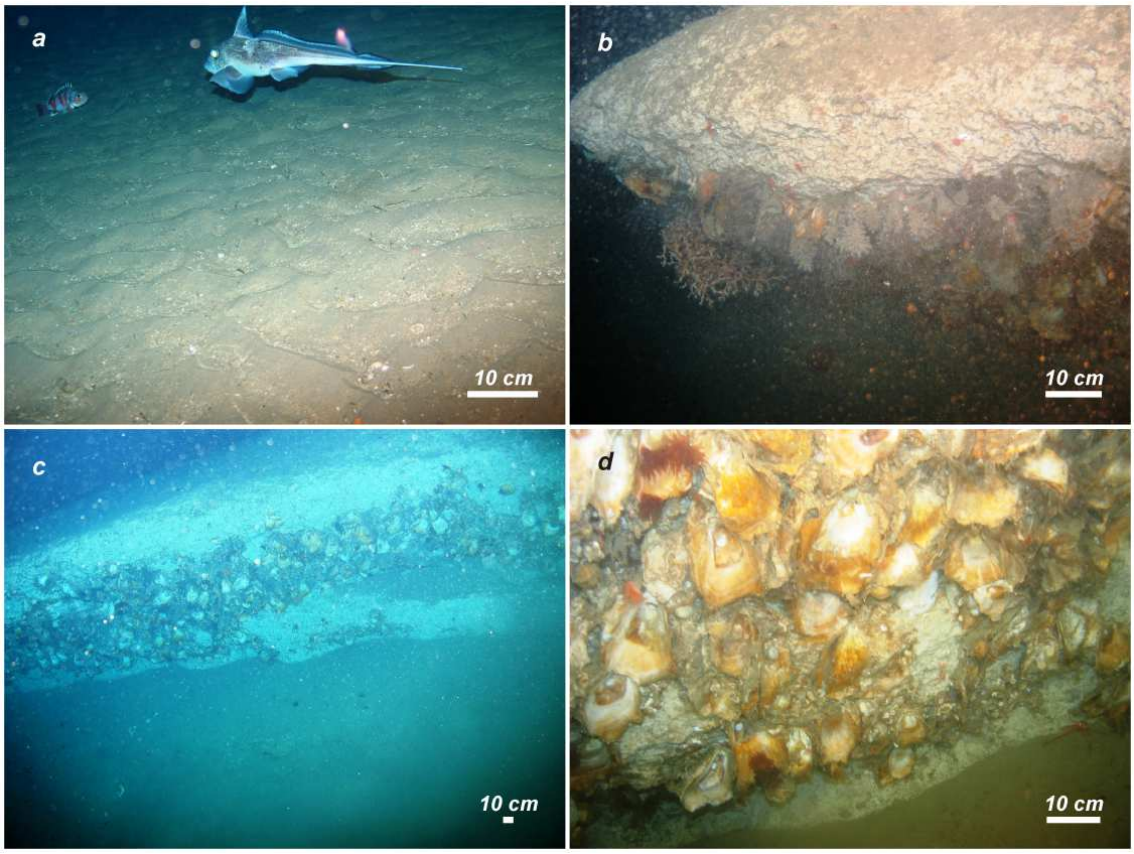

Fig. 6.9 *Stills images of oyster assemblages and facies recognised during dive B08-05 (Fig. 6.8). (A) sinuous SSE-NNW oriented sand ripple field and the fish* Chimera monstrosa *and* Helicolenus dactylopterus*, (B) overhanging cliff with a thriving mixed oyster and* Madrepora oculata *colony, (C) distant view of a S-N colonised overhanging cliff, and (D) detailed view of the densely packed deep-water oyster community.*

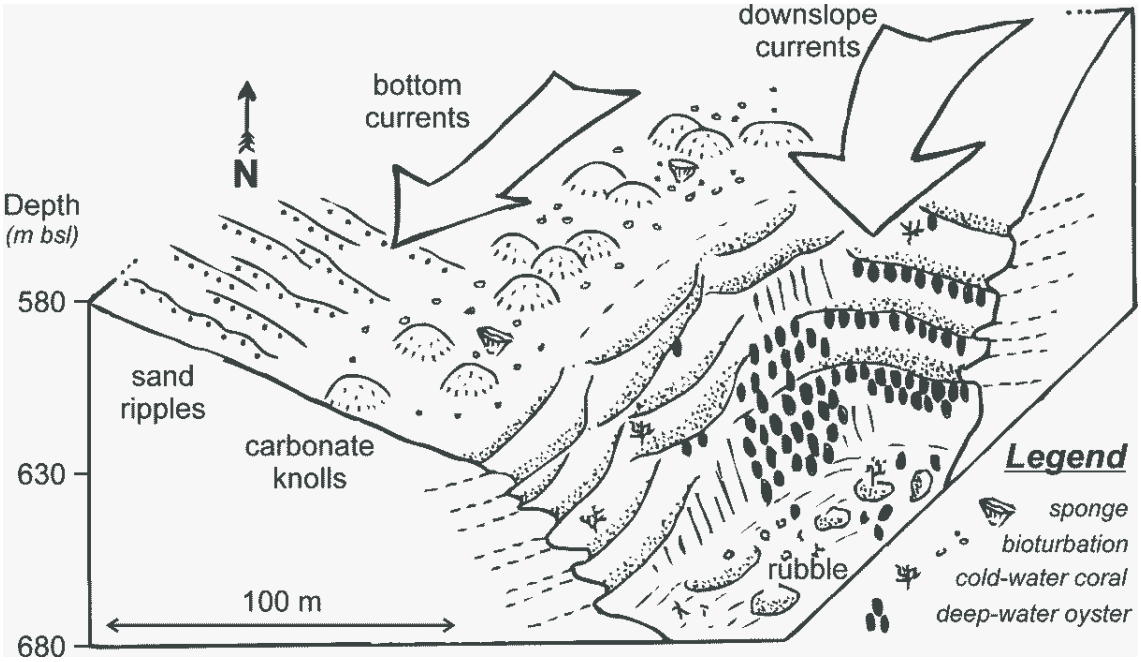

Fig. 6.10 *Conceptual sketch of the deep-water oyster environment, based on ROV dive B06-02 on the La Chapelle continental slope. The main oyster communities are located at the gully axis, fed by downslope currents enabling a suitable nutrient supply. The banks upon which the oysters are seated probably are Miocene carbonate banks (calcarenites).*

6.4.1 Influence of the physical environment on deep-water oyster colonisation

Until now, within the Bay of Biscay, the deep-water oyster *N. zibrowii* has only been observed on hard substrates. More specifically, only the areas underneath overhanging cliffs, banks or steep escarpments seem to be successful colonization surfaces with relative abundances from 30 to 100 individuals per m² (Figs. 6.5, 6.9 and 6.7). These specific deep-water oyster substrata, which can be considered as limiting along the continental margins, are concentrated within canyons, where they still are relatively sparsely developed (less than 5% of the surface area in this dataset).

Generally, the morphology of canyons flanks is relatively irregular and no significant cover of draping sediments is observed (Figs. 6.1 and 6.3). This zone is most likely subject to reworking by along-slope (contouritic) or downslope (turbiditic) current processes during respectively interglacial and glacial times (Arzola et al., 2008; Bourillet et al., 2006b; Huthnance, 1995; Toucanne et al., 2009). Within the depth window corresponding to the ROV observations, seismic profiles show single, high-amplitude reflections or diffraction hyperbolae, which might correspond to lithified calcarenite or calcilutites banks (Figs. 6.3 and 6.5d) from the Miocene Jones or Cockburn Formations (Bourillet et al., 2003; Paquet et al., 2010). Within canyons and gullies, predominantly downslope erosion has gradually exposed these consolidated carbonate-like sedimentary sequences, which have been shaped into step-like banks or escarpments (Figs. 6.5c-d and 6.10). This process is more intense towards the centre (thalweg) of the canyon or gully, providing a higher availability of suitable substrates for epibenthos colonization. Evidently, this will also affect the nature of the sessile organisms that colonize these substrates. If this epifauna is too exposed, they may be removed by episodic turbiditic currents. The overhanging banks and the vertical escarpments may provide a sufficiently sheltered habitat for the deep-water oysters, which are able to settle on such surfaces. Along the steeper La Chapelle continental slope, suitable substrates with abundant deep-water oysters were more prevalent compared to the Guilvinec area (Figs. 6.4 and 6.6). Only occasionally, and in reduced numbers, were co-occurring species such as cold-water corals observed on identical substrates (Figs. 6.7b and 6.9b). Such vertical substrates and overhangs could be considered as a challenging surface to be colonised by cold-water corals, given their relatively weak attachment and delicate skeletal structure.

The asymmetry of the Guilvinec Canyon clearly is a second factor influencing the location of the deep-water oyster habitats (Fig. 6.3). Both morphologically and stratigraphically the (north-)western slope of the Guilvinec Canyon shows more evidence of erosion than the eastern slope, which is characterised by depositional features (Figs. 6.1c and 6.3). Both ROV observations have shown the presence of seabed ripples on different parts of this slope between 300 and 950 m (Figs. 6.1, 6.6 and 6.8), inferring an enhanced E-W bottom current with average velocities between 20 to 40 cm/s (Stow et al., 2009). These observations fit the

cyclonic flow circulation and observed depth of the MOW in the Bay of Biscay (Fig. 6.2). The (north-)western slope of the canyon(s) could act as an obstacle that might intensify the easterly bottom currents through isopycnal doming, leading to erosion (Hernández-Molina et al., 2003; Iorga and Lozier, 1999; Van Rooij et al., 2010b). A similar process was also observed on the upper part of the Portimao Canyon (Marches et al., 2007). This effect does not operate on the eastern slope, leading to a preferential deposition of sediment on this side of the canyon and making it nearly devoid of banks and escarpments (Figs. 1c and 3). This example also demonstrates how a combination of turbiditic and contouritic currents may influence canyon morphology and hence the spatial structure deep-water ecosystems. Since the banks, as well as the cliffs, will not be susceptible to sediment burial, they can provide a suitable hard substrate for this type of filter feeders.

6.4.2 Oceanographic drivers for deep-water oyster occrrence

In addition to suitable substrates on which to settle, the oysters also require a favourable oceanographic environment and sufficient nutrients. During some of the ROV dives, dense marine snow was present in the area where the oyster community was discovered (Figs. 6.5a, 6.7c-d and 6.9c). This aggregated particulate matter, composed of phytodetritus and faecal pellets sinking from the upper water layers, is an important constituent of the trophic input to this community. Compared to shallow-water oysters, the occurrence of oysters at these depths is remarkable given the higher salinities and generally lower food input. On the other hand, this part of the margin is characterised by relatively high surface primary production (Joint et al., 2001; Pingree and Le Cann, 1990). Moreover, according to the available hydrographic data, the depth range in which *N. zibrowii* is observed lies just beneath the boundary between the upper Eastern North Atlantic Water and the intermediate saline Mediterranean Outflow Water (Fig. 6.2). The lower limit of the oyster's occurrence coincides with a local salinity and temperature maximum. Within this zone of upper MOW, the observation of straight sand ripples during dive B06-02 (Figs. 6.4, 6.6 and 6.8) indicates the presence of strong bottom currents between 10 to 40 cm/s (Stow et al., 2009). Apart from the average cyclonic flow velocity of the MOW, these bottom currents may be enhanced by strong internal tides (White, 2007) and funnelled along the canyon axis, as observed along the Armorican margin (Pingree and Le Cann, 1989, 1990) and within the Portimao Canyon (Marches et al., 2007). Within the canyons, these tidally induced transports may be channelled and result in regions of locally increased flow, resuspension and local circulations (Pingree and Le Cann, 1990). Upper slope internal tides are considered to be responsible for the entrapment and downward transport of enhanced fluxes of surface-derived phytodetritus (Holligan et al., 1985; Pingree et al., 1982), as recently inferred for the Nazaré Canyon (Arzola et al., 2008) and above giant carbonate mound provinces colonised by reef-forming cold-water corals (Mienis et al., 2007; White, 2007). The significance of submarine canyons as hotspot for deep-water ecosystems may be due to their capacity to accumulate organic debris (Canals et al., 2006; Mortensen and Buhl-

Mortensen, 2005; Roberts et al., 2006). It is highly likely that this water-mixing above the seabed results in enhanced concentrations of suspended material and favors aggregations of filter/suspension feeders (de Stigter et al., 2007).

The oyster banks occur within a potential density envelope of 27.4 – 27.7 kg/m³ (Fig. 6.2), overlapping the range of values that are considered to be a prerequisite for the development, growth and distribution of cold-water coral reefs along the Celtic and Nordic European margin (Dullo et al., 2008) and within the Guilvinec area (De Mol et al., 2011b). This relationship to potential density may be linked to the formation of intermediate nepheloid layers, indicating an increased nutrient supply and resuspension (de Stigter et al., 2007; Mienis et al., 2007). Thus, in contrast to shallow marine oyster occurrences, the dynamic oceanography within deep-sea canyons has the potential to support a stable ecosystem in which oysters co-exist with sponges, hydrozoans, gorgonians and scleractinians (De Mol et al., 2011b).

6.5 Conclusions

The use of ROV technology enabled detailed observations to be made of *Neopycnodonte zibrowii* oysters in water depths between 540 and 846 m along the French Atlantic continental margin. This recently described species can be regarded as a distinct deep-sea relative of *N. cochlear* with specific adaptations allowing it to thrive at upper bathyal depths. Although *N. zibrowii* was previously observed in non-canyon environments, for example, in the Azores Archipelago (Wisshak et al., 2009a) and the Gorringe Bank (Auzende et al., 1984), this species commonly requires steep slopes with overhanging banks and escarpments. In the northern Bay of Biscay, suitable physical habitats can only be generated within canyons by the interplay of turbiditic and contouritic processes, which erode and gradually expose consolidated carbonate-like sedimentary sequences, shaping them into step-like banks. Moreover, within these canyons, the delivery and resuspension of nutrients is facilitated through funnelling of internal tides near the ENAW/MOW interface. Only when these unusual physical habitats and hydrographic conditions coincide can *N. zibrowii* be observed in relatively high numbers of up to 100 individuals per m².

This little-known population located in an inaccessible environment sheds light on the richness of filter-feeding species in canyon systems. Because they occupy vertical habitats, acoustic hull-mounted systems and bottom sampling with conventional towed devices are unsuitable for a proper description of these communities. Further in situ observations and habitat mapping using ROVs should improve our understanding of the biogeographic distribution of this unusual bivalved mollusc along the Bay of Biscay and the European margin. It typifies an overlooked deep-water community, which represents part of the still vastly underestimated biodiversity of bathyal benthic communities, especially within canyons.

Acknowledgements

This research was supported by the HERMES project (EC contract n^{o} GOCE-CT-2005-511234), funded by the European Commission's Sixth Framework Programme under the priority 'Sustainable Development, Global Change and Ecosystems' and by ESF EuroDIVERSITY MiCROSYSTEMS (05_EDIV_FP083-MICROSYSTEMS). A follow-up of this research will be performed within the framework of the EC FP7 IP HERMIONE project (grant agreement n° 226354). We are indebted to the entire ROV *Genesis* technical team of Ghent University (Belgium). The captains, crews and shipboard scientific parties of the R/V *Belgica* ST0612 and ST0813a campaigns are also acknowledged for their enthusiastic efforts. We are grateful to Dr. L. Chou (ULB, Belgium) for kindly providing CTD data (Station 3 cast B). The authors also kindly acknowledge H. Pirlet, three anonymous reviewers, the editor and associated editor of DSR I for the useful comments and suggestions which significantly helped improving this manuscript. LDM acknowledges the support through an IWT-grant. The research of DVR was funded through an FWO Flanders post-doctoral fellowship.

Part 4

Conclusions

Chapter 7

Conclusions and outlook

7.1 Conclusions

After many years of intensive research SW of Ireland, other areas (e.g. the Gulf of Cadiz) were targeted in order to compare the environmental setting and check the representativeness of the existing mound growth model. Based on visual observations and sediment core analyses, the architecture of the cold-water coral mounds on top of the Pen Duick Escarpment in the southern Gulf of Cadiz was investigated, aiming to reconstruct the paleoenvironmental record. However, early diagenesis (e.g. dissolution of carbonates, the formation of pyrite and the formation of lithified layers) in combination with a shallow methane transition zone has a major impact on the preservation of that record, especially in Alpha and Beta Mound. In contrast, the uppermost 470 cm of Gamma Mound seems not to be influenced by diagenetic processes, making it an ideal mound to reveal the paleoenvironmental conditions and recent build-up of the mounds. Previous studies in this area (e.g. Wienberg et al., 2009; Wienberg et al., 2010) mainly focussed on the distribution, appearance and diversity of cold-water corals in relation to climatic and oceanographic changes. Hence, we went a step further and tried to unravel the growth and evolution of the cold-water coral mounds and to link this mound growth with climate changes on the NW African continent. Especially the input of aeolian dust seemed to be very important within mound growth in the southern Gulf of Cadiz. Up to now, indications for a similar growth pattern as well as similar environmental conditions as the cold-water coral mounds SW of Ireland and off Mauritania are present, although further research is necessary. All mounds are characterised by a periodic growth with intervals containing coral bearing sediments and intervals marked by numerous hiatuses that represent periods without cold-water coral growth on the mounds. However, cold-water coral growth in the Gulf of Cadiz and off Mauritania is assigned to glacial periods while off Ireland coral growth is restricted to interglacial periods. One of the major differences between the different mound provinces is the sediment source. While the terrigenous fraction in the Porcupine mounds is built up of ice-rafted debris, mainly linked to the development of the British-Irish Ice Sheet, the terrigenous fraction of the mounds on the PDE consists of aeolian dust derived from the NW African continent. Hence, the terrigenous component of mound growth is not restricted to a certain type of sediment source but a large input of terrigenous sediment is more important in order to stimulate vertical growth, next to the ideal environmental conditions for cold-water coral growth.

Based on the results of chapters 3 and 4, the following conclusions are highlighted:

- Based on the sediment nature and the macrofaunal assemblages, four different facies were distinguished on the mounds. The coral distribution pattern is most likely the result of local variations in bottom current strength and direction, inducing local areas of deposition, non-deposition and erosion. Additionally, this process is influenced by differences in the morphology of the escarpment between the SE and

NW part. This explains the rather similar distribution pattern on Alpha and Beta Mound on one hand and on Gamma Mound on the other hand.

- A preference of *L. pertusa* and *M. oculata* for the north-western part of the Pen Duick Escarpment is observed, while *Dendrophyllia* sp. mostly occurs on the south-eastern end. Mainly fossil cold-water corals were found, except for a few living *Dendrophyllia* sp. specimens on the north-eastern flank of Beta Mound. U-series datings revealed that these *Dendrophyllia* sp. started to grow after the extinction of *L. pertusa* and *M. oculata*. This confirms that *Dendrophyllia* sp. prefers warmer conditions with reduced bottom currents while *L. pertusa* and *M. oculata* prefer colder environments.
- The observed cold-water coral rubble fields can be considered as ideal hotspots for biodiversity. Although the cold-water corals are dead, creating open frameworks, they can still act as habitat for many other organisms, e.g. poriferans, crinoids, octocorals, crustaceans, fish. The slimy decay products of these associated sponges and other metazoans, observed on the coral framework elements, may fuel thriving microbial microcosms and may play a significant role in sediment fixing.
- The outcropping hard substrate, observed on Alpha and Beta Mound, can be related to authigenic carbonate slabs. Several hypotheses (e.g. early diagenetic lithification, organomineralisation, influence of methane) are proposed in order to explain the formation of carbonate slabs on top of a cold-water coral mound. However, further research, including intensive sampling of the carbonate slabs on different locations, is necessary in order to ascertain their origin.
- Cold-water coral fragments are observed throughout the whole core but species and amount of corals vary. *L. pertusa* and *M. oculata* are the dominant framework building species although some *Dendrophyllia* sp. fragments are also observed. 88 % of the U-series dating results of the first two species refer to glacial times while *Dendrophyllia* sp. linked to warmer conditions during interglacial periods such as the Holocene (MIS 1).
- The growth and evolution of cold-water coral mounds on the Pen Duick Escarpment is related to the climate on the NW African continent. During glacial periods, a more arid climate results in increased wind intensity and a scarce plant cover, providing high dust input in the NE Atlantic Ocean. This dust input not only favours cold-water coral growth (nutrient supply due to the high Fe content) but also mound growth as on average more than 80 % of the terrigenous fraction of the mound sediments consists of this aeolian dust. Aeolian dust is transported to the southern Gulf of Cadiz by the northern branch of the Saharan air layer and some additional smaller wind trajectories from southern Morocco. Mound growth can be mainly assigned to MIS 8 and MIS 2-4 for Gamma Mound, although MIS 6 is also represented in Alpha and Beta Mound.
- During interglacial periods, the terrestrial climate becomes more humid which increases the supply of fluvial material towards the continental shelf. During these periods, mound growth is slowed down or even interrupted, creating hiatuses.

However, the presence of *Dendrophyllia* sp. fragments in the deeper part of the mounds indicates possible mound growth during interglacial periods. Due to the bad preservation of the coral fragments it is not possible to date these fragments and thus to trace coral and mound growth during past interglacial periods on the Pen Duick mounds.

In the Gulf of Cadiz and the Porcupine Seabight, specific conditions stimulate mound growth, which are not present in the Bay of Biscay. Different sites, earlier described by Le Danois in 1948, were revisited in order to better understand the physical and oceanographic setting of the cold-water coral habitats along the NE Atlantic continental margin. During these exploratory cruises large cold-water coral and oyster ecosystems were discovered. Deep-sea canyons such as the Penmarc'h and Guilvinec Canyons are suitable habitats for the settlement of cold-water corals (*M. oculata* and *L. pertusa*) due to (1) their role as transport pathways of organic matter from the shelf to the abyssal plain, (2) the mixing of different water masses resulting in enhanced suspended material, (3) increased bottom currents, and (4) the presence of hard substrate. The Bay of Biscay can be considered as a transition zone between the temperate Atlantic (below 50°N) and the cold north-eastern Atlantic between 50° and 70°N. After the Late Glacial Maximum, cold-water corals started to grow along the Armorican margin but migrated likely during the mid-Holocene.

The most important conclusions from chapters 5 and 6 are listed below.

- Two cold-water coral settings were distinguished within the canyons: a shallow setting in water depths of 280-290 m with only dead coral rubble (mostly *L. pertusa*) and a deep-water setting (700-920 m) with mostly living *M. oculata* species on top of coral rubble. Mini mounds occur at an unusually shallow water depth (~ 280 m) compared to most other cold-water coral (reef) occurrences along the NE Atlantic margin.
- Coral growth in the Penmarc'h and Guilvinec Canyons started at the beginning of the Holocene. The older age of the corals in the shallow setting compared to the deeper setting indicates a migration of the coral habitats towards greater water depths. Moreover, indications of bio-erosion and disintegration on the shallow coral fragments suggest that they have already been exposed on the seabed for a significant amount of time. In contrast, the corals in the deeper setting are much better preserved, in accordance with the younger age for these species. The cause of the downslope migration of the corals is still uncertain. However, the changing sea level and the rising temperatures, might have forced corals to deeper water depths, where they found better living conditions.
- The density range of 27.35 to 27.65 $kg.m^{-3}$ (Dullo et al., 2008) is also valid for the living cold-water corals (mostly *M. oculata*) in the Bay of Biscay, which makes it a good prerequisite for the distribution and growth of living cold-water corals along the

northeast Atlantic margin. It can be used as a predictive tool in order to discover more cold-water coral habitats along the European continental margin.

- Seabed observations resulted in the discovery of giant deep-water oyster banks and cliffs at depths between 540 to 846 m along the French Atlantic continental margin. This recently described species can be regarded as a distinct deep-sea relative of *N. cochlear* with specific adaptations allowing it to thrive at upper bathyal depths. Although *N. zibrowii* was previously observed in non-canyon environments, this species commonly requires steep slopes with overhanging banks and escarpments.
- In the northern Bay of Biscay, suitable physical habitats for these oysters can only be generated within canyons by the interplay of turbiditic and contouritic processes, which erode and gradually expose consolidated carbonate-like sedimentary sequences, shaping them into step-like banks. Moreover, within these canyons, the delivery and resuspension of nutrients is facilitated through funnelling of internal tides near the ENAW/MOW interface. Only when these unusual physical habitats and hydrographic conditions coincide *N. zibrowii* can be observed in relatively high numbers of up to 100 individuals per m^2.
- This little-known population located in an inaccessible environment sheds light on the richness of filter-feeding species in canyon systems. It typifies an overlooked deep-water community, which represents part of the still vastly underestimated biodiversity of bathyal benthic communities, especially within canyons.

7.2 Outlook

During this research new questions raised which can be tackled during future research.

- In order to obtain a full 4D characterisation of the Pen Duick mounds, additional coring and ROV observations are necessary. For example, one core on top of each mound and a few cores on the flanks. This will allow to detect variations (e.g. cold-water coral abundance, sedimentation…) within the mounds itself and to reconstruct a more precise evolutionary model. In 2013, an R/V Marion Dufresne cruise is planned within the framework of the EUROFLEETS program in order to obtain additional gravity cores in the area.
- The cores described in this study (3.4, 4.5 and 6.3 m long) do not reach the mound base as the presence of lithified layers within the mounds prevents a higher penetration depth of the gravity corer. MeBo or IODP drilling can provide a possible solution for this problem. On Alpha Mound an additional coring problem occurred due to the presence of carbonate slabs. A MeBo drilling cruise has been recently confirmed and will be planned soon.
- Additional datings from the sediment are necessary as there can be a difference in age between the cold-water coral fragments and the sediment. This can provide further information on the timing of infill and thus of mound growth.

- The carbonate slabs on top of Alpha Mound should be further investigated in order to reveal their origin. It is remarkable that such hard substrate is observed on top of a coral mound and that they are heavily disturbed. Authigenic methane-derived carbonates are promising archives since they preserve the geochemical signature of the interstitial water and therefore reflect varying methane seepage activity and gas hydrate decomposition (Bahr et al., 2010 and references therein).
- Another important issue is the relationship and impact of proximal mud volcanoes, e.g. Gemini mud volcano, which is located at a distance of only 1 km from Alpha Mound. This latter mound is heavily altered by diagenetic processes under influence of methane. The further away from the mud volcano the impact of methane becomes smaller, e.g. Gamma Mound where the significant impact of early diagenesis only starts at a depth of 470 m.
- A detailed hydrodynamic study of the southern Gulf of Cadiz does not exist at the moment. This can be useful in order to (1) define transport patterns of the sediment before settling on the Pen Duick Escarpment and (2) reveal the impact of reworking of the sediments during transport and on the mounds.
- Surface water productivity seems to play an important role in mound building in the Porcupine Seabight (Thierens et al., in prep.) as well as along the Mauritanian continental margin (Eisele et al., 2011). Further research (e.g. planktonic foraminifera assemblages) is necessary on the Pen Duick mounds in order to define the importance of surface water productivity in the build-up of the mounds in the southern Gulf of Cadiz. Additionally, the role of upwelling (Fe supply) should be investigated.
- The source area of aeolian input is defined based on previous studies along the NW African margin and in the Mediterranean Sea. However, additional lab experiments (e.g. XRD analyses) are necessary to locate the source area for dust input to the Pen Duick Escarpment.

References

Adkins, J.F., Cheng, H., Boyle, E.A., Druffel, E.R.M., Edwards, R.L., 1998. Deep-sea coral evidence for rapid change in ventilation of deep North Atlantic 15, 400 years ago. Science 280, 725–728.

Akhmetzhanov, A.M., Kenyon, N.H., Ivanov, M.K., Wheeler, A.J., Shashkin, P.V., van Weering, T.C.E., 2003. Giant Carbonate Mounds and Current-Swept Seafloors on the Slope of the Southern Rockall Trough. In: Mienert, J., Weaver, P.P.E. (Eds.), European margin sediment dynamics: side-scan sonar and seismic images. Springer-Verlag Berlin Heidelberg, pp. 203-209.

Altuna, A., 1994. El orden Scleractinia (Cnidaria, Anthozoa) en la costa vasca: consideraciones generales y especies litorales. Kobie 22, 67-82.

Altuna, A., 1995. El orden Scleractinia (Cnidaria, Anthozoa) en la costa vasca (Golfo de Vizcaya): especies batiales de la fosa de CapBreton. Munibe 47, 85–96.

Álvarez-Claudio, C., 1994. Deep-water Scleractinia (Cnidaria: Anthozoa) from southern Bay of Biscay. Les Cahiers de Biologie Marine 35, 461–469.

Álvarez-Pérez, G., Busquets, P., De Mol, B., Sandoval, N.G., Canals, M., Casamor, J.L., 2005. Deep-water coral occurrences in the Strait of Gibraltar. In: Freiwald, A., Roberts, J.M. (Eds.), Cold-water Corals and Ecosystems. Springer-Verlag Berlin Heidelberg, 207-221.

Arzola, R.G., Wynn, R.B., Lastras, G., Masson, D.G., Weaver, P.P.E., 2008. Sedimentary features and processes in the Nazaré and Sétubal submarine canyons, west Iberian margin. Marine Geology 250, 64-88.

Auzende, J.-M., Charvet, J., Le Lann, A., Le Pichon, X., Monteiro, J.-H., Nicolas, A., Olivet, J.-L., Ribeiro, A., 1984. Géologie du Banc de Gorringe, Campagne CYAGOR II. Résultats des Campagnes à la Mer 27. Publications du Centre National pour l'Exploration des Oceans (CNEXO), Brest, 65 pp.

Bahr, A., Pape, T., Abegg, F., Bohrmann, G., van Weering, T., Ivanov, M.K., 2010. Authigenic carbonates from the eastern Black Sea as an archive for shallow gas hydrate dynamics – Results from the combination of CT imaging with mineralogical and stable isotope analyses. Marine and Petroleum Geology 27, 1819-1829.

Bartoli, G., Sarnthein, M., Weinelt, M., Erlenkeuser, H., Garbe-Schönberg, D., Lea, D.W., 2005. Final closure of Panama and the onset of northern hemisphere glaciation. Earth and Planetary Science Letters 237, 33-44.

Becker, E.L., Cordes, E.E., Macko, S.A., Fisher, C.R., 2009. Importance of seep primary production to *Lophelia pertusa* and associated fauna in the Gulf of Mexico. Deep-Sea Research Part I 56, 786-800.

Beuck, L., Freiwald, A., 2005. Bioerosion patterns in a deep-water Lophelia pertusa (Scleractinia) thicket (Propeller Mound, northern Porcupine Seabight). In: Freiwald, A., Roberts, J.M. (Eds.), Cold-water Corals and Ecosystems. SpringerVerlag Berlin Heidelberg, pp. 915-936.

Blamart, D., Van Rooij, D., Leau, H., 2010. MD169 – Microsystems Cruise report. Les Rapports des Campagnes à la Mer, IPEV, Brest, OCE/2010/02.

Bloemendal, J., King, J.W., Hall, F.R., Doh, S.J., 1992. Rock magnetism of Late Neogene and Pleistocene deep-sea sediments – Relationships to sediment source, diagenetic processes, and sediment lithology. Journal of Geophysical Research - Solid Earth 97, 4361-4375.

Blott, S.J., Pye, K., 2001. Gradistat: a grain size distribution and statistics package for the analysis of unconsolidated sediments. Earth Surface Processes and Landforms 26, 1237-1248.

Boetius, A., Ravenschlag, K., Schubert, C.J., Rickert, D., Widdel, F., Gleseke, A., Amann, R., Jergensen, B.B., Witte, U., Pfannkuche, O., 2000. A marine microbial consortium appartenly mediating anaerobic oxidation of methane. Nature 407, 623-626.

Bongiorni, L., Mea, M., Gambi, C., Pusceddu, A., Taviani, M., Danovaro, R., 2010. Deep-water scleractinian corals promote higher biodiversity in deep-sea meiofaunal assemblages along continental margins. Biological Conservation 143 (7), 1687-1700.

Bourillet, J.F., Jouanneau, J.-M., Macher, C., Le Hir, P., Naughton, F., 2006a. “La Grande Vasière” mid-shelf mud belt: Holocene sedimentary structure, natural and anthropogenic impacts. 10th International Symposium on Oceanography of the Bay of Biscay, Vigo, Spain.

Bourillet, J.-F., Lericolais, G., 2003. Morphology and seismic stratigraphy of the Manche Paleoriver System, Western Approaches. In: Mienert, J., Weaver, P. (Eds.), European Margin Sediment Dynamics. Springer-Verlag Berlin Heidelberg, pp. 229-233.

Bourillet, J.-F., Reynaud, J.-Y., Baltzer, A., Zaragosi, S., 2003. The 'Fleuve Manche': the submarine sedimentary features from the outer shelf to the deep-sea fans. Journal of Quaternary Science 18 (3-4), 261-282.

Bourillet, J.-F., Zaragosi, S., Mulder, T., 2006b. The French Atlantic margin and deep-sea submarine systems. Geo-Marine Letters 26, 311-315.

Bout-Roumazeilles, V., Combourieu Nebout, N., Peyron, O., Cortijo, E., Landais, A., Masson-Delmotte, V., 2007. Connection between South Mediterranean climate and North African atmospheric circulation during the last 50,000 yr BP North Atlantic cold events. Quaternary Science Reviews 26, 3197-3215.

Boyd, P.W., Watson, A.J., Law, C.S., Abraham, E.R., Trull, T., Murdoch, R., Bakker, D.C.E., Bowie, A.R., Buesseler, K.O., Chang, H., Charette, M., Croot, P., Downing, K., Frew, R., Gall, M., Hadfield, M., Hall, J., Harvey, M., Jameson, G., LaRoche, J., Liddicoat, M., Ling, R., Maldonado, M.T., McKay, R., Nodder, S., Pickmere, S., Pridmore, R., Rintoul, S., Safi, K., Sutton, P., Strzepek, R., Tanneberger, K., Turner, S., Waite, A., Zeldis, J., 2000. A mesoscale phytoplankton bloom in the polar Southern Ocean waters stimulated by iron fertilization. Nature 407, 695–702.

Brabant, L., Vlassenbroeck, J., De Witte, Y., Cnudde, V., Boone, M., Dewanckele, J., Van Hoorebeke, L., 2011. 3D analysis of high resolution X-ray CT data with Morpho+. Microscopy and Microanalysis 17 (2), 252-263.

Broecker, W.S., 1963. A preliminary evaluation of uranium series inequilibrium as a tool for absolute age measurement on marine carbonates. Journal of Geophysical Research 68, 2817-2834.

Cairns, S.D., 1979. The deep-water Scleractinia of the Caribbean Sea and adjacent waters. Studies on the Fauna of Curaçao 57, 1-341.

Cairns, S.D., 1982. Antarctic and Subantarctic Scleractinia. Antarctic Research Series 34, 1-74.

Cairns, S.D., 1984. New records of ahermatypic corals (Scleractinia) from the Hawaiian Islands and Line Islands. Occasional Papers of the Bishop Museum 25, 1-30.

Cairns, S.D., 2001. A brief history of taxonomic research on azooxanthellate Scleractinia (Cnidaria: Anthozoa). Bulletin of the Biological Society of Washington 10, 191-203.

Canals, M., Puig, P., Durrieu de Madron, X., Heussner, S., Palanques, A., Fabres, J., 2006. Flushing submarine canyons. Nature 444, 354-357.

Caralp, M.H., 1988. Late Glacial to Recent deep-sea benthic foraminifera from the Northeastern Atlantic (Cadiz Gulf) and Western Mediterranean (Alboran Sea): paleoceanographic results. Marine Micropaleontology 13, 265-289.

Caress, D.W., Chayes, D.N., 1995. New software for processing sidescan data from sidescan-capable multibeam sonars, in: Wernli, R. (Ed.), Oceans 95 MTS/IEEE: Challenges of our Changing Global Environment, Conference Proceedings, vol. 2, Marine Technology Society Journal, Washington DC, pp. 997-1000.

Carlier, A., Le Guilloux, E., Olu, K., Sarrazin, J., Mastrototaro, F., Taviani, M., Clavier, J., 2009. Trophic relationships in a deep Mediterranean cold-water coral bank (Santa Maria di Leuca, Ionian Sea). Marine Ecology Progress Series 397, 125-137.

Castanier, S., Le Mètayer-Levrel, G., Perthuisot, J.-P., 1999. Ca-carbonates precipitation and limestone genesis - the microbiogeologist point of view. Sedimentary Geology 126 (1-4), 9-23.

Chang, T.S., Flemming, B.W., Bartholoma, A., 2007. Distinction between sortable silts and aggregated particles in muddy intertidal sediments of the East Frisian Wadden Sea, southern North Sea. Sedimentary Geology 202, 453–463.

Cheggour, M., Chafik, A., Fisher, N.S., Benbrahim, S., 2005. Metal concentrations in sediments and clams in four Moroccan estuaries. Marine Environmental Research 59, 119-137.

Chen, J.H., Curran, H.A., White, B., Wasserburg, G.J., 1991. Precise chronology of the last interglacial period: ^{234}U-^{230}Th data from fossil coral reefs in the Bahamas. GSA Bulletin 103, 82-97.

Cheng, H., Adkins, J., Edwards, R.L., Boyle, E.A., 2000. U-Th dating of deep-sea corals. Geochimica et Cosmochimica Acta 64 (14), 2401-2416.

Cheng, H., Edwards, R.L., Hoff, J., Gallup, C.D., Richards, D.A., Asmerom, Y., 2000. The half-lives of uranium-234 and thorium-230. Chemical Geology 169, 17-33.

Cnudde, V., Boone, M., Dewanckele, J., Vlassenbroeck, J., Van Hoorebeke, L., Jacobs, P., 2011. High-resolution X-ray CT applied on sandstones. Geosphere 7 (1), 54-61.

Cnudde, V., Masschaele, B., Dierick, M., Vlassenbroeck, J., Van Hoorebeke, L., Jacobs, P., 2006. Recent progress in X-ray CT as a geosciences tool. Applied Geochemistry 21 (5), 826-832.

Cole, J.M., Goldstein, S.L., deMenocal, P.B., Hemming, S.R., Grousset, F.E., 2009. Contrasting compositions of Saharan dust in the eastern Atlantic Ocean during the last deglaciation and African Humid Period. Earth and Planetary Science Letters 278, 257-266.

Colman, J.G., Gordon, D.M., Lane, A.P., Forde, M.J., Fitzpatrick, J.J., 2005. Carbonate mounds off Mauritania, Northwest Africa: status of deep-water corals and implications for management of fishing and oil exploration activities. In: Freiwald, A., Roberst, J.M. (Eds.), Cold-Water Corals and Ecosystems. Springer-Verlag Berlin Heidelberg, pp. 417-441.

Comas, M., Pinheiro, L., 2007. Discovery of carbonate mounds in the Alboran Sea: The Melilla Mound Field, The First MAPG International Convention. MAPG-AAPG, Marrakech, pp. 96-97.

Cordes, E.E., McGinley, M.P., Podowski, E.L., Becker, E.L., Lessard-Pilon, S., Viada, S.T., Fisher, C.R., 2008. Coral communities of the deep Gulf of Mexico. Deep-Sea Research Part I 55, 777-787.

Cunningham, M.J., Hodgson, S., Masson, D.G., Parson, L.M., 2005. An evaluation of along- and down-slope sediment transport processes between Goban Spur and Brenot Spur on the Celtic Margin of the Bay of Biscay. Sedimentary Geology 179, 99-116.

Davies, A.J., Wisshak, M., Orr, J.C., Roberts, J.M., 2008. Predicting suitable habitat for the cold-water coral Lophelia pertusa (Scleractinia). Deep-Sea Research I 55 (8), 1048-1062.

De Haas, H., Mienis, F., Frank, N., Richter, T.O., Steinacher, R., De Stigter, H., van der Land, C., van Weering, T.C.E., 2009. Morphology and sedimentology of (clustered) cold-water coral mounds at the south Rockall Trough margins, NE Atlantic Ocean. Facies 55, 1-26.

De Jong, J.T.M., Boyé, M., Gelado-Caballero, M.D., Timmermans, K.R., Veldhuis, M.J.W., Nolting, R.F., van den Berg, C.M.G., de Baar, H.J.W., 2007. Inputs of iron, manganese and aluminium to surface waters of the Northeast Atlantic Ocean and the European continental shelf. Marine Chemistry 107, 120–142.

De Jonge, C., 2010. A multi-proxy approach to the paleoceanographic variability within the last glacial cycle offshore Morocco. MSc thesis, Ghent University, Gent, 25 pp.

De Mol, B., 2002. Development of coral banks in Porcupine Seabight (SW Ireland): A multidisciplinary approach. PhD thesis, Ghent University, Gent, 363 pp.

De Mol, B., Henriet, J.-P., Canals, M., 2005. Development of coral banks in Porcupine Seabight: do they have Mediterranean ancestors? In: A. Freiwald, A., Roberts, J.M. (Eds.), Cold-Water Corals and Ecosystems. Springer-Verlag Berlin Heidelberg, pp. 515-533.

De Mol, B., Van Rensbergen, P., Pillen, S., Van Herreweghe, K., Van Rooij, D., McDonnell, A., Huvenne, V., Ivanov, M., Swennen, R., Henriet, J.-P., 2002. Large deep-water coral banks in the Porcupine Basin, southwest of Ireland. Marine Geology 188, 193-231.

De Mol, L., Hilàrio, A., Van Rooij, D., Henriet, J.-P., 2011a. Habitat mapping of a cold-water coral mound on Pen Duick Escarpment (Gulf of Cadiz). In: Harris, P., Baker, E. (Eds.), Seafloor Geomorphology as Benthic Habitat: GeoHab Atlas of seafloor geomorphic features and benthic habitats, 645-654.

De Mol, L., Van Rooij, D., Pirlet, H., Greinert, J., Frank, N., Quemmerais, F., Henriet, J.P., 2011b. Cold-water coral habitats in the Penmarc'h and Guilvinec Canyons (Bay of Biscay): Deep-water versus shallow-water settings Marine Geology 282, 40-52.

De Stigter, H., Boer, W., Mendes, P.A.D.J., Jesus, C.C., Thomsen, L., van den Bergh, G.D., van Weering, T.C.E., 2007. Recent sediment transport and deposition in the Nazaré Canyon, Portuguese continental margin. Marine Geology 246, 144-164.

Delongueville, C., Sciallet, R., 1999. Neopycnodonte cochlear (Poli, 1795) dans le Golfe de Gascogne. Arion 24 (2), 62.

Delongueville, C., Sciallet, R., 2009. Neopycnodonte zibrowii dans le golfe de Gascogne. Novapex 10 (1), 9–12.

deMenocal, P., Ortiz, J., Guilderson, T., Adkins, J., Sarnthein, M., Baker, L., Yarusinsky, M., 2000. Abrupt onset and termination of the African Humid Period: rapid climate responses to gradual insolation forcing. Quaternary Science Reviews 19 (1–5), 347-361.

Depreiter, D., 2009. Sources, modes and effects of seabed fluid flow. PhD thesis, Ghent University, 256 pp.

Desrochers, A., Bourque, P.A., Neuweiler, F., 2007. Diagenetic versus biotic accretionary mechanisms of bryozoan-sponge buildups (Lower Silurian, Anticosti Island, Canada). Journal of Sedimentary Research 77 (7-8), 564-571.

Díaz-del-Río, V., Somoza, L., Martínez-Frías, J., Mata, P., Delgado, A., Hernández-Molina, F.J., Lunar, R., Martín-Rubí, J.A., Maestro, A., Fernández-Puga, M.C., León, R., Llave, E., Medialdea, T., Vázquez, T., 2003. Vast fields of hydrocarbon-derived carbonate chimneys related to the accretionary wedge/olistostrome of the Gulf of Cádiz. Marine Geology 195, 177–200.

Dickson, R.R., Gould, W.J., Muller, T.J., Maillard, C., 1985. Estimates of the mean circulation in the deep (> 2000 m) layer of the eastern North Atlantic. Progress in Oceanography 14, 103-127.

Dodge, R.E., Vaisnys, J.R., 1977. Coral populations and growth patterns: responses to sedimentation and turbidity associated with dredging. Journal of Marine Research 35, 715-730.

Dorschel, B., Hebbeln, D., Foubert, A., White, M., Wheeler, A.J., 2007a. Hydrodynamics and cold-water coral facies distribution related to recent sedimentary processes at Galway Mound west of Ireland. Marine Geology 244, 184-195.

Dorschel, B., Hebbeln, D., Rüggeberg, A., Dullo, C., 2007b. Carbonate budget of a cold-water coral carbonate mound: Propeller Mound, Porcupine Seabight. International Journal of Earth Sciences 96, 73-83.

Dorschel, B., Hebbeln, D., Rüggeberg, A., Dullo, C., Freiwald, A., 2005. Growth and erosion of a cold-water coral covered carbonate mound in the Northeast Atlantic during the Late Pleistocene and Holocene. Earth and Planetary Science Letters 233, 33-44.

Dorschel, B., Wheeler, A.J., Huvenne, V.A.I., de Haas, H., 2009. Cold-water coral mounds in an erosive environmental setting: TOBI side-scan sonar data and ROV video footage from the northwest Porcupine Bank, NE Atlantic. Marine Geology 264, 218-229.

Douville, E., Sallé, E., Frank, N., Eisele, M., Pons-Branchu, E., Ayrault, S., 2010. Rapid and accurate U-Th dating of ancient carbonates using inductively coupled plasma-quadrupole mass spectrometry. Chemical Geology 272, 1-11.

Duce, R.A., Liss, P.S., Merill, J.T., Atlas, E.L., Buat-Menard, P., Hicks, B.B., Miller, J.M., Prospero, J.M., Arimoto, R., Church, T.M, Ellis, W., Galloway, J.N., Hansen, L., Jickels, T.D., Knap, A.H., Reinhardt, K.H., Schneider, B., Soudine, A., Tokos, J.J., Tsunogai, S., Wollast, R., Zhou, M., 1991. The atmospheric input of trace species to the world ocean. Global Biogeochemical Cycles 5, 193-259.

Duineveld, G.C.A., Lavaleye, M.S.S., Berghuis, E.M., 2004. Particle flux and food supply to a seamount cold-water coral community (Galicia Bank, NW Spain). Marine Ecology Progress Series 277, 13-23.

Duineveld, G.C.A., Lavaleye, M.S.S., Berman, M.J.N., de Stigter, H., Mienis, F., 2007. Trophic structure of a cold-water coral mound community (Rockall Bank, NE Atlantic) in relation to the near-bottom particle supply and current regime. Bulletin of Marine Science 81, 449-467.

Duineveld, G., Lavaleye, M., Berghuis, E., de Wilde, P., 2001. Activity and composition of the benthic fauna in the Whittard Canyon and the adjacent continental slope (NE Atlantic). Oceanologica Acta 24 (1), 69–83.

Dullo, W.-C., Flögel, S., Rüggeberg, A., 2008. Cold-water coral growth in relation to the hydrography of the Celtic and Nordic European continental margin. Marine Ecology-Progress Series 371, 165-176.

Eisele, M., Frank, N., Wienberg, C., Hebbeln, D., López Correa, M., Douville, E., Freiwald, A., 2011. Productivity controlled cold-water coral growth periods during the last glacial off Mauritania. Marine Geology 280, 143-149.

Eisele, M., Hebbeln, D., Wienberg, C., 2008. Growth history of a cold-water coral covered carbonate mound - Galway Mound, Porcupine Seabight, NE-Atlantic. Marine Geology 253, 160-169.

Etnoyer, P., Morgan, L.E., 2005. Habitat-forming deep-sea corals in the Northeast Pacific Ocean. In: Freiwald, A., Roberts, J.M. (Eds.), Cold-Water Corals and Ecosystems. Springer-Verlag Berlin Heidelberg, pp. 331-343.

Ferdelman, T., Kano, A., Williams, T., Henriet, J.-P., 2006. Modern carbonate mounds: Porcupine Drilling, Integrated Ocean Drilling Program Management International Inc.

Flinch, J., 1993. Tectonic Evolution of the Gibraltar Arc. PhD Thesis, Rice University, Houston, Texas.

Folk, R.L., Ward, W., 1957. Brazos River bar: a study in the significance of grain size parameters. Journal of Sedimentary Petrology 27, 3-26.

Fosså, J.H., Lindberg, B., Christensen, O., Lundalv, T., Svellingen, I., Mortensen, P.B., Alvsvag, J., 2005. Mapping of *Lophelia* reefs in Norway: experiences and survey methods. In: Freiwald, A., Roberts, J.M. (Eds.), Cold-Water Corals and Ecosystems. Springer-Verlag Berlin Heidelberg, pp. 359-391.

Fosså, J.H., Mortensen, P.B., Furevik, D.M., 2000. *Lophelia*-korallrev langs norskekysten forekomst og tilstand. Fisken og Havet 2, 1-94.

Fosså, J.H., Mortensen, P.B., Furevik, D.M., 2002. The deep-water coral *Lophelia pertusa* in Norwegian waters: distribution and fishery impacts. Hydrobiologia 471, 1-12.

Foubert, A., Beck, T., Wheeler, A.J., Opderbecke, J., Grehan, A., Klages, M., Thiede, J., Henriet, J.-P., the Polarstern ARK-XIX/3a shipboard party, 2005. New view of the Belgica Mounds, Porcupine Seabight, NE Atlantic: Preliminary Results from the Polarstern ARK-XIX/3a ROV cruise. In: Freiwald, A., Roberts, J.M. (Eds.), Deep-water Corals and Ecosystems. Springer-Verlag Berlin Heidelberg, pp. 403-415.

Foubert, A., Depreiter, D., Beck, T., Maignien, L., Pannemans, B., Frank, N., Blamart, D., Henriet, J.-P., 2008. Carbonate mounds in a mud volcano province off north-west Morocco: key to processes and controls. Marine Geology 248, 74-96.

Foubert, A., Henriet, J.-P., 2009. Nature and Significance of the Recent Carbonate Mound Record: The Mound Challenger Code. Springer-Verlag, Heidelberg, 350 pp.

Foubert, A., Van Rooij, D., Blamart, D., Henriet, J.-P., 2007. X-ray imagery and physical core logging as a proxy of the content sediment cores in cold-water coral mound provinces: a case study from Porcupine Seabight, SW of Ireland. International Journal of Earth Sciences 96, 141-158.

Frank, N., Freiwald, A., López Correa, M., Wienberg, C., Eisele, M., Hebbeln, D., Van Rooij, D., Henriet, J.-P., Colin, C., van Weering, T., de Haas, H., Buhl-Mortensen, P.B., Roberts, J.M., De Mol, B., Douville, E., Blamart, D., Hatté, C., 2011. Northeastern Atlantic cold-water coral reefs and climate. Geology 39, 743-746.

Frank, N., Lutringer, A., Paterne, M., Blamart, D., Henriet, J.-P., Van Rooij, D., van Weering, T., 2005. Deep-water corals of the northeastern Atlantic margin: carbonate mound evolution and upper intermediate water ventilation during the Holocene. In: Freiwald, A., Roberts, J.M. (Eds.), Cold-water Corals and Ecosystems. Springer-Verlag Berlin Heidelberg, pp. 113–133.

Frank, N., Paterne, M., Ayliffe, L., van Weering, T., Henriet, J.-P., Blamart, D., 2004. Eastern North Atlantic deep-sea corals: tracing upper intermediate water $\Delta^{14}C$ during the Holocene. Earth and Planetary Science Letters 219, 297-309.

Frank, N., Ricard, E., Paque, A., van der Land, C., Colin, C., Blamart, D., Foubert, A., Van Rooij, D., Henriet, J.-P., de Haas, H., van Weering, T., 2009. The Holocene occurence of cold

water corals in the NE Atlantic: implications for coral carbonate mound evolution. Marine Geology 266, 129-142.

Frederiksen, R., Jensen, A., Westerberg, H., 1992. The distribution of the scleractinian coral Lophelia pertusa around the Faeroe islands and the relation to internal tidal mixing. Sarsia 77, 157-171.

Freiwald, A., 2002. Reef-forming cold-water corals. In: Wefer, G., Billett, D., Hebbeln, D., Jørgensen, B.B., Schlüter, M., van Weering, T.C.E. (Eds.), Ocean Margin Systems. Springer-Verlag Berlin Heidelberg, pp. 365-385.

Freiwald, A., Beuck, L., Rueggeberg, A., Taviani, M., Hebbeln, D., 2009. The WHITE CORAL COMMUNITY in the Central Mediterranean Sea Revealed by ROV Surveys. Oceanography 22, 58-74.

Freiwald, A., Fosså, J.H., Grehan, A., Koslow, T., Roberts, J.M., 2004. Cold-water Coral Reefs. UNEP-WCMC, Cambridge, UK.

Freiwald, A., Henrich, R., 1997. Victor Hensen Cruise VH-97 Leg 1 and Leg 5. Unpublished report and station list. Institut für Paläontologie, Universität Erlangen, Erlangen, Germany.

Freiwald, A., Henrich, R., Patzold, J., 1997. Anatomy of a deep-water coral reef mound from Stjernsund, west Finnmark, northern Norway. Cool-Water Carbonates 56, 141-162.

Freiwald, A., Hühnerbach, V., Lindberg, B., Wilson, J.B., Campbell, J., 2002. The Sula Reef Complex, Norwegian shelf. Facies 47, 179-200.

Freiwald, A., Roberts, J.M., 2005. Cold-Water Corals and Ecosystems. Springer-Verlag, Heidelberg.

Freiwald, A., Schonfeld, J., 1996. Substrate pitting and boring pattern of Hyrrokkin sarcophaga (Foraminifera) in a modern deep-water coral reef mound. Marine Micropaleontology 28, 199-207.

Freiwald, A., Wilson, J.B., 1998. Taphonomy of modern deep, cold-temperate water coral reefs. History of Biology 13, 37-52.

Freiwald, A., Wilson, J.B., Henrich, R., 1999. Grounding Pleistocene icebergs shape recent deep-water coral reefs. Sedimentary Geology 125, 1-8.

Frenz, M., Hoppner, R., Stuut, J.-B.W., Wagner, T., Henrich, R., 2003. Surface Sediment Bulk Geochemistry and Grain-Size Composition Related to the Oceanic Circulation along the South American Continental Margin in the Southwest Atlantic. In: Wefer, G., Mulitza, S., Ratmeyer, V. (Eds.), The South Atlantic in the Late Quaternary: Reconstruction of Material Budgets and Current Systems. Springer-Verlag Berlin Heidelberg New York Tokyo, pp. 347-373.

Gasse, F., 2000. Hydrological changes in the African tropics since the Last Glacial Maximum. Quaternary Science Reviews 19 (1-5), 189–211.

Gofas, S., Freiwald, A., López Correa, M., Remia, A., Salas, C., Taviani, M., Wisshak, M., Zibrowius, H., 2007. Oyster beds in the deep sea. In: Jordaens, K., van Houtte, N., van Goethem, J., Backeljau, T. (Eds.), World Congress of Malacology, pp. 80.

González-Pola, C., Lavin, A., Somavilla, R., Vargas-Yanez, M., 2006. Central water masses variability in the southern Bay of Biscay from early 90s. The effect of the severe winter 2005, in: ICES Annual Science Conference, Maastricht, September 2006, C26, pp. 1–12.

Grasmueck, M., Eberli, G.P., Viggiano, D.A., Correa, T., Rathwell, G., Luo, J.G., 2006. Autonomous underwater vehicle (AUV) mapping reveals coral mound distribution, morphology, and oceanography in deep water of the Straits of Florida. Geophysical Research Letters 33.

Hall, I.R., McCave, I.N., 1998. Glacial-interglacial variation in organic carbon burial on the slope of the N.W. European Continental Margin (48°-50°N). Progress in Oceanography 42, 37-60.

Hall-Spencer, J., Rogers, A., Davies, J., Foggo, A., 2007. Deep-sea coral distribution on seamounts, oceanic islands, and continental slopes in the Northeast Atlantic. In: George, R.Y., Cairns, S.D. (Eds.), Conservation and Adaptive Management of Seamount and Deep-Sea Coral Ecosystems, pp. 135-146.

Harry, H.W., 1981. Nominal species of living oysters proposed during the last fifty years. Veliger 24, 39–45.

Hayashida, A., Hattori, S., Oda, H., 2007. Diagenetic modification of magnetic properties observed in a piston core (MD01-2407) from the Oki Ridge, Japan Sea. Palaeogeography Palaeoclimatology Palaeoecology 247, 65-73.

Haynes, R., Barton, 1990. A poleward flow along the Atlantic coast of the Iberian Peninsula. Journal of Geophysical Research 95, 11425–11441.

Henriet, J.-P., De Mol, B., Pillen, S., Vanneste, M., Van Rooij, D., Versteeg, W., Croker, P.F., Shannon, P.M., Unnithan, V., Bouriak, S., Chachkine, P., the Porcupine-Belgica 97 Shipboard Party, 1998. Gas hydrate crystals may help build reefs. Nature 391, 648-649.

Henriet, J.-P., Guidard, S., ODP "Proposal 573" Team, 2002. Carbonate mounds as a possible example for microbial activity in geological processes. In: Wefer, G., Billet, D., Hebbeln, D., Jorgensen, B.B., Schlüter, M., van Weering, T. (Eds.), Ocean margin systems. Springer-Verlag Berlin Heidelberg, pp. 439-455.

Henry, L. A., Roberts, J. M., 2007. Biodiversity and ecological composition of macrobenthos on cold-water coral mounds and adjacent off-mound habitat in the bathyal Porcupine Seabight, NE Atlantic. Deep-sea Research II 54, 654–672.

Hensen, C., Nuzzo, M., Hornibrook, E., Pinheiro, L.M., Bock, B., Magalhaes, V.H., Bruckmann, W., 2007. Sources of mud volcano fluids in the Gulf of Cadiz - indications for hydrothermal imprint. Geochimica Et Cosmochimica Acta 71 (5), 1232-1248.

Hernández-Molina, F.J., Llave, E., Somoza, L., Fernandez-Puga, M.C., Maestro, A., Leon, R., Medialdea, T., Barnolas, A., Garcia, M., de Rio, V.D., Fernandez-Salas, L.M., Vazquez, J.T., Lobo, F., Dias, J.M.A., Rodero, J., Gardner, J., 2003. Looking for clues to paleoceanographic imprints: A diagnosis of the Gulf of Cadiz contourite depositional systems. Geology 31 (1), 19-22.

Hernández-Molina, F.J., Llave, E., Stow, D.A.V., García, M., Somoza, L., Vázquez, J.T., Lobo, F.J., Maestro, A., Díaz del Río, V., León, R., Medialdea, T., Gardner, J., 2006. The contourite depositional system of the Gulf of Cádiz: A sedimentary model related to the bottom current activity of the Mediterranean outflow water and its interaction with the continental margin. Deep-Sea Research II 53, 1420-1463.

Hill, T.M., Kennett, J.P., Spero, H.J., 2003. Foraminifera as indicators of methane-rich environments: A study of modern methane seeps in Santa Barbara Channel, California. Marine Micropaleontology 49, 123-138.

Hillier, S., 1995. Erosion, sedimentation, and sedimentary origin of clays. In: Velde, B. (Ed.). Origin and mineralogy of clays – Clays and the environment. Springer, Berlin, 162-219.

Hily, C., Le Loc'h, F., Grall, J., Glémarec, M., 2008. Soft bottom macrobenthic communities of North Biscay revisited: Long-term evolution under fisheries-climate forcing. Estuarine, Coastal and Shelf Science 78, 413-425.

Hoelzmann, P., Jolly, D., Harrison, S.P., Laarif, F., Bonnefille, R., Pachur, H.-J., 1998. Mid-Holocene land-surface conditions in northern Africa and the Arabian Peninsula: a data set for the analysis of biogeophysical feedbacks in the climate system. Global Biogeochemical Cycles 12, 35–51.

Hoernle, K., Shipboard party, 2001. METEOR Cruise No. M51, Leg 1, VULKOSO - Vulkanismus Ostatlantik-Alboran. GEOMAR, Bremen, 94 pp.

Holligan, P.M., Pingree, R.D., Mardell, G.T., 1985. Oceanic solitions, nutrient pulses and phytoplankton growth. Nature 314, 348-350.

Holz, C., Stuut, J.-B.W., Henrich, R., 2004. Terrigenous sedimentation processes along the continental margin off NW-Africa: implications from grain-size analysis of seabed sediments. Sedimentology 51, 1145-1154.

Holz, C., Stuut, J.-B., Henrich, R., Meggers, H., 2007. Variability in terrigenous sedimentation processes off northwest Africa and its relation to climate changes: Inferences from grain-size distributions of a Holocene marine sediment record. Sedimentary Geology 202, 499-508.

Hounsfield, G.N., 1973. Computerized transverse axial scanning tomography: Part I description of the system. British Journal of Radiology 46, 1016–1022.

Hovland, M., 1990. Do carbonate reefs form due to fluid seepage? Terra Nova 2, 8-18.

Hovland, M., Croker, P.F., Martin, M., 1994. Fault-associated seabed mounds (carbonate knolls?) off western Ireland and north-west Australia. Marine and Petroleum Geology 11, 232-246.

Hovland, M., Mortensen, P., Brattegard, T., Strass, P., Rokoengen, K., 1998. Ahermatypic coral banks off mid-Norway: evidence for a link with seepage of light hydrocarbons. Palaios 13, 189-200.

Hovland, M., Ottesen, D., Thorsnes, T., Fossa, J.H., Bryn, P., 2005. Occurrence and implications of large *Lophelia*-reefs offshore Mid Norway. Onshore-Offshore Relationships on the North Atlantic Margin 12, 265-270.

Hovland, M., Risk, M., 2003. Do Norwegian deep-water coral reefs rely on seeping fluids? Marine Geology 198, 83-96.

Huetten, E., Greinert, J., 2008. Software controlled guidance, recording and post-processing of seafloor observations by ROV and other towed devices: The software package OFOP. Geophysical Research Abstracts 10, EGU2008-A-03088.

Huthnance, J.M., 1995. Circulation, exchange and water masses at the ocean margin: the role of physical processes at the shelf edge. Progress in Oceanography 35, 353-431.

Huvenne, V.A.I., Bailey, W.R., Shannon, P.M., Naeth, J., di Primio, R., Henriet, J.-P., Horsfield, B., de Haas, H., Wheeler, A.J., Olu-Le Roy, K., 2007. The Magellan mound province in the Porcupine Basin. International Journal of Earth Sciences 96, 85-101.

Huvenne, V.A.I., Beyer, A., de Haas, H., Dekindt, K., Henriet, J.P., Kozachenko, M., Olu-Le Roy, K., Wheeler, A., the TOBI/Pelagia 197 and CARACOLE cruise participants, 2005. The seabed appearance of different coral bank provinces in the Porcupine Seabight, NE Atlantic: results from sidescan sonar and ROV seabed mapping. In: Freiwald, A., Roberts, J.M. (Eds.), Cold-water Corals and Ecosystems. Springer-Verlag Berlin Heidelberg, pp. 535-569.

Huvenne, V.A.I., Blondel, P., Henriet, J.-P., 2002. Textural analyses of sidescan sonar imagery from two mound provinces in the Porcupine Seabight. Marine Geology 189, 323-341.

Huvenne, V.A.I., De Mol, B., Henriet, J.-P., 2003. A 3D seismic study of the morphology and spatial distribution of buried coral banks in the Porcupine Basin, SW of Ireland. Marine Geology 198, 5-25.

Huvenne, V.A.I., Masson, D.G., Wheeler, A.J., 2009. Sediment dynamics of a sandy contourite: the sedimentary context of the Darwin cold-water coral mounds, Northern Rockall Trough. International Journal of Earth Sciences 98, 865-884.

IODP 307 Expedition Scientists, 2005. Modern carbonate mounds: Porcupine drilling. IODP Preliminary Report, doi: 10.2204/iodp.pr.307.2005.

Iorga, M.C., Lozier, M.S., 1999. Signatures of the Mediterranean outflow from a North Atlantic climatology 1. Salinity and density fields. Journal of Geophysical Research - Oceans 104 (C11), 25985-26009.

Jansen, J.H.F., Van der Gaast, S.J., Koster, B., Vaars, A.J., 1998. CORTEX, a shipboard XRF-scanner for element analyses in split sediment cores. Marine Geology 151, 143-153.

Jensen, A., Frederiksen, R., 1992. The fauna associated with the bank forming deepwater coral Lophelia pertusa (Scleractinaria) on the Faroe shelf. Sarsia 77, 53-69.

Joint, I., Wollast, R., Chou, L., Batten, S., Elskens, M., Edwards, E., Hirst, A., Burkill, P., Groom, S., Gibb, S., Miller, A., Hydes, D., Dehairs, F., Antia, A., Barlow, R., Rees, A., Pomroy, A., Brockmann, U., Cummings, D., Lampitt, R., Loijens, M., Mantoura, F., Miller, P., Raabe, T., Alvarez-Salgado, X., Stelfox, C., Woolfenden, J., 2001. Pelagic production at the Celtic Sea shelf break. Deep Sea Research Part II: Topical Studies in Oceanography 48 (14-15), 3049–3081.

Jolly, D., Prentice, I.C., Bonnefille, R., Ballouche, A., Bengo, M., Brenac, P., Buchet, G., Burney, D., Cazet, J.-P., Cheddadi, R., Edorh, T., Elenga, H., Elmoutaki, S., Guiot, J., Laarif, F.,

Lamb, H., Lezine, A.-M., Maley, J., Mbenza, M., Peyron, O., Reille, M., Reynaud-Farrera, I., Riollet, G., Ritchie, J.C., Roche, E., Scott, L., Ssemmanda, I., Straka, H., Umer, M., Van Campo, E., Vilimumbalo, S., Vincens, A., Waller, M., 1998. Biome reconstruction from pollen and plant macrofossil data for Africa and the Arabian peninsula at 0 and 6000 years. Journal of Biogeography 25, 1007–1027.

Joubin, M.L., 1922. Les coraux de mer profonde nuisibles aux chalutiers. Note et Mémoires N° 18, Office Scientifique et Technique des Pêches Maritimes, Paris.

Kano, A., Ferdelman, T.G., Williams, T., 2010. The Pleistocene cooling built Challenger Mound, a deep-water coral mound in the NE Atlantic: synthesis from IODP Expedition 307. Sedimentary Record 8, 4-9.

Kano, A., Ferdelman, T.G., Williams, T., Henriet, J.-P., Ishikawa, T., Kawagoe, N., Takashima, C., Kakizaki, Y., Abe, K., Sakai, S., Browning, E.L., Li, X., the IODP Expediation 307 scientific party, 2007. Age constraints on the origin and growth history of a deep-water coral mound in NE Atlantic drilling during Integrated Ocean Drilling Program Expedition 307. Geology 35, 1051-1054.

Karlin, R., Levi, S., 1983. Diagenesis of magnetic minerals in recent hemipelagic sediments. Nature 303, 327-330.

Kennett, J.P., Cannariato, K.G., Hendy, I.L., Behl, R.J., 2000. Carbon isotopic evidence for methane hydrate instability during Quaternary interstadials. Science 288, 128-133.

Kenyon, N.H., Akhmetzhanov, A.M., Wheeler, A.J., van Weering, T.C.E., de Haas, H., Ivanov, M.K., 2003. Giant carbonate mud mounds in the southern Rockall Trough. Marine Geology 195, 5-30.

Kiriakoulakis, K., Bett, B.J., White, M., Wolff, G.A., 2004. Organic biogeochemistry of the Darwin Mounds, a deep-water coral ecosystem, of the NE Atlantic. Deep-Sea Research I 51, 1937-1954.

Kiriakoulakis, K., Freiwald, A., Fisher, E., Wolff, G.A., 2007. Organic matter quality and supply to deep-water coral/mound systems of the NW European Continental Margin. International Journal of Earth Science 96, 159-170.

Kissel, C., Kleiven, H., Morin, X., the Shipboard Scientific Party, 2008. MD168-AMOCINT/XVII IMAGES cruise report. Les rapports de campagne à la mer, IPEV, Brest, OCE/2008/02.

Knippertz, P., Christoph, M., Speth, P., 2003. Long-term precipitation variability in Morocco and the link to the large-scale circulation in recent and future climates. Meteorology and Atmospheric Physics 83, 67-88.

Lallemand, S., Sibuet, J.C., 1986. Tectonic Implications of Canyon Directions over the Northeast Atlantic Continental-Margin. Tectonics 5 (7), 1125-1143.

Larmagnat, S., Neuweiler, F., 2011. Exploring a link between Atlantic coral mounds and Phanerozoic carbonate mudmounds: Insights from pore water fluorescent dissolved organic matter (FDOM), Pen Duick mounds, offshore Morocco. Marine Geology 282, 149-159.

Laubier, L., Monniot, C., 1985. Peuplements profonds du Golfe de Gascogne campagnes BIOGAS. IFREMER, Brest, France, 629 pp.

Le Danois, E., 1948. Les profondeurs de la mer. Trente ans de recherche sur la faune sous-marine au large des côtes de France. Payot, Paris, 303 pp.

Le Guilloux, E., Olu, K., Bourillet, J.F., Savoye, B., Iglesias, S.P., Sibuet, M., 2009. First observations of deep-sea coral reefs along the Angola margin. Deep-Sea Research Part I 56, 2394-2403.

Le Suavé, R., Bourillet, J.F., Coutelle, A., 2000. La marge nord du golfe de Gascogne. Connaissances générales du rapport des nouvelles synthèses de données multifaisceaux. IFREMER, Paris.

León, R., Somoza, L., Medialdea, T., González, F.J., Díaz-del-Río, V., Fernández-Puga, M.C., Maestro, A., Mata, M.P., 2007. Sea-floor features related to hydrocarbon seeps in deepwater carbonate-mud mounds of the Gulf of Cádiz: from mud flows to carbonate precipitates. Geo-Marine Letters 27, 237-247.

León, R., Somoza, L., Medialdea, T., Maestro, A., Díaz-del-Río, V., Fernández-Puga, M.C., 2006. Classification of sea-floor features associated with methane seeps along the Gulf of Cádiz continental margin. Deep-Sea Research II 53, 1464-1481.

Lindberg, B., Berndt, C., Mienert, J., 2007. The Fugløy Reef at 70°N: acoustic signature, geologic, geomorphologic and oceanographic setting. International Journal of Earth Sciences 96, 201-213.

Lindberg, B., Mienert, J., 2005. Post-glacial carbonate production by cold-water corals on the Norwegian Shelf and their role in the global carbonate budget. Geology 33, 537-540.

Lisiecki, L.E., Raymo, M.E., 2005. A Pliocene-Pleistocene stack of 57 globally distributed benthic delta O-18 records. Paleoceanography 20 (2).

Llave, E., Schönfeld, J., Hernández-Molina, F.J., Mulder, T., Somoza, L., Díaz del Río, V., Sánchez-Almazo, I., 2006. High-resolution stratigraphy of the Mediterranean outflow contourite system in the Gulf of Cadiz during the late Pleistocene: The impact of Heinrich events. Marine Geology 227, 241-262.

Luff, R., Wallmann, K., 2003. Fluid flow, methane fluxes, carbonate precipitation and biogeochemical turnover in gas hydrate-bearing sediments at Hydrate Ridge, Cascadia Margin: numerical modeling and mass balances. Geochimica Et Cosmochimica Acta 67 (18), 3403-3421.

Luff, R., Wallmann, K., Aloisi, G., 2004. Numerical modeling of carbonate crust formation at cold vent sites: significance for fluid and methane budgets and chemosynthetic biological communities. Earth and Planetary Science Letters 221 (1-4), 337-353.

Machin, F., Pelegri, J.L., Marrero-Diaz, A., Laiz, I., Ratsimandresy, A.W., 2006. Near-surface circulation in the southern Gulf of Cadiz. Deep-Sea Research Part II - Topical Studies in Oceanography 53 (11-13), 1161-1181.

Magalhães, V.H., Pinheiro, L.M., Ivanov, M.K., Kozlova, E., Blinova, V., Kolganova, J., Vasconcelos, C., McKenzie, J.A., Bernasconi, S.M., Kopf, A.J., Díaz-del-Río, V., González, F.J., Somoza, L., 2012. Formation processes of methane-derived authigenic carbonates from the Gulf of Cadiz. Sedimentary Geology 243-244, 155-168.

Maignien, L., Depreiter, D., Foubert, A., Reveillaud, J., De Mol, L., Boeckx, P., Blamart, D., Henriet, J.-P., Boon, N., 2011. Anaerobic oxidation of methane in a cold-water coral carbonate mound from the Gulf of Cadiz. International Journal of Earth Sciences 100, 1413-1422.

Maldonado, A., Somoza, L., Pallares, L., 1999. The Betic orogen and the Iberian-African boundary in the Gulf of Cadiz: geological evolution (central North Atlantic). Marine Geology 155 (1-2), 9-43.

Marches, E., Mulder, T., Cremer, M., Bonnel, C., Hanquiez, V., Gonthier, E., Lecroart, P., 2007. Contourite drift construction influenced by capture of Mediterranean Outflow Water deep-sea current by the Portimao submarine canyon (Gulf of Cadiz, South Portugal). Marine Geology 242 (4), 247-260.

Marticorena, B., Bergametti, G., 1996. Two-year simulations of seasonal and interannual changes of the Saharan dust emission. Geophysical Research Letters 23, 1921-1924.

Masschaele, B.C., Cnudde, V., Dierick, M., Jacobs, P., Van Hoorebeke, L., Vlassenbroeck, J., 2007. UGCT: New X-ray radiography and tomography facility. Nuclear Instruments and Methods in Physics Research A – Accelerators Spectrometers Detectors and Associated Equipment 580, 266-269.

Masson, D.G., Bett, B.J., Billet, D.S.M., Jacobs, C.L., Wheeler, A.J., Wynn, R.B., 2003. The origin of deep-water, coral-topped mounds in the northern Rockall Trough, Northeast Atlantic. Marine Geology 194, 159-180.

Matsumoto, A.K., 2005. Recent observations on the distribution of deep-sea coral communities on the Shiribeshi Seamount, Sea of Japan. In: Freiwald, A., Roberst, J.M. (Eds.), Cold-Water Corals and Ecosystems. Springer-Verlag Berlin Heidelberg, pp. 345-356.

McCartney, M.S., 1992. Recirculating components to the deep boundary current of the northern North Atlantic. Progress in Oceanography 29, 283-383.

McCartney, M.S., Talley, L.D., 1982. The sub-polar mode water of the north-atlantic ocean. Journal of Physical Oceanography 12, 1169-1188.

McCave, I.N., Hall, I.R., 2006. Size sorting in marine muds: Processes, pitfalls, and prospects for paleoflow-speed proxies. Geochemistry, Geophysics, Geosystems 7 (10), Q10N05, doi:10.1029/2006GC001284.

McCave, I.N., Hall, I.R., Antia, A.N., Chou, L., Dehairs, F., Lampitt, R.S., Thomsen, L., van Weering, T.C.E., Wollast, R., 2001. Distribution, composition and flux of particulate material over the European margin at 47°-50°N. Deep-Sea Research II 48, 3107-3139.

McCave, I.N., Hall, I.R., Bianchi, G.G., 2006. Laser vs. settling velocity differences in silt grainsize measurements: estimation of palaeocurrent vigour. Sedimentology 53, 919-928.

Medialdea, T., Somoza, L., Pinheiro, L.M., Fernández-Puga, M.C., Vázquez, J.T., León, R., Ivanov, M.K., Magalhaes, V.H., Díaz-del-Río, V., Vegas, R., 2009. Tectonics and mud volcano development in the Gulf of Cádiz. Marine Geology 261, 48-63.

Medialdea, T., Vegas, R., Somoza, L., Vázquez, J.T., Maldonado, A., Díaz-del-Río, V., Maestro, A., Córdoba, D., Fernández-Puga, M.C., 2004. Structure and evolution of the "Olistostrome" complex of the Gibraltar Arc in the Gulf of Cádiz (eastern Central Atlantic): evidence from two long seismic cross-sections. Marine Geology 209, 173-198.

Mienis, F., De Stigter, H.C., De Haas, H., Van der Land, C., van Weering, T.C.E., 2012. Hydrodynamic conditions in a cold-water coral mound area on the Renard Ridge, southern Gulf of Cadiz. Journal of Marine Systems 96-97, 61-71.

Mienis, F., de Stigter, H.C., White, M., Duineveld, G., de Haas, H., van Weering, T.C.E., 2007. Hydrodynamic controls on cold-water coral growth and carbonate-mound development at the SW and SE Rockall Trough Margin, NE Atlantic Ocean. Deep-Sea Research Part I 54, 1655-1674.

Mienis, F., van der Land, C., de Stigter, H.C., van de Vorstenbosch, M., de Haas, H., Richter, T., van Weering, T.C.E., 2009. Sediment accumulation on a cold-water carbonate mound at the Southwest Rockall Trough margin. Marine Geology 265, 40-50.

Mienis, F., van Weering, T., de Haas, H., de Stigter, H., Huvenne, V., Wheeler, A., 2006. Carbonate mound development at the SW Rockall Trhough margin based on high resolution TOBI and seismic recording. Marine Geology 233, 1-19.

Moreno, A., Targarona, J., Henderiks, J., Canals, M., Freudenthal, T., Meggers, H., 2001. Orbital forcing of dust supply to the North Canary Basin over the last 250 kyr. Quaternary Science Reviews 20, 1327–1339.

Mortensen, P., Buhl-Mortensen, L., 2005. Deep-water corals and their habitats in The Gully, a submarine canyon off Atlantic Canada. In: Freiwald, A., Roberts, J.M. (Eds.), Cold-Water Corals and Ecosystems. Springer-Verlag Berlin Heidelberg, pp. 247-277.

Mortensen, P.B., Hovland, M., Brattegard, T., Farestveit, R., 1995. Deep-Water Bioherms of the Scleractinian Coral Lophelia-Pertusa (L) at 64-Degrees-N on the Norwegian Shelf - Structure and Associated Megafauna. Sarsia 80 (2), 145-158.

Mortensen, P.B., Hovland, M.T., Fossa, J.H., Furevik, D.M., 2001. Distribution, abundance and size of *Lophelia pertusa* coral reefs in mid-Norway in relation to seabed characteristics. Journal of the Marine Biological Association of the United Kingdom 81, 581-597.

Neulinger, S.C., Gartner, A., Jarnegren, J., Ludvigsen, M., Lochte, K., Dullo, W.C., 2009. Tissue-Associated "Candidatus Mycoplasma corallicola" and Filamentous Bacteria on the Cold-Water Coral Lophelia pertusa (Scleractinia). Applied and Environmental Microbiology 75 (5), 1437-1444.

Neuweiler, F., Daoust, I., Bourque, P.A., Burdige, D.J., 2007. Degradative calcification of a modern siliceous sponge from the Great Bahama Bank, the Bahamas: A guide for interpretation of ancient sponge-bearing limestones. Journal of Sedimentary Research 77 (7-8), 552-563.

Neuweiler, F., Gautret, P., Thiel, V., Lange, R., Michaelis, W., Reitner, J., 1999. Petrology of Lower Cretaceous carbonate mud mounds (Albian, N-Spain): insights into organomineralic deposits of the geological record. Sedimentology 46, 837-859.

Neuweiler, F., Turner, E.C., Burdige, D.J., 2009. Early Neoproterozoic origin of the metazoan clade recorded in carbonate rock texture. Geology 37, 475-478.

Nicholson, S.E., 2000. The nature of rainfall variability over Africa on time scales of decades to millennia. Global and Planetary Change 26 (1-3), 137-158.

Noé, S., Titschack, J., Freiwald, A., Dullo, W.-C., 2006. From sediment to rock: diagenetic processes of hardground formation in deep-water carbonate mounds of the NE Atlantic. Facies 52, 183-208.

Normand, A., Mazé, J.-P., 2000. Cartes bathymétriques au 1/250 000ème: Marge celtique Est, Marge armoricaine Nord, Sud Trevelyan, Dôme Gascogne, Marge armoricaine sud, Marge Aquitaine, in: Le Suavé, R. (Ed.). Synthèse bathymétrique et imagerie acoustique, Zone Economique Exclusive Atlantique Nord-Est, Editions IFREMER.

O'Reilly, B.M., Readman, P.W., Shannon, P.M., Jacob, A.W.B., 2003. A model for the development of a carbonate mound population in the Rockall Trough based on deep-towed sidescan sonar data. Marine Geology 198, 55-66.

Øvrebø, L.K., Haughton, P.D.W., Shannon, P.M., 2006. A record of fluctuating bottom currents on the slopes west of the Porcupine Bank, offshore Ireland – implications for Late Quaternary climate forcing. Marine Geology 225 (1-4), 279-309.

Paillet, J., Mercier, H., 1997. An inverse model of the eastern North Atlantic general circulation and thermocline ventilation. Deep-Sea Research I 44 (8), 1293-1328.

Pairaud, I.L., Lyard, F., Auclair, F., Letellier, T., Marsaleix, P., 2008. Dynamics of the semi-diurnal and quarter-diurnal internal tides in the Bay of Biscay. Part 1: Barotropic tides. Continental Shelf Research 28 (10–11), 1294-1315.

Palanques, A., Puig, P., Latasa, M., Scharek, R., 2009. Deep sediment transport induced by storms and dense shelf-water cascading in the northwestern Mediterranean basin. Deep-Sea Research I 56 (3), 425–434.

Paquet, F., Menier, D., Estourn_es, G., Bourillet, J.-F., Leroy, P., Guillocheau, F., 2010. Buried fluvial incisions as a record of Middle–Late Miocene eustasy fall on the Armorican Shelf (Bay of Biscay, France). Marine Geology 268 (1-4), 137-151.

Paull, C.K., Neumann, A.C., Ende, B.A.A., Ussler, W., Rodriguez, N.M., 2000. Lithoherms on the Florida-Hatteras slope. Marine Geology 166, 83-101.

Pingree, R.D., 1973. Component of Labrador Sea-Water in Bay-of-Biscay. Limnology and Oceanography 18 (5), 711-718.

Pingree, R.D., Griffiths, D.K., 1982. Tidal Friction and the Diurnal Tides on the Northwest European Shelf. Journal of the Marine Biological Association of the United Kingdom 62 (3), 577-593.

Pingree, R.D., Le Cann, B., 1989. Celtic and Armorican slope and shelf residual currents. Progress in Oceanography 23, 303-338.

Pingree, R.D., Le Cann, B., 1990. Structure, strength and seasonality of the slope currents in the Bay of Biscay region. Journal of the Marine Biological Association of the United Kingdom 70, 857-885.

Pinheiro, L.M., Ivanov, M.K., Sautkin, A., Akhmanov, G., Magalhaes, V.H., Volkonskaya, A., Monteiro, J.H., Somoza, L., Gardner, J., Hamouni, N., Cunha, M.R., 2003. Mud volcanism in the Gulf of Cadiz: results from the TTR-10 cruise. Marine Geology 195 (1-4), 131-151.

Pingree, R.D., Mardell, G.T., Holligan, P.M., Griffiths, D.K., Smithers, J., 1982. Celtic Sea and Armorican current structure and the vertical distributions of temperature and chlorophyll. Continental Shelf Research 1 (1), 99–116.

Pirlet, H., 2010. The matrix of cold-water coral mounds: origin and early-diagenetic interactions. PhD thesis, Ghent University, 180 pp.

Pirlet, H., Colin, C., Thierens, M., Latruwe, K., Van Rooij, D., Foubert, A., Frank, N., Blamart, D., Huvenne, V.A.I., Swennen, R., Vanhaecke, F., Henriet, J.-P., 2011. The importance of the terrigenous fraction within a cold-water coral mound: A case study. Marine Geology 282, 13-25.

Pirlet, H., Wehrmann, L.M., Brunner, B., Frank, N., Dewanckele, J., Van Rooij, D., Foubert, A., Swennen, R., Naudts, L., Boone, M., Cnudde, V., Henriet, J.P., 2010. Diagenetic formation of gypsum and dolomite in a cold-water coral mound in the Porcupine Seabight, off Ireland. Sedimentology 57 (3), 786-805.

Pirlet, H., Wehrmann, L.M., Foubert, A., Brunner, B., Blamart, D., De Mol, L., Van Rooij, D., Dewanckele, J., Cnudde, V., Swennen, R., Duyck, P., Henriet, J.-P., 2012. Unique authigenic mineral assemblages reveal different diagenetic histories in two neighbouring cold-water coral mounds on Pen Duick Escarpment, Gulf of Cadiz. Sedimentology 59, 578-604.

Pollard, S., Griffiths, C.R., Cunningham, S.A., Read, J.F., Perez, F.F., Ríos, A.F., 1996. Vivaldi 1991 - a study of the formation, circulation and ventilation of Eastern North Atlantic Central Water. Progress in Oceanography 37, 167–192.

Prins, M.A., Bouwer, L.M., Beets, C.J., Troelstra, S.R., Weltje, G.J., Kruk, R.W., Kuijpers, A., Vroon, P.Z., 2002. Ocean circulation and iceberg discharge in the glacial North Atlantic: Inferences from unmixing of sediment size distributions. Geology 30, 555-558.

Prins, M.A., Postma, G., Cleveringa, J., Cramp, A., Kenyon, N.H., 2000. Controls on terrigenous sediment supply to the Arabian Sea during the late Quaternary: the Indus Fan. Marine Geology 169, 327-349.

Prins, M.A., Weltje, G.J., 1999. End-member modelling of siliciclastic grain-size distributions: the late Quaternary record of eolian and fluvial sediment supply to the Arabian Sea and its paleoclimate significance. In: Harbaugh, J. (Ed.), Numerical Experiments in Stratigraphy: Recent Advances in Stratigraphic and Sedimentologic Computer Simulations. SEPM (Society for Sedimentary Geology) Special Publication, pp. 91-111.

Radon, J., 1917. Über die Bestimmung von Funktionen durch ihre Integralwerte längs gewisser Mannigfaltigkeiten. *Berichte über die Verhandlungen der Sächsische Akademie der Wissenschaften* 69, 262–277. Translation: Radon, J., Parks, P.C., 1986. On the determination of functions from their integral values along certain manifolds. IEEE Transactions on Medical Imaging 5 (4), 170–176.

Raes, M., Vanreusel, A., 2005. The metazoan meiofauna associated with a cold-water coral degradation zone in the Porcupine Seabight (NE Atlantic). In: Freiwald, A., Roberts, J.M. (Eds.), Cold-Water Corals and Ecosystems. Springer-Verlag Berlin Heidelberg, pp. 821-847.

Raes, M., Vanreusel, A., 2006. Microhabitat type determines the composition of nematode communities associated with sediment-clogged cold-water coral framework in the Porcupine Seabight (NE Atlantic). Deep-Sea Research I 53, 1880-1894.

Ratmeyer, V., Balzer, W., Bergametti, G., Chiapello, I., Fischer, G., Wyputta, U., 1999. Seasonal impact of mineral dust on deep-ocean particle flux in the eastern subtropical Atlantic Ocean. Marine Geology 159, 241-252.

Ravelo, A.C., Hillaire-Marcel, C., 2007. The use of oxigen and carbon isotopes of foraminifera in paleoceanography. In: Hillaire-Marcel, C., De Vernal, A. (Eds.), Proxies in Late Cenozoic Paleoceanography. Developments in Marine Geology, Elsevier, 862 pp.

Reveillaud, J., Freiwald, A., Van Rooij, D., Le Guilloux, E., Altuna, A., Foubert, A., Vanreusel, A., Roy, K.O.L., Henriet, J.P., 2008. The distribution of scleractinian corals in the Bay of Biscay, NE Atlantic. Facies 54, 317-331.

Richter, T.O., van der Gaast, S., Koster, B., Vaars, A., Gieles, R., de Stigter, H.C., de Haas, H., van Weering, T.C.E., 2006. The Avaatech XRF Core Scanner: technical description and applications to NE Atlantic sediments. In: Rothwell, R.G. (Ed.), New Techniques in Sediment Core Analysis. The Geological Society, Special Publication 267, London.

Ritchie, J.C., Eyles, C.H., Haynes, C.V., 1985. Sediment and pollen evidence for an early to mid-Holocene humid period in the eastern Sahara. Nature 330, 645–647.

Roberts, J.M., Brown, C.J., Long, D., Bates, C.R., 2005. Acoustic mapping using a multibeam echosounder reveals cold-water coral reefs and surrounding habitats. Coral Reefs 24, 654-669.

Roberts, J.M., Henry, L.A., Long, D., Hartley, J.P., 2008. Cold-water coral reef frameworks, megafaunal communities and evidence for coral carbonate mounds on the Hatton Bank, north east Atlantic. Facies 54, 297-316.

Roberts, J.M., Wheeler, A.J., Freiwald, A., 2006. Reefs of the deep: the biology and geology of cold-water ecosystems. Science 312, 543-547.

Roberts, J.M., Wheeler, A.J., Freiwald, A., Cairns, S.D., 2009. Cold-Water Corals: The Biology and Geology of Deep-Sea Coral Habitats. Cambridge University Press, New York, 352 pp.

Robinson, S.G., 1986. The late Pleistocene palaeoclimatic record of North Atlantic deep-sea sediments revealed by mineral magnetic measurements. Physical Earth and Planetary International 42, 22– 57.

Rogers, C.S., 1990. Responses of Coral Reefs and Reef Organisms to Sedimentation. Marine Ecology-Progress Series 62 (1-2), 185-202.

Rogers, A.D., 1999. The biology of *Lophelia pertusa* (LINNAEUS 1758) and other deep-water reef-forming corals and impacts from human activities. International Reviews of Hydrobiology 84 (4), 315-406.

Rogerson, M., Rohling, E.J., Weaver, P.P.E., Murray, J.W. 2004. The Azores Front since the Last Glacial Maximum. Earth and Planetary Science Letters 222, 779-789.

Rogerson, M., Weaver, P.P.E., Rohling, E.J., Lourens, L.J., Murray, J.W., Hayes, A., 2006. Colour logging as a tool in high-resolution palaeoceanography. The Geological Society Special Publications 267, 99-112.

Rüggeberg, A., Dorschel, B., Dullo, W.C., Hebbeln, D., 2005. Sedimentary patterns in the vicinity of a carbonate mound in the Hovland Mound Province, northern Porcupine Seabight. In: Freiwald, A., Roberts, J.M. (Eds.), Cold-Water Corals and Ecosystems. Springer-Verlag Berlin Heidelberg, pp. 87-112.

Rüggeberg, A., Dullo, C., Dorschel, B., Hebbeln, D., 2007. Environmental changes and growth history of a cold-water carbonate mound (Propeller Mound, Porcupine Seabight). International Journal of Earth Sciences 96, 57-72.

Sabatier, P., Reyss, J.-L., Hall-Spencer, J.M., Colin, C., Frank, N., Tisnérat-Laborde, N., Bordier, L., Douville, E., 2012. ^{210}Pb-^{226}Ra chronology reveals rapid growth rate of *Madrepora oculata* and *Lophelia pertusa* on world's largest cold-water coral reef. Biogeosciences 9 (3), 1253-1265.

Sanders, D., 2003. Syndepositional dissolution of calcium carbonate in neritic carbonate environments: geological recognition, processes, potential significance. Journal of African Earth Sciences 36, 99-134.

Sarnthein, M., 1978. Sand deserts during glacial maximum and climatic optimum. Nature 272, 43-46.

Sarnthein, M., Tetzlaff, G., Koopmann, B., Wolter, K., Pflaumann, 1981. Glacial and interglacial wind regimes over the eastern subtropical Atlantic and north-west Africa. Nature 293, 193-196.

Scholz, D., Mangini, A., Felis, T., 2004. U-series dating of diagenetically altered fossil reef corals. Earth and Planetary Science Letters 218, 163-178.

Schröder-Ritzrau, A., Freiwald, A., Mangini, A., 2005. U/Th dating of deep-water corals from the eastern North Atlantic and the western Mediterranean Sea. In: Freiwald, A., Roberts, J.M. (Eds.), Cold-water Corals and Ecosystems. Springer-Verlag Berlin Heidelberg, pp. 157-172.

Schroeder, W.W., 2002. Observations of *Lophelia pertusa* and the surficial geology at a deep-water site in the northeastern Gulf of Mexico. Hydrobiologia 471, 29-33.

Schütz, L., Jaenicke, R., Pietrek, H., 1981. Saharan dust transport over the North Atlantic Ocean. Special Paper Geological Society America 186, 87-100.

Sibuet, J.-C., Monti, S., Loubrieu, B., Mazé, J.-P., Srivastasa, S., 2004. Carte bathymétrique de l'Atlantique nord-est et du golf de Gascogne: implications cinématiques. Bulletin de la Société Géologique de France 175 (5), 429-442.

Smith, J.E., Risk, M.J., Schwarcz, H.P., McConnaughey, T.A., 1997. Rapid climate change in the North Atlantic during the Younger Dryas recorded by deep-sea corals. Nature 386, 818–820.

Soetaert, K., Hofmann, A.F., Middelburg, J.J., Meysman, F.J.R., Greenwood, J., 2007. The effect of biogeochemical processes on pH. Marine Chemistry 105, 30-51.

Somoza, L., Díaz-del-Río, V., León, R., Ivanov, M., Fernández-Puga, M.C., Gardner, J.M., Hernández-Molina, F.J., Pinheiro, L.M., Rodero, J., Lobato, A., Maestro, A., Vázquez, J.T., Medialdea, T., Fernández-Salas, L.M., 2003. Seabed morphology and hydrocarbon seepage in the Gulf of Cádiz mud volcano area: Acoustic imageray, multibeam and ultra-high resolution seismic data. Marine Geology 195, 153-176.

Stadnitskaia, A., Ivanov, M.K., Blinova, V., Kreulen, R., van Weering, T.C.E., 2006. Molecular and carbon isotopic variability of hydrocarbon gases from mud volcanoes in the Gulf of Cadiz, NE Atlantic. Marine and Petroleum Geology 23 (3), 281-296.

Stow, D.A.V., Hernandez-Molina, F.J., Llave, E., Sayago-Gil, M., del Rio, V.D., Branson, A., 2009. Bedform-velocity matrix: The estimation of bottom current velocity from bedform observations. Geology 37 (4), 327-330.

Strømgren, T., 1971. Vertical and horizontal distribution of Lophelia pertusa (Linné) in Trondheimsfjorden on the west coast of Norway. Det Kongelige Norske Videnskabers Selskabs Skrifter 6, 1-9.

Stuut, J.-B.W., Kasten, S., Lamy, F., Hebbeln, D., 2007. Sources and modes of terrigenous sediment input to the Chilean continental slope. Quaternary International 161, 67-76.

Stuut, J.-B.W., Prins, M.A., Schneider, R.R., Weltje, G.J., Jansen, J.H.F., Postma, G., 2002. A 300-kyr record of aridity and wind strength in southwestern Africa: inferences from grain-size distributions of sediments on Walvis Ridge, SE Atlantic. Marine Geology 180, 221-233.

Stuut, J.-B., Zabel, M., Ratmeyer, V., Helmke, P., Shefuß, E., Lavik, G., Schneider, R., 2005. Provenance of present-day eolian dust collected off NW Africa. Journal of Geophysical Research 110, D04202.

Sumida, P.Y.G., Yoshinaga, M.Y., Madureira, L.A.S.P., Hovland, M., 2004. Seabed pockmarks associated with deepwater corals off SE Brazilian continental slope, Santos Basin. Marine Geology 207, 159-167.

Swap, R., Ulanski, S., Cobbett, M., Garstrang, M., 1996. Temporal and spatial characteristics of Saharan dust outbreaks. Journal of Geophysical Research 101, 4205-4220.

Taviani, M., Angeletti, L., Dimech, M., Mifsud, C., Freiwald, A., Harasewych, M.G., Oliverio, M., 2009. Coralliophilinae (Gastropoda: Muricidae) associated with deep-water coral banks in the Mediterranean. Nautilus 123, 106-112.

Taviani, M., Freiwald, A., Zibrowius, H., 2005a. Deep coral growth in the Mediterranean Sea: an overview. In: Freiwald, A., Roberts, J.M. (Eds.), Cold-Water Corals and Ecosystems. Springer Berlin Heidelberg, pp. 137-156.

Taviani, M., Remia, A., Corselli, C., Freiwald, A., Malinverno, E., Mastrototaro, F., Savini, A., Tursi, A., 2005b. First geo-marine survey of living cold-water *Lophelia* reefs in the Ionian Sea (Mediterranean basin). Facies 50 (3-4), 409-417.

Templer, S.P., Wehrmann, L.M., Zhang, Y., Vasconcelos, C., McKenzie, J.A., 2011. Microbial community composition and biogeochemical processes in cold-water coral carbonate mounds in the Gulf of Cadiz, on the Moroccan margin. Marine Geology 282, 138-148.

Thierens, M., Browning, E., Pirlet, H., Loutre, M.-F., Dorschel, B., Huvenne, V.A.I., Titschack, J., Colin, C., Foubert, A., Wheeler, A.J., submitted. Cold-water coral carbonate mounds as unique palaeo-archives: the Plio-Pleistocene Challenger Mound record (NE Atlantic continental margin). Quaternary Science Reviews.

Thierens, M., Pirlet, H., Colin, C., Latruwe, K., Vanhaecke, F., Lee, J.R., Stuut, J.-B., Titschack, J., Huvenne, V.A.I., Dorschel, B., Wheeler, A.J., Henriet, J.-P., 2012. Ice-rafting from the British-Irish ice sheet since the earliest Pleistocene (2.6 million years ago): implications for long-term mid-latitudinal ice-sheet growth in the North Atlantic region. Quaternary Science Reviews 44, 229-240.

Thierens, M., Titschack, J., Dorschel, B., Huvenne, V.A.I., Wheeler, A.J., Stuut, J.-B., O'Donnell, R., 2010. The 2.6 Ma depositional sequence from the Challenger cold-water coral carbonate mound (IODP Exp. 307): Sediment contributors and hydrodynamic palaeo-environments. Marine Geology 271, 260-277.

Toucanne, S., Zaragosi, S., Bourillet, J.F., Cremer, M., Eynaud, F., Van Vliet-Lanoë, B., Penaud, A., Fontanier, C., Turon, J.L., Cortijo, E., Gibbard, P.L., 2009. Timing of massive 'Fleuve Manche' discharges over the last 350 kyr: insights into the European ice-sheet oscillations and the European drainage network from MIS 10 to 2. Quaternary Science Reviews 28 (13-14), 1238-1256.

Tribble, G.W., 1993. Organic matter oxidation and aragonite diagenesis in a coral reef. Journal of Sedimentary Research 63 (3), 523-527.

Trichet, J., Défarge, C., 1995. Non-biologically supported organomineralization. Bulletin de l'Institut océanographique Monaco 14, 203-236.

Tucker, M.E., Wright, V.P., 1990. Carbonate sedimentology. Blackwell, Oxford.

Tyler, P., Amaro, T., Arzola, R., Cunha, M.R., de Stigter, H., Gooday, A., Huvenne, V., Ingels, J., Kiriakoulakis, K., Lastras, G., Masson, D., Oliveira, A., Pattenden, A., Vanreusel, A., van Weering, T., Vitorino, J., Witte, U., Wolff, G., 2009. Europe's Grand Canyon Nazaré Submarine Canyon. Oceanography 22 (1), 46-57.

Van Aken, H.M., 2000. The hydrography of the mid-latitude Northeast Atlantic Ocean II: the intermediate water masses. Deep-Sea Research I 47, 789–824.

Van der Land, C., Mienis, F., de Haas, H., Frank, N., Swennen, R., van Weering, T.C.E., 2010. Diagenetic processes in carbonate mound sediments at the south-west Rockall Trough margin. Sedimentology 57, 912-931.

Van Rensbergen, P., Depreiter, D., Pannemans, B., Moerkerke, G., Van Rooij, D., Marsset, B., Akhmanov, G., Blinova, V., Ivanov, M., Rachidi, M., Magalhaes, V., Pinheiro, L., Cunha, M., Henriet, J.-P., 2005. The El Arraiche mud volcano field at the Moroccan Atlantic slope, Gulf of Cadiz. Marine Geology 219, 1-17.

Van Rooij, D., Blamart, D., De Mol, L., Mienis, F., Pirlet, H., Wehrmann, L.M., Barbieri, R., Maignien, L., Templer, S.P., de Haas, H., Hebbeln, D., Frank, N., Larmagnat, S., Stadnitskaia, A., Stivaletta, N., van Weering, T., Zhang, Y., Hamoumi, N., Cnudde, V., Duyck, P., Henriet, J.-P., the MiCROSYSTEMS MD169 shipboard party, 2011. Cold-water coral mounds on the Pen Duick Escarpment, Gulf of Cadiz: the MiCROSYSTEMS approach. Marine Geology 282, 102-117.

Van Rooij, D., Blamart, D., the MD169 shipboard scientists, 2008. Cruise Report MD169 MiCROSYSTEMS, Brest (FR)-Algeciras (ES), 15-25 July 2008. ESF EuroDIVERSITY MiCROSYSTEMS internal report, 86 pp.

Van Rooij, D., De Mol, B., Huvenne, V., Ivanov, M.K., Henriet, J.-P., 2003. Seismic evidence of current controlled sedimentation in the Belgica mound province, upper Porcupine slope, southwest of Ireland. Marine Geology 195, 31-53.

Van Rooij, D., De Mol, L., Le Guilloux, E., Wisshak, M., Huvenne, V.A.I., Moeremans, R., Henriet, J.-P., 2010a. Environmental setting of deep-water oysters in the Bay of Biscay. Deep-Sea Research I 57 (12), 1561-1572.

Van Rooij, D., Iglesias, J., Hernández-Molina, F.J., Ercilla, G., Gomez-Ballesteros, M., Casas, D., Llave, E., De Hauwere, A., Garcia-Gil, S., Acosta, J., Henriet, J.-P., 2010b. The Le Danois Contourite Depositional System: interactions between the Mediterranean Outflow Water and the upper Cantabrian slope (North Iberian margin). Marine Geology 274 (1–4), 1–20.

Van Weering, T.C.E., de Haas, H., de Stigter, H.C., Lykke-Andersen, H., Kouvaev, I., 2003. Structure and development of giant carbonate mounds at the SW and SE Rockall Trough margins, NE Atlantic Ocean. Marine Geology 198, 67-81.

Vangriesheim, A., Khripounoff, A., 1990. Near-bottom particle concentration and flux: temporal variations observed with sediment traps and nepholometer on the Meriadzek Terrace, Bay of Biscay. Progress in Oceanography 24 (1–4), 103–116.

Videt, B., Neraudeau, D., 2003. Variability and heterochronies of Rhynchostreon suborbiculatum (Lamarck, 1801) (Bivalvia:Ostreoidea:Gryphaeidae:Exogyrinae) from the Cenomanian and the Lower Taronian of Charentes (SW France). Comptes Rendus Palevol 2 (6–7), 563–576.

Villanueva, P., Gutierrezmas, J.M., 1994. The Hydrodynamics of the Gulf of Cadiz and the Exchange of Water Masses through the Gibraltar Strait. International Hydrographic Review 71 (1), 53-65.

Vlassenbroeck, J., Cnudde, V., Masschaele, B., Dierick, M., Van Hoorebeke, L., Jacobs, P., 2007a. A comparative and critical study of X-ray CT and neutron CT as non-destructive material evaluation techniques. Building Stone Decay: From Diagnosis to Conservation 271, 277-285.

Vlassenbroeck, J., Dierick, M., Masschaele, B., Cnudde, V., Van Hoorebeke, L., Jacobs, P., 2007b. Software tools for quantification of X-ray microtomography at the UGCT. Nuclear Instruments and Methods in Physics Research Section A: Accelerators, Spectrometers, Detectors and Associated Equipment 580, 442-445.

Voelker, A.H.L., Lebreiro, S.M., Schönfeld, J., Cacho, I., Erlenkeuser, H., Abrantes, F., 2006. Mediterranean outflow strengthening during northern hemisphere coolings: A salt source for the glacial Atlantic? Earth and Planetary Science Letters 245, 39-55.

Weaver, P.P.E., Gunn, V., 2009. Introduction to the special issue Hermes Hotspot Ecosystem Research on the Margins of European Seas. Oceanography 22 (1), 12–15.

Webster, G., Blazejak, A., Cragg, B.A., Schippers, A., Sass, H., Rinna, J., Tang, X.H., Mathes, F., Ferdelman, T.G., Fry, J.C., Weightman, A.J., Parkes, R.J., 2009. Subsurface microbiology and biogeochemistry of a deep, cold-water carbonate mound from the Porcupine Seabight (IODP Expedition 307). Environmental Microbiology 11 (1), 239-257.

Wehrmann, L.M., Knab, N.J., Pirlet, H., Unnithan, V., Wild, C., Ferdelman, T.G., 2009. Carbon mineralization and carbonate preservation in modern cold-water coral reef sediments on the Norwegian shelf. Biogeosciences 6 (4), 663-680.

Wehrmann, L.M., Templer, S.P., Brunner, B., Bernasconi, S.M., Maignien, L., Ferdelman, T.G., 2011. The imprint of methane seepage on the geochemical record and early diagenetic processes in cold-water coral mounds on Pen Duick Escarpment, Gulf of Cadiz. Marine Geology, 282, 118-137.

Weldeab, S., Siebel, W., Wehausen, R., Emeis, K.-C., Schmiedl, G., Hemleben, C., 2003. Late Pleistocene sedimentation in the Western Mediterranean Sea: implications for productivity changes and climatic conditions in the catchment areas. Palaeogeography Palaeoclimatology Palaeoecology 190, 121– 137.

Weltje, G.J., 1997. End-Member Modeling of Compositional Data: Numerical-Statistical Algorithms for Solving the Explicit Mixing Problem. Mathematical Geology 29, 503-549.

Weltje, G.J., Prins, M.A., 2003. Muddled or mixed? Inferring palaeoclimate from size distributions of deep-sea clastics. Sedimentary Geology 162, 39-62.

Weltje, G.J., Prins, M.A., 2007. Genetically meaningful decomposition of grain-size distributions. Sedimentary Geology 202, 409-424.

Wessel, P., Smith, W.H.F., 1991. Free software helps map and display data. EOS Transactions AGU 72 (441), 445–446.

Wheeler, A.J., Beyer, A., Freiwald, A., de Haas, H., Huvenne, V.A.I., Kozachenko, M., Olu-Le Roy, K., Opderbecke, J., 2007. Morphology and environment of cold-water coral carbonate mounds on the NW European margin. Internation Journal of Earth Sciences 96, 37-56.

Wheeler, A.J., Kozachenko, M., Beyer, A., Foubert, A., Huvenne, V.A.I., Klages, M., Masson, D.G., Olu-Le Roy, K., Thiede, J., 2005. Sedimentary processes and carbonate mounds in the Belgica Mound province, Porcupine Seabight, NE Atlantic. In: Freiwald, A.,

Roberts, J.M. (Eds.), Cold-Water Corals and Ecosystems. Springer-Verlag Berlin Heidelberg, pp. 571-603.

Wheeler, A.J., Kozachenko, M., Henry, L.-A., Foubert, A., de Haas, H., Huvenne, V.A.I., Masson, D.G., Olu, K., 2011. The Moira Mounds, small cold-water coral banks in the Porcupine Seabight, NE Atlantic: Part A - an early stage growth phase for future coral carbonate mounds? Marine Geology 282, 53-64.

Wheeler, A.J., Kozachenko, M., Masson, D.G., Huvenne, V.A.I., 2008. Influence of benthic sediment transport on cold-water coral bank morphology and growth: the example of the Darwin Mounds, north-east Atlantic. Sedimentology 55, 1875-1887.

White, M., 2007. Benthic dynamics at the carbonate mound regions of the Porcupine Sea Bight continental margin. International Journal of Earth Sciences 96, 1-9.

White, M., Dorschel, B., 2010. The importance of the permanent thermocline to the cold water coral carbonate mound distribution in the NE Atlantic. Earth and Planetary Science Letters 296 (3-4), 395-402.

White, M., Mohn, C., de Stigter, H., Mottram, G., 2005. Deep-water coral development as a function of hydrodynamics and surface productivity around the submarine banks of the Rockall Trough, NE Atlantic. In: Freiwald, A., Roberts, J.M. (Eds.), Cold-Water Corals and Ecosystems. Springer-Verlag Berlin Heidelberg, pp. 503-514.

Wienberg, C., Beuck, L., Heidkamp, S., Hebbeln, D., Freiwald, A., Pfannkuche, O., Monteys, X., 2008. Franken Mound: facies and biocoenoses on a newly-discovered “carbonate mound” on the western Rockall Bank, NE Atlantic. Facies 54, 1-24.

Wienberg, C., Frank, N., Mertens, K.N., Stuut, J.-B., Marchant, M., Fietzke, J., Mienis, F., Hebbeln, D., 2010. Glacial cold-water coral growth in the Gulf of Cadiz: Implications of increased palaeo-productivity. Earth and Planetary Science Letters 298 (3-4), 405-416.

Wienberg, C., Hebbeln, D., Fink, H.G., Mienis, F., Dorschel, B., Vertino, A., López Correa, M., Freiwald, A., 2009. Scleractinian cold-water corals in the Gulf of Cádiz - First clues about their spatial and temporal distribution. Deep-Sea Research I 156, 1873-1893.

Williams, T., Kano, A., Ferdelman, T.G., Henriet, J.P., Abe, K., Andres, M.S., Bjerager, M., Browning, E., Cragg, B.A., De Mol, B., Dorschel, B., Foubert, A., Frank, T.D., Fuwa, Y., Gaillot, P., Gharib, J.J., Gregg, J.M., Huvenne, V., Léonide, P., Li, X., Mangelsdorf, K., Tanaka, A., Monteys, X., Novosel, I., Sakai, S., Samarkin, V.A., Sasaki, K., Spivack, A.J., Takashima, C., Titschak, J., 2006. Cold-Water Coral Mounds Revealed. EOS Transactions 87, 525-526.

Wilson, J.B., 1979. ‘Patch’ development of the deep-water coral Lophelia pertusa (L.) on rockall bank. Marine Biology Association of the UK 59, 165.

Wisshak, M., Freiwald, A., Lundalv, T., Gektidis, M., 2005. The physical niche of the bathyal *Lophelia pertusa* in a non-bathyal setting: environmental controls and palaeoecological implications. In: Freiwald, A., Roberts, J.M. (Eds.), Cold-Water Corals and Ecosystems. Springer-Verlag Berlin Heidelberg, pp. 979-1001.

Wisshak, M., López Correa, M., Gofas, S., Salas, C., Taviani, M., Jakobsen, J., Freiwald, A., 2009a. Shell architecture, element composition, and stable isotope signature of the giant deep-sea oyster Neopycnodonte zibrowii sp. n. from the NE Atlantic. Deep-Sea Research I 56 (3), 374–407.

Wisshak, M., Neumann, C., Jakobsen, J., Freiwald, A., 2009b. The 'living-fossil community' of the cyrtocrinid Cyathidium foresti and the deep-sea oyster Neopycnodonte zibrowii (Azores Archipelago). Palaeogeography, Palaeoclimatology, Palaeoecology 271 (1-2), 77–83.

Zaragosi, S., Auffret, G.A., Faugeres, J.-C., Garlan, T., Pujol, C., Cortijo, E., 2000. Physiography and recent sediment distribution of the Celtic Deep-Sea Fan, Bay of Biscay. Marine Geology 169, 207–237.

Zaragosi, S., Bourillet, J.-F., Eynaud, F., Toucanne, S., Denhard, B., Van Toer, A., Lanfumey, V., 2006. The impact of the last European deglaciation on the deep-sea turbidite systems of the Celtic-Armorican margin (Bay of Biscay). Geo-Marine Letters, 26, 317-329.

Zhu, Z.R., Wyrwoll, K.-H., Collins, L.B., Chen, J.H., Wasserburg, G.J., Eisenhauer, A., 1993. High-precision U-series dating of Last Interglacial events by mass spectrometry : Houtman Abrolhos Islands, Western Australia. Earth and Planetary Science Letters 118, 281-293.

Zibrowius, H., 1973. Scléractinairies des Iles Saint Paul et Amsterdam (sud de l'Océan Indien). Tethys 5, 747-777.

Zibrowius, H., 1980. Les Scléractiniens de la Méditerranée et de l'Atlantique nord-oriental. Bulletin de l'Institut Océanographique de Monaco 11, 1-284.

Zibrowius, H., 1985. Scléractiniaires bathyaux et abyssaux de l'Atlantique nord-oriental: campagnes BIOGAS (POLGAS) et INCAL. In: Laubier, L., Monniot, C. (Eds.), Peuplements profonds du Golfe de Gascogne. IFREMER, Brest, France, pp. 311–324.

Zibrowius, H., Southward, E.C., Day, J.H., 1975. New observations on a little-known species of *Lumbrineris* (Polychaeta) living on various cnidarians, with notes on its recent and fossil scleractinian hosts. Journal of the Marine Biological Association of the United Kingdom 55, 83–108.

Zitellini, N., Gràcia, E., Matias, L., Terrinha, P., Abreu, M.A., DeAlteriis, G., Henriet, J.P., Dañobeitia, J.J., Masson, D.G., Mulder, T., Ramella, R., Somoza, L., Diez, S., 2009. The quest for the Africa-Eurasia plate boundary west of the Strait of Gibraltar. Earth and Planetary Science Letters 280 (1-4), 13-50.

Zühlsdorff, C., Wien, K., Stuut, J.B.W., Henrich, R., 2007. Late Quaternary sedimentation within a submarine channel-levee system offshore Cap Timiris, Mauritania. Marine Geology 240, 217-234.